LBL-7002

MICROSEISMS IN GEOTHERMAL EXPLORATION: STUDIES IN GRASS VALLEY, NEVADA

Alfred Liang-Chi Liaw
(Ph. D. thesis)

MASTER

November 1977

Prepared for the U. S. Department of Energy
under Contract W-7405-ENG-48

LBL-7002

DISCLAIMER

DEDICATION

This dissertation is dedicated to my wife Julie Yu-Chu for her patient encouragement and understanding.

MN ONLY

TABLE OF CONTENTS

MICROSEISMS IN GEOTHERMAL EXPLORATION: STUDIES IN GRASS VALLEY, NEVADA

Alfred Liang-Chi Liaw

Lawrence Berkeley Laboratory
University of California, Berkeley

ABSTRACT

Frequency-wavenumber (f-k) spectra of seismic noise in the bands $1 \leq f \leq 10$ Hz in frequency and $|\underline{k}| \leq 35.7$ cycles/km in wavenumber, measured at several places in Grass Valley, Nevada, exhibit numerous features which can be correlated with variations in surface geology and sources associated with hot spring activity. Exploration techniques for geothermal reservoirs, based upon the spatial distribution of the amplitude and frequency characteristics of short-period seismic noise, are applied and evaluated in a field program at a potential geothermal area in Grass Valley, Nevada. A detailed investigation of the spatial and temporal characteristics of the noise field was made to guide subsequent data acquisition and processing. Contour maps of normalized noise-level derived from carefully sampled data are dominated by the hot spring noise source and the generally high noise levels outlining the regions of thick alluvium. Major faults are evident when they produce a shallow lateral contrast in rock properties. Conventional seismic noise mapping techniques cannot differentiate noise anomalies due to buried seismic sources from those due to shallow geological effects. The noise radiating from a deep reservoir ought to be evident as body waves of high phase velocity with time-invariant source azimuth. A small two-dimensional array was placed at 16 locations in the region

to map propagation parameters. The f-k spectra reveal local shallow sources, but no evidence for a significant body wave component in the noise field was found. With proper data sampling, array processing provides a powerful method for mapping the horizontal component of the vector phase velocity of the noise field. This information, as well as the accurate velocity structure, will enable us to carry out seismic ray tracing and eventually to locate the source region of radiating microseisms. In Grass Valley, and probably in most areas, the 2-10 Hz microseismic field is predominantly fundamental mode Rayleigh waves controlled by the very shallow structure.

ACKNOWLEDGMENTS

This work was supported by the U.S. Energy Research and Development Administration through the University of California, Lawrence Berkeley Laboratory.

I wish to express my deep gratitude to all those who have helped in this work. I am very grateful to the members of my thesis committee, especially the Chairman, Professor T. V. McEvilly, for his advice, stimulating discussions, and encouragement at all stages of the work; to Professor H. F. Morrison and Professor W. E. Farrell for their many constructive criticisms and the arrangement of financial aids during this period of study.

I am grateful to Steven Palmer, Jack Yatou, Glen Melosh, Ernie Majer, and the technical personnel of Lawrence Berkeley Laboratory for their helpful field assistance in various stages of the field experiment.

A final note of thanks goes to my parents for their love and encouragement.

I. INTRODUCTION

Two methods have been proposed for attempting to utilize microseisms for delineating geothermal reservoirs. The first is based on the speculation that hydrothermal processes deep in the reservoir radiate seismic wave energy in the frequency band 1 to 100 Hz. If this phenomenon exists, the exploration method becomes a relatively straightforward "listening" survey, using stations on a 0.5 to 2 km grid. Contours of noise power on the surface should delineate noise sources. This is the "standard" noise survey used widely in geothermal exploration. A second approach interprets the noise field as propagating elastic waves of appropriate type, e.g., fundamental mode Rayleigh waves, and inverts their propagation characteristics to obtain the distribution of medium properties, i.e. velocity and attenuation, both laterally and vertically. The propagation parameters of ambient microseisms so measured will also locate distinctive radiation sources. With sufficient knowledge of the wave nature of the microseisms and a reasonably accurate velocity-depth model, a fixed, non-aliased array can be used in a beam-steering mode to define the source region of radiating noise. Both approaches, as used in typical surveys, suffer greatly when data are contaminated by non-seismic noise, by interfering seismic wave trains, or by improper temporal and spatial data sampling. These pervasive problems have combined to render noise analysis at best a qualitative geophysical method and have substantially limited the acceptance of the seismic noise survey as an integral element in geothermal exploration.

This study attempts to avoid such problems by sophisticated analysis of microseismic data in an evaluation of the feasibility of ground noise studies in geothermal site delineation. We report a series of investigations undertaken near Leach Hot Springs in Grass Valley, within the region of generally high heat flow in northern Nevada. We first quantify the spatial and temporal variations of ground noise in the region and find that the seismic noise spectrum is strongly affected by the near-surface geology at the recording site. In fact, with broad-band seismic sensors in a mapping technique using amplitudes and frequencies, one can outline lateral variations in alluvial thickness. This "standard" mapping technique cannot differentiate noise enhancement due to shallow structure from noise enhancement due to buried seismic source. On the other hand, we find that the mapping of wave propagation parameters provides additional information about the noise field. However, the successful application of this technique requires some understanding of the wave nature of microseisms. We used multiple-sensor arrays to study the seismic coherency as a function of frequency and spatial separation. Based on this information, we designed an array to collect propagating microseismic data. The array data were processed by both the frequency domain beam-forming method (BFM) and the maximum-likelihood method (MLM). From the dispersion curves obtained in our array study, we verify that the seismic noise consists primarily of fundamental mode Rayleigh waves.

In Chapter 2, I consider the geothermal ground noise within the content of wide-band microseisms and discuss the origin of seismic noise in three different period ranges. In Chapter 3, I describe the area of field study and the systems used for field data acquisition. The conventional seismic noise power contour technique is evaluated in Chapter 4. Finding weakness in the conventional mapping method, I present a sophisticated array mapping technique in Chapter 5, along with field procedures, data processing schemes, and the results of the Grass Valley study. In the concluding chapter, I summarize the results of the study and present recommendations for extensions of the work.

II. EARTH NOISE

2.1 Introduction

The study of microseisms, or earth noise, involves interplay of meteorology, oceanography and seismology. The investigation of microseisms has attracted seismologists since the beginning of this century. A bibliography covering work up to 1955 (Gutenberg and Andrews, 1956) lists over 600 articles on the subject. In a recent review, Båth (1974) provided an additional 69 articles related to spectral studies of microseisms.

A typical seismic noise spectrum recorded at a quiet site (Figure 2.1) shows:

1) The amplitude increases with period for periods longer than 30 sec. Over this band seismic noise is due to atmospheric loading (Savino, et al., 1972).
2) Two distinctive maxima appear around 6-8 sec and 14-20 sec. These are related to ocean waves.
3) Low amplitude short-period noise ($T < 0.8$ sec) associated with human activity and local natural disturbances, including weather.

A distinct worldwide minimum in seismic noise occurs around 30 to 40 sec, separating the very long-period microseisms of atmospheric origin from those long-period waves due to ocean swell. (Savino, et al., 1972; Whorf, 1972). Another prominent minimum around 0.8 sec separates short-period local noise from long-period ocean swell (Figures 2.1 and 2.2).

The noise spectrum, S(f) can be expressed as

$$S(f) = I(f)\ E(f)\ G(f) \tag{2.1}$$

where:

I(f) = the source spectrum,

E(f) = the transfer function of entire path, excluding near surface effects at the sensor, and

G(f) = the transfer function of the shallow section at the recording site.

The noise spectrum reflects the nature of the source spectrum, and the acoustic properties of the medium both along the path and beneath the recording site. At a quiet bedrock location, away from strong local surface or subsurface sources, the noise spectrum generally exhibits a frequency dependence of f^{-1} to f^{-3}, with local reversals at the peaks (Figures 2.1 and 2.2). In Figure 2.1 the power spectral density obtained by Fix (1972) corresponds to the minimum value recorded at a quiet site (Brune and Oliver, 1959) and to the typical background noise spectrum in 10 to 100 sec range at Albuquerque (Peterson et al., 1976). The results of Peterson et al. (1976) were recorded by the broad-band borehole seismometers of the Seismic Research Observatories.

In this chapter, I discuss the sources of seismic noise, emphasizing those observations of particular relevance for geothermal ground noise. In the last section, I discuss the effect of local geology on seismic noise.

2.2 Short-period seismic noise ($T < 0.8$ sec)

Microseisms in the period range 0.8 sec to 0.01 sec (1.25 Hz to 100 Hz) are generated by human activity such as traffic or machinery (usually called "cultural" noise), by natural surface disturbances due to wind, or by subsurface activity such as microearthquakes or geothermal processes. Over this frequency range the seismic energy attenuates rapidly with increasing distance from the source. As indicated by Douze (1967), short-period surface seismic noise consists mostly of fundamental mode Rayleigh waves. He also found that at depths of 2 to 3 km beneath the earth's surface, where the fundamental Rayleigh mode has decreased to negligible amplitude, the remainder of the noise consists of random body waves.

Cultural noise. Noise sources related to human activity are responsible for diurnal variations of background noise level as seen in the Waiotapu region of New Zealand (Whiteford, 1970), and at East Mesa, California (Iyer, 1974), both geothermal regions. At East Mesa the freeway, with frequent truck traffic, produces wide-band (up to 10 Hz) noise as well as large amplitude variations which can be detected at distances up to 8 km. Measurements near roads in the Waiotapu region show that traffic can produce ground motion up to 700 x 10^{-9} m/sec about 13 dB above a quiet site, in 0.5 - 100 Hz, at a distance of 0.5 km (Whiteford, 1970).

Rivers, canals, and waterfalls. Iyer and Hitchcock (1976) reported that the river flowing in Long Valley, California, generates noise at frequencies above 6 Hz and that the noise is attenuated by 12 dB 1 km from the river. In East Mesa, irrigation canals seem to be continuous wide-band sources of noise attenuating rapidly with distance, reaching a fairly steady level beyond 3 km. At the power drops (small waterfalls) along the canals, however, a distinctive noise component is generated in a narrow frequency band around 2.5 Hz (Iyer, 1974). Iyer and Hitchcock

(1974) found that in Yellowstone National Park the waterfalls generate a narrow band seismic noise at 2 Hz which is clearly different in appearance from the noise generated by the hydrothermal process.

Wind. Although both Whiteford (1970) and Iyer (1974) reported poor correlation between the amplitude of short-period seismic noise with wind speed, Frantti (1963) reported that high wind influenced short-period noise. His results are presented in Figure 2.3 for three components of motion. The wind effect influences a broad frequency range, particularly on the horizontal component oriented parallel to the wind direction. Peterson *et al.* (1976) have shown that the effect of wind-generated noise decreases as the depth of sensor location increases.

Geysers, hot springs, and fumaroles. Reports relating short-period microseisms to geothermal processes are numerous. We will discuss this topic in more detail in Section 2.5.

2.3 Long-period seismic noise (2 sec < T < 20 sec)

Early studies of microseisms concentrated on the observation and the origin of 6 - 8 sec microseisms which have been reported as a world-wide phenomenon. The amplitude of microseisms varies from site to site and it varies temporally at a given site. The term "microseismic storm" is used to refer to the occasional periods of unusually large amplitude microseismic activity. Since the dominant microseism period at 6 - 8 sec corresponds to half the period of a pronounced peak in the ocean wave spectrum, and since large amplitude microseisms are always observed near the coast, these microseisms are inferred to be of oceanic origin. Longuet-Higgins (1950) has shown theoretically that the 6 - 8 sec microseisms are generated by the standing wave phenomenon in ocean wave motion. The standing waves are caused by the interference of groups of waves of the same wavelength, but not necessarily of equal amplitude, travelling in opposite directions. The mean pressure on the bottom beneath a train of standing waves is not constant, as in a progressive wave, but fluctuates with an amplitude independent of the depth and proportional to the square of the wave height. The oscillation of standing waves produces the type of energy required for the generation of ground movement. This type of energy is unattenuated by water depth, and in phase at all points of the bottom, suitable for producing coherent seismic waves. Further, the frequency of this pressure variation is twice the fundamental frequency of the waves. The favorable environments in which the standing wave motion may be strong are:

1) the wake of a moving storm,
2) the center of a storm, and
3) reflection from a coast.

The generation of 6-8 sec microseisms by ocean storms has been reported (Iyer, 1958; Toksöz and Lacoss, 1968; Haubrich and McCamy, 1969; and Vinnik, 1971), suggesting the first or second possible source of generation. Other observations related to ocean waves near the coastline indicate the third possible source (Haubrich _et al._, 1963).

The double-peaked spectral feature characterized by two distinctive maxima at 6-8 sec and 14-20 sec respectively has attracted attention since the development of high gain long period seismographs. Microseisms with the same dominant period as ocean surface waves are referred to as primary frequency microseisms (PF), as distinct from double frequency microseisms (DF) or secondary microseisms, which have half this period. The microseisms of the double frequency contain more energy than those of the primary frequency. The primary and secondary microseisms are generated from the same meteorological disturbances at the east and west coasts of the United States (Oliver and Page, 1963; Haubrich *et al.*, 1963). The primary microseisms are probably generated as a result of the incidence of gravity waves in water upon a coastline; this is in general agreement with the classical "surf" theory. The generative strip is presumably confined to shallow water, 100 miles up or down the coast (Haubrich *et al.*, 1963). The secondary microseisms are apparently due to standing water wave oscillation, in agreement with Longuet-Higgins' theory, in shallow and/or deep water.

2.4 Very long period seismic noise (T > 30 sec)

The power spectral density of very long period seismic noise in 30 to 130 sec range rises smoothly with period, as shown in Figure 2.1 for the vertical component. Haubrich and Mackenzie (1965) and Capon (1969) have observed that noise in this period range consists of non-propagating energy, as indicated by low coherency between two seismometers separated a few km, plus some fundamental Rayleigh mode energy. The non-propagating seismic noise is apparently generated by atmospheric pressure variations. Sorrells *et al.* (1971) have noted that during windy intervals there is strong correlation between local atmospheric pressure changes and the noise recorded by a vertical seismograph located on the surface. In contrast, over the same range of periods, there is no correlation between seismic noise recorded in a mine at a depth of 183 m and local atmospheric pressure changes, except during the passage of acoustic gravity waves. The model for generating earth noise in this period range is related to atmospheric pressure disturbances that are relatively coherent over a fraction of a wavelength and propagate with jet stream velocities (30-100 m/sec) which are much slower than seismic waves (Savino, et al., 1972). An idealization of this model corresponds to a static, atmospheric pressure loading consisting of random pressure disturbances acting over equal areas on the earth surface. This idealized model explains the level and shape of the spectrum of very long-period earth noise and the attenuation of microseismic ground motion with depth.

2.5 Geothermal ground noise

New Zealand. Clacy (1968) first suggested that seismic noise increased near geothermal reservoirs. His first results northeast of Lake Taupo, New Zealand, were based on contours of total noise amplitude in the frequency band 1 to 20 Hz. In subsequent surveys at Wairakei, Waiotapu, and Broadlands geothermal areas, he found that the local noise amplitude anomalies were characterized by a dominant frequency of 2 Hz, whereas, away from the area of the anomaly, frequencies higher than 3 Hz predominated. On the other hand, Whiteford (1970) found in repeat surveys of the same areas that neither the shape of the frequency spectrum nor its dominant frequency conformed to any regional pattern. Whiteford measured the absolute ground motion in the Waiotapu geothermal area and found that, within a distance of 1 to 2 km of the high heat flow area, the average minimum ground particle velocity was greater than 150×10^{-9} m/sec, while further away, the amplitude of the ground movement decreased by a factor of about 3 and, in addition, exhibited pronounced diurnal variations.

Imperial Valley, California. In the United States, a similar survey was first carried out southeast of the Salton Sea by Goforth *et al.* (1972) who suggested an empirical relationship for geothermal reservoirs between high temperature gradient and high seismic noise level. Their results showed a significant increase in the noise power in the frequency band of 1 to 3 Hz at sites above the reservoir. They estimated the power spectrum at each site with ten 200-second data segments taken over eight hours of night-time recording. The contour map of the total power in the frequency band of 1 to 3 Hz was similar to the temperature gradient contour map. Douze and Sorrells (1972) conducted a similar survey over the nearby East Mesa area, where they found that the total seismic power in the 3 to 5 Hz band exhibited spatial variations similar, in general, to the gravity and heat flow fields. East Mesa was later surveyed by Iyer (1974), with significantly different results. Iyer measured seismic noise by averaging 20 of the lowest values of the RMS amplitude in several narrow frequency bands, using data blocks of 81.92 sec selected from four hours of digital data. He did not find an anomaly in seismic noise associated with geothermal activity but only the noise from canals and freeway traffic.

Yellowstone National Park. The seismic pulsation associated with several geysers in Yellowstone National Park is believed to be indicative of the heating of water in the underground reservoir and the eruption triggered by the superheated system. Nicholls and Rinehart (1967) have studied the seismic signature of several geysers in the park and inferred that their predominant pulse frequencies are quite similar, in the range of 20-60 Hz, presumably due to steam action. The very low frequency seismic pulses recorded at Old Faithful, Castle, Bead, Plume and Jewel geysers are believed to be associated with some type of water movement. The maximum amplitude of seismic pulses recorded in the park is 5.08×10^{-5} m/sec. At Old Faithful Geyser the maximum amplitude is 2.54×10^{-5} m/sec at 30-50 Hz.

Iyer and Hitchcock (1974) have also found good correlation between geothermal activity and high seismic noise levels in 1 to 26 Hz in the park. The ground noise level in non-geothermal areas of the park is approximately 13 to 15×10^{-9} m/sec at 1 to 26 Hz. In the Lower and Upper Geyser Basins where there are numerous geysers and hot springs, the average noise level is in general higher than 50×10^{-9} m/sec, and reaches a value of 672×10^{-9} m/sec near the Old Faithful Geyser. In the Norris Basin, another highly active geyser basin in the park, the noise level varies from 50 to 500×10^{-9} m/sec. Part of the observed noise in the Lower, Upper, and Norris Geyser Basins is no doubt generated by the hydrothermal activity at the surface. The measurements near Old Faithful indicate that high-frequency noise, in the 8 to 16 Hz band, is generated during the geyser eruption; the noise level of lower frequencies is not affected by the eruption cycles. Noise levels around Mammoth Hot Springs are two to five times higher than in the surrounding area. There is no geyser or fumarole here, and the geothermal water is relatively cooler than at Norris and the other geyser basins. Hence, it is very unlikely that the seismic noise observed here is generated near the surface. The noise anomaly observed in the area between Lower Falls and Mud Volcano could be caused by ground amplification effects in the soft sedimentary deposits.

Other Areas. Correlations have also been reported between geothermal activity and high seismic ground noise in the Vulcano Islands, Italy (Luongo and Rapolla, 1973), the Coso geothermal area, China Lake, California (Combs and Rotstein, 1975), and Long Valley, California (Iyer and Hitchcock, 1976). High frequency noise, $f > 8$ Hz, in the vicinity of geysers, fumaroles, and hot springs is associated with hydrothermal activity near the surface and during the geyser eruption. Low frequency noise, $f < 8$ Hz, is not affected by geyser eruption cycles and is probably generated at depth. Other than those active sources the noise power anomaly may also result from lateral variation in near-surface velocity, particularly where low velocity alluvium is involved.

2.6 Local geological structure effects

It has been noted that the seismic waves observed from earthquakes and explosions are strongly affected by the near-surface geology at the recording site. The amplitude of seismic waves is generally smaller at a bedrock site than at an alluvium site. Low-velocity surface materials tend to amplify incident body waves (Borcherdt, 1970; Murphy et al., 1972) and surface waves (Lysmer and Drake, 1972) in selective frequency bands. The amplification effects of body waves result from resonance phenomena caused by large reflection coefficients related to velocity and thickness of the overburden. In the case of the surface waves, the shallow structure can provide a waveguide at particular frequencies corresponding to the maxima and minima in the group velocity dispersion curve. Similar effects have been reported for seismic noise, where amplitude and dominant frequency are characterized by the geology of the recording site (Kanai and Tanaka, 1961; Borcherdt, 1970; Iyer and Hitchcock, 1976). In general, the seismic noise at a quiet bedrock site exhibits a smooth spectrum and small amplitude, whereas on a surface of deep weathering or thick sedimentary overburden, the noise spectrum shows a large peak in a particular frequency band.

For a normally incident-plane SH wave at the lower boundary of an elastic layer over an elastic half-space, the theoretical resonance frequencies are

$$f = \frac{(2n-1)\beta}{4h} \qquad \text{for } n = 1, 2, 3, \ldots N,$$

where β = shear-wave velocity of the layer and

h = thickness of the layer.

This relation also holds for the case of P-wave, using the compressional wave velocity. Consequently, the spectrum of recorded motion will show distinctive peaks at the resonance frequencies. In practice, however, complex geological structure will complicate the nature of the spectrum (Kanai and Tanaka, 1961; Kanai, et al., 1966).

FIGURE CAPTIONS

Figure 2.1 Power spectral density of the vertical component earth noise recorded at the Queen Creek Seismological station, Arizona (after Fix, 1972). This spectrum is typical of a quiet site. The distinctive humps at 8 and 15 sec arise from ocean sources.

Figure 2.2 Power spectral density of the vertical component short-period earth noise recorded at the surface and at a depth of 5486 m in Grapevine, Texas (after Douze, 1967). Note the attenuation with depth.

Figure 2.3 Earth noise spectra showing the effect of high wind (>20 mph) and low wind (<5 mph) in three components of short-period particle motion at Rural Valley, Pennsylvania (after Frantti, 1963).

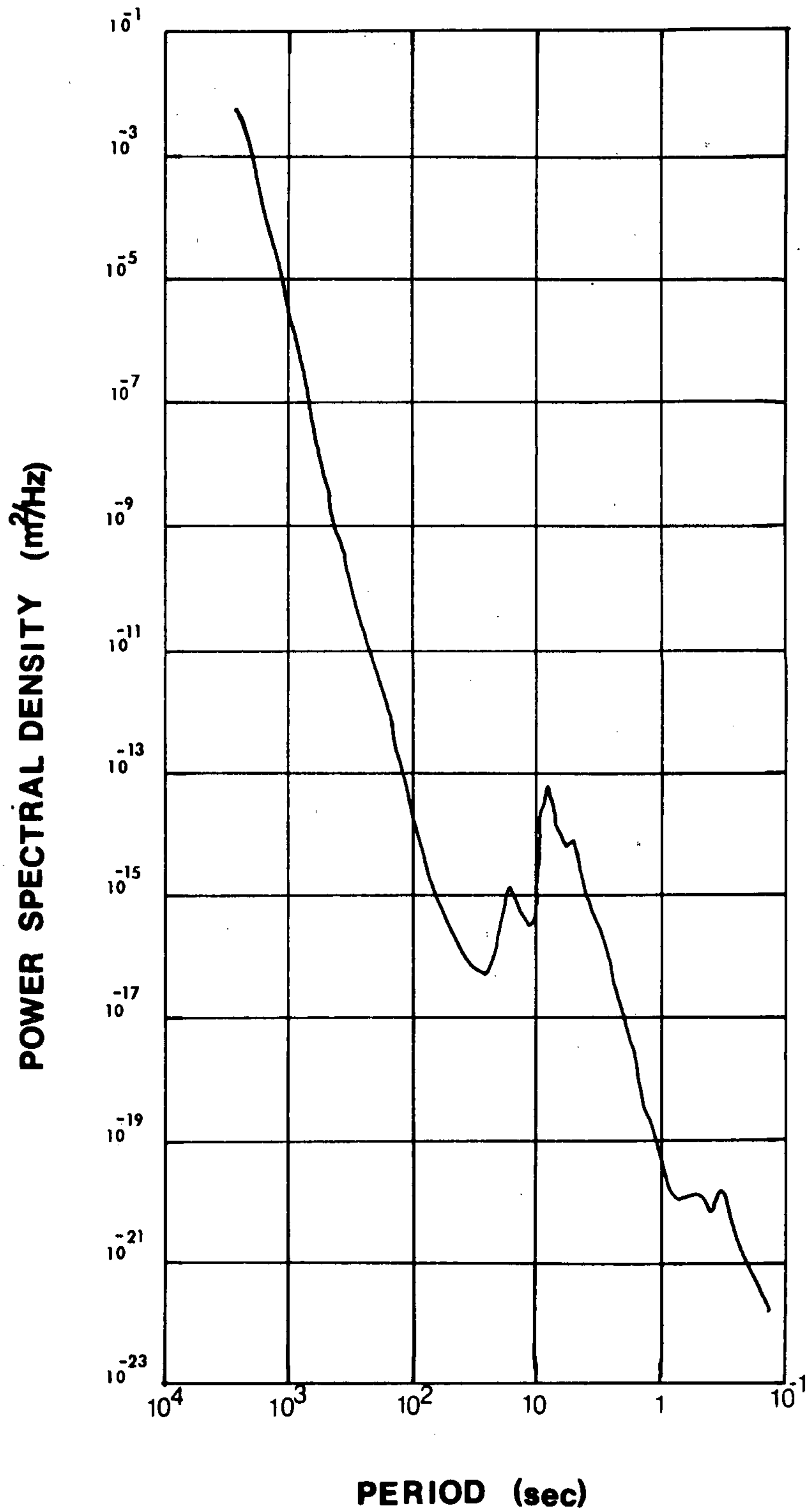

XBL 779-2461

Figure 2.1

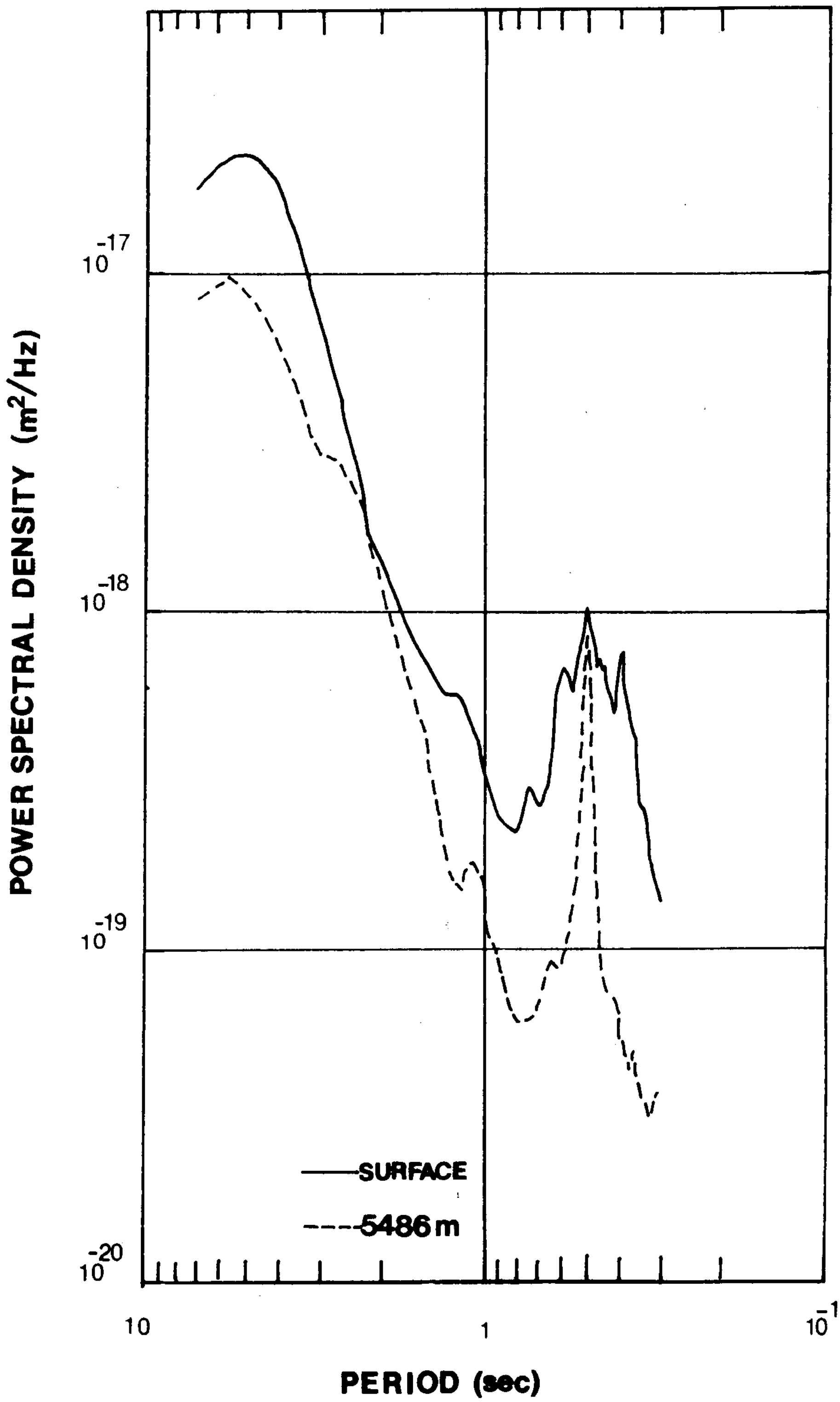

XBL 779-2462

Figure 2.2

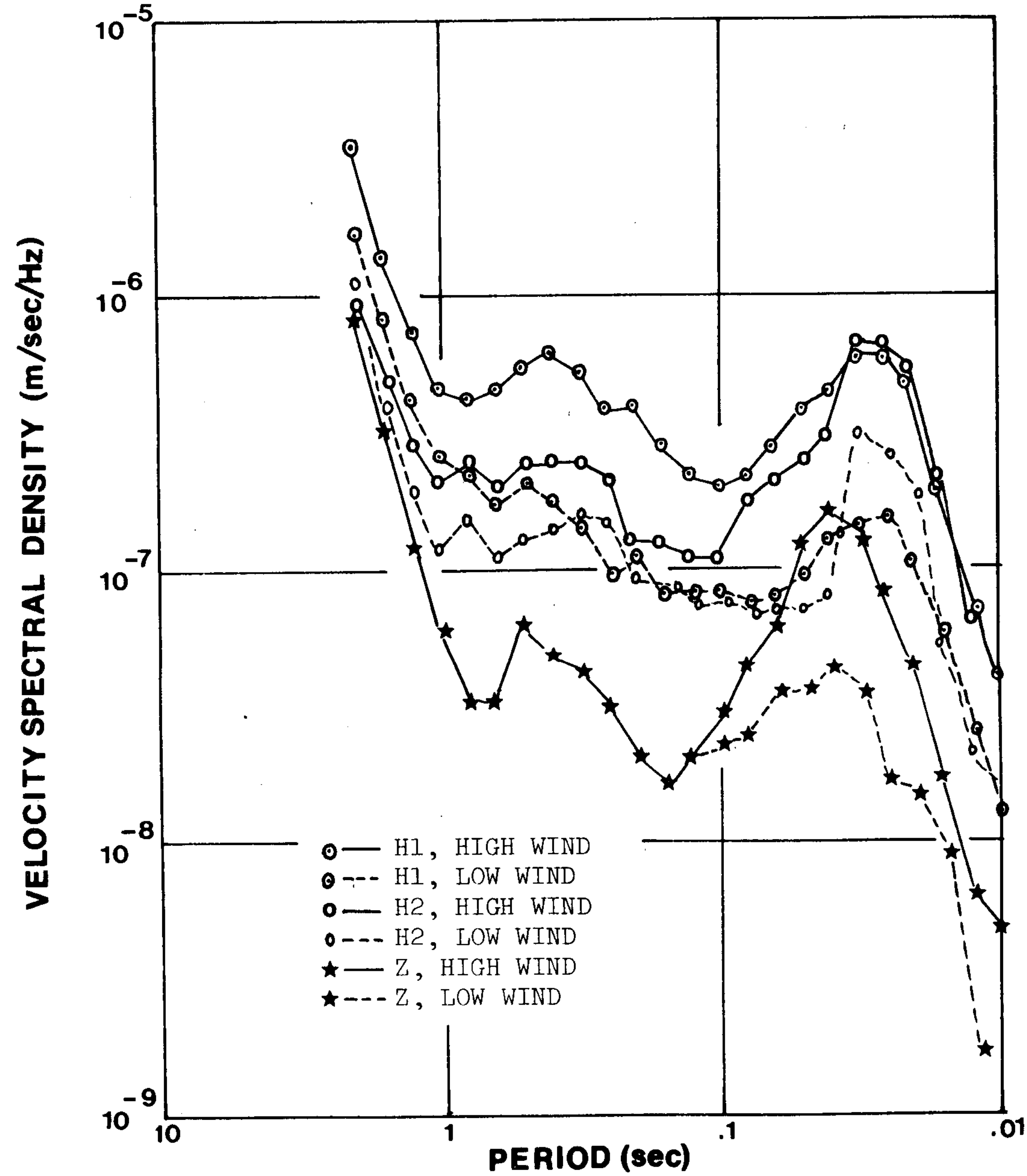

XBL 779-2460

Figure 2.3

III. FIELD PROGRAMS

3.1 Introduction

In this chapter I discuss the data collection phase of the seismic ground noise study. The location, geological setting and tectonic history of the potential geothermal resource region are presented. Data acquisition is discussed in the concluding sections.

3.2 Area of Study

Leach Hot Springs, in Grass Valley, Nevada, is located 30 km south of Winnemucca (Figure 3.1). Grass Valley is a typical valley of the Basin and Range province with normal faulting, major earthquakes, and hot springs occurring along the valley margins. The valley is bounded by the Sonoma and Tobin Ranges to the east, and the basalt-capped East Range to the west. The valley narrows south of the hot springs as it approaches the Goldbanks Hills (Figure 3.2). These ranges are composed of Paleozoic sedimentary rocks, or Triassic siliceous clastic and carbonate rocks. Some granitic intrusions, probably of Triassic age, are found in the Goldbanks Hills; elsewhere the granites are probably of Cretaceous age. The valley is filled with Quaternary alluvial sediments. There are sparse occurrences of Tertiary rhyolite and basalt, and in the vicintiy of Leach Hot Springs there are Quaternary sinter deposits. The distribution of major lithologic units in the region is illustrated on the geologic map (Figure 3.3).

As is characteristic of hot spring systems found in northern Nevada, Leach Hot Springs is located on a fault, strongly expressed by a 10 to 15 m high scarp trending NE. Normal faulting since mid-Tertiary has offset rock units vertically several tens to several hundreds of meters. As shown on the fault and lineament map (Figure 3.2), the present day hot springs occur at the intersection of a major NE-trending fault and the more common NNW-SSE trending lineament on the eastern side of the valley.

Leach Hot Springs is within the high heat flow area of northern Nevada indicated in Figure 3.1. This high heat flow area is often called the "Battle Mountain high" (Sass et al., 1971) and exhibits heat flow values in the range of 1.5 to 3.5 HFU (1 HFU = 10 cal/m^2 sec). The diffuse region of elevated heat flow over the Basin and Range province is generally thought to be an expression of high temperature in the lower crust and upper mantle, and it seems reasonable to interpret the localized Battle Mountain high as an effect of fairly recent intrusion of magma into the earth's crust. Quaternary volcanism within the province supports this hypothesis.

3.3 Other geophysical data in this area

Geophysical data were obtained primarily along 17 survey lines (Figure 3.4), although not all methods were employed on every line. Line E is typical. Bouguer gravity anomaly, P-wave delay data, and seismic reflection data, presented in Figure 3.5 for line E, indicate that the greatest thickness of sediments and major faulting occur near the eastern valley margin. The major lithologic units from the seismic reflection section are Quaternary alluvium (1.8 km/sec), Tertiary sedimentary and volcanic rocks (2.9 km/sec), Paleozoic rocks (4.0 km/sec), and deep basement (5.0 km/sec), respectively. The basement surface rises gently to the west, but is apparently up-faulted at the eastern boundary faults as indicated by the Bouguer gravity map (Figure 3.6).

The low apparent resistivity zone beneath E2W-E4W (Beyer, et al., 1976), found in the dipole-dipole resistivity survey, has been identified with Tertiary sediments. Since the heat flow value in this zone is not high by Battle Mountain standards (2.24 HFU), the accumulation of conductive sediments, such as ancient playa deposits in the deepest portion of the valley, is probably responsible for the resistivity anomaly.

The only portion of the Grass Valley area that is seismically active is in Panther Canyon and in the valley immediately west of it. This seismic zone is one of complicated faulting and frequent micro-earthquakes. The area is dominated by a strong NE trending gravity feature which offsets topography and the Bouguer gravity anomaly (Figure 3.6). There is a strong electrical conductivity high and a high heat flow of 4.9 HFU. More details of the geophysical data obtained in the Grass Valley area are given by Beyer, et al., (1976).

3.4 Seismic data acquisition system

A portable seismic network, with up to 12 stations linked by radio telemetry to a recording system mounted in a small two-wheeled trailer, was designed for simplicity, flexibility and ease of installation. It proved possible for two men to deploy the sensors and check out the telemetry in about one day. Ease of network emplacement made it possible to modify the array as data were collected and to design field experiments with multiple objectives.

A 4.5 Hz vertical-component geophone, a high-gain amplifier (60-120 dB), a voltage controlled oscillator, and a radio transmitter constitute the station site equipment. The block diagram of one typical station is shown in Figure 3.7. A 0.1 watt transmitter gives a range of about 20 km for average topography. In applications using all 12 geophones spaced over a small aperture array (50m), the radio links were eliminated and signals were transmitted by wire to the recording trailer. In the trailer are housed the radio receivers, FM discriminators, a 14-channel slow-speed FM tape recorder (0.12 ips, 0-40 Hz, 8 days; or 0.24 ips, 0-80 Hz, 4 days), the timing system, and batteries. A slow-speed smoked-paper recorder was used as a monitor. Figure 3.8 gives the details of the central recording system housed in the trailer. The system has about 40 dB dynamic range (peak-to-peak measurement), limited primarily by the tape recorder.

Data are played back at the Seismographic Station on the Berkeley campus and selectively digitized at a rate of 40 samples per second. The transfer function (ground particle velocity to volts from playback discriminator) of the recording and playback system before digitization is expressed as the product over the transfer function of all system elements

$$H(f) = H_g(f) \cdot |H_A \cdot H_{RC}(f) \cdot \frac{4}{VCOFS} \cdot H_p(f)| \text{ volts/m/sec.} \qquad (3.1)$$

The phase term of $H_g(f)$ is different in some channels. Other terms are recording/playback/digitization systems which are the same for all channels, so no phase term is involved.

$$H_g(f) = G \cdot \frac{R_D}{R_S+R_D} \cdot \frac{f^2}{[(f_S^2-f^2)^2+(2\zeta f_S f)^2]^{1/2}} \exp[j(\theta-\frac{\pi}{2})], \qquad (3.2)$$

where G = generator constant of geophone = 77 volt/m/sec for the GEOSPACE GSC-8D and HS-1 geophones,

R_D = damping resistance in ohms, typically 2000 to 3000 ohms,

R_S = coil resistance of geophone = 3400 ohms or 1310 ohms,

f_S = natural frequency of geophone, nominally 4.5 Hz,

ζ = damping factor,

$$\theta = \tan^{-1} \frac{2\zeta f f_S}{f^2 - f_S^2} \quad . \tag{3.3}$$

The exponential term in Equation (3.2) is the phase difference introduced by the geophone. In the small-aperture array data acquisition mode, we have used geophones of two different damping factors, i.e. $\zeta = 0.3$ and $\zeta = 0.6$. The phase correction is, therefore, necessary to correct those data used for f-k analysis. The geophone phase is the only phase correction term required in the data processing, since we have used matched phase responses to every other system element. We define the positive phase term $\exp[j\theta(f)]$ to be phase delay for $\theta > 0$. The characteristics of geophones used in this study are listed in Table 1.

The modulus of transfer functions of the two-pole RC low-pass filter and the high-pass filter in the SPRENGNETHER AS-110 amplifier with mid-band gain, H_A, is

$$|H_A \cdot H_{RC}(f)| = |H_A| \cdot \frac{1}{1+(\frac{f}{f_H})^2} \cdot \frac{1}{1+(\frac{f_L}{f})^2} \quad , \tag{3.4}$$

where f_H and f_L are cut-off frequencies of the filters. "VCOFS" in Equation (3.1) represents the maximum voltage of the amplified signal set to correspond to ± 250 Hz of full-scale FM modulation about the

TABLE 1

Damping Characteristics of Geophones

Geophone identification	Damping resistance R_D(kΩ)	Coil resistance R_S(kΩ)	Damping factor
3	3.3	1.31	0.6
4	1.5	1.31	0.6
5	3.0	1.31	0.6
6	3.0	1.31	0.6
7	4.3	1.31	0.6
9	5.0	1.31	0.6
11	2.0	1.31	0.6
12	3.0	1.31	0.6
13	3.5	1.31	0.6
14	3.0	1.31	0.6
16	3.0	1.31	0.6
17	3.5	1.31	0.6
18	3.0	1.31	0.6
B1	infinite	3.4	0.3
B2	infinite	3.4	0.3
B3	infinite	3.4	0.3
B4	infinite	3.4	0.3
B5	infinite	3.4	0.3
BY1	infinite	3.4	0.3
BY2	infinite	3.4	0.3

VCO (voltage controlled oscillator) frequency. The tapes playback discriminators contain 4-pole Butterworth filters with

$$|H_p(f)| = \frac{1}{[1+(\frac{f}{f_p})^8]^{1/2}} \quad , \tag{3.5}$$

where f_p is the tape recorder bandwidth (e.g., 40 or 80 Hz, depending on the tape recorder used). Since full-scale voltage from the tape playback discriminator is $\pm$4V, and the digitizer full-scale is $\pm$2048 counts, the transfer function to the digitized signal is

$$H_D(f) = H(f) \cdot \frac{2048}{4} \cdot |H_{BW}(f)| \text{ counts/m/sec.} \tag{3.6}$$

where $H_{BW}(f)$ is the anti-alias filter (3 four-pole Butterworth filters) at low-pass corner f_{BW};

$$|H_{BW}(f)| = \frac{1}{[1+(\frac{f}{f_{BW}})^8]^{3/2}} \quad . \tag{3.7}$$

The modulus of transfer function of the system in counts/millimicron/second is shown in Figure 3.9 , assuming R_D /(R_S + R_D) to be unity. This is the only correction required for VSD estimation, since the phase information is not essential.

FIGURE CAPTIONS

Figure 3.1 Prominent thermal springs and the Battle Mountain high heat flow region in northwestern Nevada. Leach Hot Springs is located in the center of the high heat flow area.

Figure 3.2 Mapped faults and pertinent geophysical traverses in the Leach Hot Springs area. Hachured lines indicate down-faulted sides of scarplets; ball symbols indicate downthrown side of other faults. Star shows location of Leach Hot Springs. Heavy solid lines are survey lines E, B, and G with tick marks every 1 km. AC, A2N, and GP are observation sites discussed in text.

Figure 3.3 Lithologic map, Leach Hot Springs area, Qal: Alluvium, Qos: older sinter deposits, Qsg: sinter gravels, Qtg: Quaternary-Tertiary gravels and fanglomerates, Tb: Tertiary basalt, Tr: Tertiary rhyolite, Tt: tuff, Ts: Tertiary sedimentary rocks, Kqm: quartz monzonite, Kg: granitic rock, md: mafic dike, TRg: Triassic granitic rocks, TR: Undifferentiated Traissic sedimentary rocks, P: undifferentiated Paleozoic sedimentary rocks.

Figure 3.4 Geophysical survey lines in Grass Valley, Nevada.

Figure 3.5 Profiles on line E of Bouguer gravity anomaly, P-wave delay, migrated seismic reflection section, and the instantaneous microseismic field, showing east margin fault (trace at 1E) and the maximum sediment thickness around 2W. Averaged section compressional velocities shown: (A) 1.8 km/sec Quaternary alluvium,

(B) 2.9 km/sec Tertiary sediments, and (C) 4.0 km/sec Paleozoic rocks. A detailed explanation of the microseismic field contour is given in Figure 4.6.

Figure 3.6 Bouguer gravity anomaly map of Grass Valley, Nevada. Station locations are shown as dots on the map. The gravity low axis along the eastern side of the valley corresponds to the greatest thickness of sediment.

Figure 3.7 Block diagram of a typical seismic station.

Figure 3.8 Block diagram of the central receiving and recording system. The splitter box at the center of the figure indicates the device distributing a multiplexed signal to two or more discriminators.

Figure 3.9 The modulus of transfer function of data acquisition, playback, and digitizing systems. The gain of the amplifier is 120 dB. ζ represents the geophone damping factor. $H_p(f)$ and $H_{RC}(f)$ are not included in the response shown (see text). R_D / $(R_S + R_D)$ of $H_g(f)$ is assumed to be unity in calculating these responses.

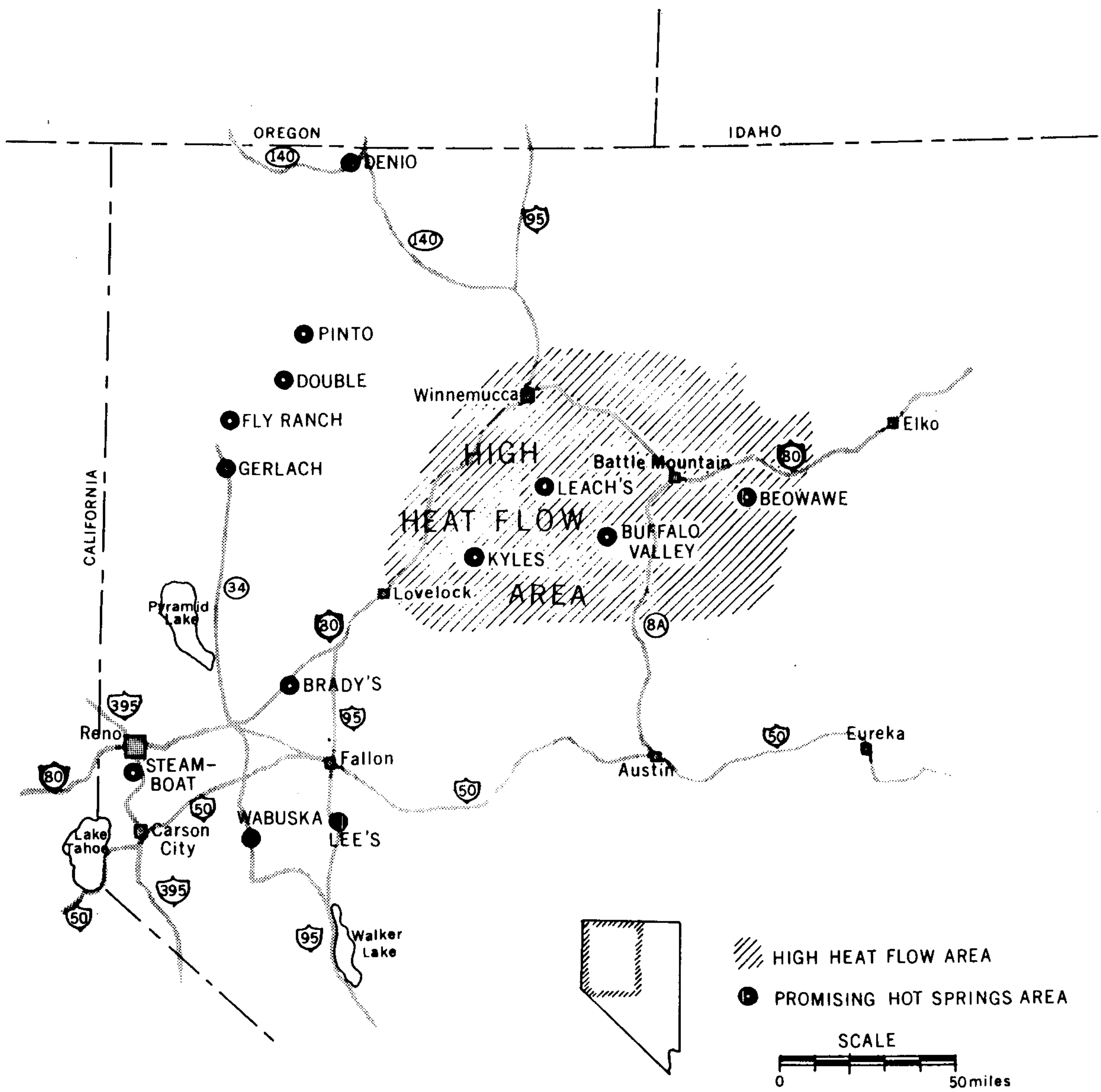

Hot Springs in Northwestern Nevada

XBL 735 676

Figure 3.1

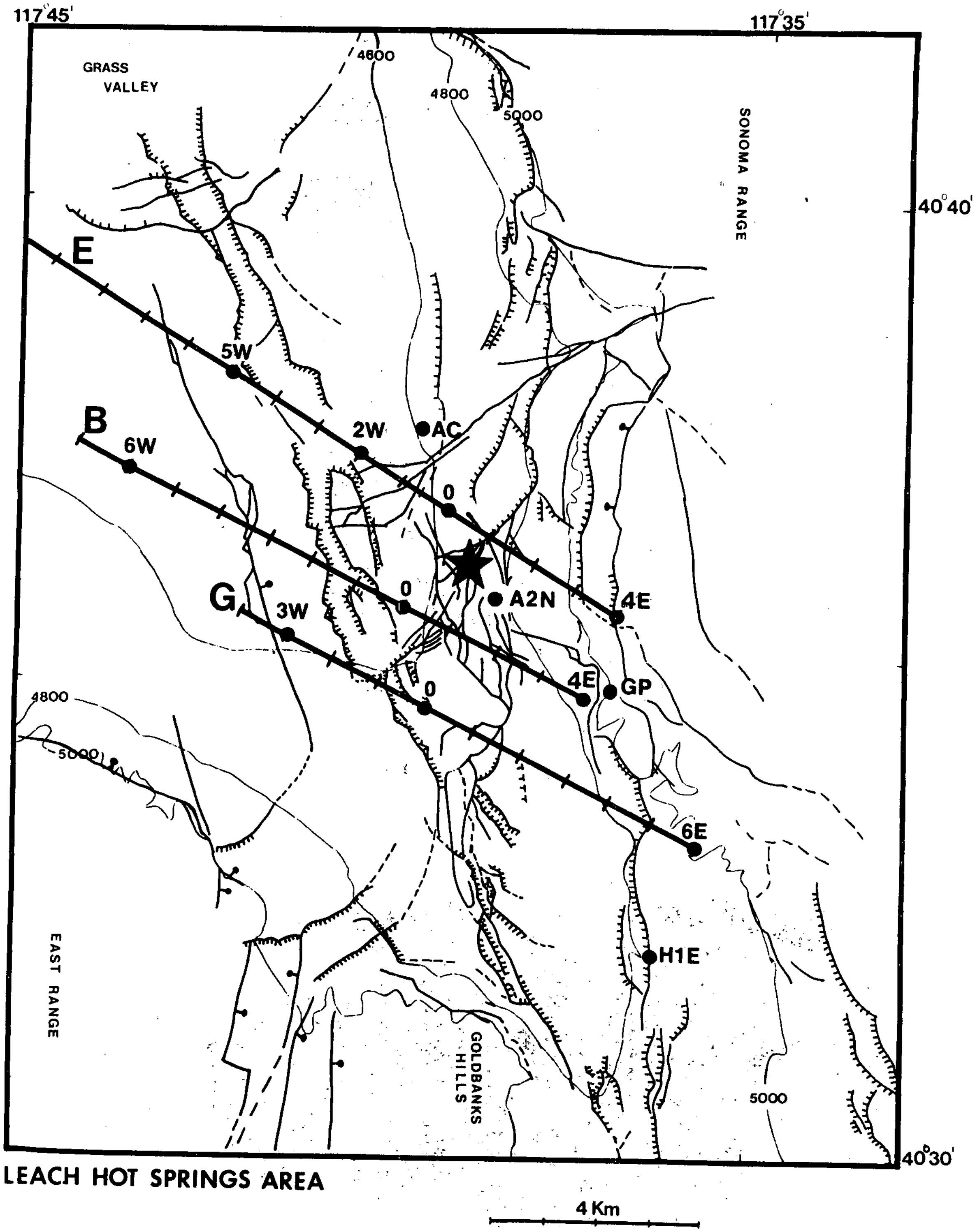

XBL 771-7423

Figure 3.2

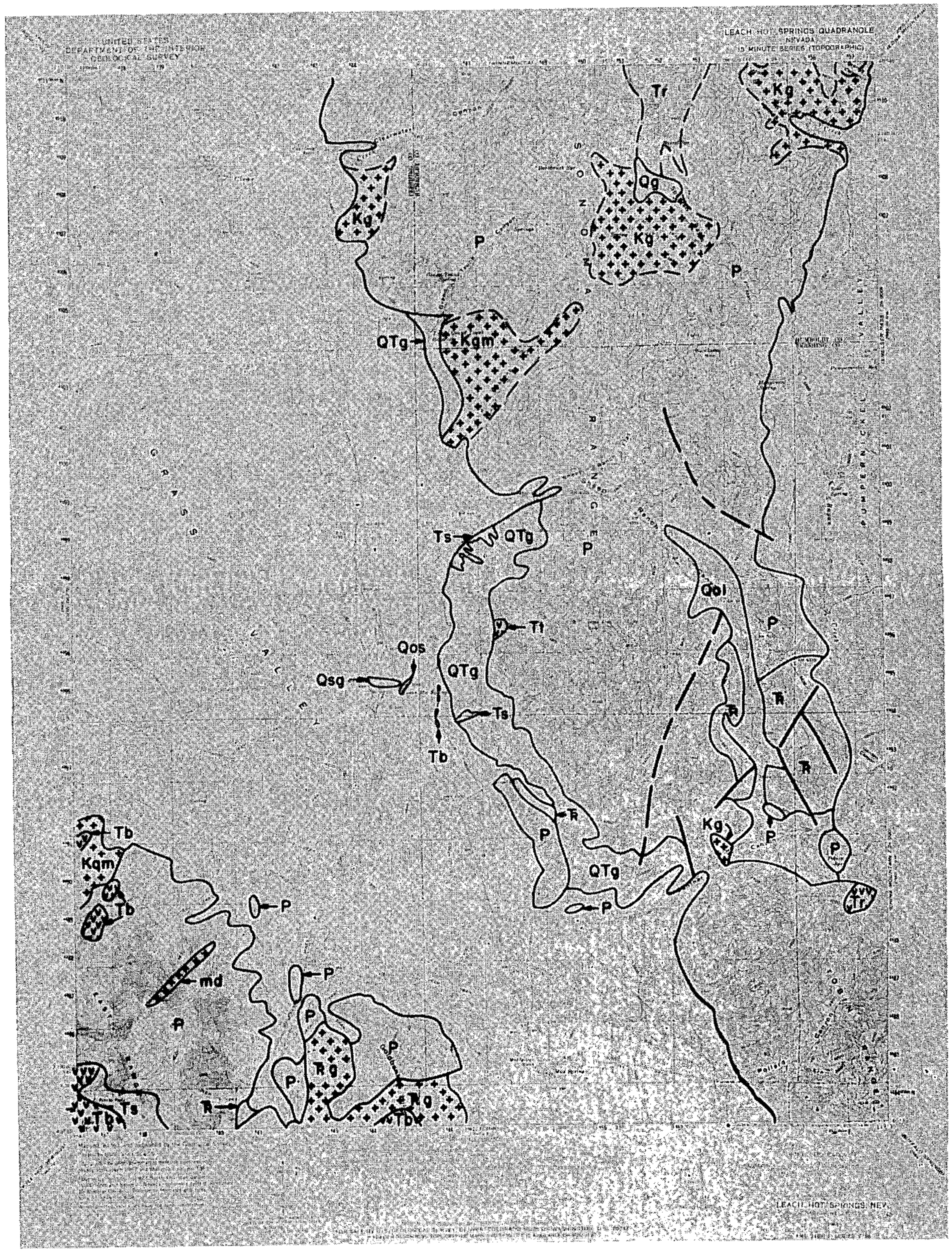

CBB 751-49

Figure 3.3

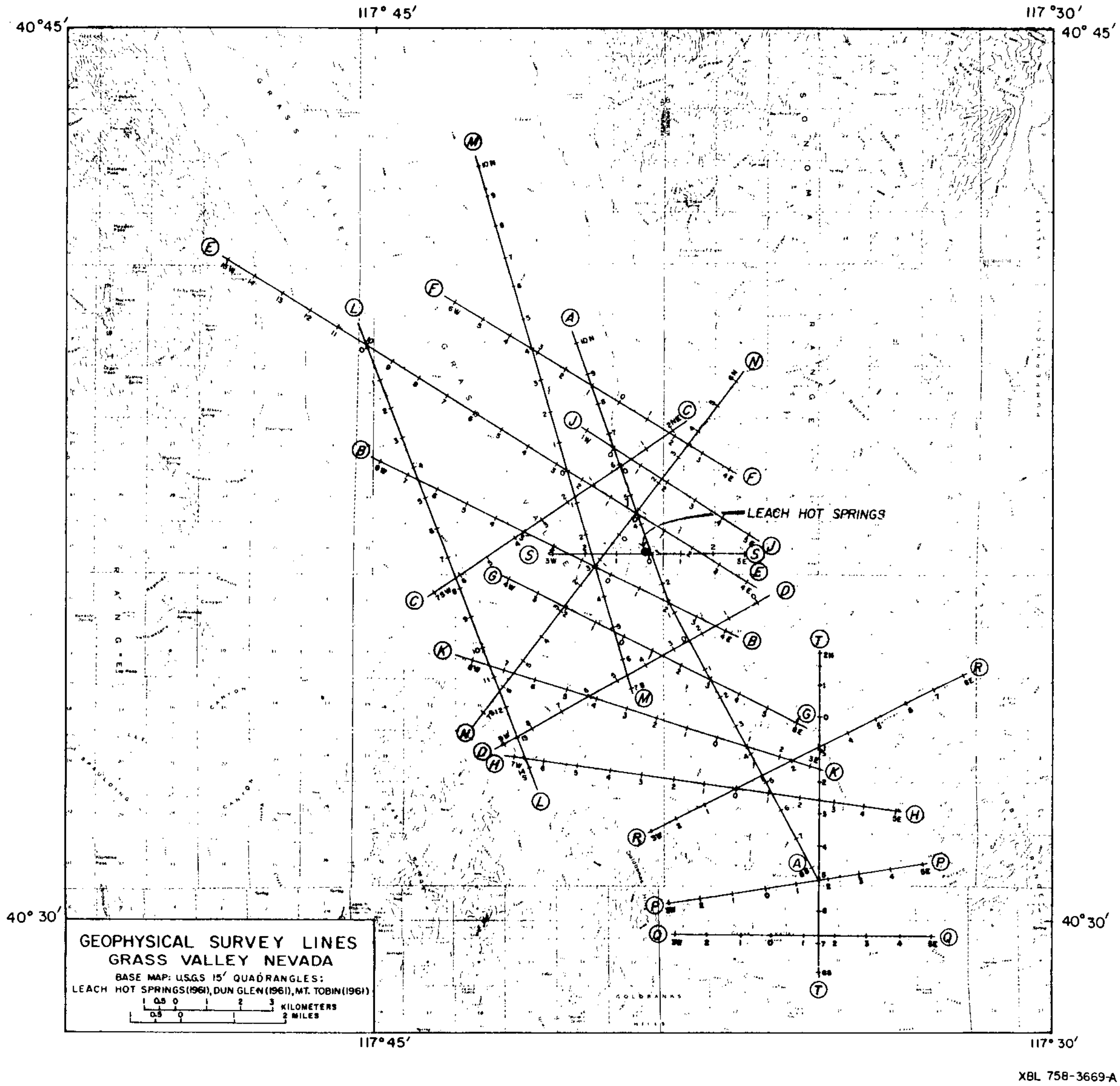
117° 45'
117° 30'
40° 45'
40° 30'
LEACH HOT SPRINGS
GEOPHYSICAL SURVEY LINES
GRASS VALLEY NEVADA
BASE MAP: U.S.G.S 15' QUADRANGLES:
LEACH HOT SPRINGS(1961), DUN GLEN(1961), MT. TOBIN(1961)
KILOMETERS
MILES
XBL 758-3669-A

Figure 3.4

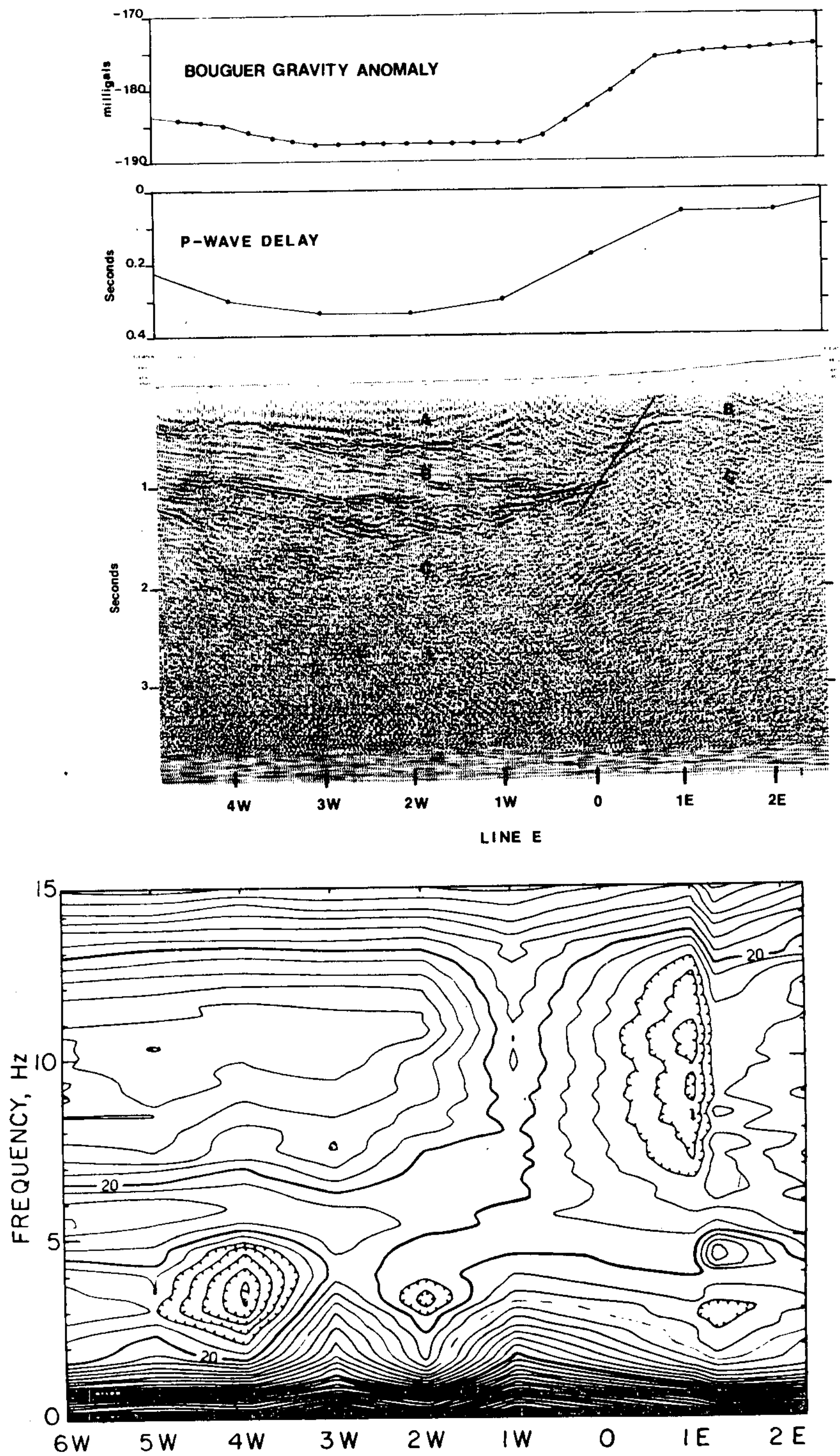

XBL 777-9469A

Figure 3.5

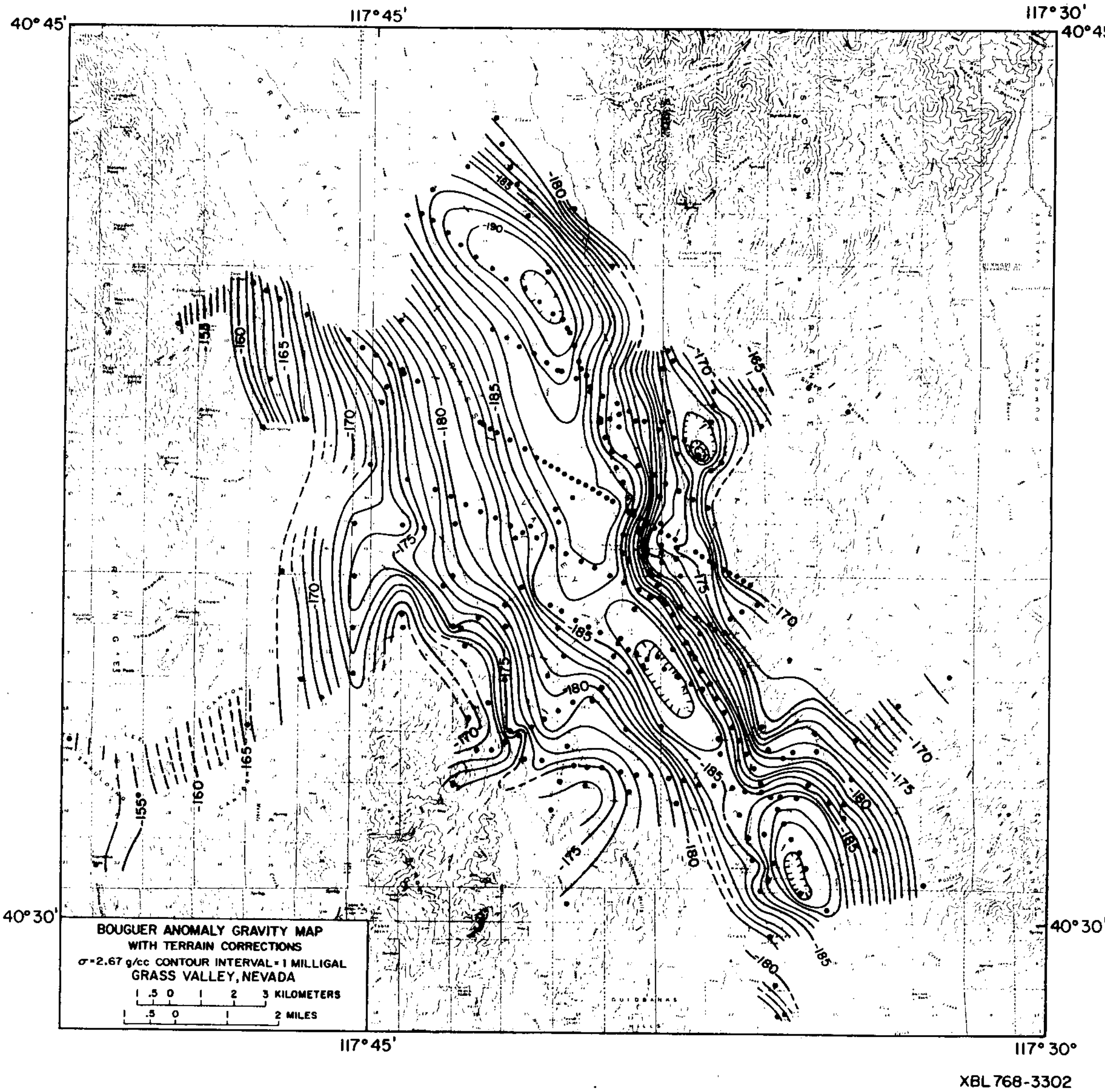
40° 45'
117° 45'
117° 30'
40° 45'
40° 30'
40° 30'
117° 45'
117° 30°
BOUGUER ANOMALY GRAVITY MAP
WITH TERRAIN CORRECTIONS
σ=2.67 g/cc CONTOUR INTERVAL=1 MILLIGAL
GRASS VALLEY, NEVADA
3 KILOMETERS
2 MILES
XBL 768-3302

Figure 3.6

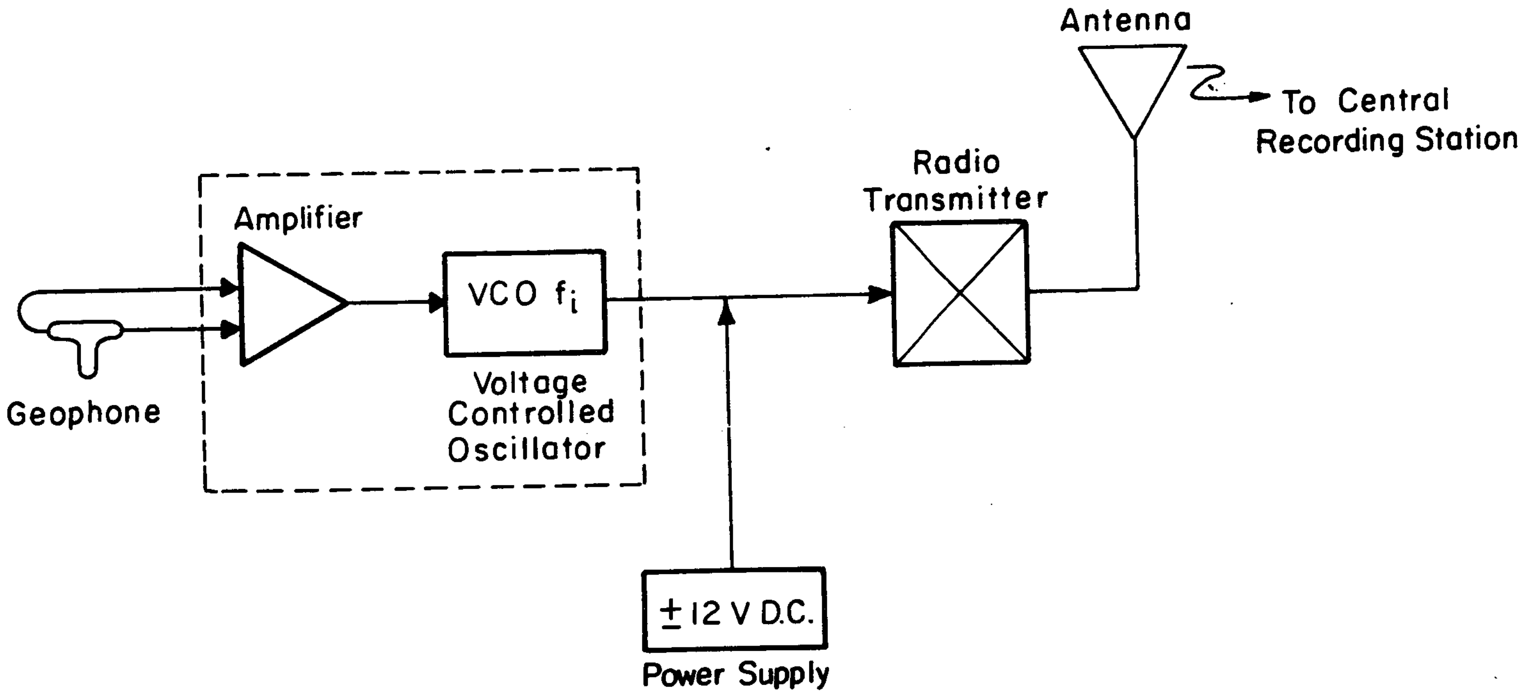

Figure 3.7

XBL 778-5997

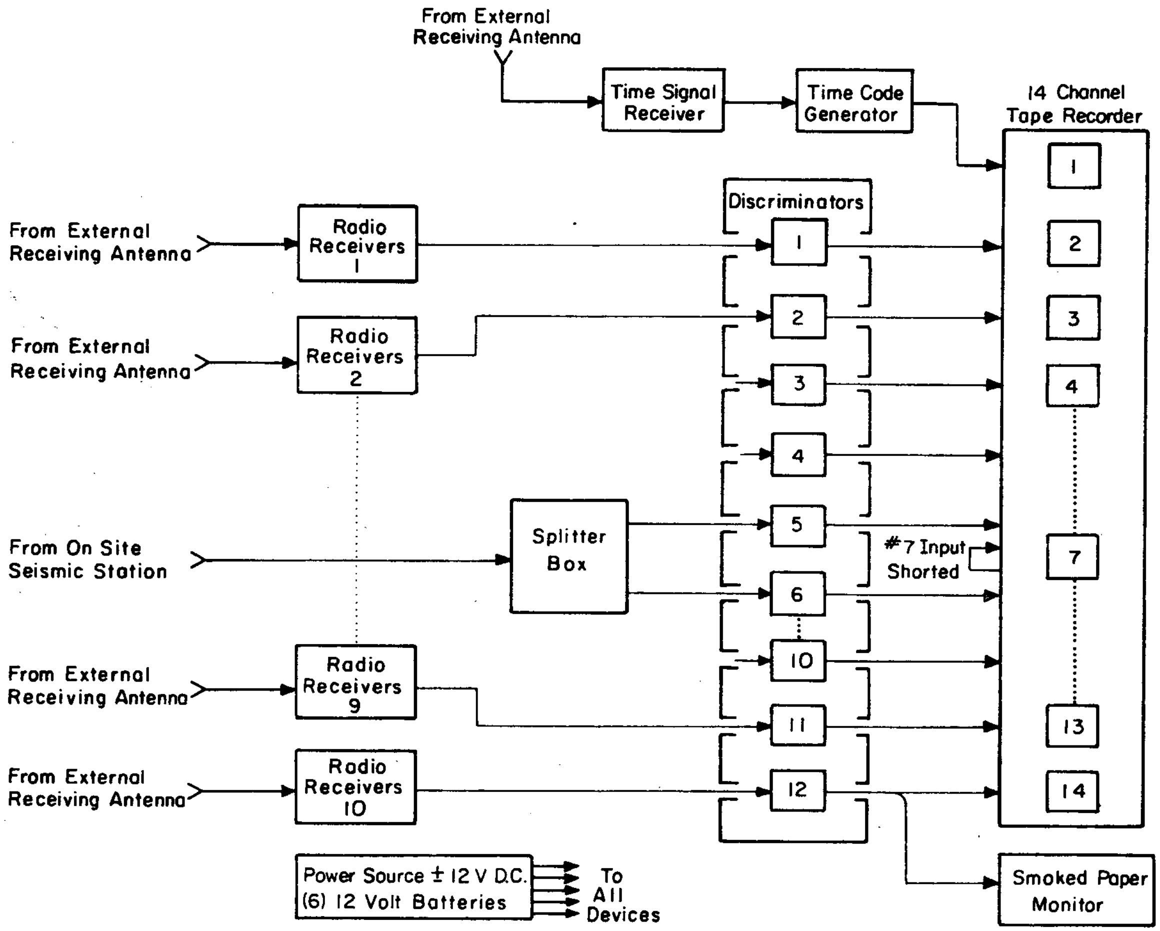

XBL778-5996

Figure 3.8

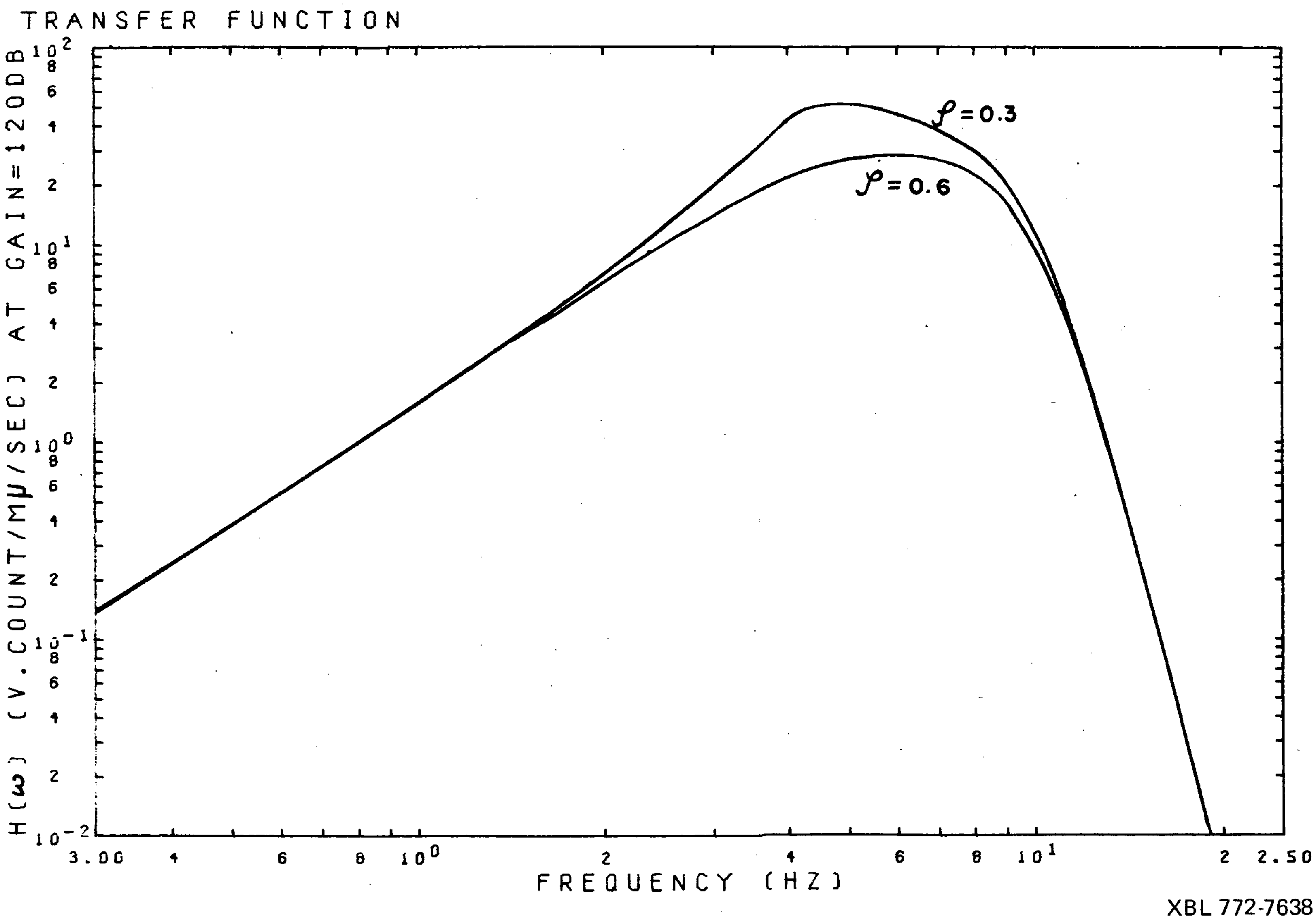
TRANSFER FUNCTION
H(ω) (V.COUNT/Mμ/SEC) AT GAIN=120DB
ρ=0.3
ρ=0.6
FREQUENCY (HZ)
XBL 772-7638

Figure 3.9

IV. AMPLITUDE VARIATIONS OF GROUND NOISE

4.1 Introduction

The mapping of ground noise amplitude in selected frequency bands has often been used to locate presumed noise sources in geothermal areas. Such surveys, however, rarely give repeatable or easily interpretable results. We have investigated this exploration technique in Grass Valley by first establishing the general characteristics of the microseismic field, and then using this knowledge to design and execute an appropriate survey for more quantitative measurements. In this chapter, the field procedures, data processing techniques, and the observed temporal and spatial variations of seismic noise in Grass Valley are discussed. Weaknesses of the amplitude mapping technique in delineating buried noise sources are revealed in the discussion. In the final section of this chapter, the characteristic site-responses along line E and line G are compared for seismic noise and for waves from mine explosions. This comparison illustrates the amplification effects by the valley alluvium with respect to bedrock sites for shallow surface waves and for body waves.

4.2 Field Procedures

To study the spatial variations of ground noise amplitude, we occupied a reference site at E2W (see Figure 3.2) throughout the survey period. Normally, we recorded overnight, with stations spaced at 1 km intervals along the survey lines. The smoked-paper monitor record was checked every morning to verify the occurrence of low seismic noise level at the reference site; otherwise, the sites were re-occupied another night, until low-noise conditions prevailed. Geophones were buried about one foot below the surface. Before and after a survey, all geophones were buried in a common hole to verify uniformity of their responses.

4.3 Data processing techniques: frequency spectrum estimation

It is well known that a stationary random process can be characterized by means of a power spectral density function. This function provides information on the power as a function of frequency for the process. For random processes, there are two power spectral density estimating techniques widely used, the autocorrelation method and the modified periodogram method.

4.3.1 Autocorrelation method

The power spectrum, $S_{nn}(f)$ of a function $\phi_n(t)$ is defined as the Fourier transform of its autocorrelation function, $C_{nn}(\tau)$. To estimate the power spectrum, we filter, pre-whiten and detrend the time series, and then calculate the unbiased autocorrelation function for the ith data window of length L samples by the discrete formula,

$$ {}^{i}C_{nn}(\tau) = \frac{1}{L-\tau} \sum_{\ell=0}^{L-1-\tau} {}^{i}\phi_n(\ell)\, {}^{i}\phi_n(\ell+\tau), \quad \begin{matrix} \tau=0,\ 1,\ .\ .\ .\ .\ ,\ J-1, \\ i=1,\ 2,\ .\ .\ .\ .\ ,\ I. \end{matrix} \tag{4.1} $$

The autocorrelation functions are averaged to give

$$ \hat{C}_{nn}(\tau) = \frac{1}{I} \sum_{i=1}^{I} {}^{i}C_{nn}(\tau), \quad \tau=0,\ 1,\ .\ .\ .\ .\ ,\ J-1. \tag{4.2} $$

We utilize the Fast Fourier transform to obtain the power spectral density estimate by:

$$\hat{S}_{nn}(f_R) = \sum_{\tau=0}^{J-1} w(\tau)\hat{C}_{nn}(\tau)\exp(-j2\pi f_R \tau), \tag{4.3}$$

where $f_R = \frac{R}{L}$ frequencies of discrete Fourier transform, $-\frac{1}{2},\ldots,0,\ldots,\frac{1}{2}$, and $w(\tau)$ is a data window function, or so-called lag window.

The autocorrelation method is a reasonable technique to estimate the smooth spectrum. However, problems may arise in obtaining the power spectral density from the autocorrelation function due to certain kinds of the data window $w(\tau)$. Unless the transform of the window is entirely positive, there is a possibility that the computed power spectral density may be negative, a highly undesirable result, if the spectrum has a sharp peak. This is because the computed power spectral density is the convolution of the window transform and the transform of the estimated correlation functions. Unless the transform of the window is positive for all frequencies, the possibility exists that, due to statistical variation in estimating the correlation function, the resulting convolutions may produce negative values for the power spectrum at some frequencies. There are windows whose transforms are entirely positive, e.g., the triangular window, etc., and such windows should be used in cases where other windows lead to the undesirable result.

4.3.2 Method of modified periodogram

The second and entirely equivalent estimation technique is based on the relation:

$$S_{nn}(f) = \lim_{T\to\infty} \frac{1}{2T} \left| \int_{-T}^{T} \phi(t)\exp(-j2\pi ft)dt \right|^2 . \tag{4.4}$$

For a finite duration of time series, Equation (4.4) can be approximated to be

$$^{i}S_{nn}(f) = \frac{1}{T}\left|\int_0^T {}^{i}\phi_n(t)\exp(-j2\pi ft)dt\right|^2. \tag{4.5}$$

The left hand side of Equation (4.5) results from the modulus-squared of the finite Fourier transform, which is called the periodogram. In terms of discrete time series, the periodogram can be expressed as

$$^{i}\Phi_n(f_R) = \sum_{\ell=0}^{L-1} w(\ell)\,^{i}\phi_n(\ell)\exp[-j2\pi\ell(\tfrac{R}{L})] \tag{4.6}$$

$$= \sum_{\ell=0}^{L-1} w(\ell)\,^{i}\phi_n(\ell)\exp[-j2\pi\ell f_R],\ R=-\tfrac{L}{2},\ldots,-1,0,1,\ldots,\tfrac{L}{2}, \tag{4.7}$$

where $w(\ell)$ is a data window whose purpose is to reduce the side-lobe amplitude hence reducing the effect of spectral leakage. The transform of Equation (4.7) is effected through the Fast Fourier transform algorithm, which requires the correction factor:

$$^{i}X_n(f) = 2(\Delta t)\,^{i}\Phi_n(f_R), \tag{4.8}$$

where Δt is the sampling interval of the discrete time series.

The disadvantage of the periodogram as an estimate of the power spectrum is that the variance of $^{i}\Phi_n(f_R)$ is approximately $S^2_{nn}(f)$, under conditions of reasonable regularity, even when based on a lengthy stretch of data (Brillinger, 1975). One way to reduce the variance of the estimate is to average several statistically independent periodograms according to

$$\hat{S}_{nn}(f) = \frac{1}{U}\frac{1}{I}\sum_{i=1}^{I}\left|^{i}X_n(f)\right|^2, \tag{4.9}$$

where I is the number of periodograms, and U is the energy in the data window, defined as

$$U = [\frac{1}{L} \sum_{\ell=0}^{L-1} w^2(\ell)]T. \tag{4.10}$$

where $T = \Delta t(L-1)$.

As L approaches infinity $\hat{S}_{nn}(f)$ approaches asymptotically $S(f)\chi_\nu^2/\nu$ if $2\pi f \equiv 0 \pmod{\pi}$, and asymptotically $S(f)\chi_\nu^2\ /(\nu/2)$ if $2\pi f = \pm\pi, \pm 3\pi, \ldots$ etc. (Brillinger, 1975), where χ_ν^2 is a chi-squared variate with ν degrees of freedom. The number of degress of freedom ν of the smoothed estimator is

$$\nu = 2 \cdot I \cdot b_1, \tag{4.11}$$

where b_1 is the standardized bandwidth of data window (Jenkins and Watts, 1968) given by

$$b_1 = \frac{L}{\sum_{\ell=0}^{L-1} w^2(\ell)} . \tag{4.12}$$

$b_1 = 1$ for rectangular data window. This leads to the 100γ percent confidence interval for S(f) to be:

$$\frac{\nu\hat{S}_{nn}(f)}{\chi_\nu^2(\frac{1+\gamma}{2})} < S(f) \quad \frac{\nu\hat{S}_{nn}(f)}{\chi_\nu^2(\frac{1-\gamma}{2})} \text{ for } 2\pi f \not\equiv 0 \pmod{\pi}, \tag{4.13}$$

where $\gamma = 0.9$ for 90% confidence limits. The velocity spectral density, VSD or $V_n(f)$, is obtained by taking the square root of the power spectral density and correcting it for system response $H_D(f)$ as follows:

$$V_n(f) = \frac{\sqrt{\hat{S}_{nn}(f)}}{|H_D(f)|} \text{ m sec}^{-1}\text{Hz}^{-1/2}, \tag{4.14}$$

where $H_D(f)$ is given in Equation(3.6). We normally present VSD in units of millimicrons (nanometers, 10^{-9}m)$\sec^{-1}$Hz$^{-1/2}$.

4.3.3 Grass Valley data processing method

Data were selected from the quietest recording period in the early morning hours. At least 28 simultaneous blocks of data were chosen from each of the recording stations, avoiding any spurious transient events. Each data block of length 12.8 seconds was filtered and digitized. The resulting 512-point records were tapered by a 10% cosine data window and Fourier transformed. The power spectral density function is estimated by the method of modified periodogram.

4.4 Temporal variation of ground noise

The total seismic noise amplitude $\sigma(x,y,t,f)$ can be modeled very generally as the sum of three sorts of noises,

$$\sigma(x,y,t,f) = \sigma_i(x,y,t,f) + \sigma_m(x,y,t,f) + \sigma_\ell(x,y,t,f), \qquad (4.15)$$

where

$\sigma_i(x,y,t,f)$ is the intrinsic noise at the site, including geothermal noise,

$\sigma_m(x,y,t,f)$ is the microseismic component from distant sources, and

$\sigma_\ell(x,y,t,f)$ is the noise generated locally at the surface by human activity and atmospheric distrubances.

If we are interested only in intrinsic noise, the sampling and processing procedures must exclude the effect of the other two noise sources. To minimize local sources, $\sigma_\ell(x,y,t,f)$, the data must be taken between midnight and dawn, because normally the noise level is low.

Figure 4.1 presents the diurnal variation of seismic noise at the reference site E2W. To construct this figure, transient-free noise data were chosen to estimate the VSD every hour for a 30 hour period. Roughly 6 minutes of seismic noise actually went into each hourly average. The spectral density was then contoured as a function of time and frequency. It can be seen that noise is high over the whole band of analysis from 9 A.M. to 7 P.M., the result of more disturbed daytime meteorological conditions and cultural activity. This confirms a well known result that seismic noise VSD is minimum at 2-4 A.M. local time, and this was the period we sampled for the best data.

We found, in Grass Valley, that the time of minimum ground noise at the reference site, E2W, coincides with the quietest period at all other sites in the region. For example, simultaneous data were sampled every hour from stations E2W and K1.5E, located approximately 11 km apart. The time-varying VSD over a 12 hour period from 9 P.M. to 9 A.M. next morning are presented in Figure 4.2. The figure indicates that at 2 A.M. the data are the quietest at both sides.

A typical survey is carried out over a period of several days, so that long term secular variations are apparent in the data. The nature of this variation over a 9 day period at the reference site, E2W, is shown in Figure 4.3. We estimate one VSD every 24 hours, using the quietest data during early morning hours, and contour the VSD from day 211 to day 219. In this figure, the high amplitude seismic noise appears from day 214 to day 216 and is related to regional weather conditions. On those three days, there were thunderstorms starting in the afternoon and ending in the early evening throughout the region.

In order to eliminate temporal variations of the observed microseisms, the band-limited power of seismic noise at each site, obtained by integrating VSD over the frequency band of interest, is normalized by the simultaneous power in the same frequency band at the reference site, provided that data are both sampled from the quiet period in early morning. Mapping the normalized power gives the spatial distribution of relative intrinsic noise power level.

4.5 Spatial variation of ground noise

Estimation of ground noise VSD from simultaneous sampling in the early morning, with stations at 1 km spacing, yields relative intrinsic noise power contour maps as illustrated for the frequency band of 2-4 Hz (Figure 4.4A), 5-7 Hz (Figure 4.4B) and 10-12 Hz (Figure 4.4C). High noise levels are found at Leach Hot Springs and near the center of Grass Valley, as anticipated, but there are also local anomalies such as in the areas around G2W and G3W, H1E and H2E (see Figure 3.2 for site locations). Those ground noise anomalies, especially in 5-7 Hz band, correlating spatially with the occurrence of Bouger gravity anomalies (Figure 3.6), imply the occurrence of thickest alluvial deposits. The long-term stability of these anomalies is reproducible as indicated by close agreement with the results of a preliminary survey carried out in the summer of 1975, a year earlier than the time at which data shown were taken.

Leach Hot Springs clearly generates seismic noise, but the noise is localized and does not propagate unattenuated more than a few km. In the vicinity of the springs, noise spectra show the high amplitude seismic noise over a wide frequency band; 500 meters northwest of the hot springs (A3.7N) the amplitude of the noise at all frequencies greater than 1 Hz has attenuated nearly 20 dB. The spectrum of the hot springs noise can be seen in Figure 4.5 (top) which compares the hot springs site with A3.7N and the valley edge site, AC. Note the wide-band nature of the hot springs noise.

In the valley center, station E5W, the noise has a distinctive broad peak around 5.5 Hz, as can be seen at the bottom of Figure 4.5. The character of the broad valley peak varies from site to site, probably as a consequence of changes in near surface properties. In Figure 4.4B, the areas of high amplitude seismic noise in 5-7 Hz band generally correspond to the areas of thick alluvium. The details of noise variation across the valley are illustrated by data for three typical survey lines, E, B, and G, shown in Figures 4.6, 4.7, and 4.8.

The instantaneous ground noise level along 8.25 km of line E is presented in Figure 4.6 for three different times of recording. Data were taken simultaneously from sites at E6W, 5W, 4W, 3W, 2W, 1W, 1E, 1.25E, and 2.25E. In this figure there is a clear peak at 5.5 Hz extending westward. The source of this well-defined and band-limited peak is not clearly understood, though it is doubtless related to near-surface properties. (We know it is a surface wave with a wave-length of about 50m). A wide-band ridge of relatively large amplitude noise appears at E3W, and is frequently seen to extend to 1W. Maximum valley fill and lowest topography occurs around 2W. A remarkable feature seen in the figure is the dramatic 10 dB contrast between points 1E and 1.25E, spanning the Hot Springs fault. It seems the local noise field, generated by hot springs, is less attenuated east of the fault than west of it, probably due to high-Q surface rocks on the east being in faulted contact with alluvium west of the fault. This geological feature can be seen in the faults map (Figure 3.2) as well as in the Bouguer gravity anomaly, the P-wave delay profiles, and the seismic reflection section (Figure 3.5).

Asymmetrical ridges of wide-band noise with sharp gradients to the east are seen near 2W in line B (Figure 4.7) and near 1E in line G (Figure 4.8). These ridges in the noise contours, as was the case for line E, correspond in position to the location of the minimum Bouguer anomaly along each line and to the location of the thickest alluvium (Beyer, <u>et al</u>., 1976). The positions of high gradients in ground noise east of the noise ridges on lines B and G apparently correlate with locations of shallow faults. The prominent broad peak of 6.5 to 7 Hz, seen at G3W in Figure 4.8 and C2.5W and C4.5W in Figure 4.9, are probably also related to properties of shallow alluvium.

At the south end of Grass Valley, the ground noise level is generally lower than at the north, and this contrast is presumably due to larger distance from the hot springs and thinner alluvial deposits to the south. The noise profiles along those survey lines in the southern part of the valley, e.g. line H (Figure 4.10), line K (Figure 4.11) and line R (Figure 4.12), do not show high gradients. The close similarity in the noise profiles along lines H,K is not surprising since the shallow geology is similar along the lines. The consistent anomaly appearing in the vicinity of H2E, K1.5E and R1E in the frequency band of 3 to 6 Hz may result from the localized occurrence of thick alluvium.

We see strong evidence, then, that the conventional ground noise survey reveals anomalies due not only to radiating sources, but also to variation in shallow geological structure, even after diurnal and secular variations are carefully eliminated. The noise power mapping technique cannot discriminate between the anomaly due to a buried seismic source and that associated with alluvial response. The method does provide an alternate way to map shallow geology and to detect lateral variations of near-surface structure.

4.6 Site-response characteristics

We conclude from the previous section that the spatial distribution of microseismic amplitude in a particular frequency band is strongly affected by the properties of near-surface material. The VSD of a bedrock site, away from active sources, always shows a smooth spectrum with no dominant peaks, whereas the VSD at an alluvium site always shows a well-defined peak in the spectrum. The spectral peak doubtless results from frequency-selective amplification related to the propagation characteristics of surface waves in the section of alluvium. Similar site-responses have been reported by Kanai and Tanaka (1961) and Katz (1976). Kanai and Tanaka (1961) suggested that at a given site the microtremor response correlates with the period distribution curve of local earthquakes. In Japan, microtremor recording is used extensively to determine the predominant frequency associated with various subsoil structures (Kanai, et al., 1966). The results of such measurement have been used to determine "foundation coefficients" in earthquake-resistant construction. In a similar study in the San Francisco Bay area, Borcherdt (1970) compared the microseism-derived site-responses with the spectral amplification factors derived from nuclear explosion data. Borcherdt observed that the spectral peaks of the horizontal component of the microseisms agree with those of the nuclear explosion data, but that the predominant frequencies of horizontal microseisms do not always coincide with those of the vertical component. In contrast to the above authors, Udwadia and Trifunac (1973) found no correlation between the spectra of microtremors and the ground's response to earthquakes recorded in El Centro, California.

In Grass Valley, we have investigated the correlation between earth noise spectra and seismic event spectra using signals generated by mine blasts at the Duval Mine, some 50 km to the east. Vertical-component data were recorded simultaneously along survey lines. The VSD of the explosion arrival at each site is estimated from a data block of 6.4 sec (256 data points) and averaged over 5 adjacent frequency components. The explosion arrivals along line E are presented in Figure 4.13. The corresponding background noise data taken a few minutes before the explosion arrivals are shown in Figure 4.14. The analog records of the explosion do not show significant differences in amplitude and frequency characteristics over the line, while the background noise in the valley sites (E2W, E3W, E4W, E5W, and EbW) is apparently different from that in hill sites (E2, 25E, E1, 25E, E1E, E1W). The spectra of explosion arrivals and background noise, presented in Figure 4.15, show little similarity. We removed the source characteristics of mine blast arrivals by normalizing the VSD at each recording site, using the VSD of site E1E as a reference. The identical normalization was applied to the VSD of background noise. The normalized results along line E are shown in Figure 4.16, where the resonant effect of valley fill in the band around 5 Hz is clearly shown on the noise spectrum but not on the blast spectrum. There is very little similarity between variation in the mine blast arrival and variation in background noise. The similar data set along the survey line G also shows very little correlation between blast arrivals and noise (Figure 4.17).

FIGURE CAPTIONS

Figure 4.1 Diurnal variation of ground noise level at reference site E2W, from hour 10, day 212 to hour 16, day 213, in 1976. Noise levels are normalized with respect to 10^{-11} m/sec/$\sqrt{Hz}$, (OdB), and contour interval is 2 dB. Note the minimum noise level (hachured) between 2-4 A.M. for all frequencies greater than 2 Hz.

Figure 4.2 The simultaneous temporal variation of ground noise over a 12 hour period at sites E2W and K1.5E, approximately 11 km apart. Noise levels are normalized with respect to 10^{-11} m/sec/$\sqrt{Hz}$, (OdB), and contour interval is 5 dB. Note that the minimum noise level is coincident at both sites in the early morning.

Figure 4.3 Secular variation of early morning quiet ground noise level from day 211 to day 219 of 1976 at E2W with repsect to 10^{-11} m/sec/$\sqrt{Hz}$, (OdB). Contour interval is 2 dB. Thunderstorm and unsettled regional weather characterized days 214-216, the period of greatest early morning noise level.

Figure 4.4 The power contours of relative intrinsic noise with respect to reference site E2W in three frequency bands. Contour interval is 3 dB. Solid circles indicate sampling points. (A) 2-4 Hz, (B) 5-7 Hz, (C) 10-12 Hz.

Figure 4.5 Velocity spectral density (VSD) of ground noise at Hot Springs and at site A3.7N, 500 m NW of the hot springs (upper) and at E5W, at center of the valley (lower) compared to bedrock site AC, at the valley edge. The error bars for A3.7N and AC sites are 95% confidence limits for the estimated VSD. Data represent spectral averages over 32 data blocks of 12.8 sec length, for each site.

Figure 4.6 Instantaneous noise field along survey line E for three different quiet periods. Abscissa is station location, with 1 km spacing, and ordinate is frequency. Contour interval is 2 dB. Note the high wide-band noise level at 1W (A and B) and 3W (C), the region of thick alluvium, and also the consistently sharp gradient across the valley margin fault traced to 1E. Note also the typical valley resonant peak near 6 Hz to the west.

Figure 4.7 Instantaneous noise field along survey line B. Abscissa is station location, with 1 km spacing, and ordinate is frequency. Contour interval is 2 dB. Note the high wide-band noise level at the valley center near 2W.

Figure 4.8 Instantaneous noise field along survey line G. Abscissa is station location, with 1 km spacing, and ordinate is frequency. Contour interval is 2 dB. Note the high wide-band noise level at the valley center near 1E. Sharp gradients may indicate valley faults.

Figure 4.9 Instantaneous noise field along portion of survey line C. Abscissa is station location, with 1 km spacing, and ordinate is frequency. Contour interval is 2 dB. Note the band-limited peaks at both 2.5 W and 4.5 W, probably the result of alluvial resonant effects.

Figure 4.10 Instantaneous noise field along survey line H. Abscissa is station location, with 1 km spacing, and ordinate is frequency. Contour interval is 2 dB. Note the gentle increase in noise level toward the east reaching a peak at 2E, which may correspond to resonance of the alluvial layer.

Figure 4.11 Instantaneous noise field along survey line K. Abscissa is station location, with 1 km spacing, and ordinate is frequency. Contour interval is 2 dB. Note the gentle increase in noise level toward the east, reaching a high frequency ridge at 1W and a low frequency peak at 1.5E, which corresponds to local thick alluvial layer.

Figure 4.12 Instantaneous noise field along survey line R. Abscissa is station location, with 1 km spacing, and ordinate is frequency. Contour interval is 5 dB. Note the quiet nature of the noise field along the line, the low frequency peak at 1E corresponds to the same features at H1E, H2E and K1.5E.

Figure 4.13 Mine blast arrivals recorded at sites along survey line E. Note the early arrival at E1E, in the vicinity of Leach Hot Springs. The scale factor is 1230×10^{-9} m/sec per cm of the amplitude of displayed record at 4.5 Hz. The geophones of identical response were used.

Figure 4.14 Typical seismic noise data at sites along survey line E. The scale factor is 129×10^{-9} m/sec per cm of the amplitude of displayed record at 4.5 Hz. The geophones of identical response were used.

Figure 4.15 Velocity spectral densities (VSD) of the mine explosion event (upper curve) and the seismic noise (lower curve) at each recording site along line E. Abscissa is frequency and ordinate is VSD in 10^{-9} m/sec/$\sqrt{Hz}$. Scale is indicated in Frame H.

Figure 4.16 Relative VSD at sites along survey line E. VSD in Figure 4.15 are normalized with respect to site E1E. Solid curves are mine blast arrivals and the dotted curves are seismic noise.

Figure 4.17 Velocity spectral densities (VSD) of the mine explosion event (upper curve) and the seismic noise (lower curve) at each recording site along line G. Abscissa is frequency and ordinate is VSD in 10^{-9} m/sec/$\sqrt{Hz}$.

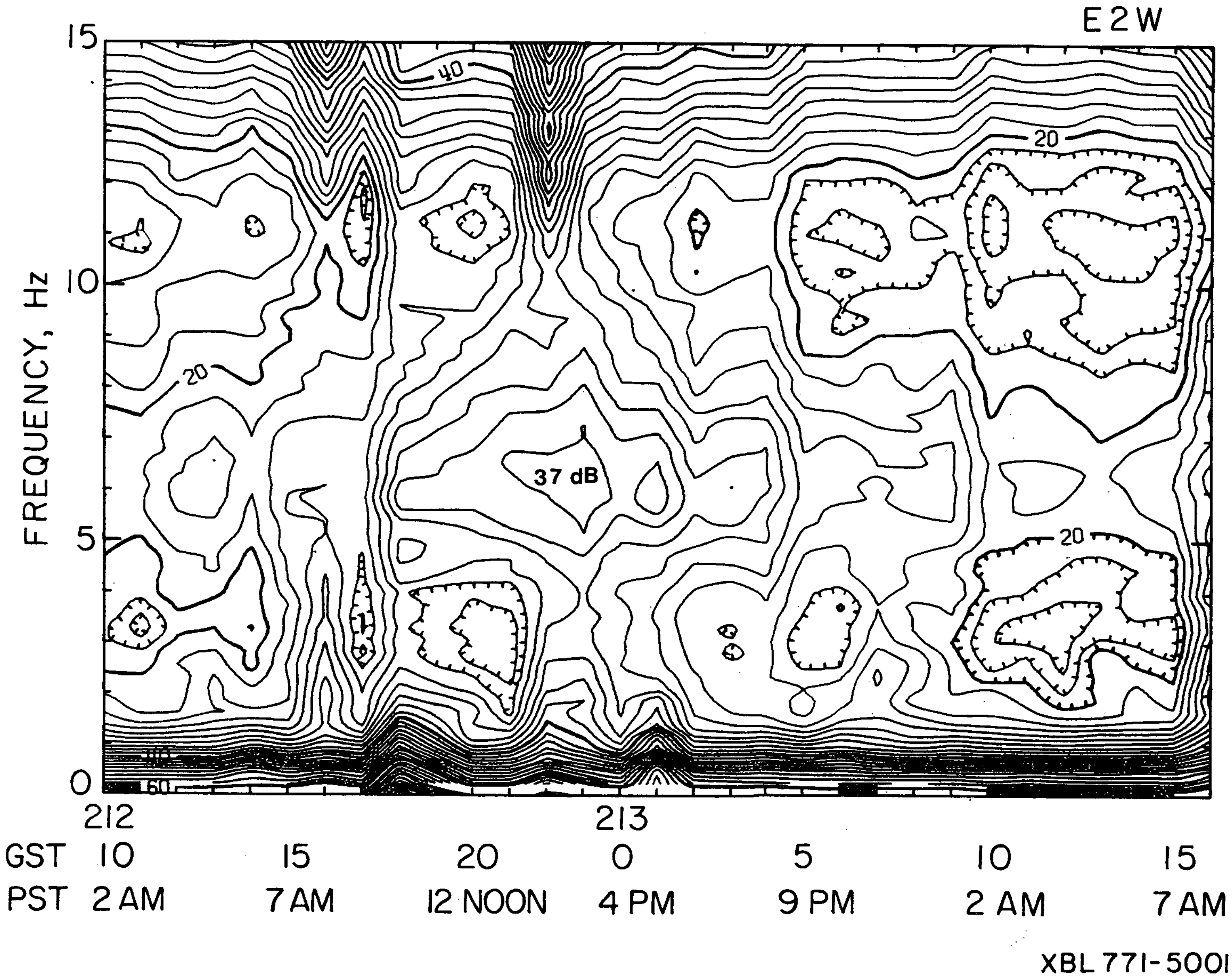
E2W
15
10
5
0
FREQUENCY, Hz
40
20
37 dB
20
20
40
60
212
213
GST 10 15 20 0 5 10 15
PST 2 AM 7 AM 12 NOON 4 PM 9 PM 2 AM 7 AM
XBL 771-5001

Figure 4.1

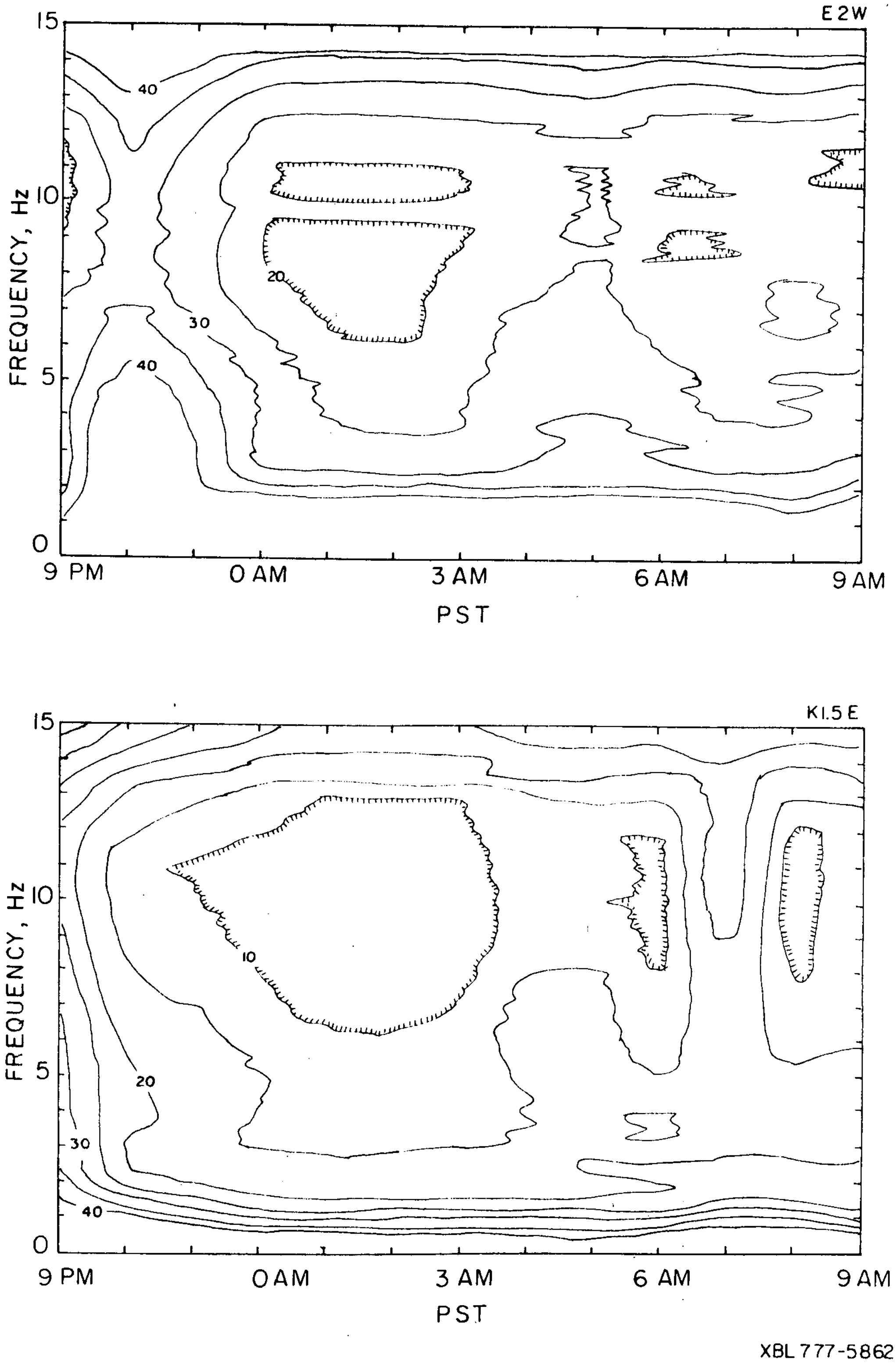
E2W
15
10
5
0
FREQUENCY, Hz
40
40
30
20
9 PM
0 AM
3 AM
6 AM
9 AM
PST
K1.5 E
15
10
5
0
FREQUENCY, Hz
10
20
30
40
9 PM
0 AM
3 AM
6 AM
9 AM
PST
XBL 777-5862

Figure 4.2

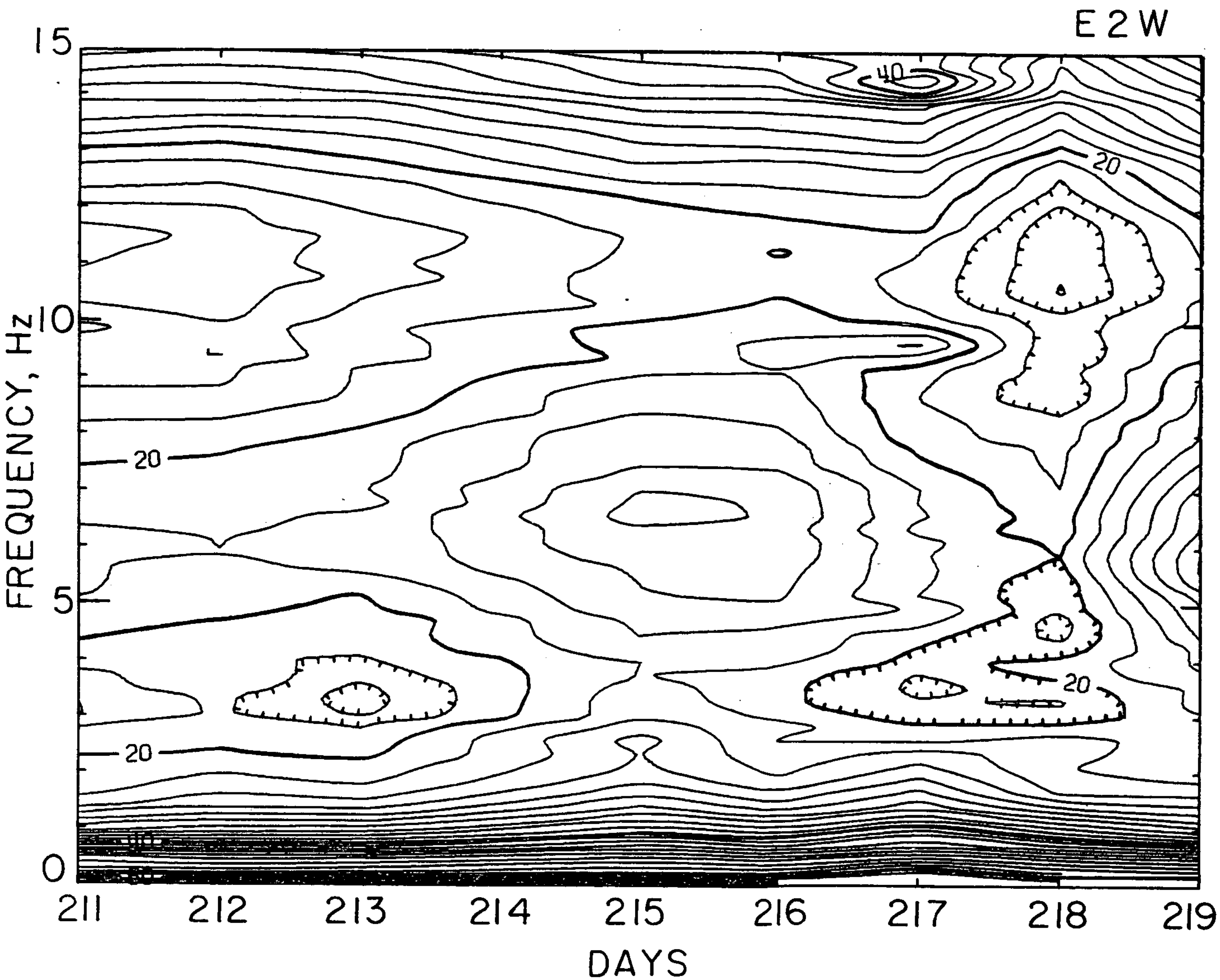

XBL771-5000

Figure 4.3

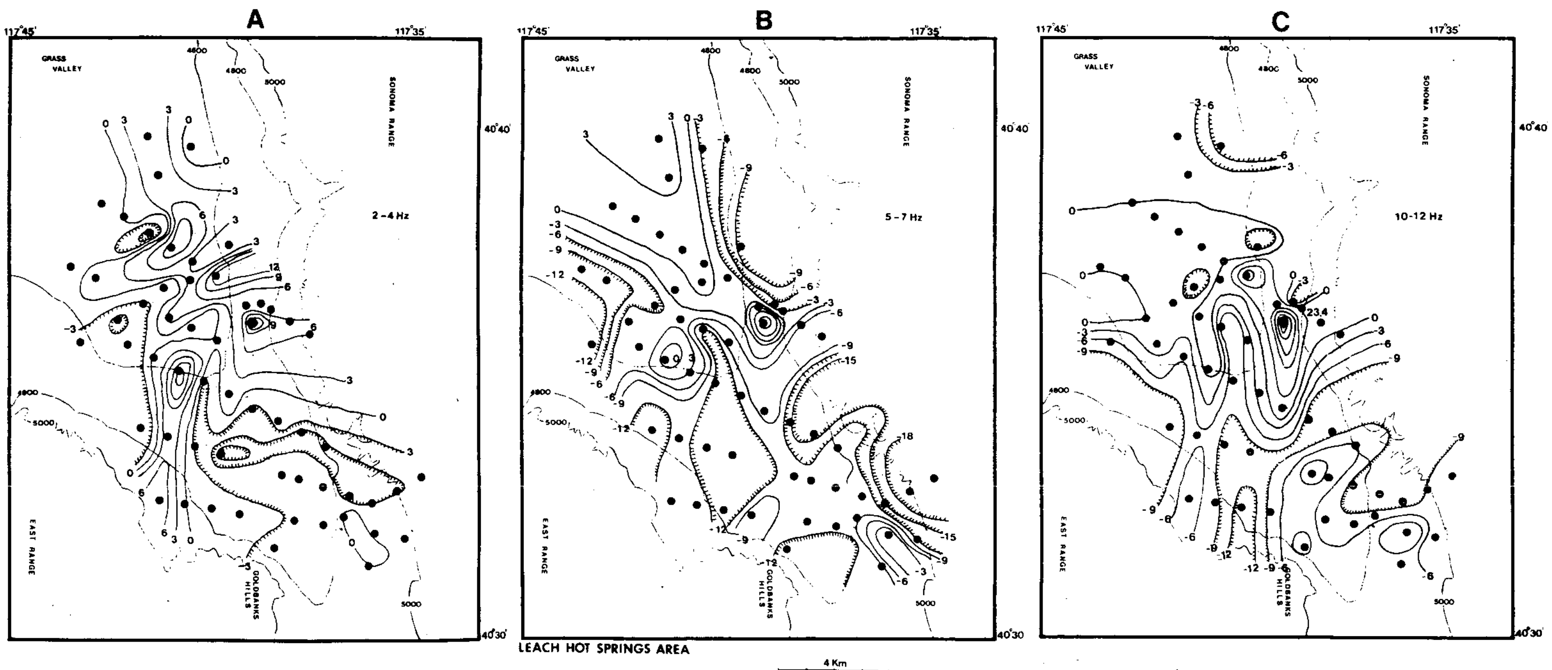
A
B
C
117°45'
117°35'
40°40'
40°30'
GRASS VALLEY
SONOMA RANGE
EAST RANGE
GOLDBANKS HILLS
2-4 Hz
5-7 Hz
10-12 Hz
LEACH HOT SPRINGS AREA
4 Km
XBL 776-9499

Figure 4.4

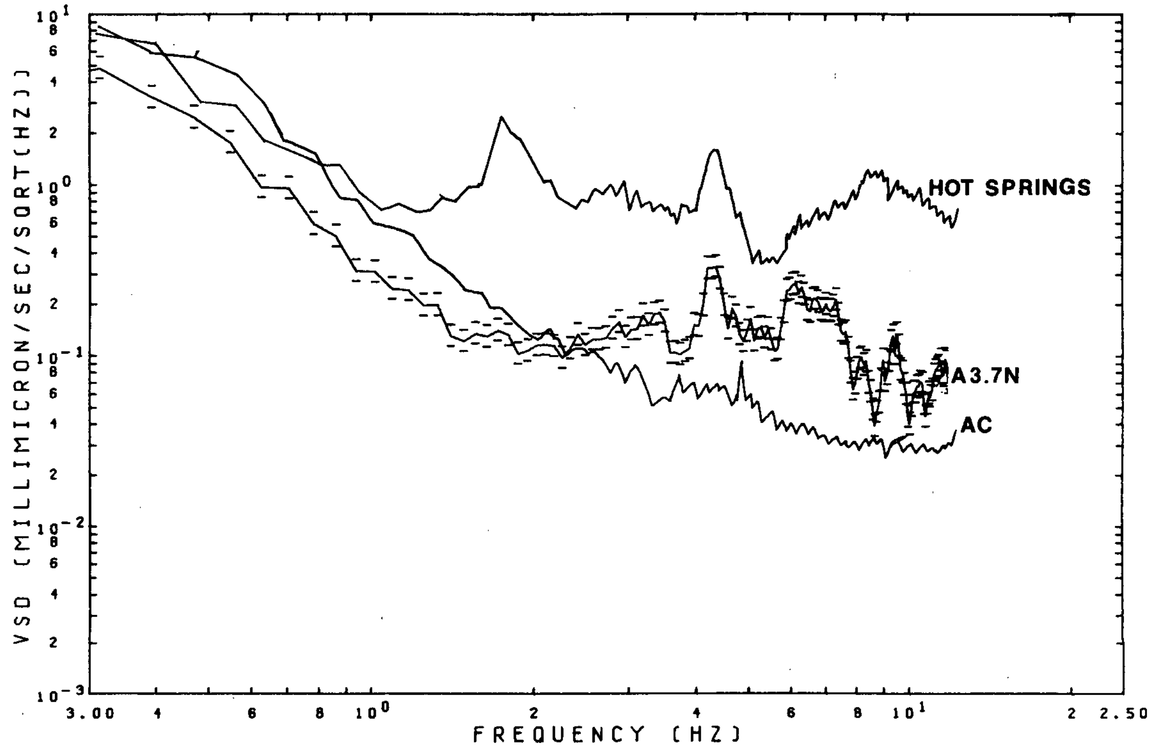

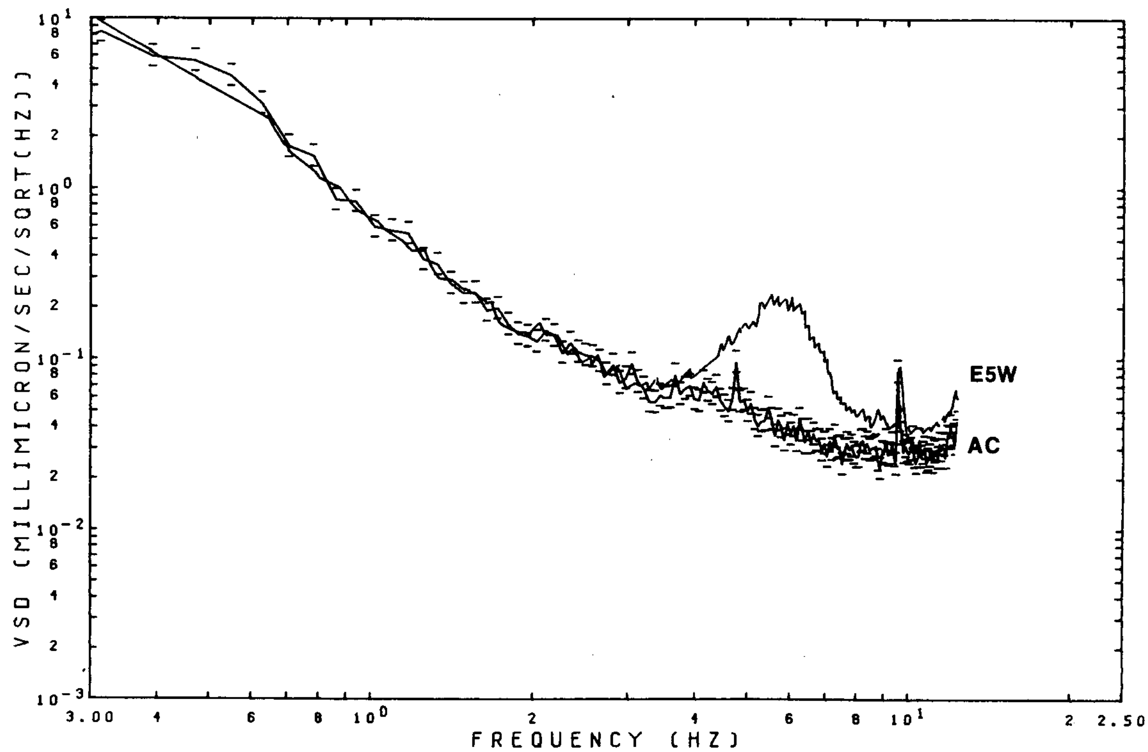

XBL 776-9466

Figure 4.5

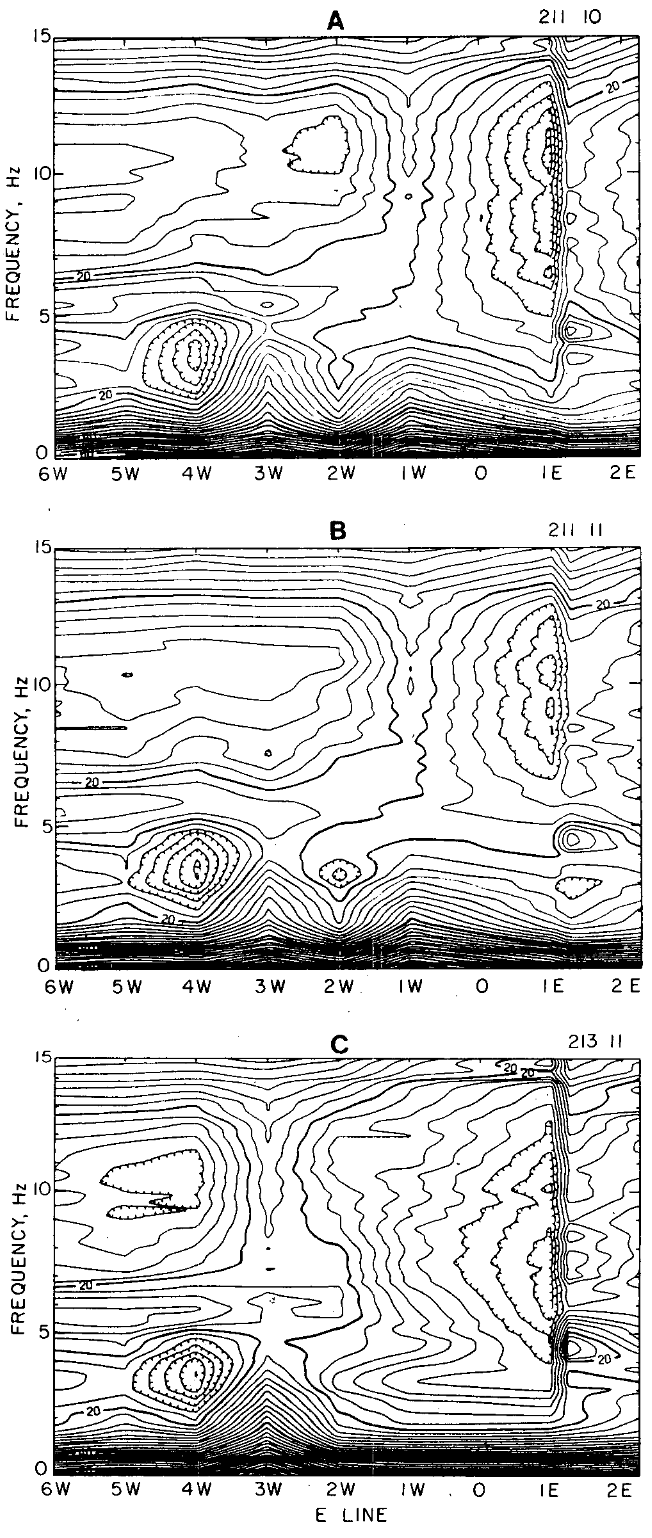
A
211 10
B
211 11
C
213 11
FREQUENCY, Hz
0
5
10
15
20
6W
5W
4W
3W
2W
1W
0
1E
2E
E LINE
XBL 771-4993A

Figure 4.6

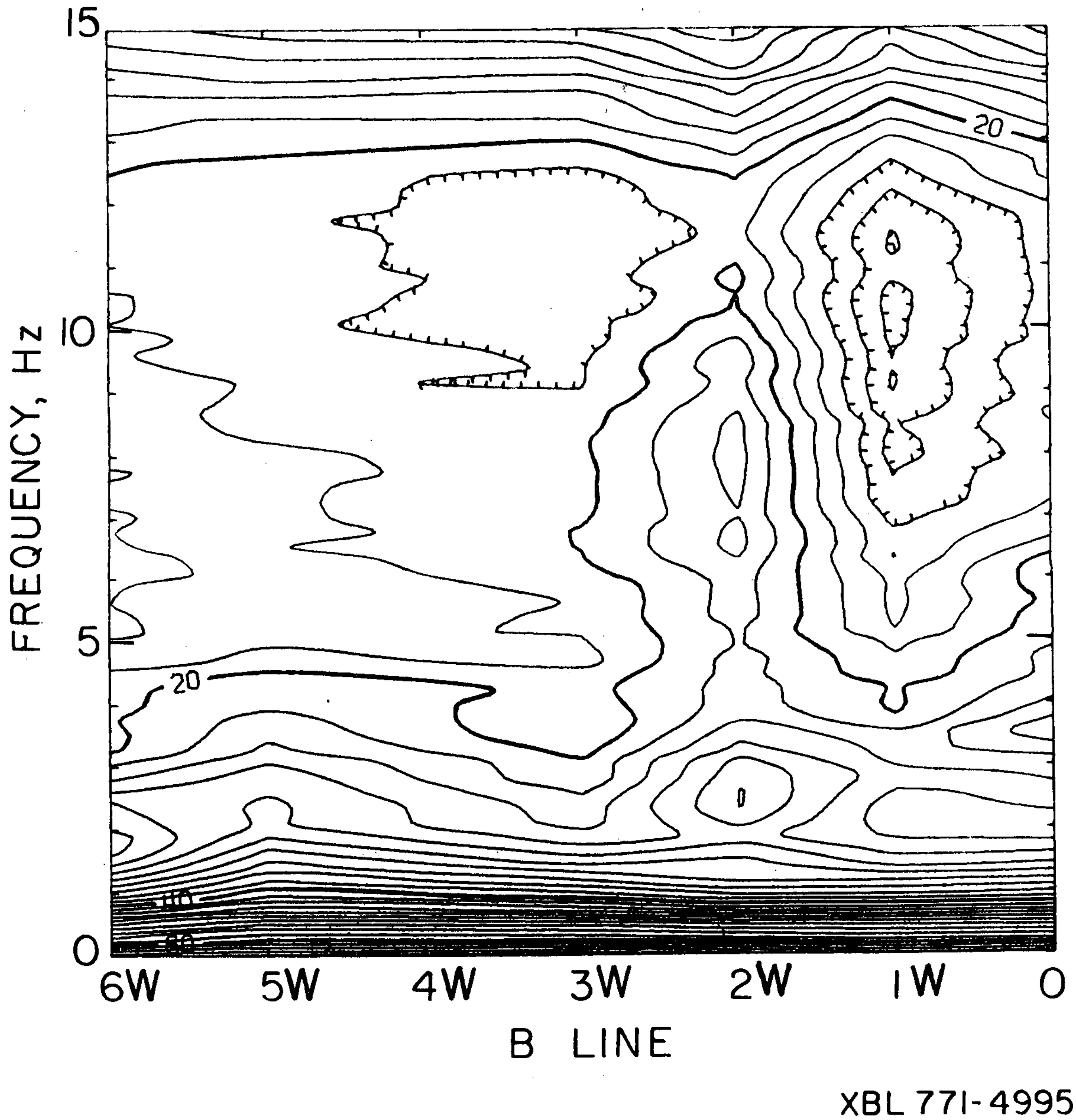

Figure 4.7

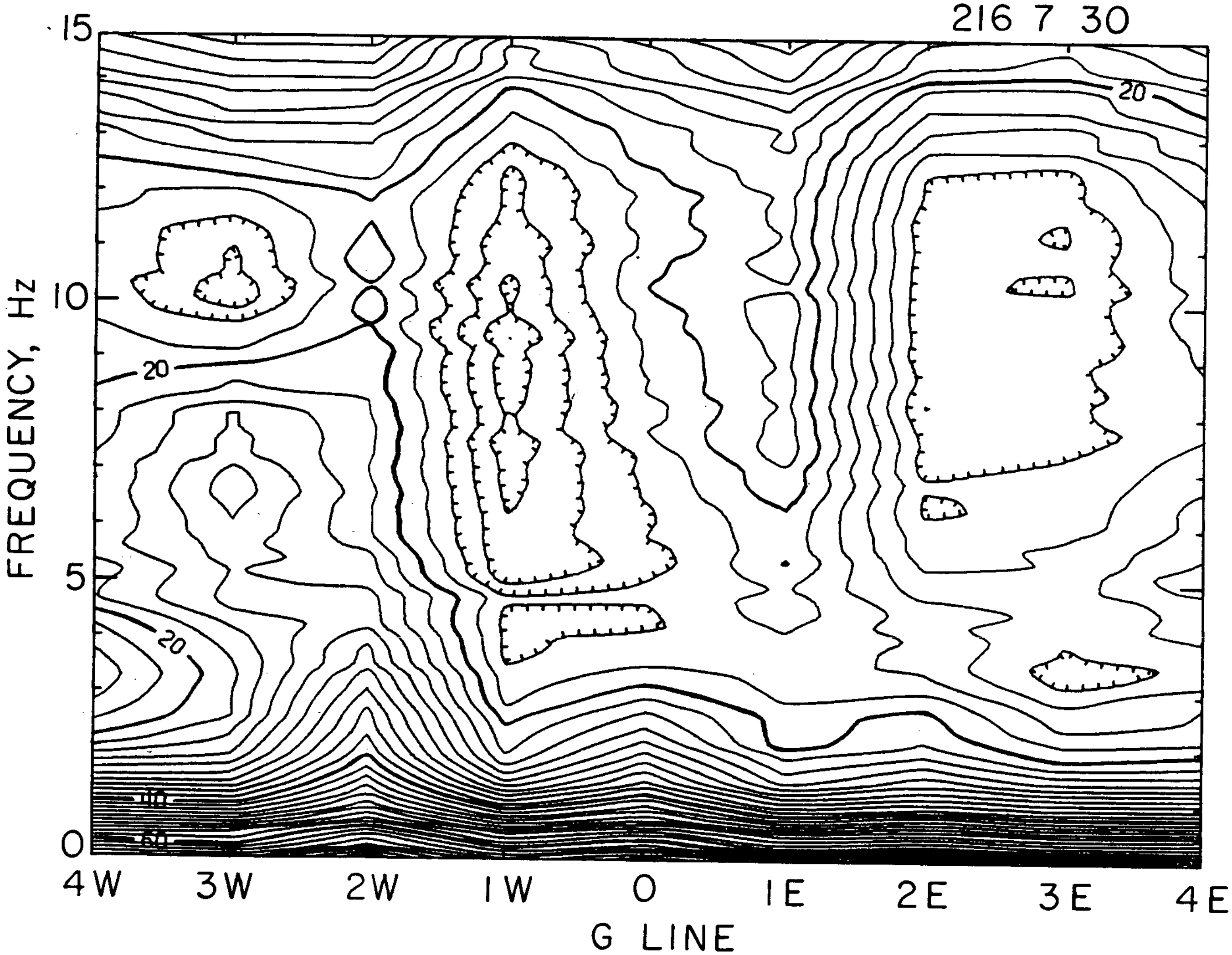

XBL 771-4997

Figure 4.8

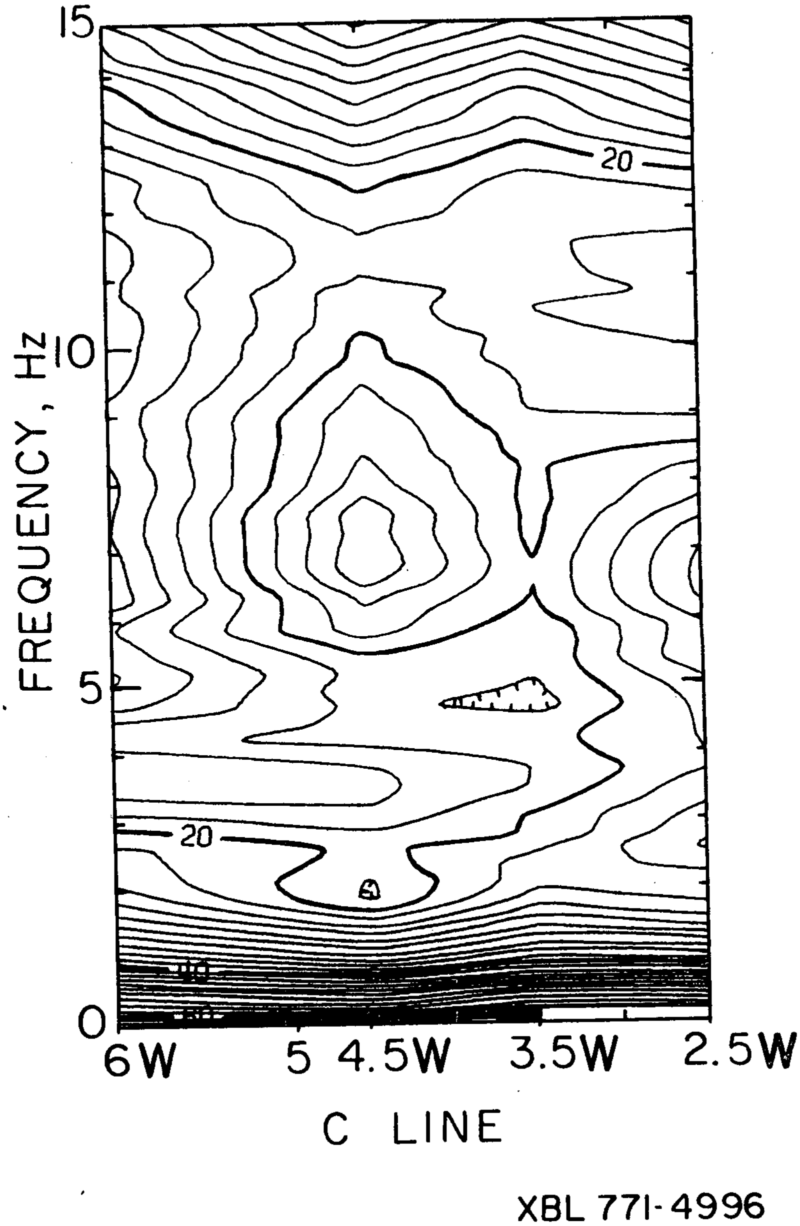

Figure 4.9

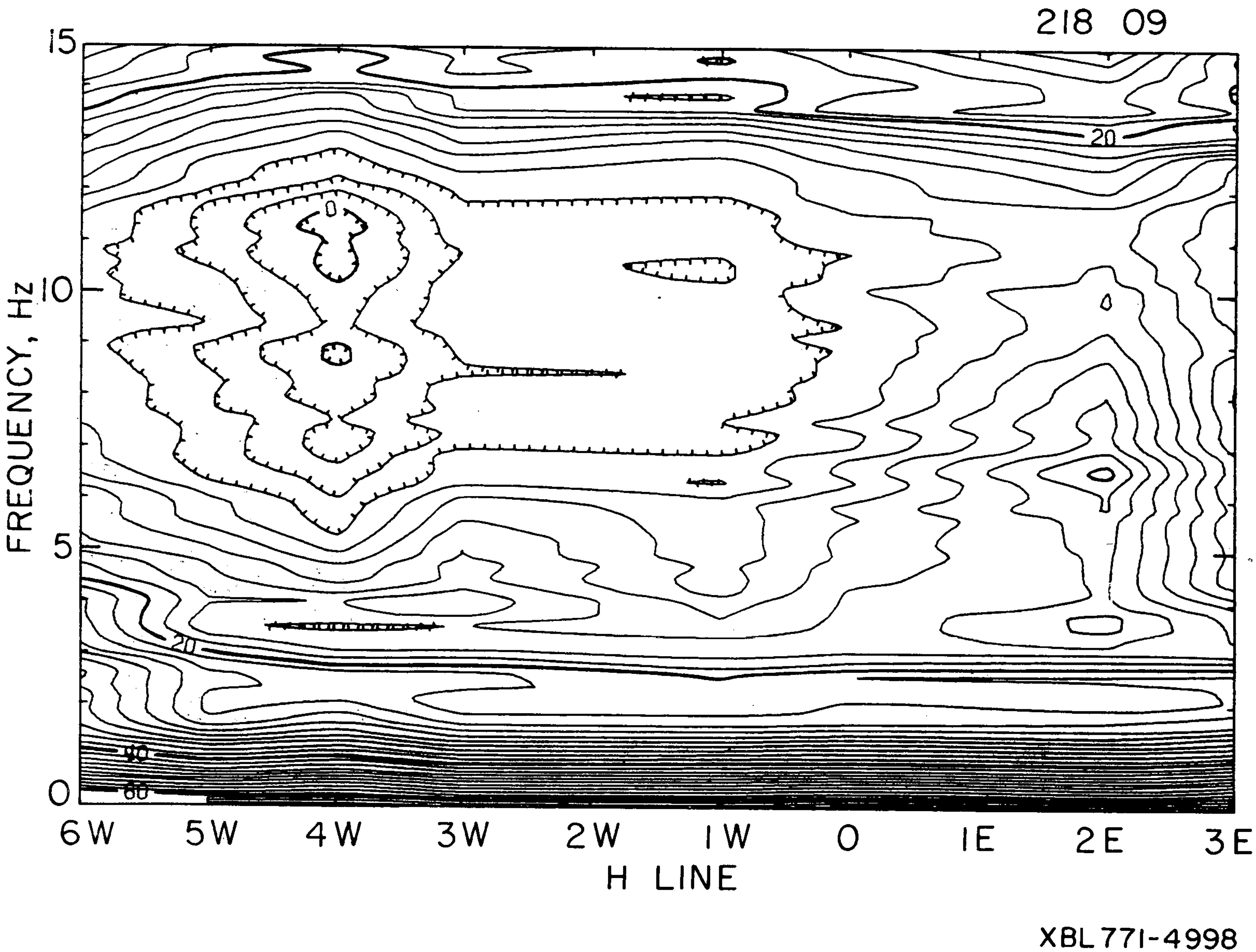
218 09
15
10
5
0
FREQUENCY, Hz
20
40
60
6W
5W
4W
3W
2W
1W
0
1E
2E
3E
H LINE
XBL 771-4998

Figure 4.10

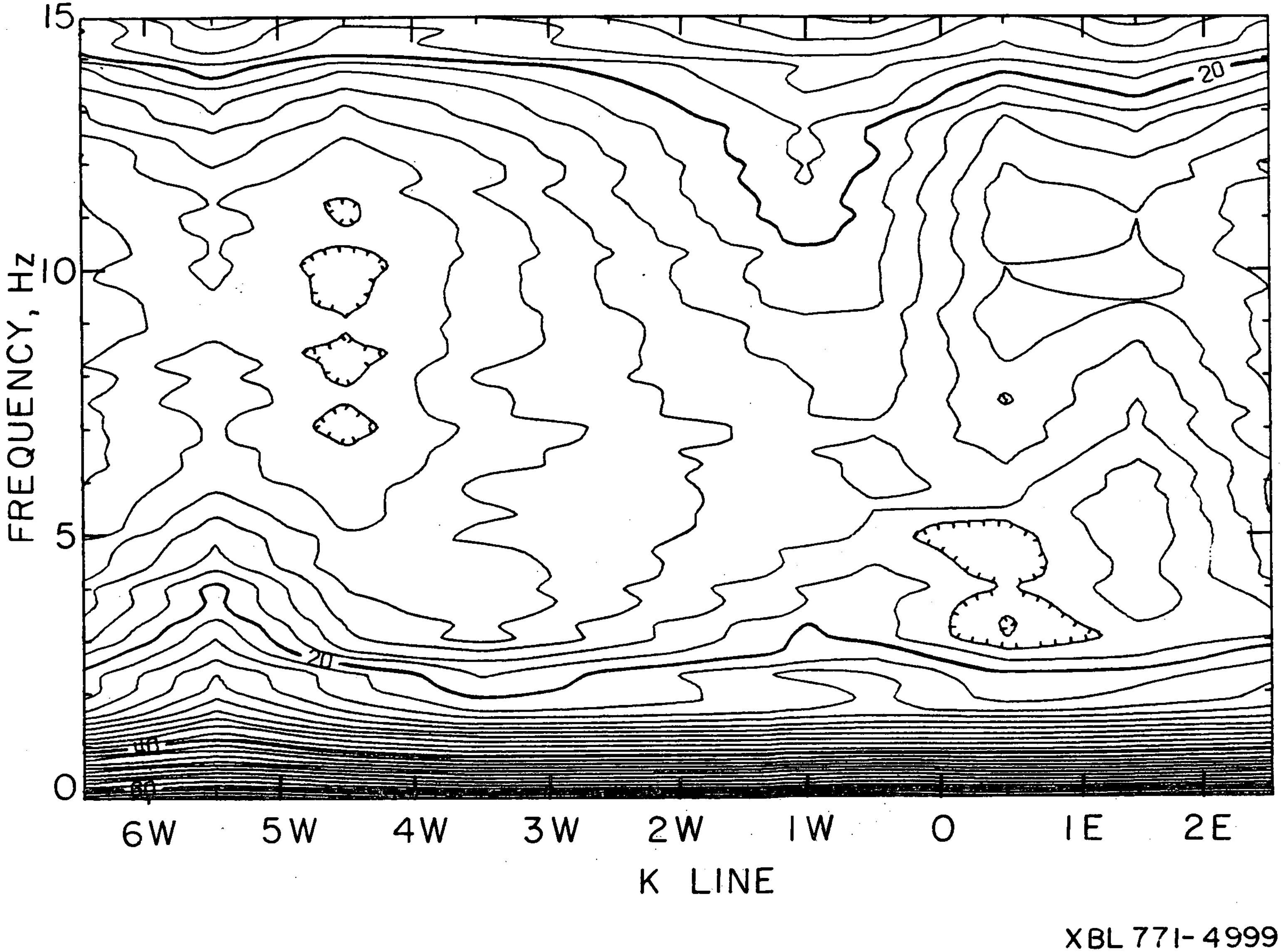
15
10
5
0
FREQUENCY, Hz
20
20
6W
5W
4W
3W
2W
1W
0
1E
2E
K LINE
XBL 771-4999

Figure 4.11

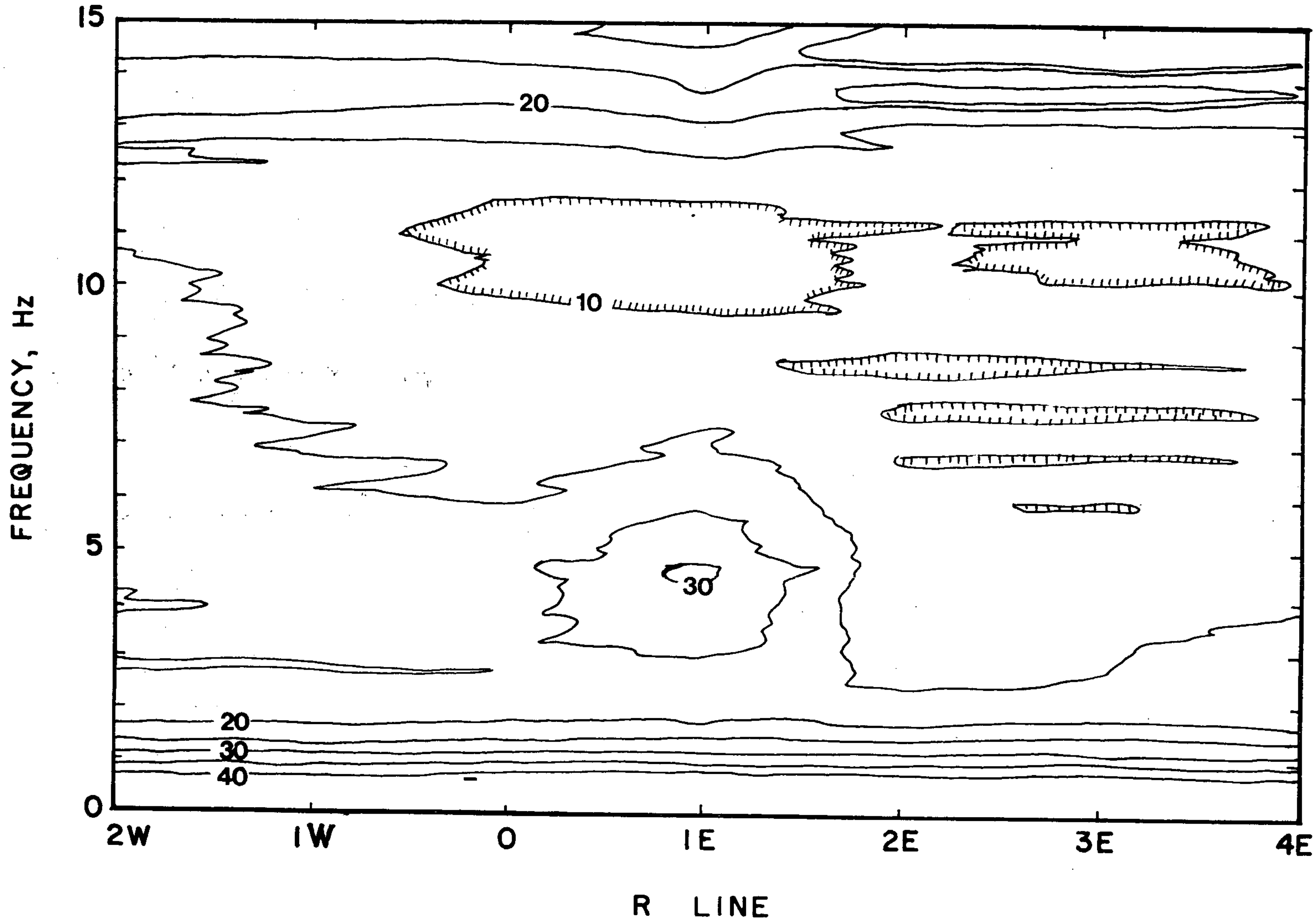

XBL 779-2472

Figure 4.12

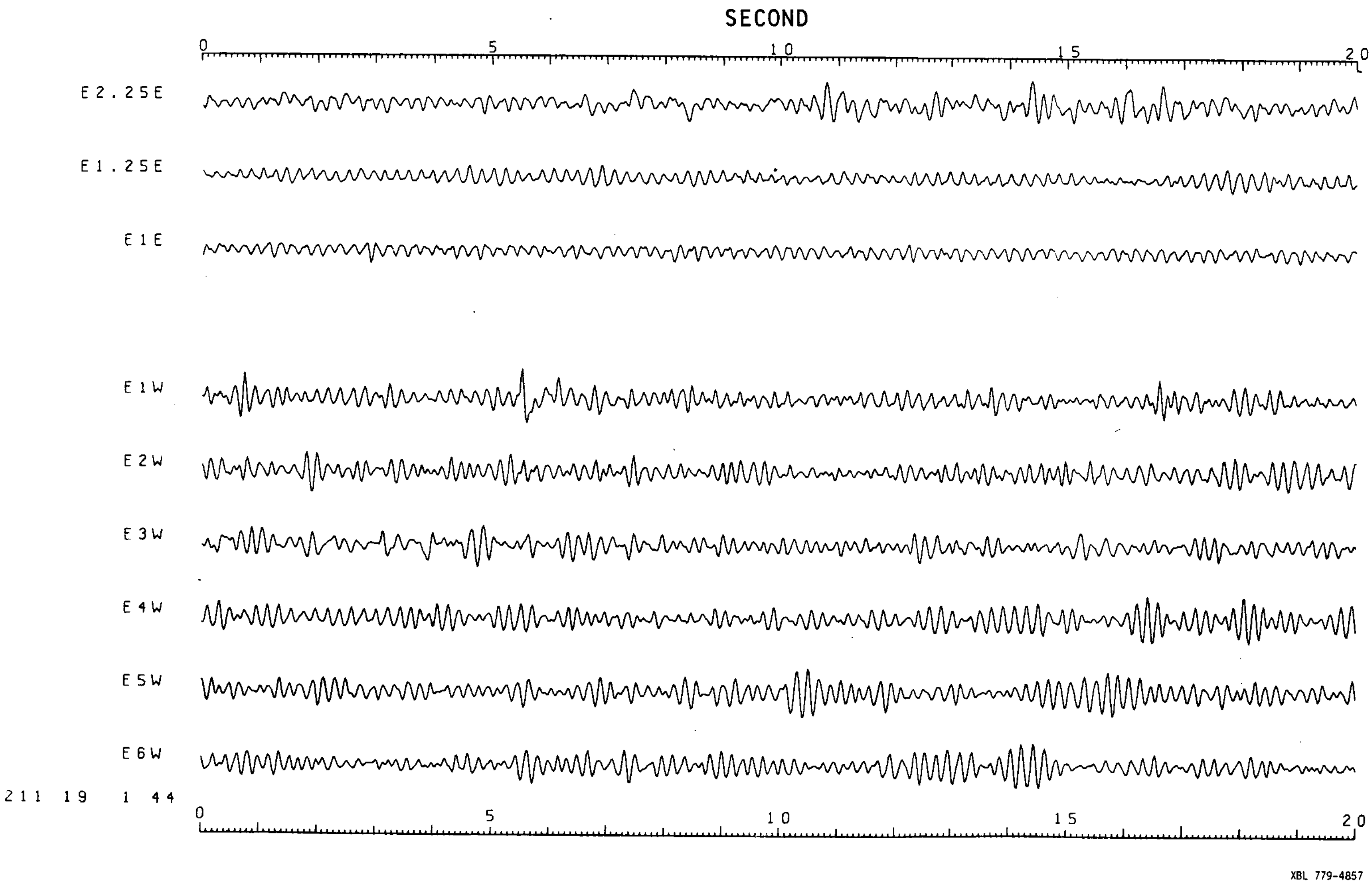
SECOND
0
5
10
15
20
E2.25E
E1.25E
E1E
E1W
E2W
E3W
E4W
E5W
E6W
211 19 1 44
XBL 779-4857

Figure 4.13

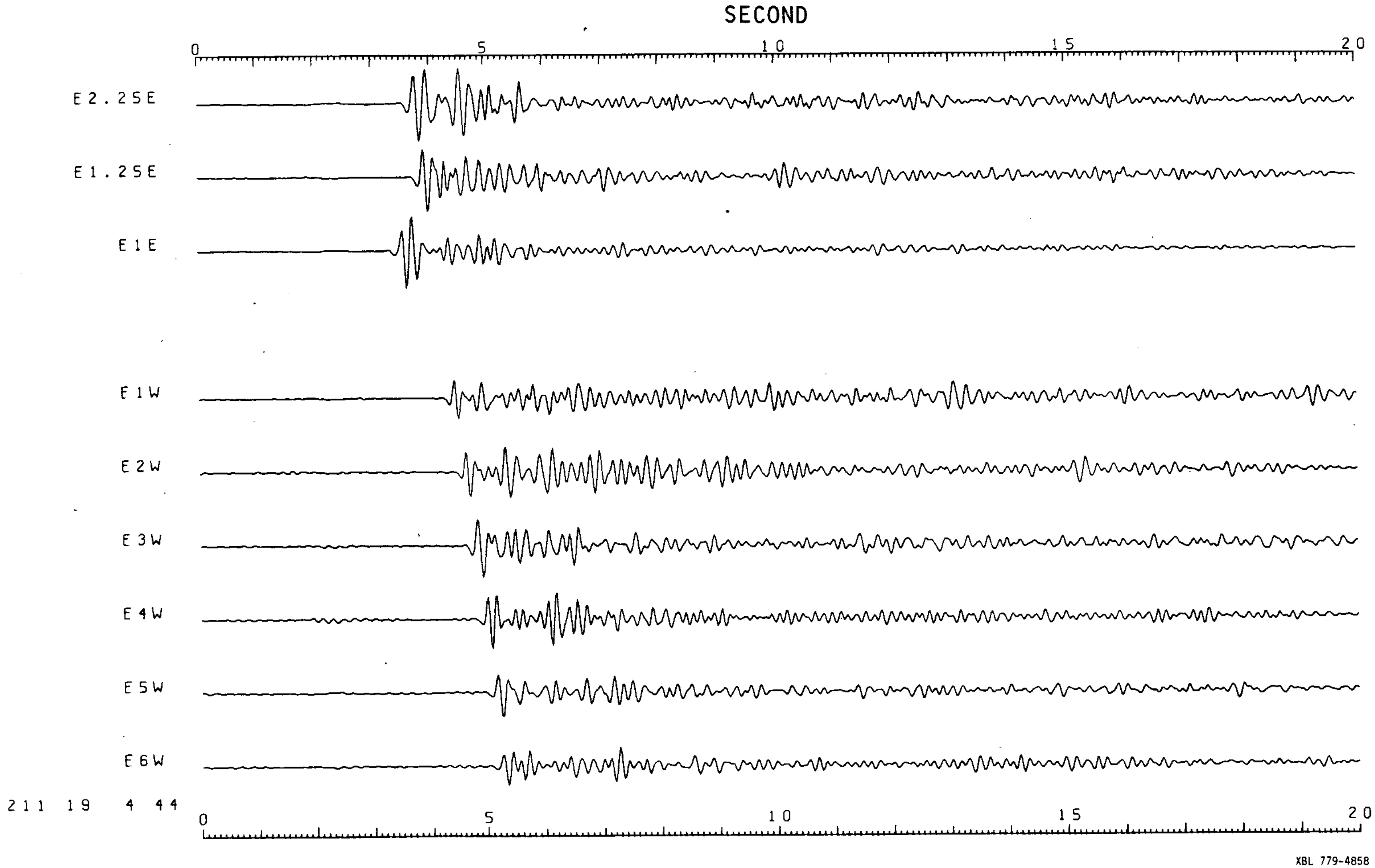
SECOND
0
5
10
15
20
E2.25E
E1.25E
E1E
E1W
E2W
E3W
E4W
E5W
E6W
211 19 4 44
XBL 779-4858

Figure 4.14

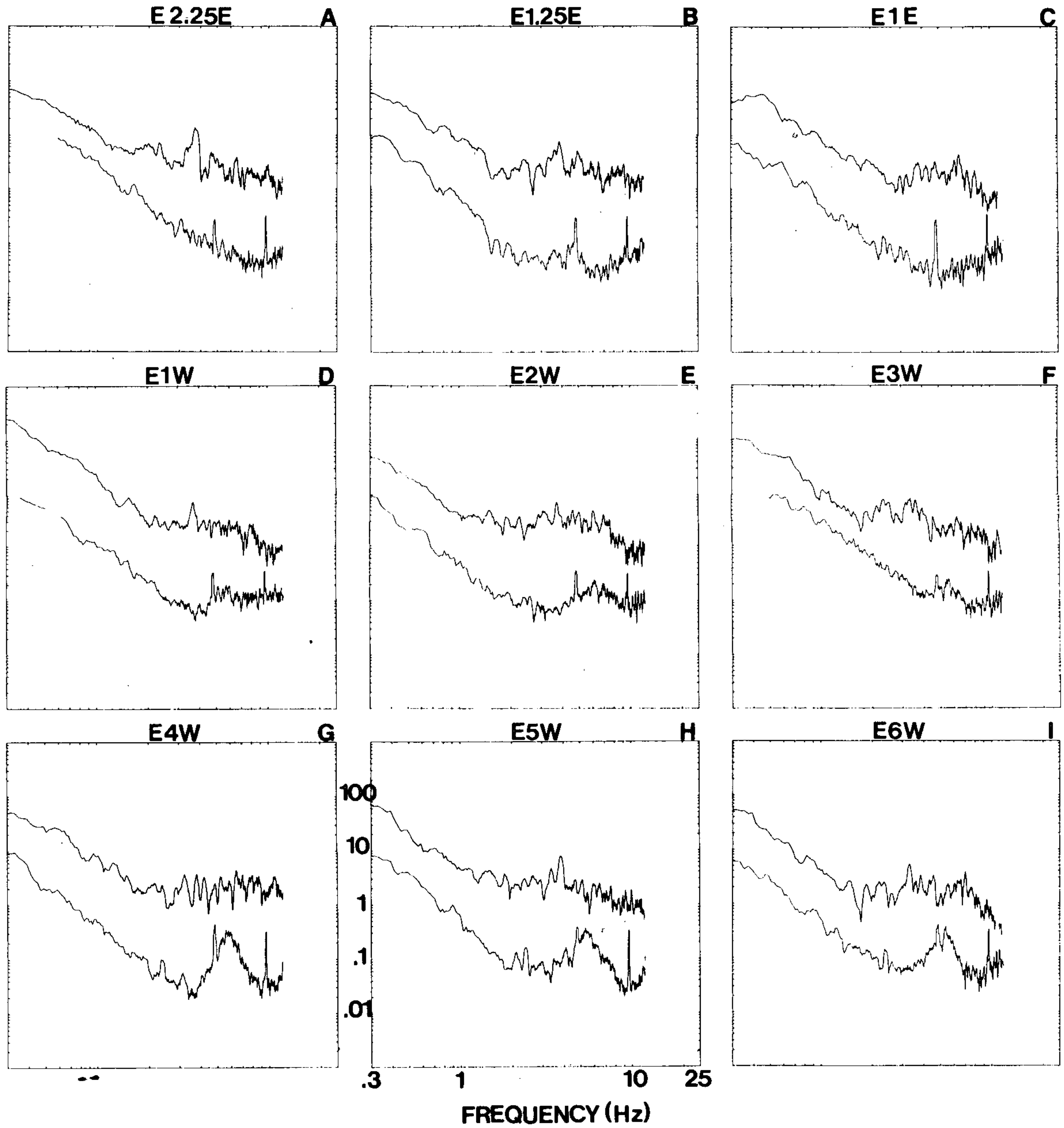

XBL 778-9828

Figure 4.15

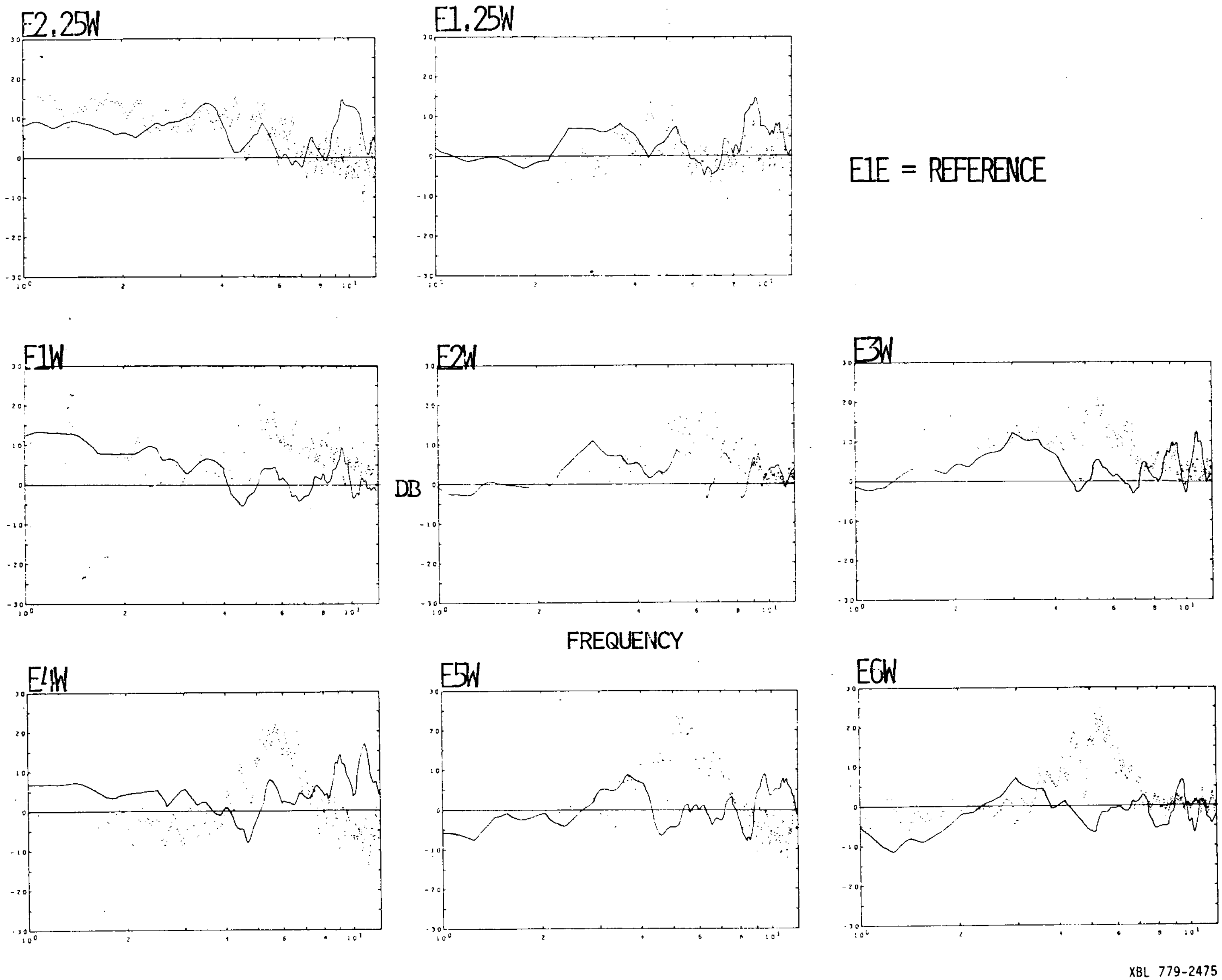
E2.25W
E1.25W
E1E = REFERENCE
E1W
E2W
E3W
DB
FREQUENCY
E4W
E5W
E6W
XBL 779-2475

Figure 4.16

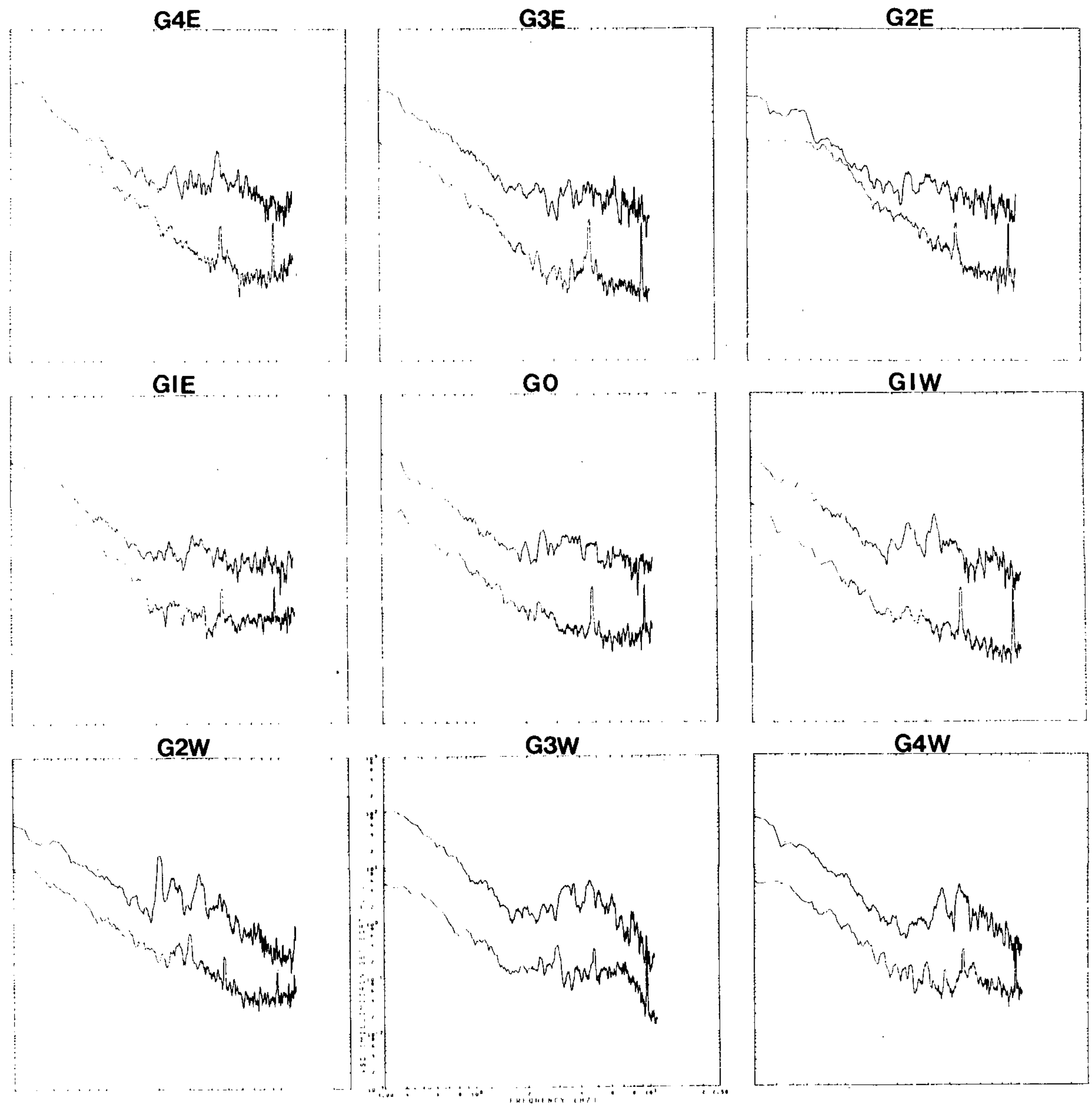

Figure 4.17

V. PROPAGATION CHARACTERISTICS OF GROUND NOISE

5.1 Introduction

We have shown in Chapter 4 that conventional noise power mapping techniques provide little information to make it possible to differentiate the effects of shallow geology from those due to buried sources. Seismic waves emitted from a buried reservoir source should be amenable to detection through local array measurements, because such vertically incident body waves have high apparent phase velocity and time-invariant propagation direction. The measurement of apparent phase velocity and azimuth is complicated for microseisms by multipath arrivals of both body waves and ambient surface waves. The reliable estimation of these propagation parameters therefore requires a properly designed array in conjunction with frequency-wavenumber (f-k) analysis. The horizontal propagating surface waves will appear in the f-k diagram as low velocity waves crossing the array, differing from the vertically incident body waves. The accurate estimation of the propagation parameters can provide the added data necessary to interpret the ambiguous noise power anomaly obtained by the method described in the previous chapter.

This chapter opens with a coherence study of seismic noise in Grass Valley conducted in order to design the array. The array design and the field program are presented in the following section. To my knowledge this work represents a first attempt at mapping the propagation parameters of microseisms in a geothermal area by using a non-aliasing roving array and advanced array processing techniques. The frequency-wavenumber (f-k) processing schemes used are the frequency domain beam-forming method, BFM (Lacoss et al., 1969), and the maximum-likelihood method, MLM (Capon, 1969). We compare the two array processing techniques in terms of their response to identical input data. The f-k analyses of Grass Valley data are presented in the last two sections.

5.2 Coherence of ground noise

To design a full-scale ground noise survey, we first deployed a pilot 12-element L-shaped array on alluvium and at the hot springs to determine the coherence properties of the noise field as a function of sensor separation.

The coherence function estimate, $\hat{R}_{mn}(f)$, between signals m and n is given by

$$\hat{R}_{mn}(f) = \frac{|\hat{S}_{mn}(f)|}{\sqrt{\hat{S}_{mm}(f)\hat{S}_{nn}(f)}} \quad , \tag{5.1}$$

where $\hat{S}_{mn}(f)$ is the estimate of cross-power spectral density. $\hat{S}_{mm}(f)$ and $\hat{S}_{nn}(f)$ are estimates of auto-power spectral density. This was defined in Equation (4.9). The 100% confidence interval for coherence estimates in the range of $0.59 \leqslant R_{mn}(f) \leqslant 0.97$ with $2I \geqslant 40$ degrees of freedom is calculated, according to Equation (6.111) of Bendat and Piersol (1971), by

$$\begin{aligned} &[\tanh\{g(f) - (2I - 2)^{-1} - \sigma_g Z_{\gamma/2}\}]^{1/2} < R_{mn}(f) \\ &[\tanh\{g(f) - (2I - 2)^{-1} + \sigma_g Z_{\gamma/2}\}]^{1/2} \quad , \end{aligned} \tag{5.2}$$

where $Z_{\gamma/2}$ is a standard normal variate and

$$g(f) = \frac{1}{2}\ln\left[\frac{1 + \hat{R}_{mn}(f)}{1 - \hat{R}_{mn}(f)}\right] = \tanh^{-1}\hat{R}_{mn}(f) \ , \qquad (5.3)$$

and I = number of data blocks being averaged, and

$$\sigma_g = \sqrt{\frac{2I}{2I - 2}} \qquad (5.4)$$

with 2I degrees of freedom.

Coherence of ground noise in Grass Valley decreases as the geophone spacing increases, the relation between coherence and geophone spacing varying from site to site. In the vicinity of Leach Hot Springs, high coherence between two geophones 10 m apart is seen in the frequency bands of 2 to 8 Hz and 10 to 20 Hz (Figure 5.1). As geophone spacing increases to 30 m, 40 m, and 60 m, the coherence decreases at high and low frequencies. At 60 m separation we can still observe high coherence in the 5-7 Hz band. There seems no obvious correlation between frequency bands with high coherence and the VSD (Figure 5.1E). In the valley, for example, at the intersection of line E and line M (EM), the frequency band of maximum coherence is 2 to 5 Hz when geophones are separated by 20 m (Figure 5.2). The coherence level and the width of the coherent frequency band decrease with increased geophone spacing to 40 m-60 m separation. The estimated coherence at nearby site E2.75W indicates some degree of coherence at 3 to 6 Hz, even at 120 m separation (Figure 5.2E). The degree of coherence seen, while variable, is generally low at valley sites, presumably the result of attenuation effects and interference from multi-path arrivals. Phase velocity and wavelength can be measured for the coherent part. Wavelengths as short as 10-20 m are present at the valley sites.

5.3 Roving array experiment

A small-aperture 12-geophone array was used. The array configuration and its impulse response in wavenumber space are shown in Figure 5.3. The existence of short wavelength noise components and the low coherence seen at large geophone separation, both dictated the tight array spacing used. An array of 100 m element separation or more, commonly used in ground noise studies elsewhere, would give spurious results because spatial aliasing folds the high-wavenumber noise components (which we have seen dominant in the valley alluvium) into low-wavenumber noise components. The spatial aliasing results in the detection of erroneously high-velocity microseisms, which are interpreted as body waves. We illustrate the effect of spatial aliasing due to inadequate element separation in Figure 5.4, where we processed a simulated 4 Hz plane wave with 50 m wavelength, propagating with phase velocity of 200 m/sec across four arrays. Those arrays have identical array shapes and numbers of sensors but different sensor spacing. The diameters of the arrays are 50 m, 75 m, 250 m, and 500 m, such that the sensor spacing for each array is proportional to the array size. Since the plane waves are propagating toward the azimuth of 60°, the folding effects are evident along the directions of 60° and 240°. Many interpretations of microseisms as body waves, based on coarse sensor separation, may well be incorrectly based on aliased low-velocity surface waves, as seen in Figure 5.4C. It is true, of course, that when the array is made small enough to accommodate the short-wavelength noise components, resolution for near-vertically incident body waves is seriously degraded, though the evidence of body waves should be visible and could be studied by appropriate array expansion and spatial filtering.

To map the propagation parameters of the microseismic field, this 12-element array was placed each evening at a site. Sixteen sites in the region have been occupied. Data were transmitted by cable to the recording vehicle some 500 m from the array.

5.4 Frequency-wavenumber power spectral density estimation

5.4.1 Definition

The frequency-wavenumber power spectral density function (FKPSD) was introduced into seismology by Burg (1964) in the development of the optimum three-dimensional filter derived from the Wiener multichannel theory. Burg (1964) illustrated the optimum three-dimensional filter by a theoretical problem of P-wave enhancement in the presence of ambient Rayleigh waves. The FKPSD, a three-dimensional equivalent of ordinary spectral density function, is given by the relation

$$P(f,\underline{k}) = \int_{-\infty}^{\infty}\int_{-\infty}^{\infty}\int_{-\infty}^{\infty} c(\tau,\underline{\rho})\exp[-j2\pi(f\tau + \underline{k}\cdot\underline{\rho})]\,d\tau\, d\rho_x\, d\rho_y \quad , \tag{5.5}$$

where $c(\tau,\underline{\rho})$ is the correlation function with time delay τ and spatial lag $\underline{\rho}$, $\underline{k}$ is the vector wavenumber in cycles/km.

The correlation function of the noise field is defined as

$$c(\tau,\underline{\rho}) = E[\phi(t,\underline{r})\cdot\phi(t+\tau,\underline{r}+\underline{\rho})] \quad , \tag{5.6}$$

where E denotes the averaged value, or expectation, and $\phi(t,\underline{r})$ is the time series of the noise field at seismometer locations $\underline{r} = (x,y)$.

The array processing is normally carried out in the frequency domain rather than in the time domain because of computation time considerations.

With carefully designed filter coefficients, however, the time domain operation has the advantage of better resolution than the frequency domain operation (Capon, et al., 1967 and Lacoss, et al., 1969). In the following sections, I compare the techniques for estimating FKPSD using the conventional and maximum-likelihood method in the frequency domain.

5.4.2 Conventional method (BFM)

The conventional method, commonly known as the frequency domain beam forming method (BFM), estimates the FKPSD, $P(f,\underline{k})$, by the relation

$$\hat{P}(f,\underline{k}) = \frac{1}{N^2}\,\underline{a}' \cdot \underline{\underline{S}} \cdot \underline{a}\ , \tag{5.7}$$

where N is the number of geophones in the array and $\underline{a}'$, the conjugate transpose of $\underline{a}$, is the row vector

$$\underline{a}' = (e^{j2\pi\underline{k}\cdot\underline{r}_1},\ e^{j2\pi\underline{k}\cdot\underline{r}_2},\ e^{j2\pi\underline{k}\cdot\underline{r}_3},\ .\ .\ .\ ,\ e^{j2\pi\underline{k}\cdot\underline{r}_N})\ , \tag{5.8}$$

where $\underline{r}_n$ is the coordinate of n^{th} geophone location. $\hat{\underline{\underline{S}}}$ is the estimate of the spectral matrix between sensors. Each entry of $\hat{S}$, $\hat{S}_{mn}(f)$, is obtained from the averaged cross-power,

$$\bar{S}_{mn}(f) = \frac{1}{I}\sum_{i=1}^{I} {}^{i}\Phi_m(f)\,{}^{i}\Phi_n^*(f)\ , \tag{5.9}$$

by the normalization

$$\hat{S}_{mn}(f) = \frac{\bar{S}_{mn}(f)}{\sqrt{\bar{S}_{mm}(f)\bar{S}_{nn}(f)}}\ , \tag{5.9A}$$

where ${}^{i}\Phi_n(f)$ is the Fourier transform of block noise sample i, from seismometer n located at $\underline{r}_n$.

The BFM estimate of FKPSD, by re-arranging Equation (5.7), is

$$\hat{P}(f,\underline{k}) = \frac{1}{N^2}\sum_{m=1}^{N}\sum_{n=1}^{N} W_m W_n^* \hat{S}_{mn}(f)\exp[-j2\pi\underline{k}\cdot(\underline{r}_m - \underline{r}_n)] \ , \qquad (5.10)$$

or

$$\hat{P}(f,\underline{k}) = \frac{1}{I}\sum_{i=1}^{I} \left|\frac{1}{N}\sum_{n=1}^{N} W_n \, {}^{i}\Phi_n(f)\exp[-j2\pi\underline{k}\cdot\underline{r}_n]\right|^2 . \qquad (5.11)$$

The term $\exp(-j2\pi\underline{k}\cdot\underline{r}_n)$ in Equation (5.11) has the effect of advancing the phase of sinusoid observed at $\underline{r}_n$ by the amount of the time delay with respect to the origin of the array assuming a plane wave propagating toward the azimuth $\underline{k}$ with phase velocity $\underline{V}$. $\underline{V}$ is given by

$$\underline{V} = \frac{f}{|\underline{k}|} \text{ km/sec} . \qquad (5.12)$$

Taking $W_m = W_n = 1$, the BFM applies uniform weighting to each array element before the delay-and-sum operation. The BFM is efficient in computational time and provides an accurate estimate of azimuth and phase velocity if the noise field has high signal-to-noise ratio in a unique direction and represents a single mode of wave propagation. On the other hand, in the presence of multi-path propagation, the result in wavenumber space always shows an ambiguous pattern of peaks due to smearing of the true spectrum. The big side-lobes in the impulse response of the array (Figure 5.3) cause serious leakage in estimating spectral density.

Statistical properties of the estimator $\hat{P}(f,\underline{k})$ were given by Capon and Goodman (1970). The *a priori* assumptions in deriving the probability distribution are the following:

1) The sensor outputs comprise a multi-dimensional Gaussian random process with zero mean and stationary discrete time series, and

2) The length of the segments employed is long so that ${}^{i}\Phi_m(f)$ is statistically independent of ${}^{k}\Phi_n(f)$, $m \neq n$, then $\zeta_1, \zeta_2, \zeta_3, \ldots, \zeta_I$ are I independent and identically distributed N-variate complex Gaussian random variables, where ζ_i is a column vector defined as

$$\zeta_i = \mathrm{Col}[\Phi_{1i}(f), \Phi_{2i}(f), \Phi_{3i}(f), \ . \ . \ . \ , \Phi_{Ni}(f)] \ , \tag{5.13}$$

where $\Phi_{Ni}(f)$ is the Fourier transform of data in the i^{th} segment, n^{th} channel, frequency f.

The N × N matrix-valued random variables, $\hat{\underline{\underline{S}}}(f)$ defined in Equation (5.9), have a complex Wishart distribution of dimension N and 2I degree of freedom (when $|\underline{k}_o| \neq 0$). The random variable $\hat{P}(f,\underline{k})$ thus is a multiple of a Chi-square variable with mean and variance given by

$$E\{\hat{P}(f,\underline{k})\} = \int_{-f_N}^{f_N}\int_{-\infty}^{\infty}\int_{-\infty}^{\infty} P(x,\underline{k})\,|B(\underline{k}-\underline{k}_o)W_L(x-f_o)|^2 dx dkx dky \ , \tag{5.14}$$

$$\mathrm{var}\{\hat{P}(f,\underline{k})\} = \begin{cases} \frac{1}{I}[E\{\hat{P}(f_o,\underline{k}_o)\}^2], & f_o \neq 0, f_N \\ \frac{2}{I}[E\{\hat{P}(f_o,\underline{k}_o)\}^2], & f_o = 0, f_N \end{cases} \ , \tag{5.15}$$

where f_N is the Nyquist frequency and $P(f,\underline{k})$ is the frequency-wavenumber power spectrum. $|B(\underline{k})|^2$ is the array response function

$$B(\underline{k}) = \frac{1}{N}\sum_{n=1}^{N} \exp(j\underline{k} \cdot \underline{r}_n) \ . \tag{5.16}$$

$|W_L(x)|^2$ is the frequency window function

$$|W_L(x)|^2 = \frac{1}{L}\left|\frac{\sin(L/2)x}{\sin(1/2)x}\right|^2 . \tag{5.17}$$

$E\{\hat{P}(f,\underline{k}_o)\}$ is obtained by means of a frequency-wavenumber window $|B(\underline{k}-\underline{k}_o)|^2 \cdot |W_L(x-f)|^2$. Hence $\hat{P}(f,\underline{k})$ will be an asymptotically unbiased estimate of $CP(f,\underline{k})$ as

$$\int_{-\pi}^{\pi}\int_{-\infty}^{\infty}\int_{-\infty}^{\infty} |W_L(x-f) \cdot B(\underline{k}-\underline{k}_o)|^2 dxdkxdky = C. \tag{5.18}$$

The var $\{\hat{P}(f,\underline{k}_o)\}$ approaches zero as I approaches infinity such that $\hat{P}(f,\underline{k})$ is a consistent estimate for $CP(f,\underline{k})$. The stability of the estimate is independent of the FKPSD, seismometer locations, or the weights W_n, $n = 1,\ldots,N$ (Lacoss, et al., 1969) and is given by

$$\nu = \frac{2E\{\hat{P}(f_o,\underline{k}_o)\}^2}{\mathrm{var}\{\hat{P}(f_o,\underline{k}_o)\}} \cdot b_1 = \begin{cases} 2Ib_1 & \text{for } f_o \neq 0 \text{ or } f_N \\ Ib_1 & \text{for } f_o = 0 \text{ or } f_N \end{cases} , \tag{5.19}$$

where b_1 is dependent on the spectral window defined in Equation (4.12) and the 100γ percent confidence interval for $\hat{P}(f_o,\underline{k}_o)$ is

$$\frac{\nu\hat{P}(f_o,\underline{k}_o)}{\chi_\nu^2\ (\frac{1+\gamma}{2})} < P(f_o,\underline{k}_o) < \frac{\nu\hat{P}(f_o,\underline{k}_o)}{\chi_\nu^2\ (\frac{1-\gamma}{2})} . \tag{5.20}$$

For 24 data blocks, each block tapered by the rectangular data window, $\nu = 48$, the 90% confidence limits are about 1.58 dB above and -1.24 dB below $\hat{P}(f_o,\underline{k}_o)$ for $f_o \neq 0$ or f_N.

5.4.3 Maximum-likelihood method (MLM)

The maximum-likelihood estimate for FKPSD is based on the application of optimal weighting functions which correspond to a maximum-likelihood filter in 2-dimensional wavenumber space to control the shape of the frequency-wavenumber window function, i.e., the beam pattern of the array impulse response. The construction of the maximum-likelihood filter is based on the coherence characteristics of the data among array sensors. These optimal weighting functions, when applied to the output of each array element, result in the maximum signal-to-noise ratio in the array signal estimation. At a selected frequency component, the maximum-likelihood filter is able to pass undistorted a monochromatic plane wave traveling at a velocity corresponding to a steering wavenumber, $\underline{k}_o$, and to suppress in an optimal least squares sense the power of those waves traveling at velocities corresponding to wavenumbers other than $\underline{k}_o$. The weighting function changes as the spectrum changes.

The maximum-likelihood estimate for FKPSD can be written as

$$\tilde{P}(f,\underline{k}) = \sum_{m=1}^{N} \sum_{n=1}^{N} A_m(f) A_n^*(f) \hat{S}_{mn}(f) \exp[-j2\pi(\underline{k} \cdot \underline{\rho})] \quad , \qquad (5.21)$$

where $A_m(f)$ and $A_n(f)$ are weights applied to the outputs of array elements m and n respectively. Note that $A_m(f)$ and $A_n(f)$ are functions of frequency, wavenumber, and spatial coordinates of the array element.

To consider the optimal weighting function in the "distortionless" sense and with optimal suppression of noise, we rearrange Equations (5.21) into the form

$$\tilde{P}(f,\underline{k}) = \sum_{m=1}^{N} \sum_{n=1}^{N} A_m(f) A_n^*(f) \tilde{S}_{mn}(f) \quad , \qquad (5.22)$$

where

$$\tilde{S}_{mn}(f) = \hat{S}_{mn}(f)\exp(-j2\pi \underline{k} \cdot \underline{x}_m)\exp(j2\pi \underline{k} \cdot \underline{x}_n) \ , \tag{5.23}$$

is the spectral matrix with delays.

Define a weighting vector

$$\underline{W} = \mathrm{col}[A_1(f), A_2(f), \ . \ . \ . \ . \ , A_n(f)] \ . \tag{5.24}$$

Equation (5.22) becomes

$$\tilde{P}(f,\underline{k}) = \underline{W}' \cdot \underline{\underline{\tilde{S}}} \cdot \underline{W} \ , \tag{5.25}$$

where $\underline{W}'$ is the conjugate transpose of $\underline{W}$.

In this optimization problem, we desire minimum array output power for $\underline{k} \neq \underline{k}_o$, which is equivalent to minimizing the quantity $(\underline{W}' \cdot \underline{\underline{\tilde{S}}} \cdot \underline{W})$. The constraint of distortionless filter response at $\underline{k} = \underline{k}_o$ requires the sum of all N coefficients to be unity over the narrow wavenumber band around $\underline{k} = \underline{k}_o$, i.e.

$$\sum_{n=1}^{N} A_n(f,\underline{k}_o) = 1 \tag{5.26}$$

or

$$\underline{C}^T \cdot \underline{W} = 1 \ , \tag{5.27}$$

where $\underline{C} = \mathrm{col}[1, 1, \ . \ . \ . \ , 1]$. (5.28)

The problem of finding the optimum set of filter weights, $\underline{W}_{opt}$, is summarized by Equations (5.25) and (5.27) as

$$\text{minimize } (\underline{W}' \cdot \underline{\underline{\tilde{S}}} \cdot \underline{W}) \text{ with respect to } \underline{W} \tag{5.29}$$

$$\text{subject to } \underline{C}^T \cdot \underline{W} = 1 \ . \tag{5.30}$$

Using the method of Lagrange multipliers in the calculus of variations, we set up the equation as:

$$H(\underline{W}) = \frac{1}{2}\, \underline{W}' \cdot \underline{\underline{\tilde{S}}} \cdot \underline{W} + \lambda(\underline{C}^T\underline{W} - 1) \quad , \tag{5.31}$$

where the coefficient 1/2 is introduced to simplify later arithmetic and λ is an undetermined Lagrange multiplier.

Taking the gradient of Equation (5.31) with respect to $\underline{W}$ and equating to zero,

$$\nabla_{\underline{W}} H(\underline{W}) = \underline{\underline{\tilde{S}}} \cdot \underline{W} + \underline{C}\lambda = 0 \tag{5.32}$$

yielding

$$\underline{W} = -\underline{\underline{\tilde{S}}}^{-1}\underline{C}\lambda \ , \tag{5.33}$$

substituting (5.33) into (5.30) we obtain

$$\lambda = -(\underline{C}^T\underline{\underline{\tilde{S}}}^{-1}\underline{C})^{-1} \ . \tag{5.34}$$

From Equations (5.33) and (5.34), the optimal weighting vector is obtained as

$$\underline{W}_{opt} = (\underline{\underline{S}}^{-1} \cdot \underline{C})(\underline{C}^T \cdot \underline{\underline{\tilde{S}}}^{-1} \cdot \underline{C})^{-1} \ , \tag{5.35}$$

and the optimal weighting functions are:

$$A_n(f) = \frac{\sum_{m=1}^{N} \tilde{q}_{mn}(f)}{\sum_{m=1}^{N}\sum_{n=1}^{N} \tilde{q}_{mn}(f)} \quad , \quad n = 1, \ldots, N \ , \tag{5.36}$$

where the matrix $\{\tilde{q}_{mn}(f)\}$ is the inverse of the delayed spectral matrix, $\{\tilde{S}_{mn}(f)\}^{-1} = \underline{\underline{\tilde{S}}}^{-1}$, as defined in Equation (5.23).

The filter obtained from the above optimization procedures is a distortionless form of a constrained least squares filter, or constrained

LMS filter (Frost, 1972). The right hand side of Equation (5.36) is identical to the coefficients of the maximum-likelihood filter derived by Capon (1973) using the maximum-likelihood estimation technique.

Substituting Equation (5.35) into Equation (5.25), the estimate for FKPSD is:

$$\tilde{P}(f,\underline{k}) = \left(\frac{\underline{C}^T \cdot \tilde{\underline{\underline{S}}}^{-1}}{\underline{C}^T \cdot \tilde{\underline{\underline{S}}}^{-1} \cdot \underline{C}}\right) \cdot \tilde{\underline{\underline{S}}} \cdot \left(\frac{\tilde{\underline{\underline{S}}}^{-1} \cdot \underline{C}}{\underline{C}^T \cdot \tilde{\underline{\underline{S}}}^{-1} \cdot \underline{C}}\right) \tag{5.37}$$

$$= (\underline{C}^T \cdot \tilde{\underline{\underline{S}}}^{-1} \cdot \underline{C})^{-1} \tag{5.38}$$

$$= (\underline{a}' \cdot \hat{\underline{\underline{S}}}^{-1} \cdot \underline{a})^{-1} \quad .$$

This is just the high-resolution estimate for $P(f,\underline{k})$ given by Capon(1969).

The justification for the usage of $\tilde{P}(f,\underline{k})$ as an estimation for $P(f,\underline{k})$ is provided by an important property of the maximum-likelihood estimator. When the maximum-likelihood estimator is used in signal estimation, it is identical to the minimum-variance unbiased estimator of the signal (Capon <u>et al</u>., 1967; and Capon, 1973). This is the consequence of minimizing the variance of the array output, $(\underline{W}' \cdot \tilde{\underline{\underline{S}}} \cdot \underline{W})$, in Equation (5.29). Therefore, $\tilde{P}(f,\underline{k})$ is a minimum-variance unbiased estimate for $P(f,\underline{k})$.

The statistical properties of $\tilde{P}(f,\underline{k})$ have been discussed by Capon and Goodman (1970), who show that $\tilde{P}(f,\underline{k})$ is a multiple of chi-square variable with $2(I - N + 1)$ degrees of freedom, if $f_o = 0$, or f_N. The mean and variance of $\tilde{P}(f,k)$ are given by

$$E\{\tilde{P}(f_o,\underline{k}_o)\} = \left(\frac{I-N+1}{I}\right)\int_{-f_N}^{f_N}\int_{-\infty}^{\infty}\int_{-\infty}^{\infty} P(x,\underline{k})\,|W_L(x-f_o)\tilde{B}(f_o,\underline{k};\underline{k}_o)|^2 dx\,dkx\,dky \tag{5.39}$$

$$\mathrm{var}\{\tilde{P}(f_o,\underline{k}_o)\} = \left(\frac{1}{I-N+1}\right)[E\{\tilde{P}(f_o,\underline{k}_o)\}]^2 , \quad f_o \neq 0 \text{ or } f_N \tag{5.40}$$

$$\text{or} \quad \left(\frac{2}{I-N+1}\right)[E\{\tilde{P}(f_o,\underline{k}_o)\}]^2 , \quad f_o = 0 \text{ or } f_N \tag{5.41}$$

The confidence limits for $\tilde{P}(f_o,\underline{k}_o)$ can be obtained in a manner similar to that discussed for the BFM. If I = 24, N = 12, and the rectangular taper is used, there are 26 degrees of freedom and the 90% confidence limits are 2.28 dB above and -1.76 dB below $\tilde{P}(f_o,\underline{k}_o)$, for $f_o \neq 0$ or f_N. In the article discussing the frequency domain beam forming method, Lacoss et al. (1969) have shown that as long as the requirement $W_{nm} = W^*_{mn}$ is satisfied, the stability of any frequency domain beam forming estimate is independent of the seismometer location, FKPSD, or the weights W_n, $n = 1, \ldots, N$. W_{mn} represents $W_m W_n$ and W_m is the weighting function applied on m^{th} sensor output. The requirement $W_{nm} = W^*_{mn}$ ensures that $\tilde{P}(f_o,\underline{k}_o)$ be real. Since the weighting function of MLM satisfies the above requirements, the confidence limits of the MLM estimate depend only on the number of data blocks and array sensors.

Equation (5.39) indicates that $E\{P(f_o,\underline{k}_o)\}$ is obtained by means of a frequency-wavenumber window, $|W_L(x-f_o) \cdot \tilde{B}(f_o,\underline{k};\underline{k}_o)|^2$ where

$$\tilde{B}(f_o,\underline{k};\underline{k}_o) = \sum_{n=1}^{N} A_n(f)\exp[j(\underline{k} - \underline{k}_o) \cdot \underline{r}_n] ; \tag{5.42}$$

therefore $\tilde{P}(f_o,\underline{k}_o)$ is an asymptotically unbiased estimator for $CP(f_o,\underline{k}_o)$, if the window approaches a three-dimensional delta function in such a way that

$$\left(\frac{I-N+1}{I}\right)\int_{-f_N}^{f_N}\int_{-\infty}^{\infty}\int_{-\infty}^{\infty} |W_L(x-f_o)\tilde{B}(f_o,\underline{k};\underline{k}_o)|^2 \, dx\,dkx\,dky = C . \tag{5.43}$$

5.4.4 Comparing the FKPSD estimation techniques

The term "high resolution f-k spectrum" is commonly used for maximum-likelihood (MLM) estimation of FKPSD, because, under favorable conditions, this method always results in a spectrum with sharper peaks and lower side-lobes than that estimated by conventional (BFM) methods. Based on theoretical analyses, however, Cox (1973) has found that the MLM has a disadvantage relative to the BFM in terms of its sensitivity to measurement errors, especially in the case of channel mismatch. Mismatch may result from distortion in the waveform during propagation, from amplitude, phase and position errors in the sensors, or in the sampling and digitization. We have examined the effects of mismatch by processing simulated data with both MLM and BFM. Input data are 4 Hz plane waves superimposed upon random noise of varying amplitude level. The 4 Hz plane wave propagates with phase velocity of 200 m/sec across an array in 50 m diameter. A block of data without random noise components is shown in Figure 5.5. We have found from the results of BFM that, regardless of the signal-to-noise ratios of input data, the f-k diagrams at 4 Hz are all identical to Figure 5.6A. This figure shows a shifted array response, centered around the wavenumber of the simulated signal. The peak value of f-k spectrum at 4 Hz is independent of the signal-to-noise ratios between 48.8 dB and 10.6 dB. On the other hand, the results of MLM analysis indicate that MLM is sensitive to signal-to-noise ratio of the input data. This effect is illustrated by the f-k plots for signal-to-noise ratio of 48.8 dB (Figure 5.6B), 30.6 dB (Figure 5.6C), 25.6 dB (Figure 5.6D), 20 dB (Figure 5.6E) and 10.6 db (Figure 5.6F). Those figures clearly indicate that MLM suppresses the side-lobes more efficiently and produces higher resolutions than BFM. The high resolution effect is a distinct advantage in the case of multiple arrivals.

The desirable characteristics of MLM are results of the combination of the side-lobe suppression and the noise rejection. We shall discuss these operations by assuming that $\hat{\underline{\underline{S}}}$ consists of signal-plus-noise, so that we may express $\hat{\underline{\underline{S}}}$ as the form

$$\hat{\underline{\underline{S}}} = \sigma_o^2 \hat{\underline{\underline{Q}}} + \sigma_1^2 \underline{d} \cdot \underline{d}' \quad , \tag{5.44}$$

where

$\sigma_o^2 \hat{\underline{\underline{Q}}}$ is the noise spectral matrix,

$\hat{\underline{\underline{Q}}}$ is normalized to have its trace equal to the number of sensors,

σ_o^2 is the input noise spectral level averaged across the sensors,

σ_1^2 is the averaged input power spectrum of the coherent microseismic signal,

$\underline{d}$ is a directional vector of microseismic field, defined as

$$d = \begin{bmatrix} \exp(j2\pi \underline{k}_o \cdot \underline{x}_1) \\ \exp(j2\pi \underline{k}_o \cdot \underline{x}_2) \\ \vdots \\ \vdots \\ \exp(j2\pi \underline{k}_o \cdot \underline{x}_N) \end{bmatrix} \tag{5.45}$$

$\underline{k}_o$ is a wavenumber vector in the direction to which the microseismic field is propagating.

We can also write a general expression for estimate FKPSD as

$$P(f,\underline{k}) = \underline{\tilde{W}}' \cdot \hat{\underline{\underline{S}}} \cdot \underline{\tilde{W}} \tag{5.46}$$

where $\underline{W}$ is the vector of generalized weighting functions,

$$\underline{\tilde{W}}' = \frac{1}{N}\,\underline{a}' \tag{5.47}$$

for BFM, and

$$\underline{\tilde{W}} = (\underline{\underline{\tilde{S}}}^{-1} \cdot \underline{C})(\underline{C}^T \cdot \underline{\underline{\tilde{S}}}^{-1} \cdot \underline{C})^{-1} = (\underline{\underline{\hat{S}}} \cdot \underline{a})(\underline{a}' \cdot \underline{\underline{\hat{S}}}' \cdot \underline{a})^{-1} \tag{5.48}$$

for MLM.

Substituting Equation (5.44) to Equation (5.46)

$$P(f,\underline{k}) = \sigma_o^2 \underline{\tilde{W}}' \cdot \underline{\underline{\hat{Q}}} \cdot \underline{\tilde{W}} + \sigma_1^2 |\underline{\tilde{W}}' \cdot \underline{d}|^2 \,. \tag{5.49}$$

We define an inner product between two column vectors $\underline{a}$ and $\underline{d}$ by $\underline{a}' \cdot \underline{\underline{C}} \cdot \underline{d}$, where $\underline{\underline{C}}$ is a positive definite Hermitian matrix, and the cosine-square of the generalized angle between $\underline{a}$ and $\underline{d}$ to be

$$\cos^2(\underline{a},\underline{d};\underline{\underline{C}}) = |\underline{a}^* \cdot \underline{\underline{C}} \cdot \underline{d}|^2 / \{(\underline{a}' \cdot \underline{\underline{C}} \cdot \underline{a})(\underline{d}' \cdot \underline{\underline{C}} \cdot \underline{d})\} \,. \tag{5.50}$$

<u>BFM</u>. For BFM, the output spectrum can be written as

$$\hat{P}(f,\underline{k};\underline{k}_o) = \frac{\sigma_o^2}{N^2}(\underline{a}' \cdot \underline{\underline{\hat{Q}}} \cdot \underline{a}) + \sigma_1^2 \cos^2(\underline{a},\underline{d};\underline{\underline{I}}) \,. \tag{5.51}$$

The first term is the noise response, the second term is the signal response, and $\cos^2(\underline{a},\underline{d};\underline{\underline{I}})$ is the array impulse response shifted by the steering vector $\underline{a}$ to the "direction" $\underline{d}$, as shown in Figure 5.6A. It is evident that signal response depends on the cosine square of the generalized angle between $\underline{a}$ and $\underline{d}$ in inner product space and is not affected by the noise spectral matrix $\underline{\underline{\hat{Q}}}$. Therefore, the signal response is relatively insensitive to small mismatch between $\underline{a}$ and $\underline{d}$, as well as input signal-to-noise ratio. The noise response is reduced by increase N which is the number of sensors in the array.

MLM. The output spectrum of MLM is obtained by substituting Equation (5.48) into Equation (5.49),

$$\tilde{P}(f,\underline{k};\underline{k}_o) = \frac{\sigma_o^2}{\underline{a}' \cdot \hat{\underline{\underline{Q}}}^{-1} \cdot \underline{a}} \left\{ 1 + \frac{[2(S/N)_{max} + (S/N)^2_{max}]\sin(\underline{a},\underline{d};\hat{\underline{\underline{Q}}}^{-1})}{[1 + (S/N)_{max}\sin^2(\underline{a},\underline{d};\hat{\underline{\underline{Q}}}^{-1})]^2} \right\}$$
$$+ \sigma_i^2 \left(\frac{\underline{d}' \cdot \hat{\underline{\underline{Q}}}^{-1} \cdot \underline{d}}{\underline{a}' \cdot \hat{\underline{\underline{Q}}}^{-1} \cdot \underline{a}} \right) \left(\frac{\cos^2(\underline{a},\underline{d};\hat{\underline{\underline{Q}}}^{-1})}{\{1 + (S/N)_{max}\sin^2(\underline{a},\underline{d};\hat{\underline{\underline{Q}}}^{-1})\}^2} \right), \tag{5.52}$$

where $(S/N)_{max}$ is the maximum output signal-to-noise spectral ratio defined as:

$$(S/N)_{max} = (\underline{d}' \cdot \hat{\underline{\underline{Q}}}^{-1} \cdot \underline{d}) \frac{\sigma_1^2}{\sigma_o^2} \quad , \quad \text{and} \tag{5.53}$$

$$\sin^2(\underline{a},\underline{d};\hat{\underline{\underline{Q}}}^{-1}) = 1 = \cos^2(\underline{a},\underline{d};\hat{\underline{\underline{Q}}}^{-1}) \quad . \tag{5.54}$$

The expressions for signal and noise responses appearing in Equation (5. 52) are more complicated than those of the BFM. It is evident from Equation (5.52) that both $(S/N)_{max}$ and $\sin^2(\underline{a},\underline{d};\underline{\underline{Q}}^{-1})$ play important roles in signal expression and noise rejection. The suppression of spurious side-lobes due to finite dimension array response can be seen from the behavior of the second term in Equation (5.4). As $\underline{a}$ deviates away from $\underline{d}$, the quantity of $\cos^2(\underline{a},\underline{d};\hat{\underline{\underline{Q}}}^{-1})$ becomes smaller while $\sin^2(\underline{a},\underline{d};\hat{\underline{\underline{Q}}}^{-1})$ becomes larger. The signal suppression can be significant at $\underline{a} \neq \underline{d}$ when $(S/N)_{max}$ is larger than unity.

Let us turn our attention to the first term of Equation (5.52), i.e. the noise response. To examine the unusual nature of the noise response, we let $\hat{\underline{\underline{Q}}} = \underline{\underline{I}}$, such that the quantity $(\underline{a}' \cdot \hat{\underline{\underline{Q}}}^{-1} \cdot \underline{a})$ is a constant. Then as $\sin^2(\underline{a},\underline{d};\underline{\underline{I}})$ varies from zero to one, the noise response increases from the value σ_o^2/N at $\sin^2(\underline{a},\underline{d};\underline{\underline{I}}) = 0$, until it reaches a maximum of $(\frac{\sigma_o^2}{N}) \frac{[2+(S/N)_{max}]^2}{4+4(S/N)_{max}}$ at $\sin^2(\underline{a},\underline{d};\underline{\underline{I}}) = 1/(2+(S/N)_{max})$.

This peculiar noise response is due to the fact that the MLM estimator treats the mismatched signal as an unwanted interference and performs a compromise between suppressing the signal and rejecting the real noise. The stronger the mismatched signal, the more importance the estimator puts on suppressing it. In suppressing the mismatched signal it accepts a lesser rejection of noise. Near the point $\sin^2(\underline{a},\underline{d};\underline{\underline{I}}) = 0$, the signal suppression is minimum. As $\sin^2(\underline{a},\underline{d};\underline{\underline{I}})$ increases, the greater suppression of the signal is possible with a corresponding increasing penalty in noise rejection. Eventually the mismatch reaches the point where the signal suppression is sufficient so that a further penalty in noise response is not justified. The processor then reverses the trend and places greater emphasis on rejecting the noise.

The MLM, however, is not an optimal array processor. The terms in large braces in Equation (5.52) deviate the output spectrum of MLM away from that of an optimal array processor. We will discuss the optimal array processor later in this section. Look back at Equation (5.36) where we used the cross-power spectral matrix of the signal-plus-noise to construct the weighting function for MLM.
The optimal array processor, on the other hand, uses the cross-power spectral

matrix of noise alone to construct the weighting functions in order to enhance the transient signal, such as earthquake or explosion arrivals. Unfortunately, such an optimal array processor is not applicable to microseismic data because of the difficulty in separating signal from noise in microseismic data. It appears that, at present, MLM is the best way to process two-dimensional array data for high resolution in the presence of multi-path interference, the normal situation in ground noise studies. It is worthwhile, nevertheless, to consider the responses of the optimal array processor.

Optimal Array Processor. The output spectrum given by Cox (1973) is

$$P(f,\underline{k};\underline{k}_o) = \frac{\sigma_o^2}{(\underline{a}' \cdot \hat{\underline{\underline{Q}}}^{-1} \cdot \underline{a})} + \sigma_1^2\left(\frac{\underline{d}' \cdot \hat{\underline{\underline{Q}}}^{-1} \cdot \underline{d}}{\underline{a}' \cdot \hat{\underline{\underline{Q}}}^{-1} \cdot \underline{a}}\right)\cos^2(\underline{a},\underline{d};\hat{\underline{\underline{Q}}}^{-1}) \tag{5.55}$$

which results from substituting $\tilde{\underline{W}}' = (\hat{\underline{\underline{Q}}}^{-1} \cdot \underline{a})(\underline{a}' \cdot \hat{\underline{\underline{Q}}}^{-1} \cdot \underline{a})^{-1}$ into Equation (5.49). Again, the first term corresponds to the noise response and the second term corresponds to the signal. Notice that Equation (5.55) reduces to Equation (5.51) for the case of spatially uncorrelated noise, $\hat{\underline{\underline{Q}}} = \underline{\underline{I}}$, and $\underline{a} = \underline{d}$.

In order to realize the effects of optimization, one must understand the effect of the matrix $\hat{\underline{\underline{Q}}}^{-1}$, since we have defined $\hat{\underline{\underline{Q}}}$ as a noise spectral matrix in Equation (5.44), the small eigenvalues of $\hat{\underline{\underline{Q}}}$ correspond to the elements of array with less noise. The effect of introducing $\hat{\underline{\underline{Q}}}^{-1}$ in $\cos^2(\underline{a},\underline{d};\hat{\underline{\underline{Q}}}^{-1})$ can be compared with $\cos^2(\underline{a},\underline{d};\underline{\underline{I}})$ of Equation (5.51) where there is no optimization involved. Cox (1973) pointed out that $\hat{\underline{\underline{Q}}}^{-1}$ in $\cos^2(\underline{a},\underline{d};\hat{\underline{\underline{Q}}}^{-1})$ is equivalent to $\cos^2(\underline{a},\underline{d};\underline{\underline{I}})$ with multiplications of scaling factors to the projections of $\underline{a}$ and $\underline{d}$ on the eigenvectors of $\hat{\underline{\underline{Q}}}$.

Since $\underline{\underline{\hat{Q}}}$ has been normalized to have its trace equal to N, $\sum_{n=1}^{N} \lambda_n = N$. The scaling factors associated with $\underline{\underline{\hat{Q}}}^{-1}$ are $\sqrt{1/\lambda_n}$ which emphasizes components of $\underline{a}$ and $\underline{d}$ corresponding to small eigenvalues of $\underline{\underline{\hat{Q}}}$, and de-emphasizes components corresponding to large eigenvalues of $\underline{\underline{\hat{Q}}}$. Therefore the quantity $\left\{\frac{\underline{d}' \cdot \underline{\underline{\hat{Q}}}^{-1} \cdot \underline{d}}{\underline{a}' \cdot \underline{\underline{\hat{Q}}}^{-1} \cdot \underline{a}}\right\} \cos^2(\underline{a},\underline{d};\underline{\underline{\hat{Q}}}^{-1})$ gives rise to signal gain, for the assumed signal direction. $\left\{\frac{\underline{d}' \cdot \underline{\underline{\hat{Q}}}^{-1} \cdot \underline{d}}{\underline{a}' \cdot \underline{\underline{\hat{Q}}}^{-1} \cdot \underline{a}}\right\}$ defines the maximum possible gain, and $(\underline{a}' \cdot \underline{\underline{\hat{Q}}}^{-1} \cdot \underline{a})$ suppresses the noise. The choice of $\underline{\tilde{W}}'$ results in the optimal estimator which provides the maximum gain for $\underline{a} = \underline{d}$ and optimal suppression for $\underline{a} \neq \underline{d}$.

5.4.5 Grass Valley data processing method

Transient-free quiet-interval data blocks from each of the 12 elements of the array are selected for processing. The number and length of the data blocks are selected on the basis of resolution and statistical stability of the estimated power spectral density. A MLM comparison for different numbers and lengths of data blocks, holding the total number of data points constant, is illustrated with array data from site E5.9W (Figure 5.7). The results of processing the identical data using three different lengths are shown in Figure 5.8 for 12 blocks x 128 points, 24 blocks x 64 points, and 48 blocks x 32 points. The 12 blocks x 128 points (Figure 5.8A) provides the highest resolution, indicating the multiple directions of propagation. However, the greater number of data points in the time domain requires the analysis of more frequency components and the FKPSD estimated in such a way is statistically less stable than the smaller number of data points. The 48 blocks x 32 points (Figure 5.8C) has only 16 discrete frequency components from DC to Nyquist frequency. In this case, the coarse frequency interval may result in an erroneous phase velocity estimate. I, therefore, have selected 24 blocks x 64 data points (Figure 5.8B). to process Grass Valley array data; this combination provides adequate resolution in wavenumber space and reasonable stability in the statistical estimation. In the figures, FKPSD are estimated for a desired frequency component at each of 41 x 41 grid points in wavenumber space, then normalized with respect to peak value and contoured in dB. Normally, data are processed in a wide frequency band and the maximum FKPSD of each frequency component is plotted as shown in Figure 5.9 for data from sites E5.9W, GP, and A2N. Those frequencies corresponding to the FKPSD maxima are selected for interpretation. The wavenumber and frequency of a FKPSD maximum provides the estimate of apparent phase velocity and direction of propagation for the most coherent propagating plane wave in the data sample. In case the microseismic field has very low coherence across the array sensors, the plot of maximum FKPSD over a wide frequency band will show a low normalized curve without distinct peaks. Accordingly, in Figure 5.9, the coherence of array data recorded at site A2N is higher than that recorded at site GP in the frequency band of 2.54 Hz to 12.9 Hz. A comparison of BFM and MLM is provided in Figures 5.8B and 5.8D for the case of 24 blocks x 64 points. The greater resolution in MLM is apparent in resolving the multiple directions of propagation. Consequently, our processing method was normally MLM using 24 blocks x 64 points.

5.5 Grass Valley data interpretation

Valley sites. The noise anomaly in the center of the valley, e.g. E5.9W at 5 to 7 Hz (Figure 4.4B), can be explained by the superposition of multi-path surface waves propagating in the shallow alluvial section. The absence of a unique and time-invariant propagation direction, as seen in Figure 5.10, indicates clearly that the high amplitude ground noise at this site is not due to a local buried source. Further, the uniform propagation velocity, $|k| \cong 16$ cycles/km, seen at all azimuths suggests a surface wave nature of the noise field. Similar multi-azimuth surface waves are seen also in the f-k results at 5.71 Hz for the array data at sites E0.5W and M2.9N (see Figure 3.4 for site locations).

Leach Hot Springs. Time-invariant azimuths of propagating noise fields are seen at sites A2N, B0.35W, E2.9E, and GP (see Figure 3.2 for site locations) in the vicinity of Leach Hot Springs. Typical noise data recorded in this area show highly coherent energy in the array. Data from site A2N are shown in Figure 5.11. Except at B0.35W, the dominant frequency of the propagating noise field in the area is 4.4 Hz. The f-k plots at this frequency are shown in Figures 5.12A, 5.12C, and 5.12E. The unique azimuth in each plot is in a direction away from the hot springs. At B0.35W the dominant frequency of noise field is 2.8 Hz. In the same frequency band, we also see distinct 2.5 Hz noise components at sites A2N and GP. Noise in this lower frequency band propagates constantly during quiet recording periods at an azimuth around 210°, as indicated in Figures 5.12B, 5.12D, and 5.12F for sites A2N, GP, and B0.35N. The phase velocities estimated from these plots indicate that the microseisms are apparently fundamental mode Rayleigh waves.

Another interesting feature appears at C6W and at the intersection of lines L and H (site LH) where f-k analyses indicate that the noise fields at both sites propagate away from the hills (Figures 5.13C, 5.13D, 5.13E and 5.13F). There is a possibility that the hills respond to gusty winds and generate ground noise.

5.6 Dispersion characteristics and shallow structure

On the assumption that the microseismic field consists of surface waves, the f-k analysis technique allows direct measurement of the local dispersion curve by selecting phase velocities corresponding to the frequencies with peak FKPSD. As an example, in Figure 5.14 we show phase velocities so estimated, along with computed fundamental and first higher mode Rayleigh wave dispersion curves, for a model based on P-wave velocities from a shallow refraction survey in the area. The effect of the very shallow velocity structure is illustrated clearly. Lateral variations in the upper 10-20 m will control the surface wave propagation characteristics. In estimating dispersion curves, we do not restrict sampling to the quiet periods, since larger microseisms are very coherent across the array. The dispersion measurements, besides providing local observations of phase velocity for shallow structure mapping, also provide a method of verifying the wave nature of the microseisms. It is clear that waves with periods of 1 sec and greater must be analyzed for structural information at geothermal target depths, if the microseisms are fundamental mode Rayleigh waves (see, for example, McEvilly and Stauder, 1965).

FIGURE CAPTIONS

Figure 5.1 Estimated coherence near Leach Hot Springs for various geophone spacings of (A) 10 m, (B) 30 m, (C) 40 m, and (D) 60 m in a single line. Note the coherence decreases as geophone spacing increases, along with narrower coherent frequency bands. Frame E is the typical VSD of this site.

Figure 5.2 Estimated coherence at valley sites, EM (A-D) and E2.75W (E), for linear geophone spacings of (A) 20 m (NS direction), (B) 20 m (EW direction), (C) 40 m, (D) 60 m, and (E) 120 m.

Figure 5.3 Array configuration and its contoured impulse response in wavenumber space, plotted to kx and ky = 71 cycles/km. The effective Nyquist wavenumber can be seen to vary with azimuth in the range of about 50 - 70 cycles/km. The interior square outlines the standard f-k plot range of 35.7 cycles/km, used in subsequent figures. Radii of the concentric circles in array are indicated.

Figure 5.4 High-resolution f-k power spectral density estimates for a simulated 4 Hz plane wave signal propagating N60°E across the array at horizontal phase velocity 200 m/s (k=20 cycles/km), to illustrate spatial aliasing. The array configuration is the same as shown in Figure 5.3. The array dimension scales are (A) 1 time, (B) 1.5 times, (C) 5 times, (D) 10 times, the radii values indicated in Figure 5.3. The maximum kx and ky values in the plots are (A) 71.4, (B) 47.6, (C) 14.3, (D) 7.1 cycles/km corresponding approximately to the effective Nyquist wavenumbers for the arrays.

The f-k power spectral density contours are -1.0, -3.0, -6.0, -9.0, -12.0 dB below the main peak. Circles indicate the constant velocities shown, expanding with array size. Aliasing is apparent in the high phase velocities in Frames (B), (C), and (D), easily misinterpreted as detected body waves. The 90% confidence limits on the estimated FKPSD are ± 1.9 dB, based on the multiple of chi-square variable with approximately 26 degrees of freedom.

Figure 5.5 Noise-free simulated 4 Hz plane waves crossing the array of Figure 5.3 with horizontal phase velocity of 200 m/sec.

Figure 5.6 Comparison of f-k resolutions using BFM (A) and MLM (B to F) on the simulated plane waves shown in Figure 5.5, with noise added. MLM resolution deteriorates as the signal-to-noise ratio of the input data varies from (B) 48.8 dB, (C) 30.6 dB, (D) 25.6 dB, (E) 20 dB, to (F) 10.6 dB, whereas BFM is insensitive to signal-to-noise ratio in the same range. The BFM resolutions for all noise levels are all identical to (A). Contoured lines are at -1, -3, -6, -9, and -12 dB below the main peak.

Figure 5.7 Typical seismic noise data in the valley, at site E5.9W, recorded by the array shown in Figure 5.3. The difference in signal amplitude among traces is a consequence of the difference in geophone damping resistor of each channel. The scale factor, in 10^{-9} m/sec per cm of displayed record amplitude, at 4.5 Hz, are shown for each trace on the right margin.

Figure 5.8 f-k results for site E5.9W for different data block lengths, comparing MLM and BFM.

(A) 12 data blocks, each with 128 points, processed by MLM, with 90% confidence limits of ± 7.7 dB.

(B) 24 data blocks, each with 64 points, processed by MLM, with 90% confidence limits of ± 1.96 dB,

(C) 48 data blocks, each with 64 points, processed by MLM with 90% confidence limits of ± 1.16 dB,

(D) 24 data blocks, each with 64 points, processed by BFM, with 90% confidence limits of ± 1.4 dB.

The frequency on each frame corresponds to a maximum FKPSD (see Figure 5.9). The range of wavenumber plotted is 35.7 cycles/km. Contour lines are at -1, -3, -6, -9, and -12 dB below the main peak.

Figure 5.9 Examples of maximum FKPSD plots as a function of frequency, independent of the wavenumber. The maximum FKPSD at each frequency is normalized with respect to a common, reference power level. Array data are taken from sites A2N, E5.9W and GP.

Figure 5.10 The time-variant nature of propagating seismic noise at valley site E5.9W. Data are selected from the 4th, 5th, 7th, 8th, 9th, and 10th hours of the recording period, as indicated, and processed by MLM using 24 blocks with 64 points per data block. Circles indicate velocities of peaks given along with azimuth in each plot.

Figure 5.11 Typical seismic noise data at site A2N, 1 km SE of Leach Hot Springs, recorded by the array shown in Figure 5.3. Note the high coherence across the array. The difference in signal amplitude among traces is resulted from the different geophone damping resistor of each channel. The scale factor, in 10^{-9} m/sec per cm of displayed record amplitude, at 4.5 Hz, are shown for each trace on the right margin.

Figure 5.12 High-resolution f-k results in wavenumber space for sites A2N, GP, E2.9E, and B0.35W located near Leach Hot Springs. The frequency on each frame corresponds to a maximum in the maximum FKPSD plot (Figure 5.9). The maximum wavenumber plotted is 35.7 cycles/km, except for frame (F), where it is 17.9 cycles/km. The contoured lines are -1, -3, -6, -9, and -12 dB below the main peak. The horizontal phase velocity and the time-invariant direction of the propagating seismic noise field are indicated on each frame. These noise components are apparently fundamental mode Rayleigh wave generated at the hot springs, where near-surface velocities exceed 4 km/sec.

Figure 5.13 High-resolution f-k results in wavenumber space for sites B2.6W, C6W and LH. The maximum wavenumber plotted in 35.7 cycles/km. The contoured lines are -1, -3, -6, -9, and -12 dB below the main peak.

Figure 5.14 Rayleigh wave dispersion curves for fundamental and first higher modes, computed for the model shown, compared with observed ground noise phase velocities at site E5.9W.

The observed phase velocities were determined at various times by f-k analysis, the hour indicated by symbol type.

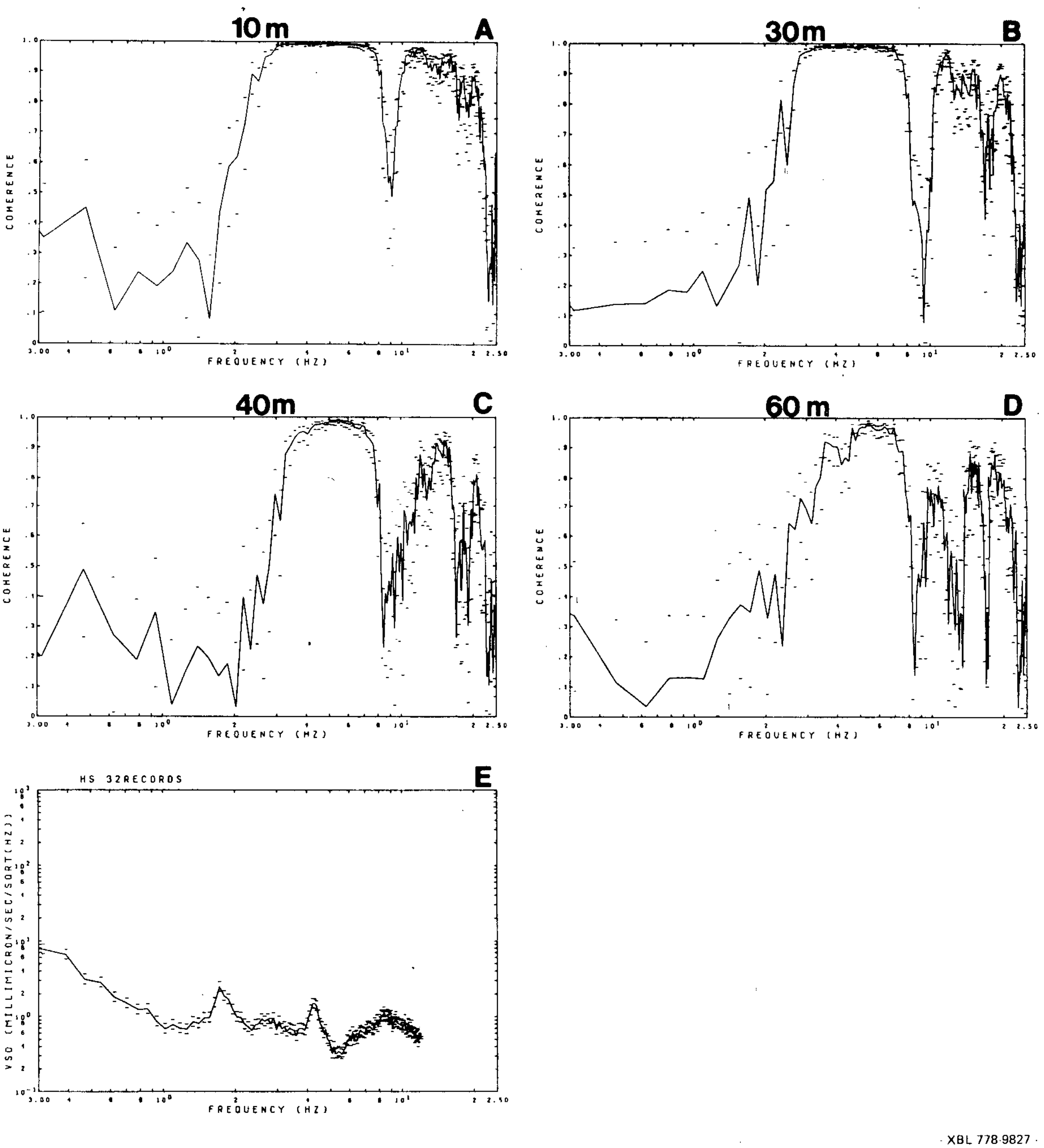
10m
A
30m
B
40m
C
60m
D
HS 32RECORDS
E
COHERENCE
FREQUENCY (HZ)
VSD (MILLIMICRON/SEC/SQRT(HZ))
XBL 778-9827

Figure 5.1

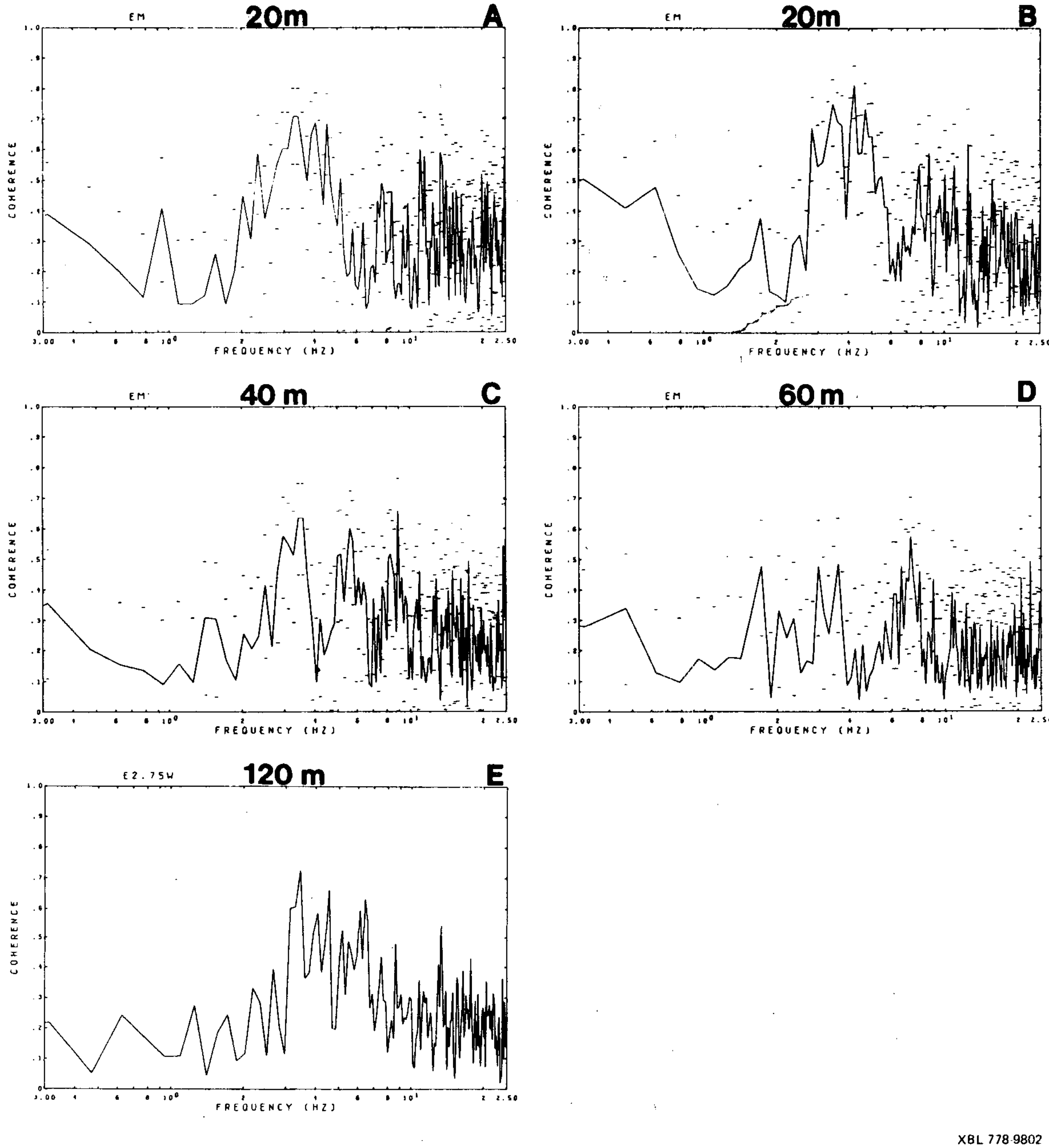
EM
20m
A
COHERENCE
FREQUENCY (HZ)
EM
20m
B
COHERENCE
FREQUENCY (HZ)
EM
40 m
C
COHERENCE
FREQUENCY (HZ)
EM
60 m
D
COHERENCE
FREQUENCY (HZ)
E2.75W
120 m
E
COHERENCE
FREQUENCY (HZ)
XBL 778-9802

Figure 5.2

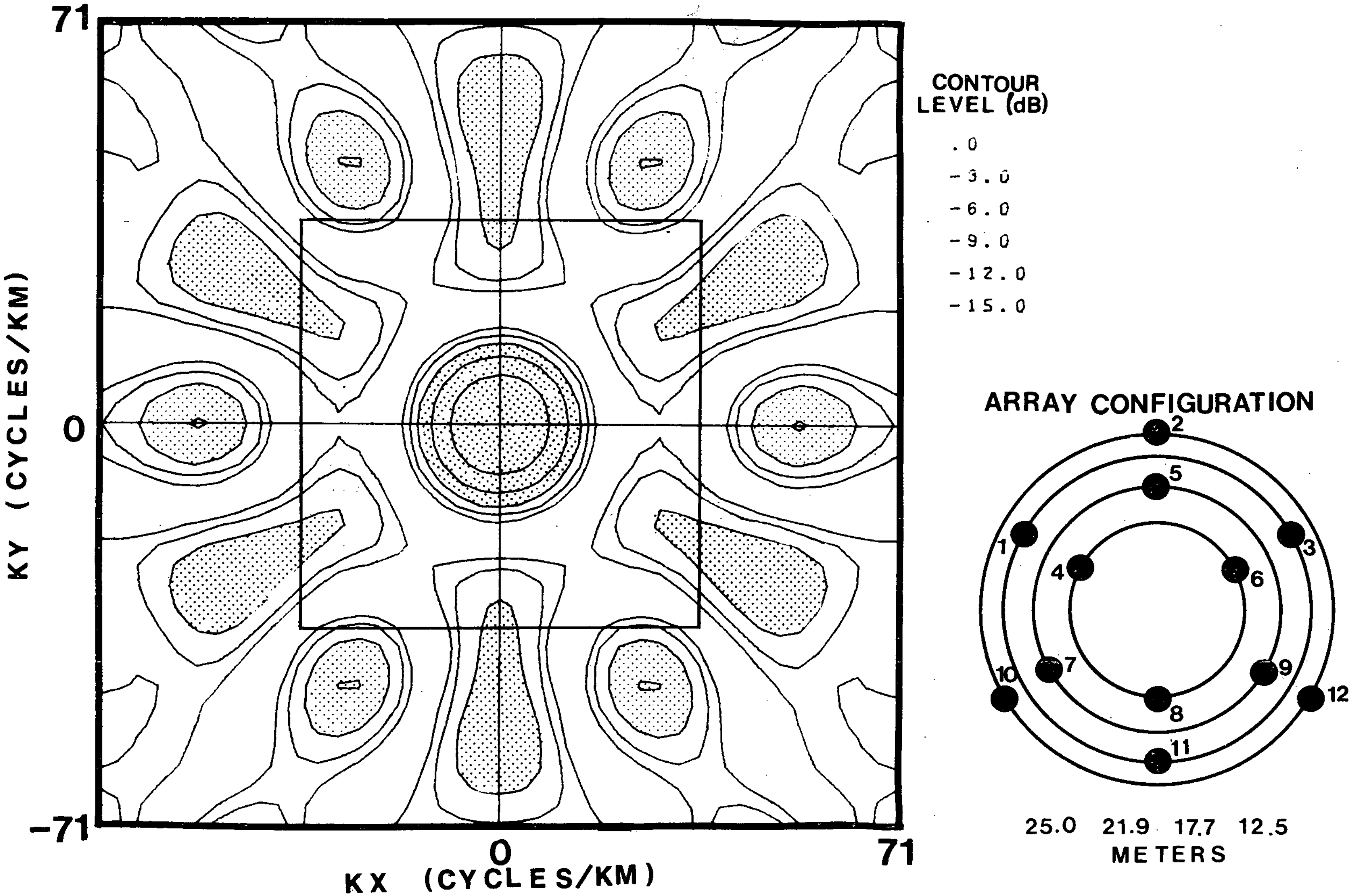

XBL 7610- 4980

Figure 5.3

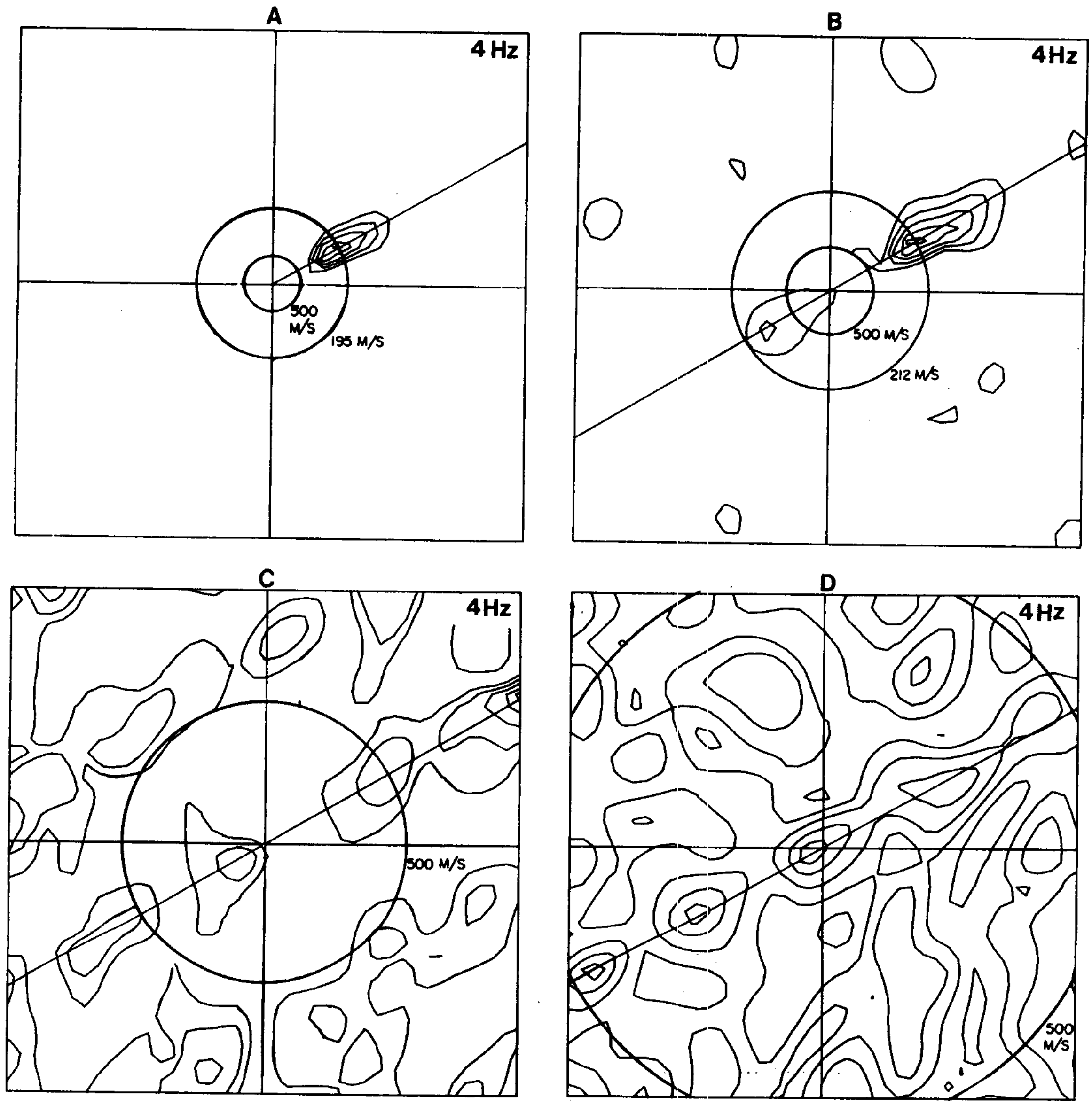

XBL 776=9467

Figure 5.4

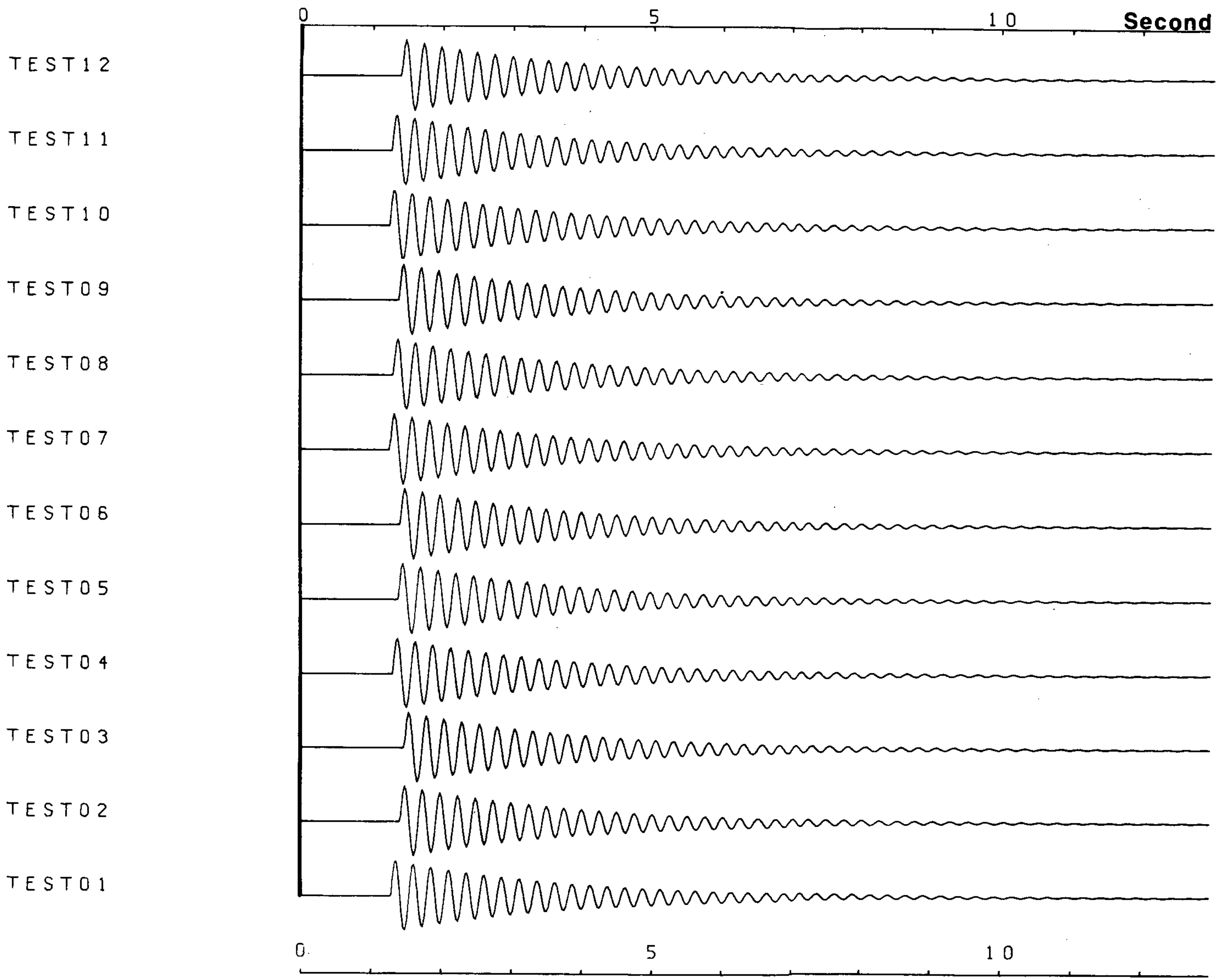

XBL 773-8115

Figure 5.5

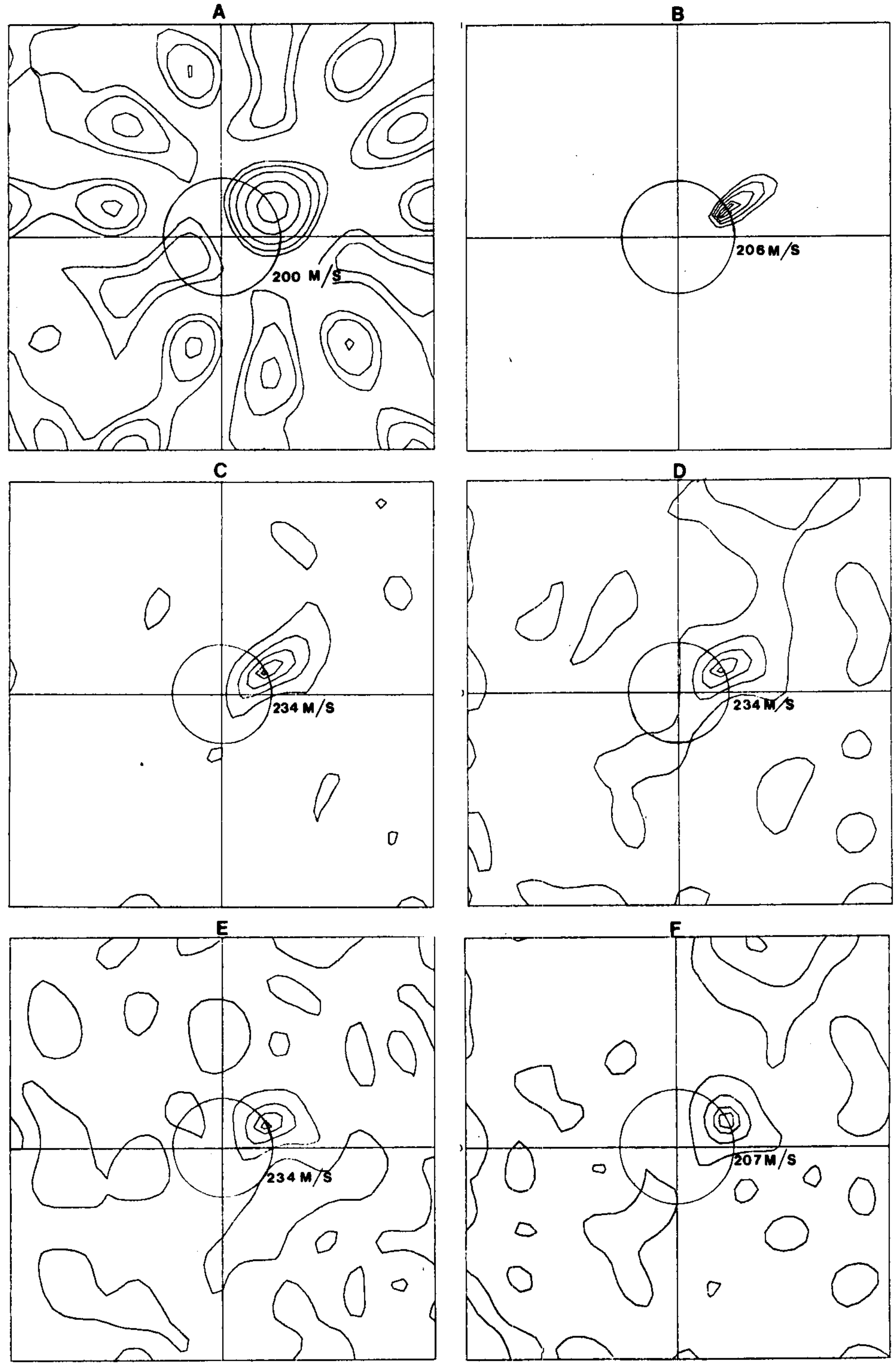

Figure 5.6

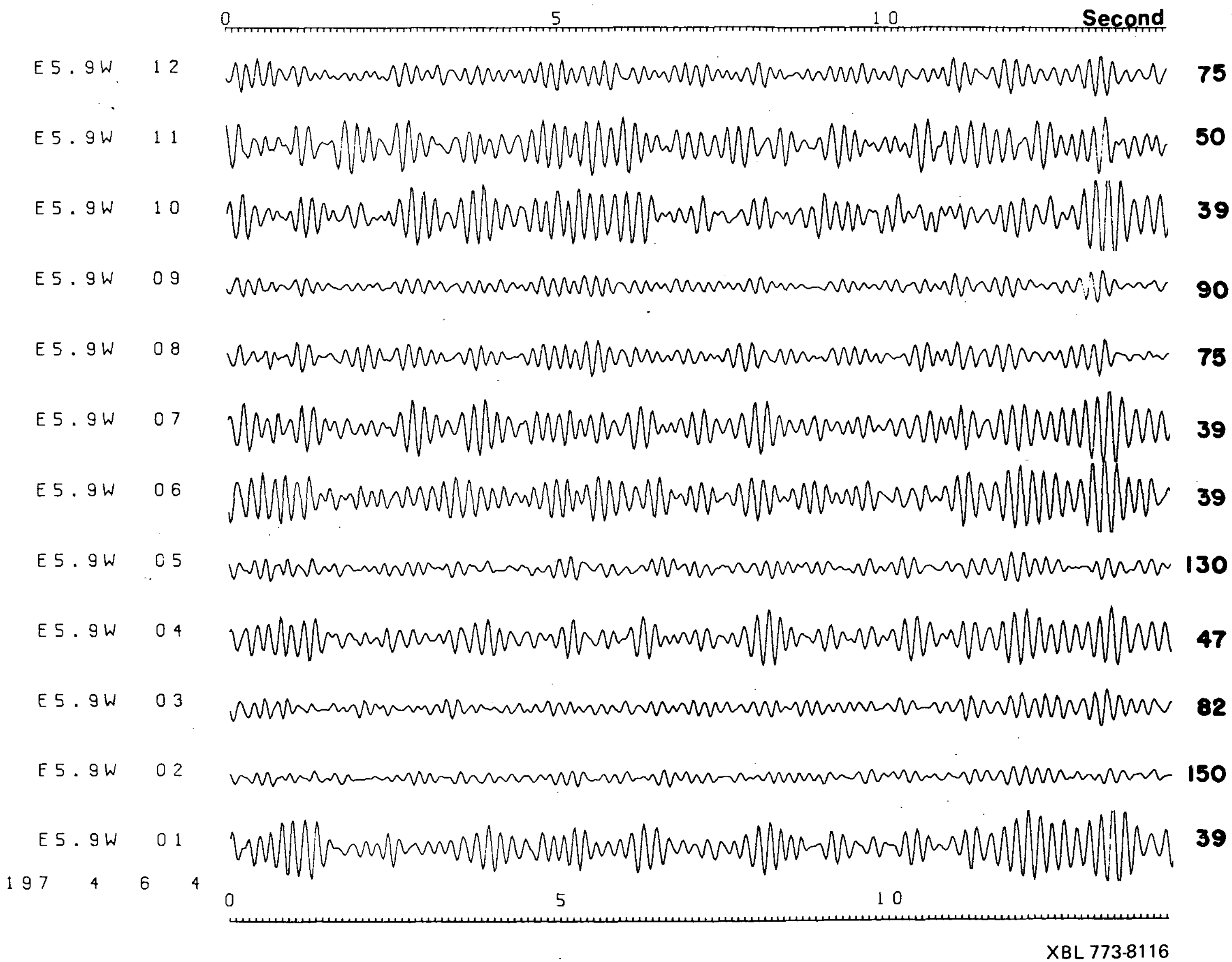

0
5
10
Second
E5.9W 12
75
E5.9W 11
50
E5.9W 10
39
E5.9W 09
90
E5.9W 08
75
E5.9W 07
39
E5.9W 06
39
E5.9W 05
130
E5.9W 04
47
E5.9W 03
82
E5.9W 02
150
E5.9W 01
39
197 4 6 4
0
5
10
XBL 773-8116

Figure 5.7

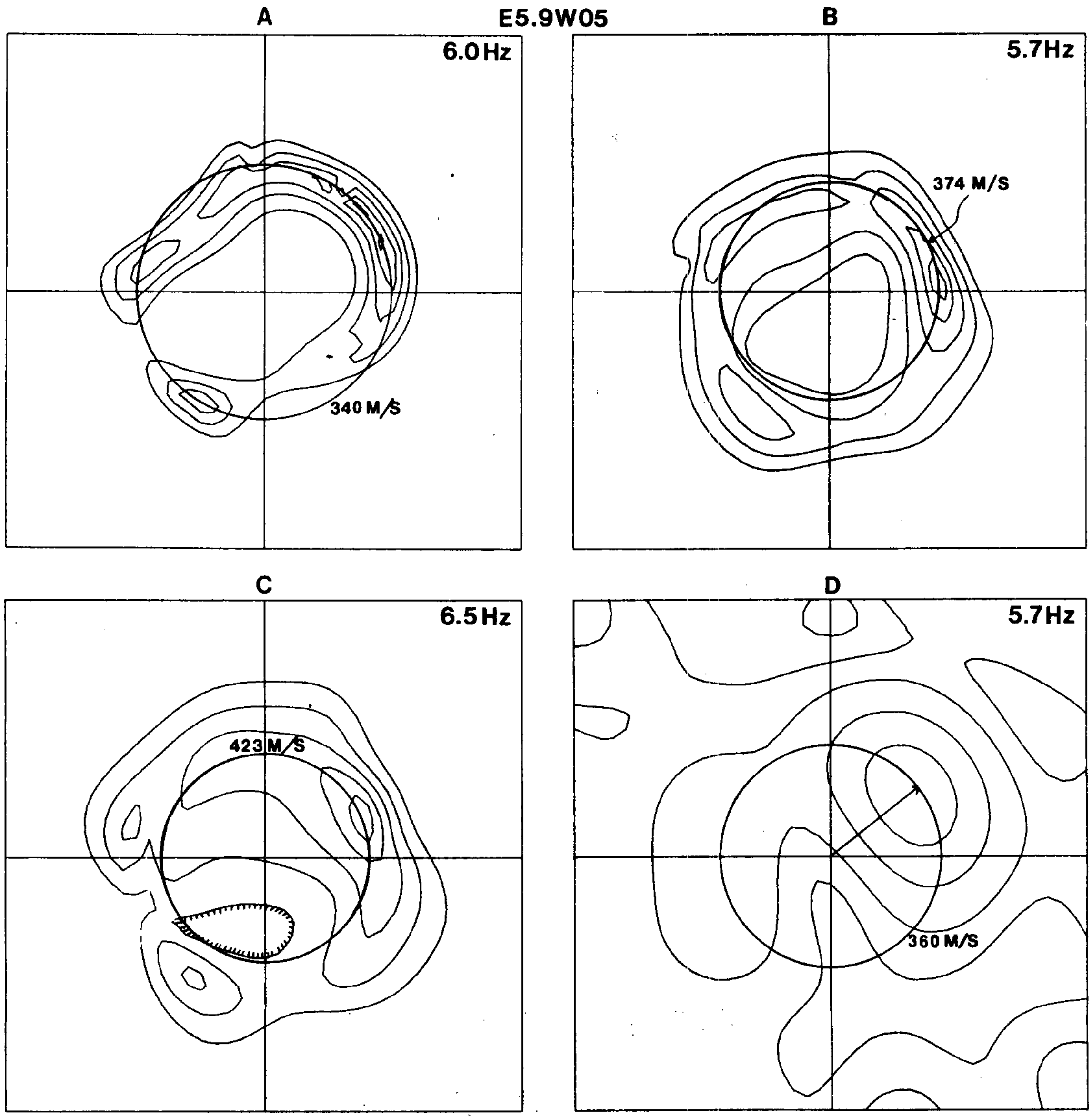

XBL 776-9468 A

Figure 5.8

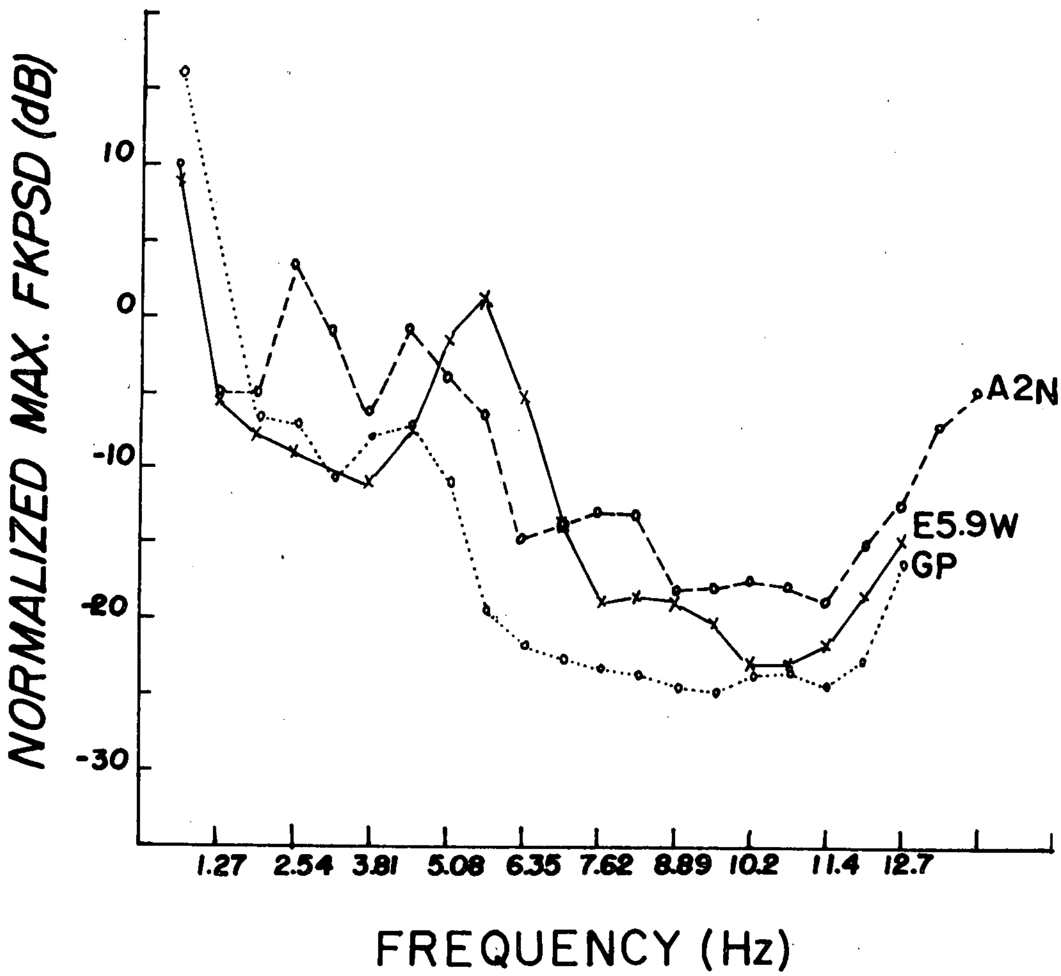

XBL 779-2463

Figure 5.9

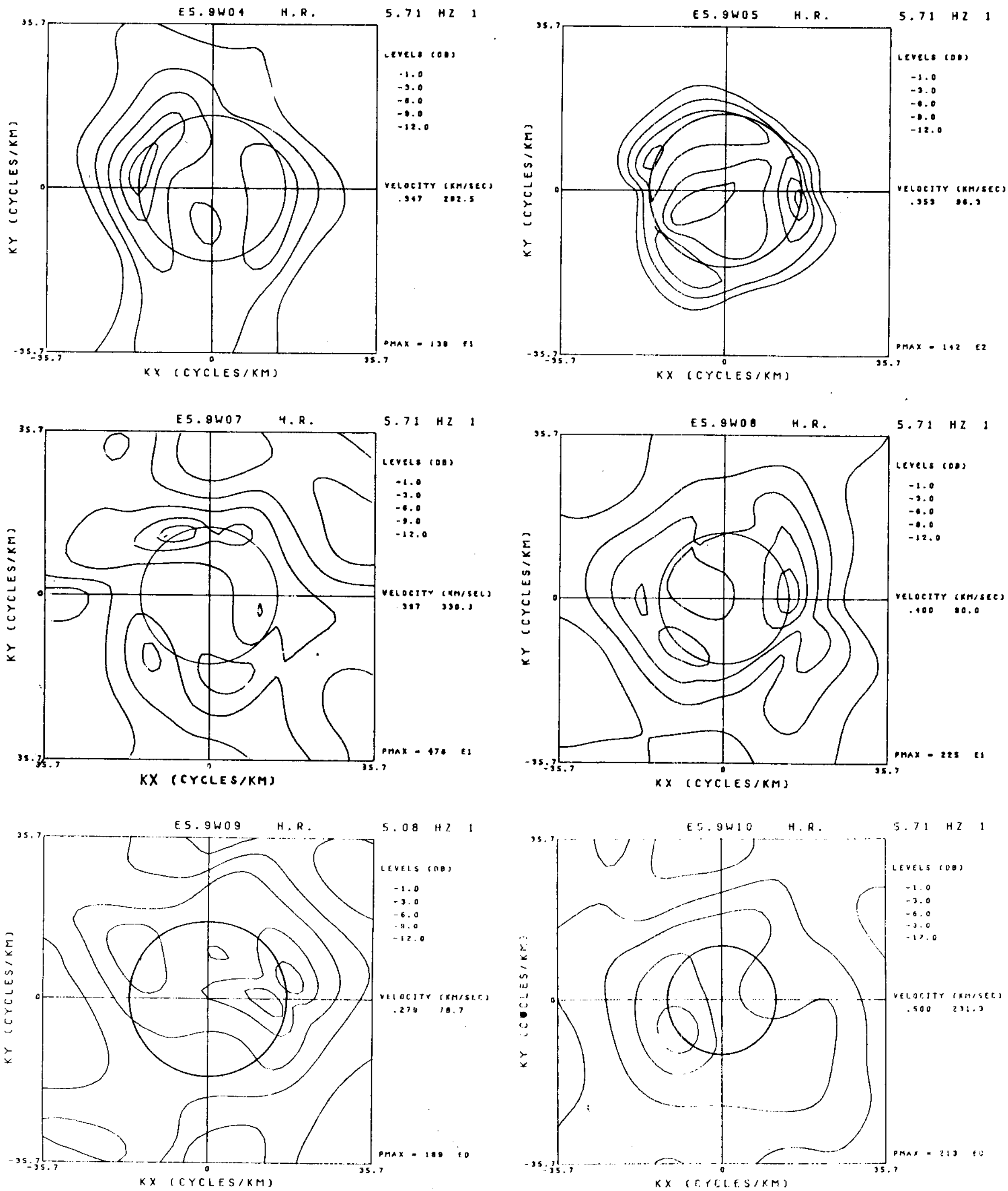

XBL 772-7631

Figure 5.10

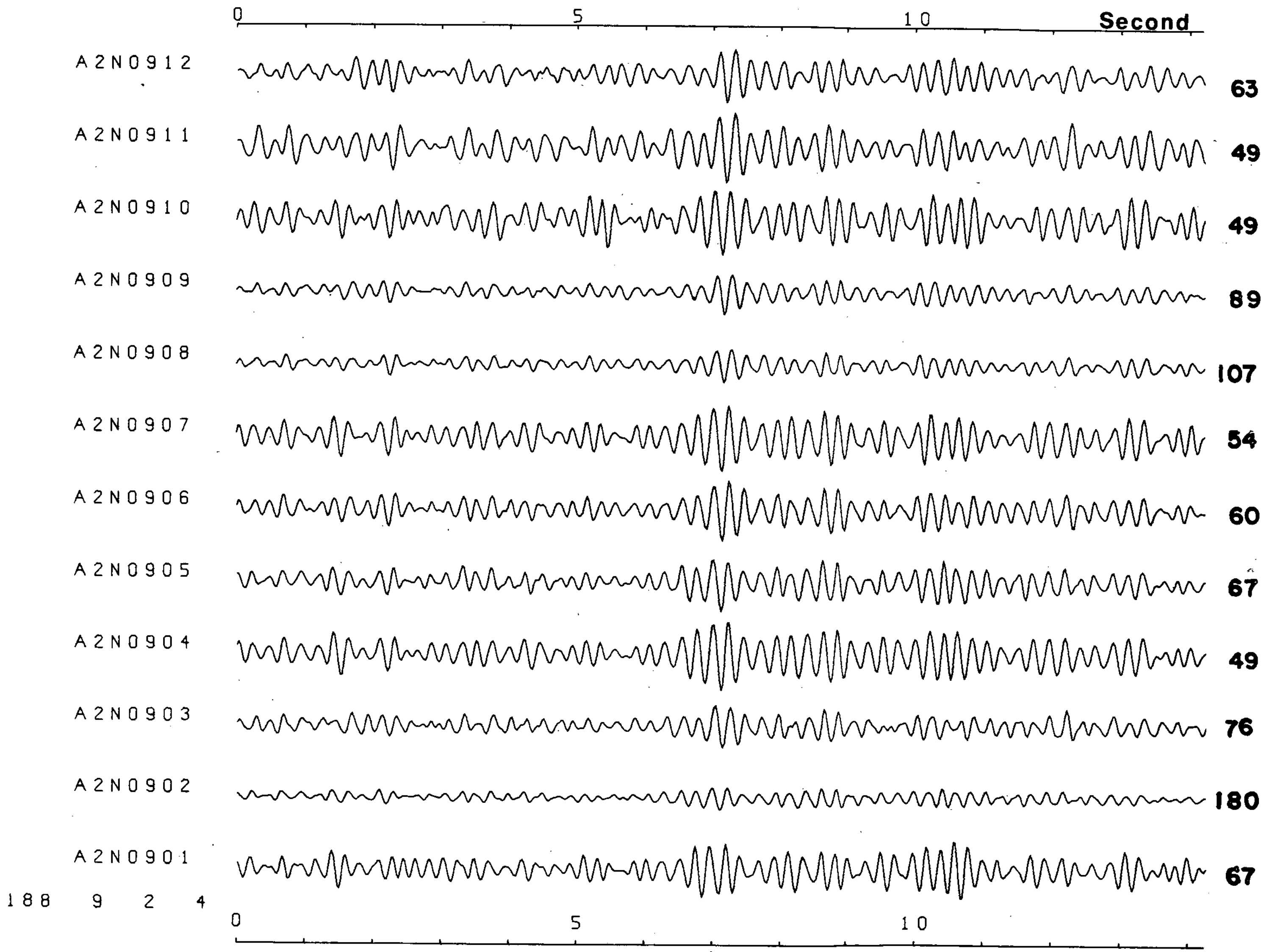

XBL 773-8117

Figure 5.11

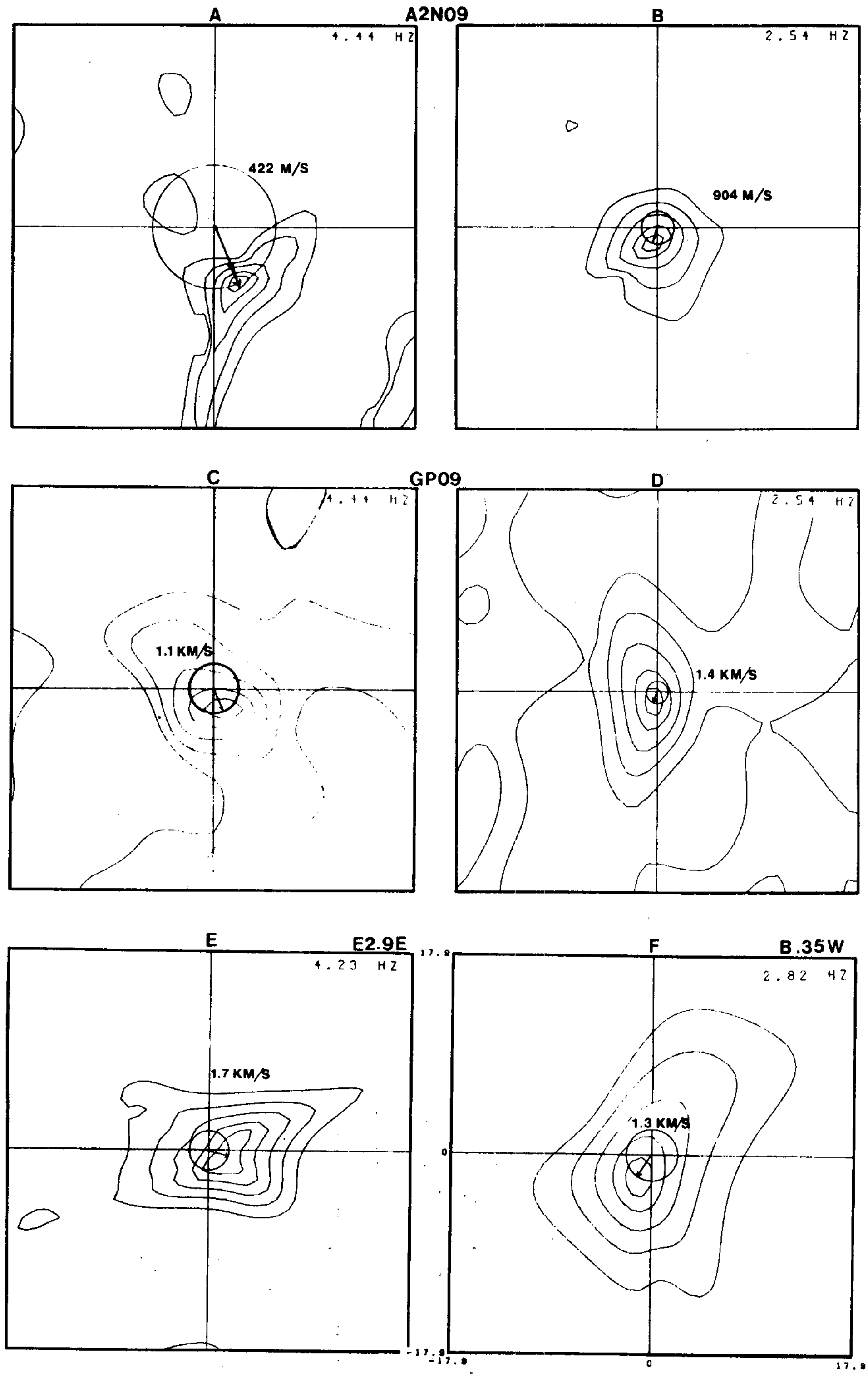

XBL 778 9801

Figure 5.12

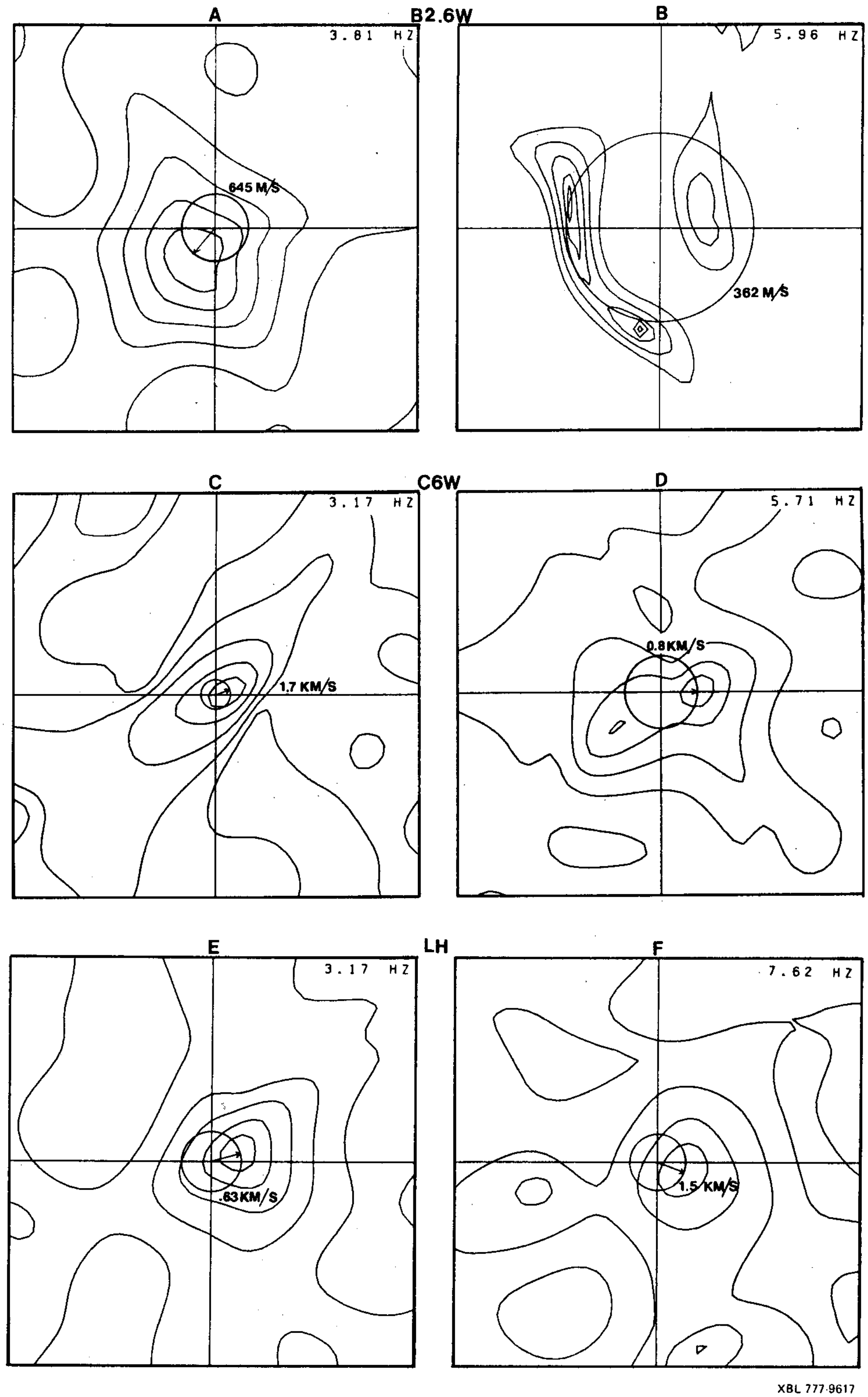
A
B2.6W
B
3.81 HZ
5.96 HZ
645 M/S
362 M/S
C
C6W
D
3.17 HZ
5.71 HZ
1.7 KM/S
0.8KM/S
E
LH
F
3.17 HZ
7.62 HZ
.63KM/S
1.5 KM/S
XBL 777-9617

Figure 5.13

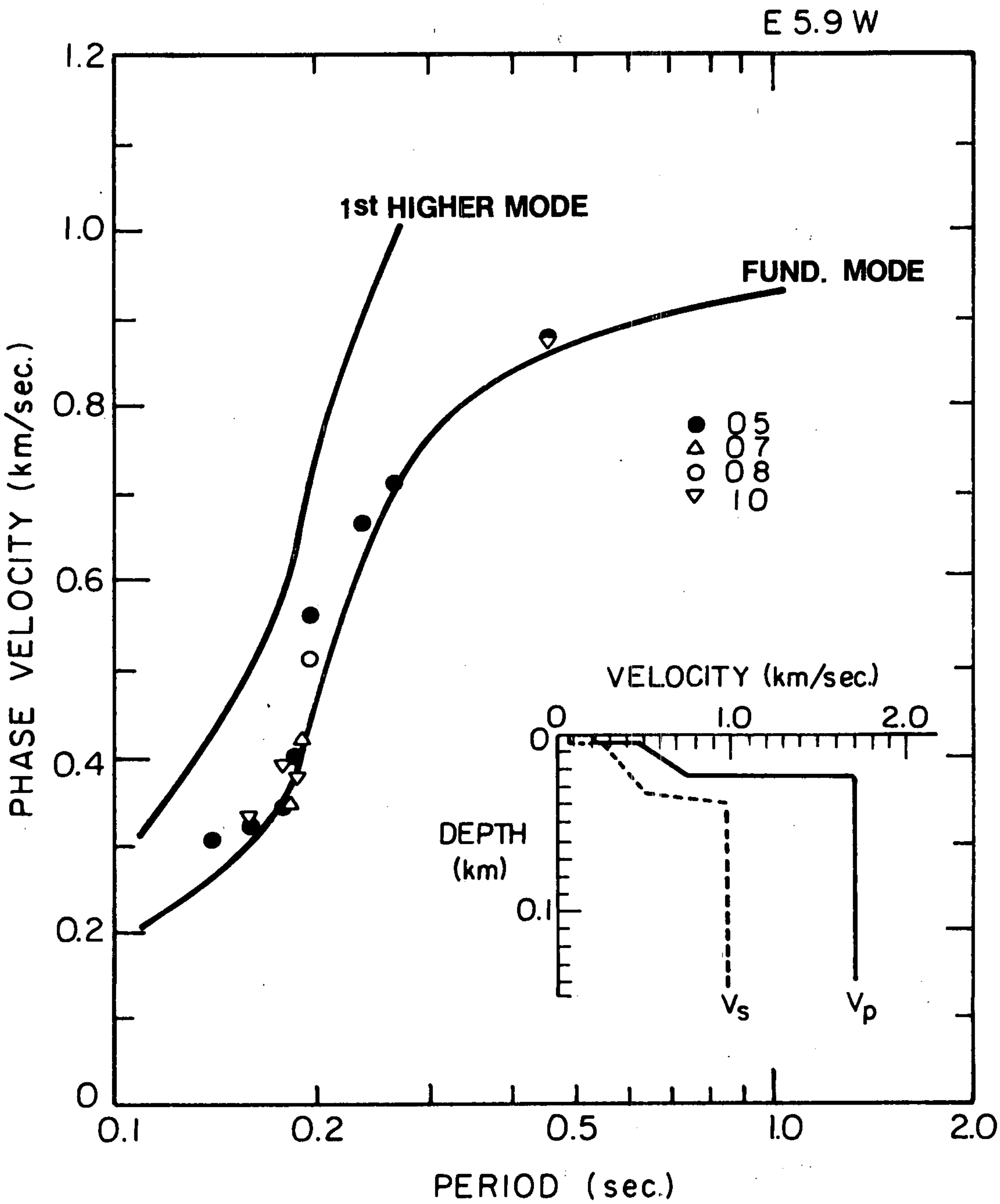

XBL 771-5005

Figure 5.14

VI. SUMMARY AND RECOMMENDATIONS

6.1 Summary

The main results of a study of microseisms in Grass Valley, Nevada, using a simple field system, are summarized below:

Diurnal variation in the 2-20 Hz noise field is regular. A consistent diurnal variation that repeats from day to day is due apparently to meteorological and cultural sources, with typically 15 dB variation seen from the mid-day high noise level to the low noise level in the early morning hours of 2-4 A.M. Secular variations, due to regional weather patterns, can produce a 5-10 dB range in the early morning minimum noise levels over a duration of a few days.

For spectral stability in investigating spatial variation of noise, at least 28 quiet data blocks, each 12.8 sec long, were taken simultaneously at the network stations and the spectra were averaged for each site. This procedure produced consistent results throughout the area, revealing a characteristically low amplitude smooth noise spectra at hard rock sites, a prominent peak at 4-6Hz at valley sites, and wideband, high amplitude noise, apparently due to very shallow sources, at hot springs sites. Contour maps of noise level, normalized to a reference site, are dominated by the hot springs noise levels outlining the regions of maximum alluvium thickness. Major faults are evident when they produce a shallow lateral contrast in rock properties.

Microseisms in the 2-10 Hz band are predominantly fundamental mode Rayleigh waves, characterized by low velocities and wavelengths as small as 20 m, requiring closely spaced arrays for adequate spatial sampling.

High resolution f-k processing, with proper data sampling, provides a powerful technique for mapping the phase velocity and the direction of propagation of the noise field, revealing local sources and lateral changes in shallow subsurface structure.

No evidence for a significant body wave component in the noise field was found, although it becomes clear that improper spatial sampling can give a false indication through aliasing. Noise emanating from a deep reservoir would be evident as body waves and could be traced to its source given a reasonably accurate velocity model.

6.2 Recommendations

Conventional seismic ground noise surveys, conducted as outlined in this study, require a large number of stations for economical implementation. With 100 stations, for example, a week-long survey could provide maps of noise amplitude distribution, P-wave delay time, and microearthquake locations, as well as f-k analyses at many sites, utilizing a 2-3 man crew. It is not clear, however, that such data will be of significant value in delineating a geothermal reservoir.

The amplitude mapping of ground noise in certain frequency bands is a poor exploration technique for delineating buried geothermal systems. The results of the survey described in Chapter 4 indicate that the amplitude variations of microseisms in an area are controlled by the near-surface geology, especially lateral variations in thickness of the alluvial layer. The large amplitude surface wave generated by surface sources and propagating horizontally, will mask weak seismic waves emitted from a buried source. Therefore, amplitude mapping only reveals information on the very shallow structure.

On the other hand, the technique of f-k analysis can, theoretically, map the wavenumber of the microseisms, discriminating the vertically incident body waves from the surface waves. The yet open question of whether a reservoir acts as a radiator of seismic body waves can be answered through careful f-k analyses in existent geothermal areas. The array to be used for further study must be a non-aliased array of larger diameter than that used in this study. The expansion in array size will improve the resolution around the origin of the f-k diagram. This improvement would provide a more accurate estimate for power at the small wavenumbers, such that the azimuth and the apparent velocity of the long-wavelength body waves are estimated more accurately. The amplitudes of body waves radiating from a source at depth are apparently much smaller than those of the ambient surface waves. In order to extract useful information from the body waves, a sophisticated signal detection and processing scheme is required. However, the f-k analysis technique may fail to detect the geothermal system at depth if our assumption of body wave radiation from the reservoir is not valid, or if the emanating body waves are either attenuated or completely masked by the ambient surface waves. It is fortunate that the ambient surface waves have shorter wavelengths that the body waves because then the detection of weak body waves can be improved by designing a more sophisticated array to cancel short wave-lengths, as is commonly done in conventional seismic reflection surveying.

If the assumption about radiated body waves is indeed valid, and such body waves are detectable, we can trace the recorded wavefronts to their source, given a reasonably accurate velocity model. There are two schemes which have been used for projecting waves observed at the surface back into the earth and locating the source region, and these methods may be applicable to the geothermal reservoir delineation problem.

The first method is seismic ray tracing described by Julian (1970); Engdahl and Lee (1976). If the array diameter is much smaller than the distance to the buried source, the microseismic field propagates as a plane wave across the array. Estimation of the azimuth and the apparent velocity of the propagating noise field from f-k analysis along with the knowledge of the near-surface velocity distribution, can give us the incident angle of noise. Given a reasonable velocity structure in the area and simultaneously occupied array sites, we can reconstruct ray paths to each site. The intersection of these ray paths outlines the region of the radiating source.

Another approach is much like that used in a conventional reflection survey with two-dimensional surface coverage but without a surface controlled source. The coherent noise fields recorded by a two-dimensional surface array are projected downward into the assumed subsurface model. The reconstruction of the coherent noise field propagating in an upward direction, at a selected frequency, can be carried out by the wave equation migration technique, using a finite-difference approximation such as described by Claerbout (1976). The restriction of this approach to microseismic data is that the noise field must propagate as a spherical wavefront across the geophone array. The spherical wavefront exists in the situation where the array dimension is greater than the distance to the source. In this case, we can outline the region of radiating sources in terms of the convergent pattern of the extrapolated wave fields.

It is clear that the ray tracing and the wave equation migration are applicable at different source-array distances in the application of delineating geothermal reservoirs. In a practical exploration program, we do not know the depth of geothermal reservoirs, nor do we know the shape of the wavefront across the array. One way of solving the problem is to place a non-aliased array at several sites and search for the evidence of time-invariant, high velocity body waves. As soon as the body waves are detected, one may compare several f-k diagrams, using data of identical recording periods but of different sizes of sub-array. The deterioration of the resolution in the f-k diagrams as we expand the size of the sub-array, indicates that the plane wave assumption is violated and the wavefront migration techniques should be applied. On the other hand, if the noise fields propagate as plane waves across the large array, the resolution in the f-k diagrams will be improved as we expand the size of sub-arrays and the f-k analysis with seismic ray tracing are the proper techniques to locate the noise source.

Based on this study, I conclude that, if the geothermal system is indeed emanating detectable body waves, the analysis of ambient ground motion or seismic noise, can be applied to the delineation of geothermal reservoirs. In fact, if the radiated body waves exist, the method can be one of the most effective geophysical methods in geothermal explorations.

REFERENCES

Båth, M., 1974, Spectral analysis in geophysics: p. 448-462, Elsevier Scientific Publishing Company.

Beyer, A., Dey, A., Liaw, A., Majer, E., McEvilly, T.V., Morrison, H.F., and Wollenberg, H., 1976, Geological and geophysical studies in Grass Valley, Nevada: Preliminary open file report, LBL-5262.

Bendat, J.S., and Piersol, A.G., 1971, Random data: Analysis and measurement procedures, Wiley interscience, p. 193-194.

Borcherdt, R.D., 1970, Effects of local geology on ground motion near San Francisco Bay: Bull. Seismol. Soc. Am. vol. 60, p. 29-61.

Brillinger, D.R., 1975, Time series: data analysis and theory: Holt, Rinehard and Winston Inc., p. 125 and p. 151.

Brune, J.N., and Oliver, J., 1959, The seismic noise of the earth's surface: Bull. Seismol. Soc. Am. vol. 49, p. 349-353.

Burg, J.P., 1964, Three-dimensional filtering with an array of seismometers: Geophysics. vol. 29, p. 693-713.

Capon, J., 1969, High-resolution frequency-wavenumber spectrum analysis: Proc. IEEE, vol. 57, p. 1408-1418.

Capon, J., 1973, Signal processing and frequency wavenumber spectrum analysis for a large aperture seismic array: in Methods of Computational Physics vol. 13, p. 1-59, Academic Press.

Capon, J., Greenfield, R.J., and Kolker, R.J., 1967, Multidimensional maximum-likelihood processing of a large aperture seismic array, Proc. IEEE, vol. 55, p. 192-211.

Capon, J., and Goodman, N.R., 1970, Probability distributions for estimators of the frequency-wavenumber spectrum; Proc. IEEE, vol. 58, p. 1785-1786.

Claerbout, J.F., 1976, Fundamentals of geophysical data processing, McGraw-Hill Book Company, p. 184-226.

Clacy, G.R.T., 1968, Geothermal ground noise amplitude and frequency spectra in New Zealand volcanic region: J. Geophys. Res. vol. 73, p. 5377-5383.

Combs, J., and Rotstein, Y., 1975, Microearthquake studies at the Coso geothermal area, China Lake, California: 2nd U.N.Sym. on the Dev. and Use of Geothermal Resources, San Francisco, 1975, p. 909-916.

Cox, H., 1973, Resolving power and sensitivity to mismatch of optimum array processors: Jour. Acoustical Soc. of A., vol. 54, no. 3, p. 771-785.

Douze, E.J., 1967, Short-period seismic noise: Bull. Seism. Soc. Am., vol. 57, p. 55-81.

Douze, E.J., and Sorrells, G.G., 1972, Geothermal ground-noise surveys: Geophysics, vol. 37, p. 813-824.

Engdahl, E.R., and Lee, W.H.K., 1976, Relocation of local earthquakes by seismic ray tracing: J. Geophys. Res., vol. 81, p. 4400-4406.

Fix, J.E., 1972, Ambient earth motion in the period range from 0.1 to 2560 sec.: Bull. Seism. Soc. Am., vol. 62, p. 1753-1760.

Frantti, G.E., 1963, The nature of high-frequency earth noise spectra: Geophysics, vol. 28, p. 547-562.

Frost, O.L., 1972, An algorithm for linearly constrained adaptive array processing: Proc. IEEE, vol. 60, p. 926-935.

Goforth, T.T., Douze, E.J., and Sorrells, G.G., 1972, Seismic noise measurements in a geothermal area: Geophysical Prospecting, vol. 20, p. 76-82.

Gutenberg, B., and Andrews, F., 1956, Bibliography of microseisms: 2nd ed., Seismological Laboratory, California Institute of Technology, Pasadena, 134 p.

Haubrich, R.A., Munk, W.H., and Snodgrass, F.E., 1963, Comparative spectra of microseisms and swell: Bull. SEismol. Soc. Am., vol. 53, p. 27-37.

Haubrich, R.A., and Mackenzie, G.S., 1965, Earth noise 5-500 millicycles per second: 2. Reaction of the earth to oceans and the atmosphere: J. Geophys. Res., vol. 70, p. 1429-1440.

Haubrich, R.A., and McCamy, K., 1969, Microseisms: Coastal and pelagic sources: Rev. of Geophys. Res., vol. 70, p. 539-571.

Iyer, H.M., 1958, A study of direction of arrival of microseisms at Kew Observatory, Geophys. Jour., vol. 1, p. 32-43.

Iyer, H.M., 1974, Search for geothermal seismic noise in the East Mesa area, Imperial Valley, California: U.S.G.S. Open-file report no. 74-96. 52 p.

Iyer, H.M., and Hitchcock, T., 1974, Seismic noise measurements in Yellowstone National Park: Geophysics, vol. 39, p. 389-400.

Iyer, H.M., and Hitchcock, T., 1976, Seismic noise survey in Long Valley, California: J. Geophys. Res., vol. 81, p. 821-840.

Jenkins, G.M., and Watts, D.G., 1968, Spectral analysis and its application: Holden-Day Inc., p. 255-257.

Julian, B.R., 1970, Ray tracing in arbitrary heterogeneous media: Tech. Note 1970-45, Lincoln Lab., Lexington, Mass.

Kanai, K., and Tanaka, T., 1961, On microtremors. VIII: Bull. of the Earthquake Res. Inst., vol. 39, p. 97-114.

Kanai, K., Tanaka, T., Morishita, T., and Osada, K., 1966, Observation of microtremors, XI (Matsushiro earthquakes swarm area): Bull. Earthquake Res. Inst., vol. 44, p. 1297-1333.

Katz, L.J., 1976, Microtremor analysis of local geological conditions: Bull. Seism. Soc. Am., vol. 66, p. 45-60.

Lacoss, R.T., Kelly, E.M., and Toksöz, M.N., 1969, Estimation of seismic noise structure using arrays: Geophysics, vol. 34, p. 21-38.

Lysmer, J., and Drake, L.A., 1972, A finite element method for seismology: in Methods in Computational Physics, vol. II, Academic Press.

Longuet-Higgins, M.S., 1950, A theroy of the origin of microseisms: Phil. Trans. Royal Soc. London, Ser. A., vol. 243, p. 1-15.

Luongo, G., and Rapolla, A., 1973, Seismic noise in Lipari and Vulcano Islands, Southern Thyrrenian Sea, Italy: Geothermics, vol. 2, p. 29-31.

McEvilly, T.V., and Stauder, W.S.J., 1965, Effect of sedimentary thickness on short-period Rayleigh-wave dispersion: Geophysics, vol. 30, p. 198-203.

Murphy, A.J., Savino, J., Rynn, J.M.W., Choy, G.L., and McCamy, K., 1972, Observations of long-period (10-100 sec) seismic noise at several worldwide locations: J. Geophys. Res. vol. 77, p. 5042-5049.

Nicholls, H.R., Rinehart, J.S., 1967, Geophysical study of geyser action in Yellowstone National Park: J. Geophys. Res. vol. 72, p. 4651-4663.

Oliver, J., and Page, R., 1963, Concurrent storm of long and ultralong period microseisms: Bull. Seism. Soc. Am., vol. 53, p. 15-26.

Peterson, J., Butler, H.M., Holcomb, L.G., and Hutt, C.R., 1976 , The seismic research observatory: Bull. Seism. Soc.Am.,Vol.66,p.2049-2068.

Sass, J.H., Lachenbruch, A.H., Monroe, R.J., Greene, G.W., and Moses, T.H., 1971, Heat flow in the western United States: J. Geophys. Res., vol. 76, p. 6376-6413.

Savino, J., McCamy, K., and Hade, G., 1972, Structures in earth noise beyond twenty seconds--a window for earthquakes: Bull. Seism. Soc. Am., vol. 62, p. 141-176.

Sorrells, G.G., McDonald, J.A., Der, Z.A., and Herrin, E., 1971, Earth Motion caused by local atmospheric pressure changes: Geophys. J.R. Astr. Soc., vol. 26, p. 83-98.

Toksoz, M.N., and Lacoss, R.T., 1968, Microseisms: mode structure and sources: Science, vol. 159, p. 872-873.

Udwadia, F.E., and Trifunac, M.D., 1973, Comparison of earthquake and microtremor ground motions in El Centro, California: Bull. Seismol. Soc. Am., vol. 63, p. 1227-1253.

Vinnik, L.P., 1971, Origin of longitudinal microseismic waves: Izv., Earth Physics, No. 10, p. 17-30.

Whiteford, P.C., 1970, Ground movement in Waiotapu geothermal region, New Zealand: Geothermics, (special issue on proceedings of the U.N. Sym. Dev. Util. of Geothermal Resources). 2(part III), p. 478-486.

Whiteford, P.C., 1975, Studies of the propagation and source locations of geothermal seismic noise, 2nd U.N. Sym. on the Dev. and Use of Geothermal Resource, San Francisco, 1975, p. 1263-1271.

Whorf, T., 1972, Teleseismic and earth noise monitoring with the Block-Moore Quartz accelerometer. Geophys. J.R. Astr. Soc., vol. 31, p. 205-238.

APPENDIX A
NOTATION

$A_m(f)$	maximum-likelihood filter coefficients
b_1	standardized bandwidth of data window
$\|B(\underline{k})\|^2$	array response function
$c(\tau,\underline{\rho})$	cross-correlation function
$c_{nn}(\tau)$	autocorrelation function
$\underline{d}$	directional vector of microseismic field
E	expectation
$E(f)$	transfer function of earth medium
f	frequency, Hz
f_H	cut-off frequency of a low-pass filter
f_L	cut-off frequency of a high-pass filter
f_p	tape recorder band width
f_s	natural frequency of geophone, Hz
G	generator constant of geophone
$G(f)$	transfer function of local geology
h	thickness of the layer
$H(f)$	transfer function of all system element
H_A	amplification of the amplifier
$H_{BW}(f)$	transfer function of Butterworth filter
$H_D(f)$	transfer function of the digitized signal
$H_g(f)$	transfer function of geophone
$H_p(f)$	transfer function of the low-pass filter in the playback system
$H_{RC}(f)$	transfer function of RC low-pass filter

I	number of data blocks
$I(f)$	source characteristic of seismic waves
j	complex i
$\underline{k}$	vector wavenumber
L	number of data points in each data block
m	index for m^{th} geophone
n	index for n^{th} geophone
N	number of geophones in the array
$P(f,\underline{k})$	frequency-wavenumber spectrum (FKPSD)
$\hat{P}(f,\underline{k})$	the BFM estimate for FKPSD
$\tilde{P}(f,\underline{k})$	the MLM estimate for FKPSD
$\underline{\underline{\tilde{q}}}$	the inverse of delayed spectral matrix
$\underline{\underline{\hat{Q}}}$	random noise spectral matrix
$\underline{r}=(x,y)$	vector of geophone location
R_D	damping resistance of geophone
$\hat{R}_{mn}(f)$	coherence function estimate between sensors m and n
R_S	geophone coil resistance
$S(f)$	power spectrum
$\hat{S}_{nn}(f)$	power spectral density estimate for the n^{th} sensor output
$\overline{S}_{mn}(f)$	averaged cross-power spectrum
$\hat{S}_{mn}(f)$	normalized cross-power spectrum
$\underline{\underline{\hat{S}}}$	normalized spectral matrix
t	time
T	length of each data block in seconds
Δt	sampling interval of the discrete time series

U	energy of the data window
$\underline{V}$	phase velocity vector
$V_n(f)$	velocity spectral density
VCOFS	VCO full scale
$w(\tau)$	data window, lag window, weighting function
$\underline{w}$	weighting vector; $\underline{\tilde{w}}$ = vector of generalized weighting function
${}^iX_n(f)$	Fourier transform of the time series ${}^i\phi_n(t)$
β	shear-wave velocity
ζ	damping factor of geophone
θ	phase angle
ν	number of degrees of freedom
$\underline{\rho}$	spatial lag
$\sigma(x,y,t,f)$	observed microseisms
$\sigma_i(x,y,t,f)$	intrinsic noise at the site
$\sigma_\ell(x,y,t,f)$	local noise component
$\sigma_m(x,y,t,f)$	microseismic component from the distance source
σ_o	noise component
σ_1	component of coherent microseismic signal
τ	temporal lag
$\phi_n(t)$	time series of n^{th} geophone output
${}^i\Phi_n(f)$	discrete Fourier transform of time series ${}^i\phi_n(t)$
χ^2_ν	chi-square variable with ν degrees of freedom

APPENDIX B
DATA PROCESSING NOTES

B.1 Introduction

Three programs have been written in FORTRAN IV for the CDC 7600 machine and RUN 76 compiler at the Lawrence Berkeley Laboratory. Program DUMP reads the digital data from the tape (TAPE 5) generated by the digitizer located in Haviland Hall of the University of California at Berkeley. It then unpacks each 12 bit tape word into one 60 bit CDC word, and writes the data onto another tape (TAPE 3) in binary mode. Program VSD reads the data from TAPE 3, estimates the velocity spectral density of the time series from each geophone output by the method of modified periodogram, and plots the result using both the Graphical Display System (GDS) at the University of California, Berkeley and the line printer (see subroutine YPLOTLG). Program FKPSD reads the array data from TAPE 3 and estimates the frequency wavenumber power spectral density (FKPSD) by either the conventional frequency domain beam forming method (BFM) or the maximum-likelihood method (MLM), and finally presents the result of f-k analysis by the GDS and the line printer.

B.2 Digitization

The field tape is played back at 3 inches per second, i.e., 25 times faster than the recording speed. This shifts the band of 0.25 Hz to 10 Hz up to the band of 6.25 Hz and 250 Hz, which are the limits of our filters. The 12 bit digitizer in Haviland Hall is normally set to digitize 2500 data points per record at the rate of 1000 data points per second (real time), which results in the digitization of 62.5 sec analog data into 2500 digital data in TAPE 5. The header (starting time of each record) and the tailer (the stop time of each record) are written in front of and behind each record in TAPE 5. If the header and/or tailer are not written along with the digital data, the variable NSUP needs to be reset in the subroutine READTAP which is called from the program DUMP.

B.3 Program DUMP

i) Data structure in TAPE 5

As an example, we digitize five records (NSEG = 5) from each geophone output at each channel of the tape recorder, the starting time (header) of each record is denoted by T(I), I = 1, 2, 3, 4, 5. The sequence of data in TAPE 5 is as follows:

	Ch.2	Ch.3	Ch.4	Ch.5. . . . Ch.14
T(1)	1	6	11	16 . . . . (NREC-4)
T(2)	2	7	12	17 . . . . (NREC-3)
T(3)	3	8	13	18 . . . . (NREC-2)
T(4)	4	9	14	19 . . . . (NREC-1)
T(5)	5	10	15	20 . . . . (NREC)
				End of file (EOF)

An end-of-file mark is required behind the last record.

ii) Input data cards

(1) The first input data card defines the number of records in the file and the record to be plotted by the GDS.

(2) An input data card is required for each geophone output. Each card defines the number of the record digitized from the geophone output, the correction factor for geophone polarization, the identification of the geophone output, and the gain factor of the playback system.

iii) Output

The time series of each digital record (2500 data points) with its starting time and stop time are printed, such that the bad record is recognizable and can be deleted. When the number of records in TAPE 5 is large, e.g., NREC > 50, it is recommended to dispose the output into microfiche. The unpacked digital data are written in another magnetic tape (TAPE 3) for further processing.

Three types of bad record may occur during this process. The record with a parity error can be skipped by the computer operator under the specification on the control card. In case of parity error, both the number of record in the file (NREC) and the number of the record at that particular geophone output (NSEG) must be reset in input data cards. then, the data in TAPE 5 ought to be reprocessed. Another kind of bad record may happen when the number of words per record does not equal to 502 words (when both the header and tailer are written). If this happens, the translation of this record is skipped by the program and is not written in TAPE 3. The last kind of bad record is the record with clipped amplitude. In this case, the values of clipped data points are listed in front of the printed output data. This kind of bad record shall be deleted by the user under the specifications in the input data cards of programs VSD or FKPSD.

iv) Data structure in TAPE 3

For each record, the unpacked data are written onto TAPE 3 in binary mode by the statements

(1) WRITE (3) (NDAYS, NHOURS, MIN, NSEC) for the starting time of the record,

(2) WRITE (3) (NDAYS, NHOURS, MIN, NSEC) for the stop time of the record,

(3) WRITE (3) (STAT, NB, J) for the record identification, the sequence of record at each geophone output,

(4) WRITE (3) (NVAL (I), I = 1, 2500) for the values of digital data,

(5) WRITE (3) (MORE) to indicate the last record of the geophone output if MORE = 0, otherwise MORE = 1.

v) Sample input and output

To unpack and translate one record in TAPE 5 from the site HO.5E sampled from the first record of the 10th hour (STAT = H0.5E1001), the sample input cards are:

INPUT DATA CARDS FOR PROGRAM DUMP

```
 1  0  0
1     1.0  H0.5E1001  1.0
```

and the printed output is:

RECORD NUMBER 1 CONTAINS 502 WORDS.

J = 1

DIGITISATION STARTING TIME FOR FJ.5E1001 1 IS 185 DAYS, 10 HOURS, 0 MINUTES, 4 SECONDS.
NOTE THAT DATA WILL START 3 SAMPLES LATER DUE TO THE WRITING OF THE HEADER.
STOP TIME 185 DAYS, 10 HOURS, 1 MINUTES, 6 SECONDS.

THE CORRECTIONAL FACTOR FOR POLARIZATION = 1.0 GAIN OF THE PLAY BACK SYSTEM = 1.00

-31	-91	-98	-56	0	79	90	44	0	-25	-22	-4	15	16	-7	-31	-53	-62	-36	0
37	26	2	-7	-31	-83	-108	-48	79	166	-132	16	-85	-90	-36	15	42	32	13	23
59	81	56	-15	-55	-118	-48	55	113	104	50	0	-43	-44	-40	-24	31	59	56	16
-87	-114	-52	31	93	100	66	0	-59	-52	0	63	65	40	9	-23	-71	-95	-64	15
91	104	64	2	-63	-111	-114	-48	59	115	96	36	0	-18	-11	5	10	-5	-18	0
39	71	72	32	-31	-68	-40	27	79	64	0	-79	-68	0	63	76	32	-19	-32	-20
-23	-34	-8	55	90	48	-23	-49	-32	-20	-10	11	31	24	-7	-25	-16	7	27	22
0	-30	-34	-12	11	26	30	25	19	17	17	18	21	26	17	-5	-23	-16	21	52
40	-15	-63	-42	23	74	66	32	-15	-79	-123	-104	-16	95	129	64	-31	-63	-36	-10
-12	-8	23	57	32	-39	-85	-56	0	61	52	8	-26	-26	-6	13	31	53	62	40
0	-31	-4	31	41	25	16	19	19	13	15	31	46	32	-15	-63	-60	-12	23	47
75	80	32	-55	-94	-64	-4	31	45	37	20	6	-3	-23	-29	0	59	72	32	-31
-44	-20	0	-3	-13	-22	-24	-4	23	35	29	12	-15	-45	-48	-28	-2	23	38	24
0	-20	-2	18	20	19	31	47	40	16	-4	0	17	8	-11	0	47	79	60	12
-22	-29	-8	23	28	0	-19	0	43	33	-11	-29	-2	8	-31	-82	-56	0	67	74
44	-21	-95	-116	-64	23	93	80	0	-103	-112	-40	29	73	80	58	0	-58	-52	0
71	64	0	-58	-60	-12	41	49	36	49	69	40	-31	-81	-64	0	63	72	40	16
19	25	2	-35	-36	0	31	12	-19	-31	-12	43	62	56	0	-46	-8	36	24	-15
-16	23	26	-7	-16	31	72	40	-31	-64	-32	19	51	67	64	32	-15	-54	-53	-28
0	39	62	40	-15	-46	-20	13	10	-2	5	13	-11	-55	-68	-48	-17	-3	7	43
82	64	0	-47	-20	11	4	-5	5	10	-15	-44	-36	-1	21	37	46	28	-7	-29
-16	5	19	35	42	32	8	-1	-2	-7	-17	-6	29	53	36	8	0	19	39	34
10	-15	-47	-69	-52	0	87	106	48	-31	-76	-48	0	38	44	16	-23	-41	-16	15
35	43	48	36	0	-79	-100	-32	59	107	97	64	0	-63	-93	-64	0	63	78	60
34	8	-17	-16	5	18	6	-3	-2	-11	-31	-26	15	51	42	2	-13	15	61	64
24	-21	-35	-25	-12	7	41	59	24	-31	-75	-68	-20	39	62	33	-7	-31	-43	-44
-35	-26	-17	7	43	50	16	-31	-53	-44	-8	39	83	54	64	16	-31	-48	-20	18
31	18	0	-17	-16	0	5	-15	-8	47	103	92	34	-11	-42	-79	-101	-64	0	63
88	88	52	-23	-86	-66	0	71	66	44	45	32	-31	-95	-84	-8	55	64	32	0
-23	-19	-6	0	3	6	14	22	16	-7	-35	-46	-20	19	39	28	8	0	7	38
73	68	16	-29	-44	-41	-24	15	63	80	44	-13	-59	-64	-8	63	101	88	36	-23
-63	-44	15	63	48	0	-44	-26	0	10	-7	-38	-63	-56	-8	51	76	48	-21	-79
-52	-52	0	38	46	29	10	18	26	-15	-77	-80	-16	45	68	58	42	36	16	-27
-55	-36	15	71	90	68	12	-30	-26	-9	-19	-33	-12	29	59	52	24	19	39	38
0	-26	-16	9	26	37	63	99	88	8	-87	-116	-72	0	71	88	48	-27	-66	-36
23	44	16	-19	-22	0	29	34	24	0	-43	-86	-82	-32	31	79	76	24	-39	-77
-76	-32	29	75	77	36	-31	-87	-76	-8	47	36	-11	-36	-28	-2	27	45	28	-23
-54	-24	23	32	4	7	45	59	16	-47	-66	-20	51	91	84	66	44	4	-43	-63
-44	-2	35	52	34	0	-33	-20	23	55	52	24	-31	-86	-82	0	87	100	48	-15
-38	-18	11	13	-11	-31	-18	23	61	52	0	-51	-44	-8	21	47	79	84	32	-39
-76	-53	-24	-8	31	91	112	52	-31	-58	-36	-4	35	65	32	-45	-90	-64	15	67
48	0	-13	-22	-41	-36	0	47	75	80	52	0	-71	-88	-32	47	99	98	48	-23
-74	-56	0	61	52	0	-39	-37	-12	15	47	54	26	0	9	43	45	0	-71	-88
-36	39	57	0	-49	-20	29	0	-63	-72	0	63	64	10	-23	-26	-24	-27	-16	11
41	52	20	-47	-92	-66	0	54	67	71	76	48	-31	-119	-108	-8	83	99	84	64
4	-79	-108	-48	35	52	18	0	11	37	52	44	16	-21	-55	-56	0	57	60	24

0	4	20	29	21	10	17	39	52	44	29	24	12	-15	-39	-28	0	37	36	5
-30	-33	0	31	26	-13	-36	-12	31	44	20	-11	-43	-67	-56	0	70	52	-15	-50
-42	-55	-64	-12	63	89	32	-37	-58	-24	23	59	76	64	24	-23	-47	-34	0	41
42	16	-22	-32	0	50	44	0	-37	-32	-19	0	59	117	58	0	-79	-96	-48	15
63	81	64	12	-47	-81	-60	-8	35	52	45	34	24	8	-23	-55	-58	-20	21	28
18	6	-23	-63	-80	-36	31	68	56	12	-19	-26	-6	31	62	42	2	-2	17	4
-39	-40	19	73	77	56	26	-11	-38	-26	15	50	52	20	-21	-79	-64	23	103	96
8	-63	-76	-8	63	84	52	0	-55	-93	-76	-4	63	76	40	9	4	4	2	5
8	5	9	16	4	-23	-22	31	85	84	32	-43	-55	-96	-48	27	83	92	40	-23
-37	-9	12	19	22	16	0	-7	4	19	13	3	10	19	16	3	-14	-30	-22	0
4	-27	-44	-20	15	37	36	10	-31	-77	-78	-32	31	75	68	36	4	-27	-63	-84
-48	15	63	65	44	24	0	-27	-35	-25	-14	-9	0	31	63	60	16	-23	-34	-28
-4	31	48	20	7	39	61	16	-55	-82	-50	0	63	123	128	64	0	-61	-77	-64
0	63	72	40	28	45	48	16	-18	-22	0	30	16	-30	-46	-16	27	40	34	20
2	-14	-31	-36	-20	7	24	22	31	63	72	20	-59	-89	-48	23	66	64	44	18
-13	-42	-40	-8	29	46	20	-31	-77	-56	0	47	52	20	-11	-18	-25	-36	-28	-2
0	-30	-38	-16	4	8	23	46	32	-23	-47	-20	11	12	-11	-20	0	47	72	40
-27	-69	-48	0	57	72	52	26	20	27	30	18	-9	-34	-16	39	77	64	16	-29
-49	-55	-44	0	71	88	34	-31	-65	-40	11	36	22	6	11	26	24	0	-29	-32
-4	23	16	-31	-77	-66	-16	14	10	-7	-4	31	95	139	100	0	-95	-56	-16	55
52	0	-57	-40	39	119	136	64	-39	-95	-80	-24	21	45	56	56	48	32	5	-29
-55	-48	0	71	82	16	-59	-64	-8	35	36	18	8	0	-2	14	41	22	-31	-87
-76	-4	87	145	104	0	-119	-112	-16	63	52	0	-42	-28	0	30	37	26	8	-10
-30	-46	-40	-8	31	62	65	32	-39	-89	-64	0	35	40	32	16	-7	-18	0	27
25	-11	-45	-48	-20	15	47	45	12	-19	-17	7	27	24	14	19	26	10	-15	-28
-21	-8	15	42	44	27	26	39	32	0	-35	-38	-20	-9	-4	19	59	72	32	-23
-39	-16	11	14	11	15	10	-11	-26	-12	15	31	28	24	15	10	18	38	24	-47
-99	-68	23	51	80	24	0	14	26	16	-14	-36	-25	11	20	-27	-77	-48	39	55
88	32	-39	-85	-72	-8	37	36	4	-17	-17	-5	10	31	40	20	6	23	39	16
-31	-77	-76	-24	47	103	126	106	48	-23	-63	-62	-32	31	79	74	16	-37	-57	-52
-44	-16	31	69	64	24	-27	-51	-24	19	32	0	-47	-24	55	88	32	-59	-86	-32
63	104	48	-43	-87	-64	-8	43	55	40	20	22	10	-47	-53	-64	39	119	108	16
-85	-118	-74	0	59	97	90	40	-23	-71	-82	-48	0	42	44	24	0	5	35	43
0	-53	-68	-44	-12	23	79	111	72	0	-41	-24	11	25	2	-27	-16	35	63	34
-15	-47	-44	-16	31	51	24	-11	-28	-24	0	45	18	66	16	-27	-43	-32	0	19
21	14	15	27	34	9	-31	-48	-20	6	14	31	69	72	20	-39	-48	-16	6	3
23	63	48	-31	-65	-24	19	21	6	6	4	-21	-47	-32	11	27	10	3	19	12
-27	-36	27	91	76	0	-87	-84	-16	39	38	12	15	36	38	8	-37	-59	-44	-4
30	40	24	8	7	7	0	0	19	47	62	34	-29	-79	-72	-16	47	89	72	10
-47	-66	-32	27	63	60	32	-11	-38	-32	0	43	48	20	-23	-60	-56	0	79	92
40	-23	-52	-44	-22	11	55	72	34	-23	-36	0	46	41	18	2	-27	-59	-40	23
67	64	32	-15	-63	-56	0	69	48	-19	-63	-57	-12	31	71	83	48	-47	-127	-120
-32	63	93	64	12	-31	-61	-48	0	45	40	4	-12	-1	17	26	19	15	31	44
20	-15	-16	27	63	48	0	-79	-98	-48	39	99	96	40	-23	-46	-16	39	60	32
-45	-101	-76	0	103	108	48	-27	-70	-56	-10	23	22	-7	-25	-14	-1	-9	-11	11
34	39	41	37	16	-15	-35	-24	0	18	12	6	15	25	17	0	-22	-24	-4	45
89	76	16	-22	-20	-21	-53	-79	-52	15	75	74	24	-39	-90	-84	-40	11	46	57
52	37	0	-51	-68	-32	15	39	38	20	1	0	25	55	59	32	1	3	31	55
48	18	0	-8	-5	0	1	15	59	84	40	-23	-22	0	21	17	13	11	0	-42
-58	-8	71	89	24	-39	-59	-51	-32	15	55	32	-31	-34	19	41	4	-27	-20	0
31	42	16	-31	-60	-36	-10	-11	-12	19	54	40	-11	-22	0	0	-47	-75	-34	27
42	2	-45	-56	-38	-26	-12	23	57	52	4	-38	-46	-32	-8	11	12	-11	-24	0
47	75	68	40	0	-47	-48	27	111	104	32	-19	-5	26	36	16	-3	0	29	57
58	32	0	-17	-29	-4	51	64	0	-59	-34	23	53	36	16	21	16	-31	-63	-32
21	43	36	24	8	-15	-33	-22	15	46	32	-7	-26	-12	11	31	32	25	24	18
-6	-24	0	47	48	4	-17	0	21	0	-45	-53	-24	23	39	8	-39	-48	-4	17
-23	-66	-42	0	35	40	42	32	4	-35	-79	-89	-32	63	108	56	-27	-69	-66	-46
-8	55	99	52	-39	-73	-24	25	8	-31	-32	23	79	86	32	-27	-63	-74	-42	39
109	96	24	-29	-33	-13	5	23	45	63	48	4	-12	11	30	20	12	23	35	24
-13	-35	-8	43	58	24	-22	-36	-12	23	47	55	44	0	-53	-68	-24	47	90	56
-23	-57	-16	43	66	48	16	-23	-63	-95	-72	0	70	72	32	-19	-63	-102	-98	-48
31	89	111	96	32	-63	-116	-80	0	52	34	0	-14	-5	14	43	59	40	0	-61

-77	-32	31	62	40	6	-9	-10	-9	-10	-4	18	55	79	48	-31	-75	-56	-10	39
83	52	56	26	27	24	-15	-71	-76	-16	59	78	50	16	-15	-47	-58	-51	-20	31
79	66	18	-15	-37	-47	-36	-4	17	0	-35	-42	-4	41	63	70	68	24	-63	-121
-104	-32	47	82	74	48	20	0	-25	-28	0	35	32	0	-8	23	57	56	16	-31
-60	-36	21	69	73	44	13	-15	-47	-40	0	63	64	32	-13	-55	-68	-32	47	115
106	24	-75	-124	-88	0	79	80	20	-35	-34	0	27	26	24	8	-37	-66	-32	31
67	64	52	32	-31	-107	-114	-24	95	124	64	-31	-62	-38	-28	-34	-8	43	40	-23
-62	-16	43	56	18	-31	-71	-83	-48	31	111	128	64	-47	-97	-64	0	63	73	34
4	1	7	3	-7	-9	0	8	6	10	31	57	58	32	-10	-37	-41	-30	-17	0
55	95	80	16	-23	-25	-19	-25	-34	-43	-41	-20	11	45	61	42	2	-11	13	37
18	-19	-16	35	78	48	-31	-99	-84	-10	51	78	78	40	-31	-72	-32	61	97	40
-31	-40	27	85	76	16	-47	-61	-40	-4	39	73	56	0	-63	-85	-60	-16	18	28
9	-19	-18	15	47	44	20	-5	-31	-59	-68	-42	13	51	48	16	-27	-59	-60	-24
31	61	44	12	0	7	9	-5	-39	-67	-48	23	91	90	32	-43	-72	-26	31	95
97	32	-55	-78	-40	11	55	95	114	64	-29	-72	-40	15	50	59	44	8	-27	-28
0	20	0	-4	31	60	24	-31	-40	15	79	81	8	-79	-104	-40	37	64	36	-13
-45	-28	11	16	-27	-54	-20	39	56	4	-55	-48	0	59	56	20	-6	-2	19	33

B.4 Program VSD

The program VSD estimates the velocity spectral density of each geophone output stored in TAPE 3. Each record of 2500 data points is divided into several data blocks of (2**NPOW) points per block. The maximum number of data point per block is 512 which is set by the dimension of arrays in the program. Each time series is multiplied by a 10% cosine bell taper before FFT. The power spectral density estimate of each geophone output is obtained by the method of periodogram described in section 4.3.2. This program also calculates 90% confidence limits of the estimated VSD.

i) Input data cards

(1) The first data card specifies the option for punched data deck of VSD, the NPOW to define the data point per block, and the record length in second.

(2) An input data card is required for each geophone output. This card specifies the termination of data processing, the option for VSD plot by the GDS, the identification of each geophone output, the bad records to be deleted, and the parameters of acquisition and playback systems.

ii) Output

The VSD estimate of each geophone output is plotted by subroutine YPLOTLG in a log-linear scale and GDS in a log-log scale along with 90% confidence limits. The estimated VSD are punched on decks for further processing, if the variable IPUNCH is set to be 1.

iii) Sample input and output

To estimate VSD of the digital data obtained from both site HS and site A3.7N, we need the digital data in magnetic tape (TAPE 3) and the following input data cards

INPUT DATA CARDS FOR PROGRAM VSD

0	9 62.5				
10102	HS	3.40999.00	0.30102.00	30.00	5.00310.00
00102	A3.7N	3.40999.00	0.30114.00	30.00	5.00310.00

Portion of the printed output (VSD of site HS from DC to 8.99 Hz) is presented as follows:

YPLOT...... HS
IB= 1 IE= 256 IK= 1 PMAX= 1.327E+02 PMIN= 3.168E-01

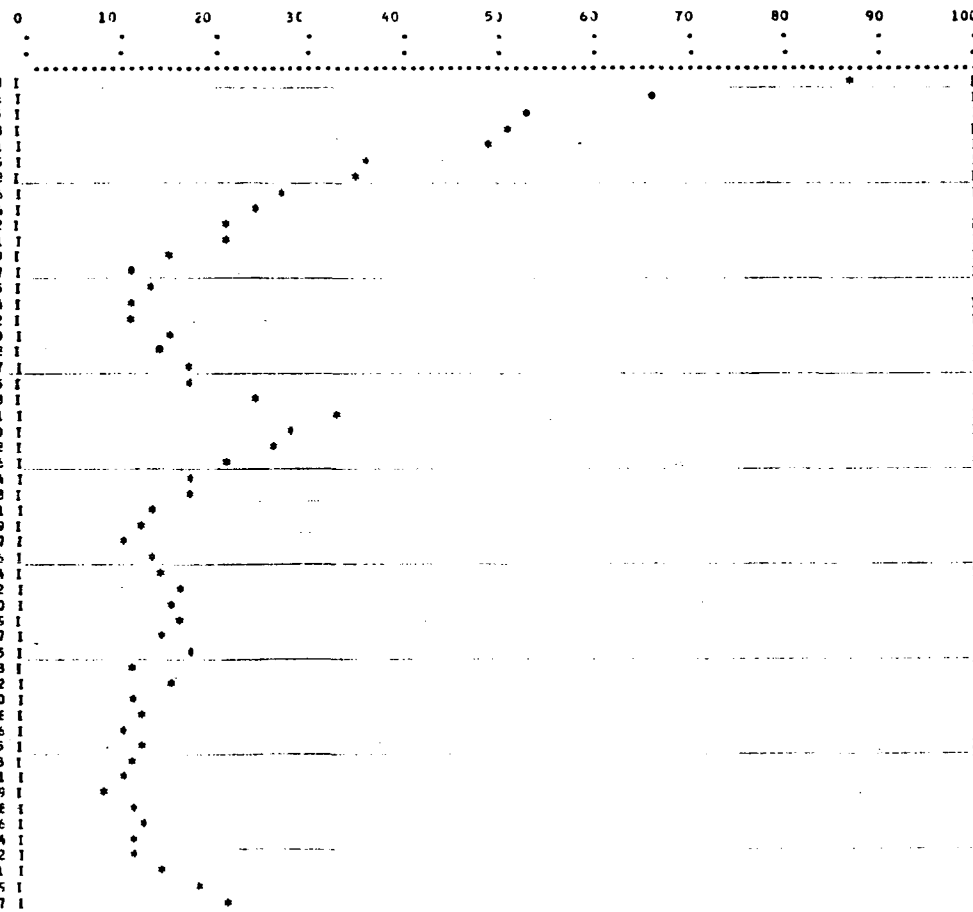

X	Y	
.078	6.606E+01	1
.156	1.905E+01	2
.235	8.480E+00	3
.313	7.659E+00	4
.391	6.505E+00	5
.469	3.072E+00	6
.548	2.787E+00	7
.626	1.780E+00	8
.704	1.480E+00	9
.782	1.227E+00	10
.861	1.244E+00	11
.939	8.494E-01	12
1.017	6.810E-01	13
1.095	7.735E-01	14
1.174	6.887E-01	15
1.252	6.718E-01	16
1.330	8.402E-01	17
1.408	8.021E-01	18
1.487	9.544E-01	19
1.565	9.641E-01	20
1.643	1.519E+00	21
1.721	2.475E+00	22
1.800	1.857E+00	23
1.878	1.680E+00	24
1.956	1.220E+00	25
2.034	9.831E-01	26
2.113	9.600E-01	27
2.191	7.830E-01	28
2.269	7.208E-01	29
2.347	6.454E-01	30
2.426	7.741E-01	31
2.504	7.949E-01	32
2.582	9.220E-01	33
2.660	8.615E-01	34
2.739	9.246E-01	35
2.817	8.015E-01	36
2.895	9.588E-01	37
2.973	6.634E-01	38
3.052	8.620E-01	39
3.130	6.866E-01	40
3.208	7.306E-01	41
3.286	6.310E-01	42
3.365	6.987E-01	43
3.443	6.695E-01	44
3.521	6.513E-01	45
3.599	5.538E-01	46
3.678	6.862E-01	47
3.756	6.975E-01	48
3.834	6.839E-01	49
3.912	6.538E-01	50
3.991	8.145E-01	51
4.069	1.006E+00	52
4.147	1.209E+00	53

4.225	1.488E+00	54
4.304	1.461E+00	55
4.382	1.360E+00	56
4.460	1.031E+00	57
4.538	8.020E-01	58
4.617	7.312E-01	59
4.695	6.031E-01	60
4.773	6.713E-01	61
4.851	5.064E-01	62
4.930	4.736E-01	63
5.008	4.128E-01	64
5.086	3.239E-01	
5.164	3.995E-01	66
5.243	3.209E-01	
5.321	3.277E-01	
5.399	3.458E-01	69
5.477	3.349E-01	
5.556	3.168E-01	
5.634	3.371E-01	72
5.712	2.725E-01	73
5.790	3.872E-01	74
5.868	4.931E-01	75
5.947	4.731E-01	76
6.025	5.591E-01	77
6.103	4.719E-01	78
6.181	6.296E-01	79
6.260	4.925E-01	80
6.338	5.480E-01	81
6.416	5.636E-01	82
6.494	5.031E-01	83
6.573	6.066E-01	84
6.651	6.552E-01	85
6.729	6.335E-01	86
6.807	6.228E-01	87
6.886	6.061E-01	88
6.964	5.954E-01	89
7.042	6.728E-01	90
7.120	7.389E-01	91
7.199	7.059E-01	92
7.277	7.508E-01	93
7.355	7.052E-01	94
7.433	6.995E-01	95
7.512	6.572E-01	96
7.590	6.859E-01	97
7.668	8.258E-01	98
7.746	7.716E-01	99
7.825	9.022E-01	100
7.903	7.269E-01	101
7.981	9.144E-01	102
8.059	8.465E-01	103
8.138	1.035E+00	104
8.216	1.027E+00	105
8.294	9.996E-01	106
8.372	1.146E+00	107
8.451	1.053E+00	108
8.529	9.942E-01	109
8.607	1.025E+00	110
8.685	1.055E+00	111
8.764	9.039E-01	112
8.842	9.840E-01	113
8.920	9.309E-01	114
8.998	1.031E+00	115

B.5 Program FKPSD

The program FKPSD estimates FKPSD of the array geophone outputs stored in TAPE 3. This program is set up to process the data obtained by the maximum of 12 array elements and the maximum of 512 data points per block. Each data block is multiplied by a Hamming window to reduce the leakage effect in the Fourier transform. The FKPSD can be estimated by either BFM described in Section 5.4.2, or MLM described in Section 5.4.3. The variable ICONVEN = 1 directs the program through the conventional BFM, and the ICONVEN = 0 directs the program through MLM. At a frequency component the FKPSD are estimated at each of 41 x 41 grid points in a two-dimensional wavenumber space. In addition to estimate FKPSD, this program also provides the options to calculate the coherence between two geophone outputs with its confidence limits and the VSD by specifying ICOHER = 1 and NVSDPL $\geq$ 1.

We have found that the starting time of each digital record can drift a few msec to 250 msec from the designated starting time on the front panel of the digitizer; this results from inconstant acceleration of the tape drive before recording the digital record on tape. In order to correct the effect of random drifting, the digital data must be plotted by the GDS and compared with the analog data before the estimation of FKPSD.

i) Input data cards

(1) The first card specifies the record length, the variable NPOW to define the number of data points per block, the number of data points per record, the maximum number of data blocks to be processed, and the number of records per sensor output

of which starting-time correction is required.

(2) The second card defines the contour levels in the f-k plot.

(3) The third card specifies the options for BFM or MLM, for f-k plot by GDS, and for VSD plot.

(4) A card specifies the termination of the data processing, the number of array elements, the parameters of the playback system, the station identification, the minimum geophone spacing in the array, the scale of output wavenumber, and the options for coherence calculation and FKPSD estimations. This card is required for each array data set.

(5) Specification of the desired frequency component for estimating FKPSD. This card is required for each array data set.

(6) Correction time for each record. This card is required for each array data set.

(7) The coordinate of array elements. This card is required for each array data set.

(8) This card specifies the identifications of each geophone output, the parameters of geophone, and the option to skip the bad record. A card is required for each geophone output.

ii) Output

The estimated FKPSD in the wavenumber space are normalized with respect to the peak-valued FKPSD at each desired frequency component. The normalized FKPSD are multiplied by -10 to save space of the sign and the decimal point, then, printed in integer format, contoured by symbols, and plotted by GDS. The maximum FKPSD over the frequency band are plotted by the subroutine YPLOT.

iii) <u>Sample input and output</u>

There are two array data sets, E5.9W04 and E5.9W05, stored in TAPE 3. This example skips the array data at E5.9W04 and estimates the FKPSD of the array data at E5.9W05 in four frequency components, i.e. the 7th, 8th, 9th and 10th discrete frequency components. The sequential number of discrete frequency components is defined by the statements FK2.153 and FK2.154 of program FKPSD. The starting-time correction for each record is as follows:

E5.0W0501(1) = 0.0 sec	,	E5.9W0501(2) = 0.04 sec
E5.0W0502(1) = 0.0 sec	,	E5.9W0502(2) = 0.04 sec
E5.9W0503(1) = 0.0 sec	,	E5.9W0503(2) = 0.02 sec
E5.9W0504(1) = 0.0 sec	,	E5.9W0504(2) = 0.0 sec
E5.9W0505(1) = 0.0 sec	,	E5.9W0505(2) = 0.04 sec
E5.9W0506(1) = 0.0 sec	,	E5.9W0506(2) = 0.04 sec
E5.9W0507(1) = 0.0 sec	,	E5.9W0507(2) = 0.04 sec
E5.9W0508(1) = 0.0 sec	,	E5.9W0508(2) = 0.0 sec
E5.9W0509(1) = 0.0 sec	,	E5.9W0509(2) = 0.0 sec
E5.9W0510(1) = 0.0 sec	,	E5.9W0510(2) = 0.04 sec
E5.9W0511(1) = 0.0 sec	,	E5.9W0511(2) = 0.04 sec
E5.9W0512(1) = 0.0 sec	,	E5.9W0512(2) = 0.04 sec.

We take only the first record of each geophone output to estimate FKPSD and set the maximum number of data blocks taken from each channel to be 24, and the number of data points per block to be $2^6 = 64$. The sample input data cards are following:

```
********************************************************************************
*                                                                              *
*                      INPUT DATA CARDS FOR PROGRAM FKPSD                      *
*                                                                              *
********************************************************************************

62.50     6 2500    24     2
    5 -1.0 -3.0 -6.0 -9.0-12.0
    0     0     0
    1     0     1     1    12     0     0     3 10.0  0.50.007    E5.9W04
   20     1     2     3     4     5     6     7     8     9    10    11    12    13    14    15
   16    17    18    19    20
0.1200.0000.1200.0000.1200.0000.1200.0000.1200.0000.0000.0000.1200.0000.1200.000
0.1200.0000.0800.0000.1200.0000.1200.000
 -0.0190  0.0110  0.0000  0.0250  0.0190  0.0110 -0.0108  0.0063  0.0000  0.0177
  0.0108  0.0063 -0.0153 -0.0089  0.0000 -0.0125  0.0153 -0.0089 -0.0217 -0.0125
  0.0000 -0.0219  0.0217 -0.0125
 E5.9W0401 2 1 3                      1.0  3.4999.0 0.30
 E5.9W0402 2 1 3                      1.0 1.35 3.00 0.60
 E5.9W0403 2 1 3                      1.0 1.35 3.00 0.60
 E5.9W0404 2 1 3                      1.0 3.40999.0 0.30
 E5.9W0405 2 1 3                      1.0 1.35 3.00 0.60
 E5.9W0406 2 1 3                      1.0 3.40999.0 0.30
 E5.9W0407 2 1 3                      1.0 3.40999.0 0.30
 E5.9W0408 3 1 2 4                    1.0 4.30999.0 0.60
 E5.9W0409 3 1 2 4                    1.0 1.35999.0 0.60
 E5.9W0410 2 1 3                      1.0 3.40999.0 0.30
 E5.9W0411 2 1 3                      1.0 3.40999.0 0.30
 E5.9W0412 2 1 3                      1.0 1.35 3.50 0.60
    0     0     1     0    12     0     0     3 10.0  0.50.007    E5.9W05
    4     7     8     9    10
0.0000.0400.0000.0400.0000.0200.0000.0000.0000.0400.0000.0400.0000.0400.0000.000
0.0000.0000.0000.0400.0000.0400.0000.040
 -0.0190  0.0110  0.0000  0.0250  0.0190  0.0110 -0.0108  0.0063  0.0000  0.0177
  0.0108  0.0063 -0.0153 -0.0089  0.0000 -0.0125  0.0153 -0.0089 -0.0217 -0.0125
  0.0000 -0.0219  0.0217 -0.0125
 E5.9W0501 2 2 3                      1.0  3.4999.0 0.30
 E5.9W0502 3 2 3 4                    1.0 1.35 3.00 0.60
 E5.9W0503 2 2 3                      1.0 1.35 3.00 0.60
 E5.9W0504 2 2 3                      1.0 3.40999.0 0.30
 E5.9W0505 2 2 3                      1.0 1.35 3.00 0.60
 E5.9W0506 2 2 3                      1.0 3.40999.0 0.30
 E5.9W0507 2 2 3                      1.0 3.40999.0 0.30
 E5.9W0508 2 2 3                      1.0 4.30999.0 0.60
 E5.9W0509 2 2 3                      1.0 1.35999.0 0.60
 E5.9W0510 2 2 3                      1.0 3.40999.0 0.30
 E5.9W0511 2 2 3                      1.0 3.40999.0 0.30
 E5.9W0512 2 2 3                      1.0 1.35 3.50 0.60
114.0  5.0 30.0

********************************************************************************
```

The printed output for the 9th Frequency component at E5.9W05 is

```
FREQUENCY WAVENUMBER POWER SPECTRAL DENSITY AT FREQUENCY =    5.71      AT    E5.9W05
MAXIMAL PSD =     1.382E+04
NOTE THAT THE VALUES PRINTED ARE (-10)(PSD/PMAX1) IN DB.
K295 =    -35.714   DELTA K =     1.786

NFY =    9

                                                  0
 .   .   .   .   .   .   .   .   .   .   .   .   .   .   .   .   .   .   .   .   .   .   .   .   .   .   .   .   .   .   .   .   .   .   .   .   .   .   .   .   .
226 216 203 189 175 164 155 150 147 147 148 150 153 156 161 167 175 183 192 199 202 201 199 195 191 187 183 179 176 173 172 172 173 175 177 180 182 184 185 185 184
214 203 191 179 169 161 155 152 150 150 151 152 153 156 159 164 170 177 185 192 196 198 197 195 192 189 185 182 180 179 179 180 182 185 188 191 193 195 195 195 193
200 190 181 175 166 161 158 156 155 154 154 154 154 155 157 160 165 171 178 185 190 193 194 193 191 189 187 186 185 185 186 189 192 196 199 202 204 205 206 205 203
188 180 174 169 166 163 161 160 159 158 157 156 155 154 155 156 159 164 170 177 182 186 189 190 190 189 189 189 190 191 194 198 202 206 209 212 214 215 215 214 212
177 174 171 169 167 166 165 164 162 161 159 156 154 152 151 151 153 156 161 167 173 178 182 184 186 187 189 191 193 197 201 205 210 214 217 220 222 223 223 222 220
171 170 169 169 169 168 167 166 164 162 159 156 152 149 146 144 145 147 151 156 162 168 172 176 180 183 187 191 195 200 205 210 215 219 223 226 228 229 229 228 226
167 168 169 169 170 169 169 167 165 161 158 153 149 144 139 136 135 135 138 143 149 155 161 167 172 177 182 188 194 200 206 212 218 223 227 230 231 232 232 232 230
165 167 169 170 170 170 169 166 163 159 154 149 143 136 130 125 122 122 124 128 134 140 148 155 162 169 176 182 190 197 205 212 219 224 228 231 233 234 234 234 233
165 168 169 170 170 169 167 164 160 155 149 142 135 127 119 112 107 105 106 109 115 122 131 140 150 158 166 174 183 193 202 211 218 224 228 231 232 234 234 234 234
166 168 170 170 169 167 165 161 155 149 142 133 124 116 105  96  89  86  85  87  92 100 110 123 135 145 154 164 175 186 197 207 215 221 225 228 230 232 233 234 234
167 169 170 169 168 165 161 155 149 141 132 122 111  99  88  77  69  64  62  63  66  73  83  98 116 130 140 151 164 178 191 202 210 215 220 223 226 228 230 232 234
169 170 170 168 166 161 156 149 141 131 120 108  94  81  68  57  49  44  42  43  44  47  54  67  88 110 124 137 153 168 182 193 201 208 212 217 220 224 227 230 233
172 172 170 168 163 158 150 142 131 119 105  90  75  60  49  41  37  36  36  37  37  38  39  43  57  82 104 121 139 156 170 182 190 197 204 209 214 219 224 228 231
175 174 171 167 161 154 145 133 120 105  88  71  54  41  36  36  38  40  43  44  44  43  42  41  45  58  80 101 120 138 154 166 177 186 194 202 208 215 220 225 230
178 176 173 167 160 151 139 125 109  90  70  49  34  32  37  43  48  52  54  54  54  54  53  53  53  56  65  80  97 115 133 149 162 175 185 195 203 211 218 224 229
182 179 175 168 160 149 135 118  98  75  50  28  24  35  46  54  60  63  64  64  65  65  66  68  69  69  67  65  71  89 111 132 149 165 178 189 199 208 216 222 228
187 184 179 171 162 149 133 114  90  62  33  17  29  46  58  66  70  72  73  73  74  76  80  85  88  86  77  62  51  66  92 117 139 157 172 185 196 206 214 221 227
193 190 184 177 166 153 136 114  88  57  27  22  39  56  68  75  79  81  82  83  85  90  96 101 103  97  83  62  41  49  78 107 132 152 169 183 195 205 214 220 225
200 197 192 184 173 160 143 122  95  65  39  34  48  64  76  84  88  90  92  95  99 106 111 113 108  97  80  56  33  38  70 102 129 151 168 183 195 205 213 219 222
208 206 201 193 183 171 155 136 113  90  65  44  55  71  84  93  98 103 107 111 116 119 118 113 104  91  73  49  22  26  68 103 130 152 169 184 195 204 210 213 214
0 213 215 211 204 196 184 171 155 138 120  81  51  61  78  93 104 112 119 124 126 125 121 115 107  98  86  69  45  15   6  56 101 130 152 169 182 192 198 202 203 201 0
227 225 222 216 208 199 187 173 156 131  86  57  67  87 105 119 129 134 134 129 123 117 111 104  96  85  69  47  18   0  33  85 120 143 160 172 181 186 188 188 186
236 235 232 227 220 211 199 183 161 128  87  63  74  99 121 135 139 137 130 124 118 114 110 105  97  87  72  51  25   7  26  68 103 128 146 158 166 170 172 173 172
244 244 241 237 229 219 205 185 158 124  88  66  80 113 135 138 133 127 122 118 115 113 110 106  99  89  75  56  34  21  33  64  94 116 133 145 152 157 160 162 162
251 251 248 245 234 222 204 182 154 122  88  65  74 111 128 123 118 115 114 114 114 113 111 107 100  91  77  60  43  34  45  69  92 112 127 137 144 149 153 155 157
257 256 252 245 234 219 200 178 151 121  90  64  59  83 100 101 103 105 108 110 112 112 110 106 100  90  78  63  50  47  59  78  97 113 126 135 141 146 150 152 155
260 258 253 243 230 214 195 173 149 122  94  67  49  54  70  80  88  95 101 105 108 108 107 103  97  88  76  64  57  60  72  89 105 118 128 136 142 146 149 152 155
260 256 248 237 223 207 189 169 148 125 100  74  50  39  46  60  73  83  92  97 101 102 101  98  91  83  73  65  64  72  86 101 114 125 133 140 144 148 151 154 156
256 249 240 227 214 199 183 167 148 129 107  84  59  39  33  42  56  69  80  87  91  93  92  89  83  76  70  68  74  86 100 113 124 133 139 145 149 152 154 157 159
247 239 229 217 205 193 179 165 150 134 115  95  73  50  34  31  40  53  65  73  79  81  81  79  75  72  72  77  88 101 114 125 134 141 146 151 154 156 159 161 162
234 226 217 207 197 187 177 165 153 139 124 107  88  67  48  35  33  40  50  59  66  70  72  73  73  77  83  94 106 118 129 137 144 150 154 157 160 162 164 165 167
219 213 205 199 191 183 175 166 156 145 132 118 102  85  68  52  42  41  46  54  62  69  75  82  90  98 108 118 127 136 144 150 155 158 161 164 166 168 169 171 172
205 201 196 191 186 181 174 167 159 150 140 128 116 102  88  75  65  61  63  70  80  91 103 114 123 130 137 142 148 153 158 161 164 166 168 170 172 174 175 177 178
193 191 189 186 183 179 175 169 163 155 147 138 127 117 106  97  90  88  91 100 111 124 136 145 151 156 159 162 165 168 170 171 172 173 174 176 178 180 182 183 184
185 185 184 183 181 178 175 171 165 159 153 145 137 129 122 115 111 111 116 124 135 146 156 163 168 172 175 178 179 180 179 178 178 178 179 181 183 186 188 190 191
179 180 181 180 179 178 175 172 168 163 157 152 146 140 134 130 128 129 134 142 151 161 169 175 181 184 187 189 190 188 186 183 181 181 182 185 188 191 194 196 198
176 178 179 179 178 177 175 172 169 165 161 156 152 148 144 142 141 143 148 155 163 172 179 186 191 195 197 198 197 194 189 185 183 182 184 187 191 195 198 202 204
175 176 177 177 176 175 173 171 169 166 163 160 156 154 151 150 151 153 158 165 173 181 188 195 200 203 206 205 202 197 190 184 181 181 184 188 192 197 202 206 209
175 176 176 175 174 173 171 170 168 166 164 161 159 158 156 156 157 160 165 172 180 188 195 202 207 210 211 210 205 197 188 181 178 179 182 187 193 199 204 209 213
176 175 174 173 171 170 168 167 165 164 163 162 161 160 159 160 161 165 170 177 184 192 200 206 211 214 214 211 204 194 184 177 174 175 180 186 193 199 206 211 216
177 175 173 171 168 166 164 163 162 162 161 161 161 161 161 162 163 167 172 179 187 195 202 209 213 215 214 208 199 188 178 171 169 172 177 184 191 199 206 212 217
 .   .   .   .   .   .   .   .   .   .   .   .   .   .   .   .   .   .   .   .   .   .   .   .   .   .   .   .   .   .   .   .   .   .   .   .   .   .   .   .   .
                                                  0

VELOCITY (KM/SEC) =      .353

AZIMUTH (DEGREE)  =      96
```

B.6 Program listing

```
*****************************************************************************
*                                                                           *
*                               PROGRAM DUMP                                *
*                                                                           *
*****************************************************************************

DUMP,7,55.471209,LIAW
DISKHOG,14000.
RUN76,SC,NL77777.
FETCHMT,TAPE5,05,P4,32264,1F.
FETCHPS,BKYULIB,TEMP,GDS.
FETCHPS,BKYLGOB,GDSCC,GDSCC.
COPYI,TEMP,LIB.
RETURN,TEMP.
LINK,X,F=LGO,P=LIB,P=BKYIC.
STAGE,TAPE3,D8,W,08665.
ENTERMT,TAPE3,08665.
RETURN,TAPE3.
EXIT.
DUMP,0.
FIN.
GDSCC.
DISPOSE,OUTPUT,MF.
RETURN,LGO,LIB.
RETURN,TAPE99,GDSCC.
      PROGRAM DUMP(INPUT,OUTPUT,PUNCH,PUNCHB,TAPE1=PUNCHB,TAPE3,TAPE5,TA
     1PE99,TAPE92,TAPE93,TAPE94)
C*************************************************************************
C
C
C         PROGRAM     DUMP
C         SUBROUTINE  REACTAP
C                     TRANS
C                     UNPK
C                     TIME
C                     APLCT
C
C

C
C.....THIS PROGRAM READS THE TAPE (TAPE 5) WRITTEN BY THE DIGITIZER
C     OF HAVILAND HALL, TRANSLATES THE DATA, AND UN-PACKS EACH WORD
C     INTO 60 BITS WORD, AND PLOTS THE TIME SERIES BY CALCOMP UNDER
C     REQUESTED.
C
C.....IPRINT, WHEN IPRINT = J THAT RECORD WILL BE PRINTED IN OCTAL FORM.
C.....J = THE SEQUENCE NUMBER OF RECORD IN TAPE 5.
C.....NB = THE SEQUENCE NUMBER OF EACH GEOPHONE OUTPUT.
C.....NNPL = THE TOTAL NUMBER OF NPL.
C.....NPL =J, THE JTH TIME SERIES WILL BE PLOTTED.
C.....NREC = THE TOTAL NUMBER OF RECORD DIGITIZED ON TAPE 5.
C.....NSEG = THE NUMBER OF RECORD FROM EACH GEOPHONE OUTPUT.
C.....NSKIP = THE SEQUENCE NUMBER IN THE TAPE TO BE SKIPPED.
C.....PB = THE GAIN FACTOR OF THE PLY-BACK SYSTEM.
C.....PULA = THE CORRECTION FACTOR OF POLARIZATION OF THE SEISMOMETER AN
C.....       D/OR AMPLIFIER.
C.....STAT = STATION IDENTIFICATION.
C
C.....THE INPUT DATA CARDS ARE AS FOLLOWING
C     (1) NREC,NNPL,NSKIP(3I3)
C     (2) NSEG,PULA,STAT,PB,IPRINT(I2,F8.2,A10,F5.2,I3) FOR EACH GEO-
```

```
C        PHONE OUTPUT.
C
C.....AUTHOR     ALFRED LIANG-CHI LIAW
C                ENGINEERING GEOSCIENCE
C                UNIVERSITY OF CALIFORNIA, BERKELEY
C.....DATE       SEPTEMBER 1977
C*****************************************************************

      DIMENSION SPECS(12)
      DIMENSION NPL(55)
      COMMON /BLK1/N1(512),LEN,MDATA
      COMMON /BLK2/NB,NSKIP
      COMMON /BLK3/N(2500),NH(12),NT(12)


C.....OVERRIDES INSUFFICIENT DATA READ ERROR ON BKYIO.
      CALL FET(5,0400 0000 0000 0000 0000B,8*64)

      SPECS(12)=99.
      MDATA=2500
      IDEC=1
      J=0
      NB=0
      READ 9,NREC,NNPL,NSKIP
    9 FORMAT (3I3)
   99 READ 10,NSEG,POLA,STAT,PB,IPRINT
   10 FORMAT (I2,F8.2,A10,F5.2,I3)
      RPB=1.0/PB
   98 J=J+1
      NB=NB+1
      CALL READTAP(NREC,J,IPRINT,NNPL,SPECS,NVAL)
      IF (NVAL.EQ.0) GO TO 51
   20 CALL TRANS (MC,SAMP,IDEC,STAT,J)

      DO 5 I=1,MDATA
      N(I)=N(I)*POLA
      IF (IABS(N(I)).LE.2040) GO TO 5
      PRINT 6,I,N(I)
    6 FORMAT (1H0,1X,*N( *,I4,*) = *,I6)
    5 CONTINUE
      IF (J.LE.NSKIP) GO TO 4
      DO 55 I=1,MDATA
      N(I)=N(I)*RPB
   55 CONTINUE
      PRINT 800,POLA,PB
  800 FORMAT (1H0,1X,*THE CORRECTIONAL FACTOR FOR POLARIZATION = *,F5.1,
     15X,*GAIN OF THE PLAY BACK SYSTEM = *,F5.2,/)
      PRINT 2,(N(I),I=1,2500)
    2 FORMAT (1X,5I6,3X,5I6,3X,5I6,3X,5I6)
    4 WRITE (3) (STAT,NB,J)
      WRITE (3) (N(I),I=1,2500)
C     PUNCH 3,(N(I),I=1,2500)
C   3 FORMAT (20O4)
      DO 40 NL=1,NNPL
      IF (J.EQ.NPL(NL)) GO TO 41
   40 CONTINUE
      GO TO 7
   41 CALL APLOT(STAT,NB)
      IF (J.GE.NREC) GO TO 7
      CALL NXTFRM(SPECS)
    7 CONTINUE
   49 MORE=1
```

```
50 CONTINUE
   IF (NB.GE.NSEG) MORE=0
   IF (NB.GE.NSEG) NB=0
   WRITE (3) (MORE)
   GO TO 52
51 PRINT 53,STAT,NB,J
53 FORMAT (1H0,5X,*THE PROGRAM SKIPS THE RECORD OF *,A10,I2,* AS REQU
  1ESTED.*,*  J = *,I3,//////////////////////////////////////////////)
   IF (J.GE.NREC) GO TO 60
   IF (NB.LT.NSEG) GO TO 98
   PRINT 54
54 FORMAT (1H0,*AAAAA*)
   MORE=0
   NB=0
52 IF (J.GE.NREC) GO TO 60
   IF (MORE.EQ.1) GO TO 98
   GO TO 99
60 CONTINUE
   CALL GDSEND(SPECS)
70 STOP
   END


   SUBROUTINE APLOT(LABEL2,NB)
   COMMON /BLK3/N(2500)
   DIMENSION SPECS(30),X(2500),Y(2500),BUFX(500),BUFY(500)
   DIMENSION GXSPEC(4),XTICK(3,2),YTICK(3,2)
   DIMENSION LINE(2)
   SPECS(1)=0.0
   SPECS(2)=1.0
   SPECS(3)=2500.0
   SPECS(4)=1.0
   SPECS(5)=2048.0
   SPECS(6)=-2048.0
   SPECS(7)=46.88
   SPECS(8)=10.0
   SPECS(11)=1.0
   SPECS(12)=99.0
   SPECS(13)=2500.0
   SPECS(14)=1.0
   SPECS(15)=1.0
   DO 1 I=1,2500
   X(I)=I
   Y(I)=FLOAT(N(I))
 1 CONTINUE
   CALL PFLILI(X,Y,BUFX,BUFY,SPECS)
   LINE(1)=LABEL2
   LINE(2)=0
   RULE =3.0
   SPECS(17)=0.2
   SPECS(18)=0.2
   SPECS(19)=0.0
   SPECS(20)=0.0
   SPECS(21)=1.0
   SPECS(22)=45.0
   SPECS(23)=10.5
   CALL TITLEG(RULE,LINE,SPECS)
   SPECS(22)=46.0
   SPECS(28)=0.
   VALUE=FLOAT(NB)
   CALL DECVAL(RULE,VALUE,SPECS)
   SPECS(7)=45.0
```

```
      GXSPEC(1)=0.0                                                      APLOT.41
      GXSPEC(2)=0.0                                                      APLOT.42
      GXSPEC(3)=2.0                                                      APLOT.43
      GXSPEC(4)=2.0                                                      APLOT.44
      XTICK(1,1)=1.0                                                     APLOT.45
      XTICK(1,2)=1.0                                                     APLOT.46
      XTICK(2,1)=0.1                                                     APLOT.47
      XTICK(2,2)=0.2                                                     APLOT.48
      XTICK(3,1)=30.0                                                    APLOT.49
      XTICK(3,2)=3.0                                                     APLOT.50
      YTICK(1,1)=1.0                                                     APLOT.51
      YTICK(2,1)=0.1                                                     APLOT.52
      YTICK(3,1)=8.0                                                     APLOT.53
      YTICK(1,2)=1.0                                                     APLOT.54
      YTICK(2,2)=0.2                                                     APLOT.55
      YTICK(3,2)=2.0                                                     APLOT.56
      CALL GXLILI(GXSPEC,XTICK,YTICK,SPECS)                              APLOT.57
      RETURN                                                             APLOT.58
      END                                                                APLOT.59
      SUBROUTINE READTAP(NREC,J,IPRINT,NNFL,SPECS,NVAL)                  READTAP.
                                                                         READTAP.
C           THIS PROGRAM READS A TAPE WRITTEN BY THE HAVILAND HALL       READTAP.
C     DIGITIZER AND DUMPS THE FILES AS PRINTED OUTPUT AND MAGNETIC TAPE  READTAP.
C     AND/OR PUNCHED DECKS.                                              READTAP.
C..... NSUP=500 FOR THE RECORD W/O  HEADER AND TAILER.                   READTAP.
C..... NSUP=501 FOR THE RECORD WITH HEADER OR TAILER ONLY.               READTAP.
C..... NSUP=502 FOR THE RECORD WITH HEADER AND TAILER.                   READTAP.
C                                                                        READTAP.
      COMMON /BLK1/N1(512),LEN,MDATA                                     READTAP.
      DIMENSION SPECS(1)                                                 READTAP.
                                                                         READTAP.
      SPECS(12)=99.0                                                     READTAP.
      NSUP=502                                                           READTAP.
      READ (5) (N1(I),I=1,NSUP)                                          READTAP.
C     IF (EOF,5) 70,12                                                   READTAP.
   12 CONTINUE                                                           READTAP.
                                                                         READTAP.
C     IF (IOCHECK,5) 14,15                                               READTAP.
C  14 PRINT 81,J                                                         READTAP.
C  81 FORMAT (1H1,* PARITY ERROR IN RECORD*,I4,///,)                     READTAP.
C  15 CONTINUE                                                           READTAP.
                                                                         READTAP.
      LEN=LENGTH(5)                                                      READTAP.
      IF(LEN.LT.0.) LEN=-LEN                                             READTAP.
   80 CONTINUE                                                           READTAP.
      IF (LEN.EQ.NSUP) GO TO 60                                          READTAP.
      PRINT 3,J,LEN                                                      READTAP.
    3 FORMAT (1H1* THE NUMBER OF WORDS IN RECORD*,I4,* IS*,I5,/,         READTAP.
     1* THIS DOES NOT AGREE WITH THE EXPECTED NUMBER*,///,)              READTAP.
      NVAL=0                                                             READTAP.
      GO TO 50                                                           READTAP.
   60 CONTINUE                                                           READTAP.
      PRINT 4,J,LEN                                                      READTAP.
    4 FORMAT(1H1,* RECORD NUMBER *,I3,* CONTAINS *,I5,* WORDS.*,///,)    READTAP.
      NVAL=1                                                             READTAP.
      IF (J.NE.IPRINT) GO TO 50                                          READTAP.
      PRINT 5,(N1(I),I=1,LEN)                                            READTAP.
    5 FORMAT (4O25)                                                      READTAP.
   50 RETURN                                                             READTAP.
C  70 CONTINUE                                                           READTAP.
C     PRINT 71                                                           READTAP.
C  71 FORMAT(* EOF ENCOUNTERED.  STOP.*)                                 READTAP.
```

```
C     IF (NNPL.EQ.0) GO TO 72                                           READTAP.
C     CALL GDSEND(SPECS)                                                READTAP.
C  72 STOP                                                              READTAP.
      END                                                               READTAP.


      SUBROUTINE TIME (L,NDAYS,NHOURS,MIN,NSEC)                         TIME.2
      DIMENSION L(12)                                                   TIME.3
      NDAYS=(L(1).AND.1)*200+(L(2).AND.4)*25+(L(2).AND.3)*40+(L(3).AND.6TIME.4
     1)*5+(L(3).AND.1)*8+(L(4).AND.7)                                   TIME.5
      NHOURS=(L(5).AND.1)*20+((L(6).AND.4)/4)*10+(L(6).AND.3)*4+(L(7).ANTIME.6
     1D.6)/2                                                            TIME.7
      MIN=(L(8).AND.7)*10+(L(9).AND.7)*2+(L(10).AND.4)/4                TIME.8
      NSEC=(L(10).AND.1)*40+(L(11).AND.6)*5+(L(11).AND.1)*8+(L(12).AND.7TIME.9
     1)                                                                 TIME.10
      RETURN                                                            TIME.11
      END                                                               TIME.12


      SUBROUTINE TRANS (MC,SAMP,ICEC,STAT,J)                            TRANS.2
                                                                        TRANS.3
COMMENT... THE FIRST DATA CARD (I2,F8.2,A10,F10.0) INDICATES THE HEADER-TRANS.4
C  OPTION,THE SAMPLE INTERVAL IN SEC.,THE STATION ID,AND THE DEFAULT OPTTRANS.5
C DEFAULT OPTION IS ALWAYS LEFT BLANK THE PROGRAM TERMINATES IF ANYTHINGTRANS.6
CHED IN THIS FIELD. THE HEADER-TAILER OPTION CODE IS AS FOLLOWS 1=NO HEATRANS.7
C  TAILER    2=HEADER AND TAILER    3=HEADER ONLY    4=TAILER ONLY.   THE ITRANS.8
C TA ARE THE WRITTEN OUTPUT OF THE PROGRAM DUMPTAPE FOR THE HAV.HALL DIGTRANS.9
                                                                        TRANS.10
      COMMON /BLK1/N1(512),LEN,MDATA                                    TRANS.11
      COMMON /BLK2/NB,NSKIP                                             TRANS.12
      COMMON /BLK3/N(2500),NH(12),NT(12)                                TRANS.13
      IF (MDATA .LE. 1) MDATA =2500                                     TRANS.14
      MD3 = MDATA-3                                                     TRANS.15
      MD2 = MDATA-2                                                     TRANS.16
C     READ 2, NCHEK,SAMP,STAT,DEFAULT                                   TRANS.17
C   2 FORMAT(I2,F8.4,A10,F10.0)                                         TRANS.18
C                                                                       TRANS.19
      NCHEK=2                                                           TRANS.20
      SAMP=0.0125                                                       TRANS.21
      DEFAULT=0.0                                                       TRANS.22
C                                                                       TRANS.23
      IF (DEFAULT.LT..0001) GO TO 110                                   TRANS.24
      PRINT 12                                                          TRANS.25
   12 FORMAT (* PROBLEM WITH NUMBER OF CARDS IN THE INPUT DECK.    PROGRTRANS.26
     1AM TERMINATED.  *)                                                TRANS.27
      STOP                                                              TRANS.28
  110 CONTINUE                                                          TRANS.29
      IF (NCHEK-2) 10,20,30                                             TRANS.30
   10 CONTINUE                                                          TRANS.31
                                                                        TRANS.32
      II=0                                                              TRANS.33
      DO 3 I=1,500                                                      TRANS.34
      DO 2 JW=1,5                                                       TRANS.35
      II=II+1                                                           TRANS.36
      N(II)=SHIFT(N1(I),12*JW).AND.7777B                                TRANS.37
    2 CONTINUE                                                          TRANS.38
    3 CONTINUE                                                          TRANS.39
                                                                        TRANS.40
C     READ (4,3) (N(I),I=1,MDATA)                                       TRANS.41
C   3 FORMAT(20O4)                                                      TRANS.42
      PRINT 11,STAT,NB                                                  TRANS.43
   11 FORMAT(1H0,*NO HEADER-TAILER INDICATED BY CONTROL CARD FOR *,A10,ITRANS.44
```

```
      12)
       GO TO 40
    20 CONTINUE
C      READ (4,4) ((NH(I),I=1,12),(N(IF),IF=1,17))
C    4 FORMAT(12O1,17O4)
C      READ (4,3) (N(IH),IH=18,MD3)
C      READ (4,5) ((N(IU),IU=MD2,MDATA),(NT(JE),JE=1,12))
C    5 FORMAT(3O4,12O1)

       CALL UNPK(IWORD)
C      PRINT 22,IWORD
C   22 FORMAT (1H0,35X,*IWORD = *,I5)
    21 DO 23 J2=1,8
       NT(J2)=SHIFT(N1(IWORD),3*J2+36).AND.7B
    23 CONTINUE
       DO 24 J2=9,12
       NT(J2)=SHIFT(N1(LEN),3*(J2-8)).AND.7B
    24 CONTINUE

       CALL TIME(NH,NDAYS,NHOURS,MIN,NSEC)


       WRITE (3) (NDAYS,NHOURS,MIN,NSEC)
       PRINT 25,J
    25 FORMAT (1H0,*  J = *,I5)
    50 CONTINUE
       PRINT 6,STAT,NB,NDAYS,NHOURS,MIN,NSEC
     6 FORMAT(1H0,* DIGITISATION STARTING TIME FOR *,A10,I2,* IS *,I3,* D
      1AYS, *,I2,* HOURS, *,I2,* MINUTES, *,I2,* SECONDS.*,/,* NOTE THAT
      1DATA WILL START 3 SAMPLES LATER DUE TO THE WRITING OF THE HEADER.*
      2)
    31 CALL TIME(NT,NDAYS,NHOURS,MIN,NSEC)


       WRITE (3) (NDAYS,NHOURS,MIN,NSEC)
    51 CONTINUE
       PRINT 7,NDAYS,NHOURS,MIN,NSEC
     7 FORMAT(* STOP TIME*,I4,* DAYS, *,I2,* HOURS, *,I2,* MINUTES, *,I2,
      1* SECONDS.*,///)
       GO TO 40
    30 CONTINUE
       IF (NCHEK.EQ.4) GO TO 35
C      READ (4,4) ((NH(IY),IY=1,12),(N(IR),IR=1,17))
C      READ (4,3) (N(KJ),KJ=18,MDATA)

       CALL UNPK(IWORD)
       CALL TIME(NH,NDAYS,NHOURS,MIN,NSEC)
       PRINT 6,STAT,NDAYS,NHOURS,MIN,NSEC
       GO TO 40
    35 CONTINUE
C      READ (4,3) (N(IW),IW=1,NDATA)
C      READ (4,9) (NT(KN),KN=1,12)
C    9 FORMAT(12O1)


       II=0
       DO 103 I=1,500
       DO 102 JW=1,5
       II=II+1
       N(II)=SHIFT(N1(I),12*JW).AND.7777B
   102 CONTINUE
   103 CONTINUE
```

```
      DO 104 J2=1,12                                                    TRANS.10
      NT(J2)=SHIFT(N1(501),3*J2).AND.7B                                 TRANS.10
  104 CONTINUE                                                          TRANS.10
                                                                        TRANS.11
      CALL TIME(NT,NDAYS,NHOURS,MIN,NSEC)                               TRANS.11
      PRINT 7,NDAYS,NHOURS,MIN,NSEC                                     TRANS.11
   40 CONTINUE                                                          TRANS.11
      IF (IDEC .LT. 1) IDEC = 1                                         TRANS.11
      MD = MDATA/IDEC                                                   TRANS.11
      SAMP = SAMP*FLOAT(IDEC)                                           TRANS.11
      DO 120 JM=1,MD                                                    TRANS.11
      JA = IDEC*(JM-1)+1                                                TRANS.11
      IF (N(JA).GE.2048) N(JA)=N(JA)-4096+1                             TRANS.11
      IF (N(JA).EQ.4095) N(JA)=-1                                       TRANS.12
  120 CONTINUE                                                          TRANS.12
      RETURN                                                            TRANS.12
      END                                                               TRANS.12

      SUBROUTINE UNPK(IWORD)                                            UNPK.2
                                                                        UNPK.3
      COMMON /BLK1/N1(512),LEN,MDATA                                    UNPK.4
      COMMON /BLK3/N(2500),NH(12),NT(12)                                UNPK.5
                                                                        UNPK.6
      DO 43 I=1,LEN                                                     UNPK.7
      IF (I.NE.1) GO TO 16                                              UNPK.8
      DO 14 II=1,12                                                     UNPK.9
      NH(II)=SHIFT(N1(1),3*II).AND.7B                                   UNPK.10
   14 CONTINUE                                                          UNPK.11
      DO 15 II=1,2                                                      UNPK.12
      N(II)=SHIFT(N1(1),12*II+36).AND.7777B                             UNPK.13
   15 CONTINUE                                                          UNPK.14
      GO TO 43                                                          UNPK.15
   16 IF (I.NE.2) GO TO 12                                              UNPK.16
      II=2                                                              UNPK.17
   12 DO 17 I2=1,5                                                      UNPK.18
      II=II+1                                                           UNPK.19
      N(II)=SHIFT(N1(I),12*I2).AND.7777B                                UNPK.20
      IWORD=I                                                           UNPK.21
      IF (II.GE.MDATA) GO TO 21                                         UNPK.22
   17 CONTINUE                                                          UNPK.23
   43 CONTINUE                                                          UNPK.24
   21 RETURN                                                            UNPK.25
      END                                                               UNPK.26

  1  0  0
 1     1.0 H0.5E1001 1.0
```

```
*****************************************************************************
*                                                                           *
*                              PRCGRAM VSC                                  *
*                                                                           *
*****************************************************************************

VSD,7,55.471209,LIAW
DISKHOG,14000.
RUN76,SC,NL77777.
FETCHMT,TAPE3,D8,32277,1F.
FETCHPS,BKYULIB,TEMP,GDS.
FETCHPS,BKYLGOB,GDSCC,GCSCC.
COPYI,TEMP,LIB.
LINK,X,F=LGO,P=LIB,PP=(LC=99999).
EXIT.
RETURN,LGO,LIB.
DUMP,0.
FIN.
DISPOSE,OUTPUT,MF.
RETURN,TAPE99,GDSCC.
      PROGRAM VSD(INPUT,OUTPLT,PUNCHB,TAPE6=PUNCHB,TAPE97,TAPE99,TAPE3,TVSD.2
     1APE92,TAPE93,TAPE94)                                              VSD.3
                                                                        VSD.4
CCCCCCCCCCCCCCCCCCCCCCCCCCCCCCCCCCCCCCCCCCCCCCCCCCCCCCCCCCCCCCCCCCCCCCCCVSD.5
C.                                                                      VSD.6
C.                                                                      VSD.7
C.    PROGRAM  VSD  READS THE DIGITAL DATA FROM TAPE 3 AND ESTIMATES    VSD.8
C.    THE VELOCITY SPECTRAL DENSITY (VSD) OF THE TIME SERIES BY THE     VSD.9
C.    METHOD OF MODIFIED PERICDOGRAM.                                   VSD.10
C.    A 10 PERCENT COSINE BELL TAPER IS APPLIED TO EACH DATA BLOCK.     VSD.11
C.    VSD IS DEFINED AS THE SQUARE ROOT OF POWER SPECTRAL DENSITY.      VSD.12
C.    THE TAPE 3 IS GENERATED BY THE PROGRAM DUMP WHICH UNPACKES AND    VSD.13
C.    TRANSLATES THE TAPE 5. THE TAPE 5 IS GENARATED BY THE DIGITIZER   VSD.14
C.    IN HAVILAND HALL. EACH DATA BLOCK CONTAINS 2**NPOW DATA POINTS.   VSD.15
C.    THE ARRAY DIMENSIONS ARE SET UP TO PROCESS THE DATA BLOCK WITH    VSD.16
C.    MAXIMUM OF 512 DATA POINTS PER DATA BLOCK. THEREFORE, EACH        VSD.17
C.    RECORD OF 2500 POINTS IN TAPE 3 IS DIVIDED INTO 4 DATA BLOCK      VSD.18
C.    WITH 512 POINTS PER BLOCK.                                        VSD.19
C.                                                                      VSD.20
C.                                                                      VSD.21
C. BWCUT = CUT OFF FREQUENCY (HZ) OF THE BUTTERWORTH FILTER(LOW-PASS).  VSD.22
C. DMPFT = DAMPING FACTOR OF THE SEISMOMETER.                           VSD.23
C. ENW = ENERGY OF THE LAG WINDOW.                                      VSD.24
C. ERRBD =  LOWER ERROR BAR AT 90 PERCENT CONFIDENCE.                   VSD.25
C. ERRBU = UPPER ERROR BAR AT 90 PERCENT CONFIDENCE.                    VSD.26
C. FS = SQRT(POWER SPECTAL DENSITY).                                    VSD.27
C. GAIN = THE GAIN OF THE AMPLIFIER, IN DECIBAL.                        VSD.28
C. IIVSPL=1 WILL PLOT THE INDIVIDUAL FOURIER SPECTRUM.                  VSD.29
C. IMVSPL=1 WILL PLOT THE AVERAGED FOURIER SPECTRUM.                    VSD.30
C. INDEX3 CAN BE ANY INTEGER.                                           VSD.31
C. INDEX4 CAN BE ANY INTEGER.                                           VSD.32
C. IPUNCH=1 WILL PUNCH VSD ON CARD.                                     VSD.33
C. LABEL1 = STATION IDENTIFICATION.                                     VSD.34
C. MORE2 =0 INDICATES NO MORE INPUT DATA CARD.                          VSD.35
C. MTAPER = THE PERCENTAGE OF THE FIRST AND THE LAST TIME DATA BEING TAPVSD.36
C.          BY A COSINE BELL.                                           VSD.37
C. NBW = NUMBER OF BUTTERWORTH FILTER USED AS ANTI-ALIASING FILTER.     VSD.38
C. NPOW   NPTT = 2**NPOW                                                VSD.39
C. NPTF = THE NUMBER OF FREQUENCY COMPONENTS.                           VSD.40
C. NPTT = THE NUMBER OF DATA POINT IN TIME DOMAIN.                      VSD.41
C. NREC = NUMBER OF VSD TO BE AVERAGED.                                 VSD.42
```

```
C. NSKIP(NNSKIP) = SEQUENTIAL NUMBER OF DATA BLOCK TO BE SKIPPED.        VSD.43
C. NVAL(NSMP) = DIGITAL TIME SERIES OF ONE RECORD BLOCK.                 VSD.44
C. NSMP = NUMBER OF SAMPLING POINT IN EACH RECORD                        VSD.45
C. POWDST = POWER SPECTRAL DENSITY                                       VSD.46
C. RCCUT = CUT OFF FREQUENCY(HZ) OF 2-POLE RC LOW-PASS FILTER.           VSD.47
C. RD = DAMPING RESISTANCE OF THE SEISMOMETER, IN KILO-OHMS.             VSD.48
C. RECLEN = LENGTH OF EACH RECORD BLOCK OF 2500 POINTS (IN SECOND).      VSD.49
C. RS = COIL RESISTANCE OF THE SEISMOMETER. IN KILO-OHMS.                VSD.50
C. SAMIN = SAMPLING INTERVAL IN REAL TIME DOMAIN.                        VSD.51
C. VCOFS = FULL SCALE VOLTAGE OF VOLTAGE CONTROLLED OSCILLATOR.          VSD.52
C. VS = VELOCITY SPECTRAL DENSITY, IN MILLIMICRON/SEC/SQRT(HZ)           VSD.53
C.                                                                       VSD.54
C.                                                                       VSD.55
C.    THE INPUT DATA CARDS ARE                                           VSD.56
C.    (1) IPUNCH,NPOW,RECLEN (2I5,F5.0)                                  VSD.57
C .   (2) MORE2,IIVSPL,IMVSPL,INDEX3,INDEX4,LABEL1,NNSKIP,(NSKIP(I),I=1,VSD.58
C.        6),RS,RD,DMPFT,GAIN,RCCUT,VCOFS,NBW,BWCUT(5I1,A10,7I2,6F6.2,   VSD.59
C.        I1,F4.1)  FOR EACH SEISMOMETER OUTPUT.                         VSD.60
C.                                                                       VSD.61
C.....AUTHOR      ALFRED LIANG-CHI LIAW
C                 ENGINEERING GEOSCIENCE
C                 UNIVERSITY OF CALIFORNIA, BERKELEY
C.....DATE        SEPTEMBER 1977
C.                                                                       VSD.62
CCCCCCCCCCCCCCCCCCCCCCCCCCCCCCCCCCCCCCCCCCCCCCCCCCCCCCCCCCCCCCCCCCCCCCCCVSD.63
                                                                         VSD.64
      COMPLEX DATA,FDATA,CFDATA,POWDST                                   VSD.65
      COMPLEX X                                                          VSD.66
      COMMON /BLK1/FREQ(257)                                             VSD.67
      COMMON /BLK2/VS(257)                                               VSD.68
      COMMON /BLK3/ ERRDU(257),ERRBD(257)                                VSD.69
      COMMON /BLK4/NREC,LABEL1                                           VSD.70
      COMMON /BLK5/INDEX1,INDEX2                                         VSD.71
        COMMON /BLK6/RLFS(257)                                           VSD.72
      COMMON /BLK7/STAT                                                  VSD.73
      COMMON /BLK8/II                                                    VSD.74
      DIMENSION NVAL(2500),DATA(512),FDATA(257),CFDATA(257),POWDST(257)  VSD.75
      DIMENSION SUMFS(257),FS(257),SPECS(12),RFFS(257)                   VSD.76
      DIMENSION PHASE(257)                                               VSD.77
      DIMENSION NSKIP(6),CHI5(10),CHI95(20)                              VSD.78
      DIMENSION DATAWID(512)                                             VSD.79
      DIMENSION A(257,12),X(12)                                          VSD.80
      DATA CHI95/0.0039,0.052,0.117,0.178,0.229,0.272,0.310,0.342,0.369,VSD.81
     10.394,0.416,0.436,0.453,0.469,0.484,0.498,0.510,0.522,0.532,0.543/VSD.82
      DATA CHI5/3.84,3.00,2.60,2.37,2.21,2.10,2.01,1.94,1.88,1.83/       VSD.83
      DATA NSMP/2500/,MTAPER/10/,Z/1.645/                                VSD.84
                                                                         VSD.85
      READ 1,IPUNCH,NPOW,RECLEN                                          VSD.86
    1 FORMAT (2I5,F5.0)                                                  VSD.87
                                                                         VSD.88
      SPECS(12)=99.                                                      VSD.89
      NPTT=2**NPOW                                                       VSD.90
      NPTF1=(NPTT/2)+1                                                   VSD.91
      NPTF=NPTF1-1                                                       VSD.92
      SAMIN=RECLEN/(NSMP-1)                                              VSD.93
      PERIOD =(SAMIN)*(NPTT-1)                                           VSD.94
      PI=4.*ATAN(1.)                                                     VSD.95
      PI2=PI*2.0                                                         VSD.96
      M1=NPTT*MTAPER/100                                                 VSD.97
      M2=NPTT-M1                                                         VSD.98
      NTAPER=0                                                           VSD.99
      NTRFUN=0                                                           VSD.100
```

```
C.....GENERATING THE ARRAY CF FREQUENCY
      DO 21 I=1,NPTF
   21 FREQ(I)=I/PERIOD
   97 IA=0
      NS=12

   98 READ 2,MORE2,IIVSPL,IMVSPL,INDEX3,INDEX4,LABEL1,NNSKIP,(NSKIP(I),I
     1=1,6),RS,RD,DMPFT,GAIN,RCCUT,VCOFS,NBW,BWCUT
    2 FORMAT (5I1,A10,7I2,6F6.2,I1,F4.1)
      PRINT 108,MORE2,IIVSPL,IMVSPL,INDEX3,INDEX4,LABEL1,NNSKIP,(NSKIP(I
     1),I=1,6),RS,RD,DMPFT,GAIN,RCCUT,VCOFS,NBW,BWCUT
  108 FORMAT (2X,5I1,A10,7I2,6F6.2,I1,F4.1)

      IA=IA+1
      IF (EOF(5LINPUT).NE.0) GO TO 999
      DO 20 KI=1,NPTF
      SUMFS(KI)=0.0
   20 CONTINUE
      NREC=0

   99 READ (3) (NDAYS,NHOURS,MIN,NSEC)
      IF (EOF(3).NE.0) GO TO 999
      READ (3) (NDAYST,NHOUST,MINT,NSECT)
      READ (3) (STATN,NB,J)
      ENCODE (10,5,STAT) STATN,NB
    5 FORMAT (R8,A2)
      READ (3) (NVAL(I),I=1,2500)
      READ (3) (MORE)

      PRINT 3,STATN,NB,J,MORE
    3 FORMAT (1H0,*  STATN IN TAPE 3 = *,A10,* NB = *,I1,* J = *,I3,* MO
     1RE = *,I1)

      IF (IMVSPL.NE.1) GO TO 33

C     PRINT 4,STAT,NPTT,IIVSPL,IMVSPL,INDEX3
    4 FORMAT (1H1,///////////////,50X,*THE FOLLOWING DATA CAME FROM *,A10
     1,/,50X,*NUMBER CF POINT IN TIME DOMAIN = *,I4,/,50X,*INDEX1 = *,I1
     1,/,50X,*INDEX2 = *,I1,/,50X,*INDEX3 = *,I1,/////////)
      DO 19 I=1,NNSKIP
      IF (NB.EQ.NSKIP(I)) GO TO 331
   19 CONTINUE
C.....ADJUSTING THE DC SHIFT.

      SHIFT=0.0
      DO 666 IDC=1,2500
      SHIFT=SHIFT+FLOAT(NVAL(IDC))
  666 CONTINUE
      SHIFT=SHIFT/2500.0
      DO 667 IDC=1,2500
      NVAL(IDC)=NVAL(IDC)-SHIFT
  667 CONTINUE
   29 LJ=1

C.....APPLYING COSINE BELL TAPER.
   90 ENW=0.0
      DO 10 J=1,NPTT
      NVAL(J)=NVAL(J+LJ)
      IF (J.LT.M1) GO TO 7
      IF (J.GT.M2) GO TO 9
      TAPER=1.0
```

```
      GO TO 8
    7 ARG=PI*(M1-J+1)/M1
      TAPER=(1.0+COS(ARG))/2.0
      GO TO 8
    9 ARG=PI*(J-M2)/M1
      TAPER=(1.0+COS(ARG))/2.0
    8 CONTINUE
      ENW=ENW+TAPER*TAPER
      DATA(J)=CMPLX(TAPER*NVAL(J),0.0)
C     DATAWID(J)=TAPER
   10 CONTINUE
C     PRINT 109,ENW
  109 FORMAT (1H0,50X,*ENW = *,E12.3)

C     IF (NTAPER.NE.0) GO TO 25
C     PMAX1=1.5
C     PMIN1=DATAWID(1)
C     CALL YPLOTLG(DATAWID,1,NPTT,1,PMAX1,PMIN1,STAT)
C     NTAPER=1
   25 CONTINUE
C     IF (LJ.LT.512) GO TO 15
C     PRINT 14
   14 FORMAT (//////)
   15 CONTINUE

C     PRINT 11, (NVAL(J),J=1,NPTT)
   11 FORMAT (2X,5I6,3X,5I6,3X,5I6,3X,5I6)
      GO TO 333
  331 PRINT 332,STAT,NB
  332 FORMAT (1H0,10X,*THE PROGRAM SKIPS THE RECORD *,A10,I3)
      GO TO 33

  333 CALL FFT(DATA,NPOW,NPTT,PI)
      DO 30 KJ=1,NPTF
      FDATA(KJ)=DATA(KJ+1)*2.0*SAMIN
      CFDATA(KJ)=CONJG(FDATA(KJ))
C     FREQ(KJ)=(KJ-1)/PERIOD
      POWDST(KJ)=FDATA(KJ)*CFDATA(KJ)
      POWDST(KJ)=POWDST(KJ)/PERIOD
      POWDST(KJ)=POWDST(KJ)/ENW
      FS(KJ)=SQRT(REAL(POWDST(KJ)))
      SUMM=FS(KJ)
      SUMFS(KJ)=SUMFS(KJ)+SUMM
   30 CONTINUE

C.....PLOT THE INDIVIDUAL FOURIER SPECTRUM BY THE YPLOT ROUTINE.


CP    PMAX1=0.00
CP    PMIN1=FS(1)
CP    DO 220 I=1,NPTF
CP    IF(FS(I).GT.PMAX1) PMAX1=FS(I)
CP    IF(FS(I).LT.PMIN1) PMIN1=FS(I)
CP220 CONTINUE
CP    CALL YPLOTLG(FS,1,NPTF,1,PMAX1,PMIN1,STAT)

      LJ=LJ+NPTT
      NREC=NREC+1
      IF (IIVSPL.NE.1) GO TO 36
      II=0
      IF (NREC.EQ.1) GO TO 34
      CALL NXTFRM(SPECS)
```

```
   34  CALL PLOTFS(NPTF)
   36 IF (LJ.LT.2049) GO TO 90
   33 IF (MORE.NE.0) GO TO 99
C  33 IF (NREC.LT.NNREC) GO TO 99
      IF (IMVSPL.NE.1) GO TO 45
      DO 40 KK=1,NPTF
      FS(KK)=SUMFS(KK)/NREC
   40 CONTINUE

C.....CORRECTING THE SYSTEM RESPONSE

      CALL GEOPHON(VS,FS,DMPFT,PI2,NPTF,RS,RD)
      IF (NBW.NE.0) CALL ANTIALI(VS,PI2,NBW,BWCUT,NPTF)
      CALL AMPVCO(VS,NPTF,GAIN,VCCFS,RCCUT)

C.....CALCULATING THE CONFIDENCE LIMITS

      NFRDM=2*NREC
      IF (NFRDM.GT.10) GO TO 51
      CHI2=CHI5(NFRDM)
      GO TO 52
   51 CALL CHISC(NFRDM,Z,CHI2)
   52 IF(NFRDM.GT.20) GO TO 53
      CHI1=CHI95(NFRDM)
      GO TO 54
   53 Z1=-Z
      CALL CHISC(NFRDM,Z1,CHI1)
   54 CONTINUE
      DO 55 KK=1,NPTF
      ERRBU(KK)=VS(KK)/SQRT(CHI1)
      ERRBD(KK)=VS(KK)/SQRT(CHI2)
   55 CONTINUE
      PRINT 35, NREC,LABEL1,CHI1,CHI2
   35 FORMAT (1H1,///////////////,35X,*THE FOLLOWING DATA ARE THE ESTIMA
     1TES OF VELOCITY SPECTRAL DENSITY*,/,35X, *OVER*,I4,* RECORDS OF *,
     1A10,/,35X,*CHISQ OVER DF =*,2F10.3)
      PRINT 350,NPTT,SAMIN
  350 FORMAT (35X,*THERE ARE*,I5,* DATA POINTS IN EACH RECORD, WITH SAMP
     1LING INTERVAL *,F12.3,* SECONDS.*)


      PMAX1=0.00
      PMIN1=VS(1)
      DO 230 I=1,NPTF
      IF(VS(I).GT.PMAX1) PMAX1=VS(I)
      IF(VS(I).LT.PMIN1) PMIN1=VS(I)
  230 CONTINUE
      CALL YPLOTLG(VS,1,NPTF,1,PMAX1,PMIN1,LABEL1)

      IF (IPUNCH.NE.1) GO TO 443


      WRITE (6) (VS(I),I=1,NPTF)
      WRITE (6) (CHI1,CHI2)
  443 CALL SECOND(TIME)
      PRINT 444, TIME
  444 FORMAT (15X,*TIME = *,F15.4)
      IF (IMVSPL.NE.1) GO TO 44
      CALL NXTFRM(SPECS)
      II=1
   50 CALL PLOTFS(NPTF)
   44 CONTINUE
```

```
   45 IF (MORE2.NE.0) GO TO 98                                          VSD.287
  999 CALL GDSEND(SPECS)                                                VSD.288
      STOP                                                              VSD.289
      END                                                               VSD.290


      SUBROUTINE AMPVCO(VS,NPTF,GAIN,VCOFS,RCCUT)                        AMPVC.2
                                                                         AMPVC.3
C.....SUBROUTINE AMPVCO IS USED TO CORRECT THE GAIN AND THE LOW-PASS     AMPVC.4
C     FILTER OF THE AMPLIFIER AND THE VCO FULL SCALE.                    AMPVC.5
C      THE LOW-PASS FILTER  AT AS110 IS A 2-POLE RC FILTER.              AMPVC.6
                                                                         AMPVC.7
      COMMON /BLK1/FREQ(257)                                             AMPVC.8
      DIMENSION VS(257)                                                  AMPVC.9
      GAIN=GAIN/20.0                                                     AMPVC.10
      GAIN=10.0**GAIN                                                    AMPVC.11
      A=GAIN*2048.0/VCOFS                                                AMPVC.12
      DO 1 I=1,NPTF                                                      AMPVC.13
      B=FREQ(I)/RCCUT                                                    AMPVC.14
      B2=B*B+1                                                           AMPVC.15
      VS(I)=VS(I)*B2/A                                                   AMPVC.16
      VS(I)=VS(I)*1.0E+09                                                AMPVC.17
    1 CONTINUE                                                           AMPVC.18
      RETURN                                                             AMPVC.19
      END                                                                AMPVC.20


      SUBROUTINE ANTIALI(VS,PI2,NBW,BWCUT,NPTF)                          ANTAL.2
                                                                         ANTAL.3
C.....SUBROUTINE ANTIALI IS USED TO COREECT MODULUS OF THE TRANSFER      ANTAL.4
C     FUNCTION OF ARBITRARY BUTTERWORTH LOW PASS FILTER USED AS ANTI-ALIANTAL.5
C      ASING FILTER.                                                     ANTAL.6
C     NBW = NUMBER OF STAGE OF FILTERS.
C     NPOLE = NUMBER OF POLE OF THE FILTER.                              ANTAL.7
                                                                         ANTAL.8
      COMMON /BLK1/FREQ(257)                                             ANTAL.9
      DIMENSION VS(257)                                                  ANTAL.10
      NPOLE=4                                                            ANTAL.11
      DO 1 I=1,NPTF                                                      ANTAL.12
      N=2*NPOLE                                                          ANTAL.13
      A=FREQ(I)/BWCUT                                                    ANTAL.14
C     FOR HIGH PASS FILTER, A=1.0/A
      A=A**N                                                             ANTAL.15
      B=SQRT(1+A)                                                        ANTAL.16
      B=B**NBW                                                           ANTAL.17
      VS(I)=VS(I)*B                                                      ANTAL.18
    1 CONTINUE                                                           ANTAL.19
      RETURN                                                             ANTAL.20
      END                                                                ANTAL.21


      SUBROUTINE CHISC(NFRDM,Z,CHI)                                      CHIS2.2

C.....THIS SUBROUTINE CALCULATES PERCENTILES OF THE CHI-SQUARE/DEGREE OFCHIS2.3
C.....FREEDOM DISTRIBUTIONS FOR LARGE VALUES OF DEGREE OF FREEDOM.       CHIS2.4
                                                                         CHIS2.5
      DF=FLOAT(NFRDM)                                                    CHIS2.6
      A=2.0/(9.0*DF)                                                     CHIS2.7
      B=SQRT(A)                                                          CHIS2.8
      C=1.0-A+Z*B                                                        CHIS2.9
      CHI=C*C*C                                                          CHIS2.10
      RETURN                                                             CHIS2.11
```

```
      END

      SUBROUTINE FFT(A,M,N,PI)

C.....THIS FFT SUBROUTINE PERFORMS THE FORWARD FAST FOURIER TRANSFORM
C     ONLY. AFTER COOLEY,LEWIS,WELCH,OBTAINED FROM L.R. RABINER AND B.
C     GOLD---- THEORY AND APPLICATION OF DIGITAL SIGNAL PROCESSING.
C.....N=2**M
C.....A(N) = THE ARRAY OF DATA TO BE TRANSFORMED.
C.....FOURIER TRANSFORM IS THE FORM OF (REAL)-I(IMAG).

      COMPLEX A(N),U,W,T
      NV2=N/2
      NM1=N-1
      J=1
      DO 7 I=1,NM1
      IF (I.GE.J) GO TO 5
      T=A(J)
      A(J)=A(I)
      A(I)=T
    5 K=NV2
    6 IF(K.GE.J) GO TO 7
      J=J-K
      K=K/2
      GO TO 6
    7 J=J+K
      DO 20 L=1,M
      LE=2**L
      LE1=LE/2
      U=(1.0,0.)
      W=CMPLX(COS(PI/LE1),SIN(PI/LE1))
      DO 20 J=1,LE1
      DO 10 I=J,N,LE
      IP=I+LE1
      T=A(IP)*U
      A(IP)=A(I)-T
   10 A(I)=A(I)+T
   20 U=U*W
      RETURN
      END

      SUBROUTINE GEOPHON(VS,FS,DMPFT,PI2,NPTF,RS,RD)

C.....MODULUS CORRECTION ONLY.
C.....SUBROUTINE GEOPHON IS USED TO CORRECT THE VELOCITY SENSITIVITY,
C     DAMPING RESISTANCE,AND GENERATOR CONSTANCE.
C.....WG = NATURAL FREQUENCY OF THE SEISMOMETER (IN HZ).
C     GS = GENERATOR CONSTANCE OF THE SEISMOMETER (IN VOLT/METER/SEC).
C     RS = COIL RESISTANCE.
C     RD = DAMPING RESISTANCE.
C     DMPFT =  DAMPING FACTOR.

      COMMON /BLK1/FREQ(257)
      DIMENSION VS(257),FS(257)
      DATA WG/4.5/,GS/77.17/
      WS=WG*PI2
      WS2=WS*WS
      RO2=2.0*DMPFT
      RD=RD*1000.0
      RS=RS*1000.0
```

```
      DO 1 I=1,NPTF                                                     GEOPH.21
      WE=PI2*FREQ(I)                                                    GEOPH.22
      WE2=WE*WE                                                         GEOPH.23
      A=WE2-WS2                                                         GEOPH.24
      A2=A*A                                                            GEOPH.25
      B=RO2*WS*WE                                                       GEOPH.26
      B2=B*B                                                            GEOPH.27
      C=SQRT(A2+B2)                                                     GEOPH.28
      AMP=WE*WE/C                                                       GEOPH.29
      VS(I)=FS(I)/AMP                                                   GEOPH.30
      VS(I)=VS(I)/GS                                                    GEOPH.31
      IF (RD.GE.999000.0) GO TO 1                                       GEOPH.32
      R=RS+RD                                                           GEOPH.33
      VS(I)=VS(I)*R/RD                                                  GEOPH.34
    1 CONTINUE                                                          GEOPH.35
      RETURN                                                            GEOPH.36
      END                                                               GEOPH.37

      SUBROUTINE PLOTFS(NPTF)                                           PLFS.2
                                                                        PLFS.3
C.....THIS SUBROUTINE PLOTS THE VELOCITY SPECTRAL DENSITY IN LOG-LOG     PLFS.4
C.....SCALE.                                                            PLFS.5
                                                                        PLFS.6
      DIMENSION SPECS(30),LINE(4)                                       PLFS.7
      COMMON /BLK1/X(257)                                               PLFS.8
      COMMON /BLK2/Y(257)                                               PLFS.9
      COMMON /BLK3/ERRBU(257),ERRBD(257)                                PLFS.10
      COMMON /BLK4/NREC,LABEL1                                          PLFS.11
      COMMON /BLK5/INDEX1,INDEX2                                        PLFS.12
      COMMON /BLK7/STAT                                                 PLFS.13
      COMMON /BLK8/I1                                                   PLFS.14
      SPECS(1)=1.0                                                      PLFS.15
      SPECS(2)=1.5                                                      PLFS.16
      SPECS(3)=25.0                                                     PLFS.17
      SPECS(4)=0.3                                                      PLFS.18
      DO 8 I=15,NPTF                                                    PLFS.19
      IF (Y(I).GT.1.0E+03) GO TO 6                                      PLFS.20
      IF (Y(I).LT.1.0E-01) GO TO 9                                      PLFS.21
    8 CONTINUE                                                          PLFS.22
      SPECS(5)=1.0E+03                                                  PLFS.23
      SPECS(6)=1.0E-01                                                  PLFS.24
      GO TO 5                                                           PLFS.25
    6 SPECS(5)=1.0E+04                                                  PLFS.26
      SPECS(6)=1.0                                                      PLFS.27
      GO TO 5                                                           PLFS.28
    9 SPECS(5)=1.0E+01                                                  PLFS.29
      SPECS(6)=1.0E-03                                                  PLFS.30
    5 SPECS(7)=7.875                                                    PLFS.31
      SPECS(8)=5.2                                                      PLFS.32
      SPECS(11)=1.0                                                     PLFS.33
      SPECS(12)=99.                                                     PLFS.34
      CALL AXLGLG(SPECS)                                                PLFS.35
      YMAX=SPECS(5)                                                     PLFS.36
      YMIN=SPECS(6)                                                     PLFS.37
      DO 10 I=1,NPTF                                                    PLFS.38
      IF (Y(I).GT.YMAX) Y(I)=YMAX                                       PLFS.39
      IF (Y(I).LT.YMIN) Y(I)=YMIN                                       PLFS.40
   10 CONTINUE                                                          PLFS.41
C     PRINT 11,(X(I),Y(I),I=1,409)                                      PLFS.42
C  11 FORMAT (10X,*FREQ = *,F10.7,10X,*AMPLITUDE SPECTRUM *,E13.3)      PLFS.43
      SPECS(25)=-0.15                                                   PLFS.44
```

```
      CALL SAXLGT(SPECS)
      SPECS(27)=-0.15
      CALL SAXLGR(SPECS)
      SPECS(13)=FLOAT(NPTF)
      SPECS(14)=1.0
      SPECS(15)=1.0
      SPECS(30)=97.
      CALL SLLGLG(X,Y,SPECS)
      IF (II.EQ.0) GO TO 15

      SPECS(13)=FLOAT(NPTF)
      DO 12 I=1,164
      Y(I)=ERRBU(I)
      IF (Y(I).GT.YMAX) Y(I)=YMAX
      IF (Y(I).LT.YMIN) Y(I)=YMIN
   12 CONTINUE
      SPECS(16)=17.0
      SPECS(17)=0.05
      SPECS(18)=0.05
      CALL PSLGLG(X,Y,SPECS)
      DO 13 I=1,NPTF
      Y(I)=ERRBD(I)
      IF (Y(I).GT.YMAX) Y(I)=YMAX
      IF (Y(I).LT.YMIN) Y(I)=YMIN
   13 CONTINUE
      CALL PSLGLG(X,Y,SPECS)
   15 SPECS(17)=.1
      SPECS(18)=.1
      SPECS(9)=10.0
      SPECS(19)=0.0
      SPECS(21)=1.0
      SPECS(24)=0.0
      SPECS(29)=2.0
      CALL NCLGB(SPECS)
      SPECS(20)=0.0
      SPECS(26)=0.0
      CALL NOLGL(SPECS)
      SPECS(17)=0.15
      SPECS(18)=0.15
      SPECS(24)=0.2
      CALL TITLEB(14HFREQUENCY (HZ),SPECS)
      SPECS(20)=90.0
      SPECS(26)=0.4
      CALL TITLEL(30HVSD (MILLIMICRON/SEC/SQRT(HZ)),SPECS)
      SPECS(17)=0.15
      SPECS(18)=0.15
      SPECS(19)=0.0
      SPECS(20)=0.0
      SPECS(21)=1.0
      SPECS(23)=6.6
      RULE=1.0
      IF (II.EQ.0) GO TO 20
      SPECS(22)=2.15
      SPECS(28)=0.0
      VALUE=NREC
      CALL DECVAL(RULE,VALUE,SPECS)
      LINE(1)=LABEL1
      LINE (2)=10H   RECORDS
      LINE(3)=0
      GO TO 21
   20 LINE(1)=STAT
      LINE(2)=0
```

```
21 SPECS(22)=0.5                                                         PLFS.107
   CALL TITLEG(RULE,LINE,SPECS)                                          PLFS.108
   RETURN                                                                PLFS.109
   END                                                                   PLFS.110

   SUBROUTINE YPLOTLG(Y,IB,IE,IK,PMAX,PMIN,TITLE)                        YPLLG.2

   COMMON /BLK1/X(257)                                                   YPLLG.3
   DIMENSION Y(1),KMAP(100),ISCALE(11)                                   YPLLG.4
   DATA KBLANK,KY/1H ,1H*/                                               YPLLG.5
   DATA ISCALE/ 0,10,20,30,40,50,60,70,80,90,100/                        YPLLG.6
   DO 2 I=1,100                                                          YPLLG.7
 2 KMAP(I)=KBLANK                                                        YPLLG.8
C....PRINT BEGINNING OF GRAPH                                            YPLLG.9
   QMAX=ALOG10(PMAX)                                                     YPLLG.10
   QMIN=ALOG10(PMIN)                                                     YPLLG.11
   C=100.0/(QMAX-QMIN)                                                   YPLLG.12
   B=C*QMIN                                                              YPLLG.13
   SCALE=1.0/C                                                           YPLLG.14
   PRINT 5,TITLE,IB,IE,IK,PMAX,PMIN                                      YPLLG.15
 5 FORMAT (1H1,10X,*YPLOT......*,A10,/,10X,*IB=*,I5,2X,*IE=*,I5,2X,*IYPLLG.16
  1K=*,I5,2X,*PMAX=*,E12.3,2X,*PMIN=*,E12.3,///)                         YPLLG.17
   PRINT 6, (ISCALE(I),I=1,11)                                           YPLLG.18
 6 FORMAT(11X,5(I2,8X),1X,I2,5(7X,I3))                                   YPLLG.19
   DO 7 I=1,2                                                            YPLLG.20
 7 PRINT 8                                                               YPLLG.21
 8 FORMAT(13X,(11(1H. ,9X)))                                             YPLLG.22
   PRINT 12                                                              YPLLG.23
12  FORMAT (  6X,1HX,7X,100H.........................................YPLLG.24
  1........................................................... ,7X,1HYPLLG.25
  1Y)                                                                    YPLLG.26
C....PRINT BODY OF GRAPH                                                 YPLLG.27
   DO 10 I=IB,IE,IK                                                      YPLLG.28
   YLG=ALOG10(Y(I))                                                      YPLLG.29
   IY=C*YLG-B                                                            YPLLG.30
C  CHECK THAT Y IS ON SCALE                                              YPLLG.31
   IF(IY .LT. 1 .OR. IY .GT. 100) GO TO 13                               YPLLG.32
                                                                         YPLLG.33
   KMAP(IY)=KY                                                           YPLLG.34
   PRINT 9, X(I),(KMAP(J),J=1,100),Y(I),I                                YPLLG.35
 9  FORMAT (  2X,F9.3,1X,1HI,100A1,1HI,2X,E10.3,1X,I4)                   YPLLG.36
   GO TO 14                                                              YPLLG.37
13 PRINT 9, X(I),(KMAP(J),J=1,100),Y(I)                                  YPLLG.38
   GO TO 10                                                              YPLLG.39
14 KMAP(IY)=KBLANK                                                       YPLLG.40
10 CONTINUE                                                              YPLLG.41
   RETURN                                                                YPLLG.42
   END                                                                   YPLLG.43

   SUBROUTINE YPLOT(Y,IB,IE,IK,PMAX,PMIN,TITLE)                          YPLLI.2

   COMMON /BLK1/X(257)                                                   YPLLI.3
   DIMENSION Y(1),KMAP(100),ISCALE(11)                                   YPLLI.4
   DATA KBLANK,KY/1H ,1H*/                                               YPLLI.5
   DATA ISCALE/ 0,10,20,30,40,50,60,70,80,90,100/                        YPLLI.6
   DO 2 I=1,100                                                          YPLLI.7
 2 KMAP(I)=KBLANK                                                        YPLLI.8
C....PRINT BEGINNING OF GRAPH                                            YPLLI.9
   C=100.0/(PMAX-PMIN)                                                   YPLLI.10
   B=C*PMIN                                                              YPLLI.11
   SCALE=1.0/C                                                           YPLLI.12
```

```
      PRINT 5,TITLE,IB,IE,IK,PMAX,PMIN
    5 FORMAT (1H1,10X,*YPLCT......*,A10,/,10X,*IB=*,I5,2X,*IE=*,I5,2X,*I
     1K=*,I5,2X,*PMAX=*,E12.3,2X,*PMIN=*,E12.3,///)
      PRINT 6, (ISCALE(I),I=1,11)
    6 FORMAT(11X,5(I2,8X),1X,I2,5(7X,I3))
      DO 7 I=1,2
    7 PRINT 8
    8 FORMAT(13X,(11(1H. ,9X)))
      PRINT 12
   12  FORMAT (   6X,1HX,7X,100H......................................
     1.................................................... ,7X,1H
     1Y)
C....PRINT BODY OF GRAPH
      DO 10 I=IB,IE,IK
      IY=C*Y(I)-B
C     CHECK THAT Y IS ON SCALE
      IF(IY .LT. 1 .OR. IY .GT. 100) GO TO 13
      KMAP(IY)=KY
      PRINT 9, X(I),(KMAP(J),J=1,100),Y(I),I
    9   FORMAT (   2X,F9.3,1X,1HI,100A1,1HI,2X,E10.3,1X,I4)
      GO TO 14
   13 PRINT 9,  X(I),(KMAP(J),J=1,100),Y(I)
      GO TO 10
   14 KMAP(IY)=KBLANK
   10 CONTINUE
      RETURN
      END
```

```
    0      9 02.5
10102        HS                  3.40999.00  0.30102.00 30.00  5.00310.00
00102      A3.7N                 3.40999.00  0.30114.00 30.00  5.00310.00
```

```
************************************************************************
*                                                                      *
*                           PROGRAM FKPSD                              *
*                                                                      *
************************************************************************

FKPSD,7,500.471209,LIAW
DISKHOG,14000.
RUN76,SC,NL77777.
FETCHMT,TAPE3,U3,22304,IF.
FETCHPS,BKYULIB,TEMP,GDS.
FETCHPS,BKYLGOB,GDSCC,GDSCC.
COPYI,TEMP,LIB.
RFL,,310000.
LINK,X,F=LGO,P=LIB,PP=[LC=99999].
EXIT.
RETURN,LGO,LIB.
DUMP,0.
FIN.
GDSCC.
RETURN,TAPE99,GDSCC.
      PROGRAM FKPSD(INPUT,OUTPUT,TAPE3,TAPE99,TAPE97,TAPE92,TAPE93,TAPE9FK2.2
     14)                                                                FK2.3
                                                                        FK2.4
CCCCCCCCCCCCCCCCCCCCCCCCCCCCCCCCCCCCCCCCCCCCCCCCCCCCCCCCCCCCCCCCCCCCCCCCFK2.5
C                                                                       FK2.6
C. THIS PROGRAM READS THE DIGITAL DATA IN TAPE 3, THEN COMPUTES THE      FK2.7
C. COHERENCE BETWEEN ANY TWO SEISMOMETER OUTPUTS AND/OR ESTIMATES THE    FK2.8
C. FREQUENCY-WAVENUMBER POWER SPECTRAL DENSITY (FKPSD) AT THE            FK2.9
C. FREQUENCIES SPECIFIED BY FREQ(NFY(NNFY)).                             FK2.10
C. THE TAPE 3 IS GENERATED BY THE PROGRAM (DUMP) WHICH UNPACKES AND      FK2.11
C. TRANSLATES THE TAPE 5. THE TAPE 5 IS GENERATED BY THE DIGITIZER IN    FK2.12
C. THE HAVILAND HALL. EACH DIGITAL RECORD OF 2500 POINTS IS NORMALLY     FK2.13
C. DIVIDED INTO 24 DATA BLOCKS EACH HAS 64 POINTS. THE NUMBERS OF DATA   FK2.14
C. BLOCK AND DATA POINTS ARE ASSIGNED BY THE INPUT CARDS AND THE         FK2.15
C. DIMENSION OF SOME VARIABLES.                                          FK2.16
C. FKPSD CAN BE ESTIMATED BY CONVENTIONAL BEAM-FORMING METHOD (BFM) OR   FK2.17
C. HIGH-RESOLUTIONAL METHOD (MAXIMUM-LIKELIHOOD METHOD, MLM) BY SPECI-   FK2.18
C. FYING ICONVEN=1 OR 0.                                                 FK2.19
                                                                        FK2.20
C. AMGAIN = GAIN OF THE AMPLIFIER SET IN THE FIELD, IN DB.              FK2.21
C. DMPFT = DAMPING FACTOR OF THE SEISMOMETER.                            FK2.22
C. GAIN = THE CORRECTIONAL FACTOR FOR AMPLIFIER AND VCO FULL SCALE AND/ FK2.23
C.        OR THE POLARIZATION OF THE SEISMOMETER.                       FK2.24
C. ICOHER=1 THE PROGRAM COMPUTES THE COHERENCE.                          FK2.25
C. ICONVEN=1 THE PROGRAM ESTIMATES THE FKPSD BY CONVENTIONAL METHOD.     FK2.26
C. IFKPLOT=1 THE PROGRAM GENERATES A DECK FOR CALCOMP PLOTTER.           FK2.27
C. IFKPSD=1 THE PROGRAM ESTIMATES FKPSD.                                 FK2.28
C. ISKARR=1 THE PROGRAM SKIPS THE DATA OF THE WHOLE ARRAY.               FK2.29
C. ITRANS=1 THE PROGRAM GIVES THE TRANSFER FUNCTION OF THE ARRAY INSTEADFK2.30
C.           OF FKPSD.                                                  FK2.31
C. MLF = MAXIMUM LIKELIHOOD FILTER.                                      FK2.32
C. MTAPER = PERCENTAGE OF DATA POINT IN THE HEAD AND THE TAIL OF EACH    FK2.33
C.           DATA BLOCK ARE TAPERED BY HAMMING WINDOW.                  FK2.34
C. (NAV1*2)+1 = NAV = NO. OF THE ADJECENT FREQUENCY COMPONENTS BEING     FK2.35
C.                     AVERAGED.                                        FK2.36
C. NBMAX = THE MAXIMUM NUMBER OF DATA BLOCK USED TO ESTIMATE FKPSD.      FK2.37
C. NB512 = NO. OF DATA BLOCK SELECTED FROM EACH SEISMOMETER OUTPUT.      FK2.38
C. NFY(NNFY) = AN ARRAY OF SEQUENTIAL NUMBERS OF FREQUENCY COMPONENT     FK2.39
C.           OF P(KX,KY,FREQ).                                          FK2.40
C. NNFY = NUMBER OF FREQUENCY COMPONENT OF P(KX,KY,FREQ) TO BE CALCULATEFK2.41
```

```
C.         D.
C. NFP = SEQUENTIAL NUMBER OF FREQUENCY COMPONENTS BEING USED  TO
C.         CALCULATE F-K SPECTRUM.
C. NKX = NO. OF THE X-WAVENUMBER COMPONENTS.
C. NKY = NO. OF THE Y-WAVENUMBER COMPONENTS.
C. NPLEV = NO. OF THE CONTOUR LEVELS IN A FKPSD PLOT.
C. NPTF = NUMBER OF FREQUENCY COMPONENT.
C. NPTT = NO. OF DATA POINT IN EACH DATA BLOCK.
C. NS = NUMBER OF SEISMOMETER IN THE ARRAY.
C. NSMP = NO. OF THE SAMPLING POINT IN EACH RECORD.
C. NVAL = DIGITAL TIME SERIES.
C. NVSD(NVSDPL) =  NO. OF ARRAY ELEMENT EXPECTING TO HAVE VSD PLOT.
C. N2500 = NO. OF RECORD (2500 DATA POINTS) OF EACH SENSOR OUTPUT
C.          NEEDS TIME CORRECTION DUE TO IMPROPER STARTING TIME IN THE
C.          TAPE DRIVER OF THE DIGITIZER.
C. PMAXREF = REFERENT POWER LEVEL FOR THE MAXIMUM FKPSD.
C. RCCUT = CUT OFF FREQUENCY OF THE RC FILTER SET IN THE AMPLIFIER.
C. RECLEN = THE LENGTH OF EACH RECORD, IN SECONDS.
C. RD = DAMPING RESISTANCE OF THE SEISMOMETER, IN KILO-OHMS.
C. RS = COIL RESISTANCE OF THE SEISMOMETER, IN KILO-OHMS.
C. SM = SPECTRAL MATRIX, COHERENCY MATRIX, NORMALIZED SPECTRAL MATRIX
C. SMNFP = OPERATIONAL MATRIX
C. SPACIN = THE MINIMUM DISTANCE BETWEEN TWO SEISMOMETERS IN THE ARRAY,
C.           READ IN METER.
C. STA = ARRAY LOCATION
C. STAT = IDENTIFICATION FOR EACH SEISMOMETER OUTPUT IN THE ARRAY.
C. X = (KM,KM) THE COORDINATE OF THE SEISMOMETER LOCATION.
C. XF = MODIFIED FOURIER COEFFICIENTS OF NVAL.
C. XKIN = LOWER LEFT CORNERED VALUE OF XKX AND YKY
C. NPLEV = SIZE OF THE ARRAY (PLEVEL).
C. PLEVEL(NPLEV) = CONTOUR LEVELS OF FKPSD PLOT, IN DB.
C. VCOFS = VCO FULL SCALE SET AT FIELD, IN VOLT.
C. VS(NPTF) = VELOCITY SPECTRAL DENSITY
C. W(NPTT) = HAMMING WINDOW WEIGHTING FUNCTION APPLIED ON TIME DOMAIN.
C. WSPA(NS) = SPATIAL WEIGHTING FUNCTION.
C.

C.....THE INPUT DATA CARDS ARE
C       (1) RECLEN,NPOW,NSMP,NFMAX,N2500(F5.0,4I5)
C       (2) NPLEV,(PLEVEL(I),I=1,10) (I5,10F5.0)
C       (3) ICONVEN,IFKPLOT,NVSDPL,(NVSD(I),I=1,12) (15I5)
C       (4) MORE2,ICOHER,IFKPSD,ISKARR,NS,NAV1,ITRANS,NBW,BWCUT,SCALK,
C           SPACIN,STA(1) (8I5,3F5.0,A10)       FOR EACH ARRAY DATA SET
C       (5) NNFY,(NFY(I),I=1,NNFY) (16I5)       FOR EACH ARRAY DATA SET
C       (6) (DTIME(I),I=1,N2500*NS) (16F5.3)    FOR EACH ARRAY DATA SET
C       (7) (X(I),I=1,NS) (10F8.4)              FOR EACH ARRAY DATA SET
C       (8) STAT,(NNSKIP,(NSKIP(I),I=1,9)),GAIN,RS,RD,DMPFT (A10,10I2,
C           4F5.0)                              FOR EACH GEOPHONE OUTPUT
C
C.....AUTHOR      ALFRED LIANG-CHI LIAW
C                 ENGINEERING GEOSCIENCE
C                 UNIVERSITY OF CALIFORNIA, BERKELEY
C.....DATE        SEPTEMBER 1977
C
CCCCCCCCCCCCCCCCCCCCCCCCCCCCCCCCCCCCCCCCCCCCCCCCCCCCCCCCCCCCCCCCCCCCCCCC

      COMPLEX CZERO,DATA,DEN,SF,EKX,X,T1,E,SUMQJL,MLF,SUMFUN,CFUN,SUMQL
      COMPLEX F,DET,FF
      COMPLEX SMTEMP
      COMPLEX V,SMNPF
      COMPLEX T,CI
      LARGE C.SM(12,12,226)
```

```
      LARGE C.XF(12,24,64)
      DIMENSION PMAXDB(20),FYP(30)
      DIMENSION SMNPF(12,12)
      DIMENSION V(12,24)
      DIMENSION NVAL(2500)
      DIMENSION X(12),MLF(12),EKX(12)
      DIMENSION NFY(50),FKPMAX(50)
      DIMENSION DATA(512),NP(41,41)
      DIMENSION SPECS(12),NSKIP(10)
      DIMENSION PHASE(226),W(512),T(226),NIB(12),WSPA(12),DTIME(72),NVSD
     1(12)
      COMMON /BLK1/FREQ(226)
      COMMON /BLK2/COH(226)
      COMMON /BLK5/STATN(12)
      COMMON /BLK7/XK(41),YK(41)
      COMMON /BLK8/P(41,41)
      COMMON /BLK9/NKX,NKY
      COMMON /BLK10/PLEVEL(10),NPLEV
      COMMON /BLK11/STA(2)
      COMMON /BLK12/VEL(5),NVEL,AZIMU(5)
      COMMON /BLK13/ERRBU(164),ERRBD(164)
      COMMON /BLK14/VS(226),NE512,NPTF
      DATA MTAPER/10/
      DATA Z95/1.645/
      DATA NKX/41/,NKY/41/
      DATA PMAXREF/10000.0/

      CALL SECOND(TIME)

C.....-----------------------------------------------------------------
C.....READ INPUT DATA
C.....-----------------------------------------------------------------
      PRINT 14,TIME
      READ 1,RECLEN,NPOW,NSMP,NBMAX,N2500
      ICON=0
      STA(2)=0
      CZERO=CMPLX(0.0,0.0)
      CI=CMPLX(0.0,1.0)
      SPECS(12)=99.
      NPTT=2**NPOW
C.    DUE TO THE LIMIT OF LCM, SET MAX. NPTF=226.
      NPTF=NPTT/2
      IF (NPTF.GE.226) NPTF=226
      SAMIN=RECLEN/FLOAT(NSMP-1)
      PERIOD =(SAMIN)*FLOAT(NPTT-1)
      PI=4.*ATAN(1.0)
      PI2=2.0*PI
      CALL HAMMIN(NPTT,PI2,W,ENW)
      M1=NPTT*MTAPER/100
      M2=NPTT-M1
      NTAPER=0
       READ 2,NPLEV,(PLEVEL(I),I=1,10)

      DO 110 I=1,NPTF
  110 FREQ(I)=FLOAT(I)/PERIOD

        READ 3,ICONVEN,IFKPLOT,NVSDPL,(NVSD(I),I=1,12)
      IF (ICONVEN.NE.1) GO TO 198
      DO 140 I=1,12
  140 WSPA(I)=1.0
  198 READ 4,MORE2,ICOHER,IFKPSD,ISKAPR,NS,NAV1,ITRANS,NBW,BWCUT,SCALK,S
     1PACIN,STA(1)
```

```
      READ 5,NNFY,(NFY(I),I=1,NNFY)                                     FK2.162
      NF1=NFY(2)-NFY(1)                                                 FK2.163
      DO 220 I=2,NNFY                                                   FK2.164
      I1=I+1                                                            FK2.165
      NF2=NFY(I1)-NFY(I)                                                FK2.166
      IF (NF1.NE.NF2) GO TO 227                                         FK2.167
      IFKYPL=1                                                          FK2.168
      IF (I1.GE.NNFY) GO TO 229                                         FK2.169
  220 CONTINUE                                                          FK2.170
      GO TO 229                                                         FK2.171
  227 IFKYPL=0                                                          FK2.172
  229 CONTINUE                                                          FK2.173
C.    STATEMENTS FK2.176 AND FK2.226 ARE USED ONLY WHEN THAT            FK2.174
C.    3 RECORDS/ARRAY ELEMENT, N2500=2, AND THE FIRST RECORD BEING TO   FK2.175
C.    ESTIMATE FKPSD.                                                   FK2.1751
      IDEL=-1                                                           FK2.176
      NDTIME=N2500*NS                                                   FK2.177
      READ 6,(DTIME(I),I=1,NDTIME)                                      FK2.178
      NAV=NAV1*2+1                                                      FK2.179
      NAV2=NPTF-NAV1                                                    FK2.180
      XKIN=(-1.0)/(2.0*SPACIN)                                          FK2.181
      XKIN=XKIN*SCALK                                                   FK2.182
      DELK=(-2.0*XKIN)/FLOAT(NKX-1)                                     FK2.183
      READ 7,(X(I),I=1,NS)                                              FK2.184
      IF (EOF(5LINPUT).NE.0) GO TO 2672                                 FK2.185
      CALL SECOND(TIME)                                                 FK2.186
      PRINT 14,TIME                                                     FK2.187
      NSKCON=0                                                          FK2.188
      DO 730 J=1,NS                                                     FK2.189
      NSCON=NSCON+1                                                     FK2.190
      READ 8,STAT,(NNSKIP,(NSKIP(I),I=1,9)),GAIN,RS,RD,DMPFT            FK2.191
      PRINT 15,STAT,NPTT,ICOFER,IFKPSD,STA(1),SPACIN,XKIN,DELK,X(J)     FK2.192
       PRINT 16,ICONVEN,IFKPLCT,NVSDPL,GAIN                             FK2.193
      NB512=0                                                           FK2.194
      M=0                                                               FK2.195
      GO TO 377                                                         FK2.196
  373 PRINT 17                                                          FK2.197
                                                                        FK2.198
  377 READ (3) (NDAYS,NHOURS,MIN,NSEC)                                  FK2.199
      IF (EOF(3).NE.0) GO TO 373                                        FK2.200
      READ (3) (NDAYST,NHOUST,MINT,NSECT)                               FK2.201
      READ (3) (STATN(J),NB,JJ)                                         FK2.202
      IF (STATN(J).NE.STAT) GO TO 2675                                  FK2.203
      READ(3) (NVAL(I),I=1,NSMP)                                        FK2.204
      READ (3) (MORE)                                                   FK2.205
                                                                        FK2.206
      IF (ISKARR.NE.0) GO TO 602                                        FK2.207
      DO 460 I=1,NNSKIP                                                 FK2.208
      IF (NB.EQ.NSKIP(I)) GO TO 602                                     FK2.209
  460 CONTINUE                                                          FK2.210
                                                                        FK2.211
C.....------------------------------------------------------------------FK2.212
C.....ADJUSTING THE DC SHIFT.                                           FK2.213
C.....------------------------------------------------------------------FK2.214
      SHIFT=0.0                                                         FK2.215
      DO 480 IDC=1,NSMP                                                 FK2.216
      SHIFT=SHIFT+FLOAT(NVAL(IDC))                                      FK2.217
  480 CONTINUE                                                          FK2.218
      SHIFT=SHIFT/FLOAT(NSMP)                                           FK2.219
      DO 510 IDC=1,NSMP                                                 FK2.220
      NVAL(IDC)=NVAL(IDC)-SHIFT                                         FK2.221
  510 CONTINUE                                                          FK2.222
```

```
      LJ=1                                                                FK2.223
                                                                          FK2.224
C.    SEE NOTE AT FK2.174 ABOUT THE STATEMENT FK2.226                     FK2.225
      IDEL=IDEL+2                                                         FK2.226
                                                                          FK2.227
      NADV=CTIME(IDEL)/SAMIN                                              FK2.228
                                                                          FK2.229
C.....--------------------------------------------------------------------FK2.230
C.....APPLYING HAMMING WINDOW                                             FK2.231
C.....--------------------------------------------------------------------FK2.232
  521 DO 540 K=1,NPTT                                                     FK2.233
      RAN=(RANF(0)-0.5)*3.65                                              FK2.234
C     NVAL(K+LJ)=NVAL(K+LJ)+RAN                                           FK2.235
      DATA(K)=CMPLX(NVAL(K+LJ+NADV)*GAIN*W(K),0.0)                        FK2.236
  540 CONTINUE                                                            FK2.237
                                                                          FK2.238
       PRINT 18,STATN(J),NB,CTIME(IDEL),NADV                              FK2.239
                                                                          FK2.240
      IF (NB512.NE.0) GO TO 633                                           FK2.241
      PRINT 19, (NVAL(JN),JN=1,NPTT)                                      FK2.242
      IF (ICON.NE.0) GO TO 633                                            FK2.243
      CALL SECOND(TIME)                                                   FK2.244
      PRINT 14,TIME                                                       FK2.245
      GO TO 633                                                           FK2.246
  602  PRINT 20,STATN(J),NB                                               FK2.247
      IF (MORE.EQ.0.AND.NB512.EQ.0) GO TO 621                             FK2.248
      GO TO 725                                                           FK2.249
  621 PRINT 21,STAT                                                       FK2.250
      IF (NSKCON.GE.NS) GO TO 198                                         FK2.251
      GO TO 730                                                           FK2.252
                                                                          FK2.253
C.....--------------------------------------------------------------------FK2.254
C.....FFT AND THE CORRECTION FOR SYSTEM RESPONSE                          FK2.255
C.....--------------------------------------------------------------------FK2.256
  633 CALL FFT(DATA,NPOW,NPTT,PI)                                         FK2.257
      DO 640 NF=1,NPTF                                                    FK2.258
      DATA(NF)=CONJG(DATA(NF))                                            FK2.259
  640 CONTINUE                                                            FK2.260
      IF (RS.GT.1.0) CALL GEOPHON(DATA,PI2,CMPFT,RD,RS,NPTF)              FK2.261
      IF (NBW.NE.0) CALL ANTIALI(DATA,PI2,NBW,BWCUT,NPTF)                 FK2.262
      IF (ICON.NE.0) GO TO 672                                            FK2.263
      ICON=1                                                              FK2.264
      CALL SECOND(TIME)                                                   FK2.265
      PRINT 14,TIME                                                       FK2.266
  672 NB512=NB512+1                                                       FK2.267
      DO 700 NF=1,NPTF                                                    FK2.268
  700 XF(J,NB512,NF)=DATA(NF+1)*2.0*SAMIN                                 FK2.269
                                                                          FK2.271
                                                                          FK2.270
      IF (NB512.GE.NBMAX) GO TO 726                                       FK2.272
                                                                          FK2.273
  720 CONTINUE                                                            FK2.274
      LJ=LJ+NPTT                                                          FK2.275
      LJCK=LJ+NPTT                                                        FK2.276
      IF (LJCK.LT.NSMP) GO TO 521                                         FK2.277
  725 IF (MORE.NE.0) GO TO 377                                            FK2.278
  726 IF (MORE.NE.0) GO TO 377                                            FK2.279
      NREC=NB512                                                          FK2.280
  730 CONTINUE                                                            FK2.281
      CALL SECOND(TIME)                                                   FK2.282
      PRINT 14,TIME                                                       FK2.283
       PRINT 22,NB512,NAV                                                 FK2.284
```

```
      IF (NB512.EQ.0) GO TO 198
      TERM2=1.0/(2.0*FLOAT(NB512*NAV)-2.0)
      TERM3=SQRT(FLOAT(NB512*NAV)*TERM2)*Z95
      CALL SECOND(TIME)
      PRINT 14,TIME


C.....-----------------------------------------------------------------
C.....CONSTRUCTING THE SPETRAL MATRIX SM(JS,LS,NF),IN THE UPPER TRIANGLE
C.....-----------------------------------------------------------------
      DO 1070 NF=1,NPTF
      DO 1060 JS=1,NS
      DO 1050 LS=JS,NS
      SF =CZERO
      DO 1040 M=1,NREC
      F=XF(JS,M,NF)
      FF=CONJG(XF(LS,M,NF))
      F=F*FF
      SF=SF+F
 1040 CONTINUE
      SM(JS,LS,NF)=SF/FLOAT(NREC)
 1050 CONTINUE
 1060 CONTINUE
 1070 CONTINUE
      CALL SECOND(TIME)
      PRINT 14,TIME
      PRINT 879,(SM(1,1,NF),NF=1,NPTF)
      PRINT 879,(SM(1,6,NF),NF=1,NPTF)
  879 FORMAT (1H0,2X,*SM1*,//,24(2X,12E10.2,/))

C.....-----------------------------------------------------------------
C.....PLOTTING VELOCITY SPECTRAL DENSITY OF INDIVIDUAL GEOPHONE OUTPUT.
C.....-----------------------------------------------------------------
      IF (NVSDPL.LT.1) GO TO 1227
      DO 1220 IVSD=1,NVSDPL
      NV=NVSD(IVSD)
       READ 24, AMGAIN,VCOFS,RCCUT
       PRINT 25, AMGAIN,VCOFS,RCCUT,ENW
      DO 1200 NF=1,NPTF
      TVS=REAL(SM(NV,NV,NF))/(PERIOD*ENW)
      VS(NF)=SQRT(TVS)
 1200 CONTINUE
      IF (VCOFS.LT.1.0) GO TO 1212
      CALL AMPVCO(VS,NPTF,AMGAIN,VCOFS,RCCUT)
 1212 CONTINUE
      PRINT 879,(VS(NF),NF=1,NPTF)
      CALL PLOTVS
      CALL NXTFRM(SPECS)
 1220 CONTINUE
 1227 CONTINUE

C.....-----------------------------------------------------------------
C.....RUNNING AVERAGE OVER  (NAV) FREQUENCY COMPONENTS.
C.....-----------------------------------------------------------------

      IF (NAV.LE.1) GO TO 1377
      DO 1360 JS=1,NS
      DO 1350 LS=JS,NS
      DO 1320 NF=1,NPTF
      IF (NF.LE.NAV1) GO TO 1316
      IF (NF.GE.NAV2) GO TO 1316
      SF=(0.0,0.0)
```

```
      DO 1300 NA=1,NAV1
      I1=NF-NA
      I2=NF+NA
      SF=SF+SM(JS,LS,I1)+SM(JS,LS,I2)
 1300 CONTINUE
      SF=SF+SM(JS,LS,NF)
      T(NF)=SF/FLOAT(NAV)
      GO TO 1320
 1316 T(NF)=SM(JS,LS,NF)
 1320 CONTINUE
      DO 1340 NF=1,NPTF
      SM(JS,LS,NF)=T(NF)
 1340 CONTINUE
 1350 CONTINUE
 1360 CONTINUE
      JS=1
      LS=1
       PRINT 26,(SM(JS,LS,NF),NF=1,NPTF)
 1377 CONTINUE

C.....-----------------------------------------------------------------
C.....CALCULATING THE COHERENCE
C.....-----------------------------------------------------------------
      IF (ICOHER.NE.1) GO TO 1569
      DO 1540 JS=1,NS
      DO 1530 LS=JS,NS
      IF (JS.EQ.LS) GO TO 1530
      DO 1460 NF=1,NPTF
      SMTEMP=SM(JS,JS,NF)*SM(LS,LS,NF)
      DEN=CSQRT(SMTEMP)
      SM(JS,LS,NF)=SM(JS,LS,NF)/DEN
      COH(NF)=CABS(SM(JS,LS,NF))
 1460 CONTINUE
      CALL CONFLIM(TERM2,TERM3,NPTF)
      CALL YPLOT (COH,1,NPTF,1,1.0,0.0,STATN(JS),LS,FREQ)
      PRINT 27,NB512
      PRINT 28
       PRINT 29,(ERRBU(IE),EPRED(IE),IE=1,NPTF)
      TSTA=STATN(JS)
      IF (JS.GT.2) GO TO 1530
      CALL PLOTCOH(TSTA,LS,NPTF)
      CALL NXTFRM(SPECS)
 1530 CONTINUE
 1540 CONTINUE
      DO 1570 JS=1,NS
      DO 1560 NF=1,NPTF
      SM(JS,JS,NF)=1.0
 1560 CONTINUE
 1570 CONTINUE
 1569 IF (IFKPSD.EQ.0) GO TO 2671

      PRINT 30


C.....-----------------------------------------------------------------
C.....DO LOOP 2600 EVALUATES THE FKPSD AT DIFFERENT FREQUENCIES.
C.....-----------------------------------------------------------------
      CALL SECOND(TIME)
      PRINT 14,TIME
      PDB=0.0
      DO 2600 NF=1,NNFY
      NVEL=0
```

```
      NFP=NFY(NF)
      FREQCY=FREQ(NFP)
      IF (FREQCY.LT.8.0) GO TO 1627
      XKIN=(-1.0)/(2.0*SPACIN)
      XKIN=XKIN*2.0*SCALK
      DELK=(-2.0*XKIN)/FLOAT(NKX-1)
 1627 CONTINUE

C.....-----------------------------------------------------------------
C.....NORMALIZED THE SPECTRAL MATRIX AT  SELECTED FREQUENCIES.
C.....-----------------------------------------------------------------
      IF (ICOHER.EQ.1) GO TO 1716
      DO 1700 JS=1,NS
      DO 1690 LS=JS,NS
      IF (JS.EQ.LS) GO TO 1690
      SMTEMP=SM(JS,JS,NFP)*SM(LS,LS,NFP)
      DEN=CSQRT(SMTEMP)
      SM(JS,LS,NFP)=SM(JS,LS,NFP)/DEN
 1690 CONTINUE
 1700 CONTINUE
      DO 1710 JS=1,NS
      SM(JS,JS,NFP)=1.0
 1710 CONTINUE
 1716 CONTINUE

      PRINT 41

 1722 PMAX1=0.0
      DO 2350 KX=1,NKX
      XK(KX)=XKIN+DELK*FLOAT(KX-1)
      DO 2340 KY=1,NKY
      YK(KY)=XKIN+DELK*FLOAT(KY-1)

      IF (ICONVEN.EQ.1) GO TO 2213

C.....-----------------------------------------------------------------
C.....CONSTRUCTING THE WAVE NUMBER MATRIX.
C.....-----------------------------------------------------------------
      DO 2050 JS=1,NS
      DO 2040 LS=JS,NS
      SMNPF(JS,LS)=SM(JS,LS,NFP)
      IF (JS.EQ.LS) GO TO 2021
      T1=X(JS)-X(LS)
      DX=REAL(T1)
      DY=AIMAG(T1)
      AEXP=XK(KX)*DX+YK(KY)*DY
      AEXP=AEXP*PI2
      E=CMPLX(0.0,AEXP)
      E=CEXP(E)
      SMNPF(JS,LS)=SMNPF(JS,LS)*E
       SMNPF(LS,JS)=CONJG(SMNPF(JS,LS))
      GO TO 2036
C.....-----------------------------------------------------------------
C.....CONSTRUCTING V MATRIX (V) = (SM,I)
C.....-----------------------------------------------------------------
 2021 V(JS,LS)=1.0
      GO TO 2040
 2036 V(JS,LS)=SMNPF(JS,LS)
      V(LS,JS)=SMNPF(LS,JS)
 2040 CONTINUE
 2050 CONTINUE
      NSS=NS+1
```

```
      NSE=NS*2
      DO 2100 JS=1,NS
      DO 2070 LS=NSS,NSE
      LS1=LS-NS
      IF (JS.EQ.LS1) GO TO 2067
      V(JS,LS)=CZERO
      GO TO 2070
 2067 V(JS,LS)=1.0
 2070 CONTINUE
 2100 CONTINUE

C.....-----------------------------------------------------------------
C.....FIND THE INVERSE OF SPECTRAL MATRIX
C.....-----------------------------------------------------------------
      CALL CMXDIV(NS,NS,DET,12,V)
      DO 2130 JS=1,NS
      DO 2120 LS=1,NS
      NSS=LS+NS
      SMNPF(JS,LS)=V(JS,NSS)
 2120 CONTINUE
 2130 CONTINUE

C.....-----------------------------------------------------------------
C-....CONSTRUCTING THE MAXIMUM LIKELIHOOD FILTER.
C.....-----------------------------------------------------------------
      SUMQJL=(0.0,0.0)
      DO 2160 JS=1,NS
      DO 2150 LS=1,NS
      SUMQJL=SUMQJL+SMNPF(JS,LS)
 2150 CONTINUE
 2160 CONTINUE
      DO 2210 JS=1,NS
      SUMQL=(0.0,0.0)
      DO 2170 LS=1,NS
      SUMQL=SUMQL+SMNPF(JS,LS)
 2170 CONTINUE
      MLF(JS)=SUMQL/SUMQJL
      MLF(JS)=CONJG(MLF(JS))
 2210 CONTINUE
      GO TO 2224

 2213 DO 2220 LS=1,NS
      MLF(LS)=CMPLX(WSPA(LS),0.0)
 2220 CONTINUE

 2224 DO 2250 JS=1,NS
      TX=REAL(X(JS))
      TY=AIMAG(X(JS))
      BEXP=XK(KX)*TX+YK(KY)*TY
      BEXP=BEXP*PI2
      E=CMPLX(0.0,BEXP)
      EKX(JS)=CEXP(E)
 2250 CONTINUE

C.....-----------------------------------------------------------------
C.....ESTIMATE FKPSD
C.....-----------------------------------------------------------------
      SUM=0.
      NBC=0
      DO 2320 M=1,NREC
      SUMFUN=CZERO
      DO 2310 JS=1,NS
```

```
      CFUN=MLF(JS)*XF(JS,M,NFP)*EKX(JS)
      SUMFUN=SUMFUN+CFUN
 2310 CONTINUE
      FUN=CABS(SUMFUN)
      SUMM=FUN*FUN
      SUM=SUM+SUMM
      NBC=NBC+1
 2320 CONTINUE
      P(KX,KY)=SUM/FLOAT(NBC)
      IF (P(KX,KY).LT.PMAX1) GO TO 2340
      PMAX1=P(KX,KY)
 2340 CONTINUE
 2350 CONTINUE
      FKPMAX(NF)=PMAX1
      IF (FKPMAX(NF).LT.PDB) GO TO 2353
      PDB=FKPMAX(NF)
 2353 CONTINUE

C.....-----------------------------------------------------------------------
C.....TRANSFORMING THE FKPSD INTO DECIBAL SCALE WITH RESPECT TO THE PEAK
C.....FKPSD IN EACH FREQUENCY COMPONENT, THEN PRINT THE RESULTS.
C.....-----------------------------------------------------------------------

      PRINT 31,FREQCY,STA(1),PMAX1,XKIN,DELK,NFY(NF)
      PRINT 32
      PRINT 33
      DO 2480 KY=1,NKY
      DO 2470 KX=1,NKX
      P(KX,KY)=10.0*ALOG10(P(KX,KY)/PMAX1)
      NP(KX,KY)=-10*P(KX,KY)
      IF (P(KX,KY).LT.0.0) GO TO 2470
      XKPMAX=XK(KX)*XK(KX)
      YKPMAX=YK(KY)*YK(KY)
      NVEL=NVEL+1
      DELKH=0.5*DELK
      TEMPK=SQRT(XKPMAX+YKPMAX)
      IF (TEMPK.LT.DELKH) GO TO 2454
      VEL(NVEL)=FREQCY/TEMPK
      GO TO 2457
 2454 VEL(NVEL)=999.999
      THETA=0.000
      AZIMU(NVEL)=0.000
      GO TO 2470
 2457 CONTINUE
      THETA=57.2958*ATAN2(YK(KY),XK(KX))
      AZIMU(NVEL)=90.0-THETA
      IF (AZIMU(NVEL).GE.0.0) GO TO 2470
      AZIMU(NVEL)=360.0+AZIMU(NVEL)
 2470 CONTINUE
 2480 CONTINUE
      DO 2530 JKY=1,NKY
      JY=NKY-JKY+1
      IF (JY.EQ.21) GO TO 2516
      PRINT 34,(NP(KX,JY),KX=1,NKX)
      GO TO 2530
 2516  PRINT 35,(NP(KX,JY),KX=1,NKX)
 2530 CONTINUE
      PRINT 33
      PRINT 32
      PRINT 36,(VEL(IV),IV=1,NVEL)
      PRINT 37,(AZIMU(IV),IV=1,NVEL)
      IF (IFKPLOT.EQ.1) CALL FKPLOT(FREQCY,ICONVEN,NAV,PMAX1)
```

```
      CALL SYMCONT(P,NKX,NKY)                                           FK2.595
      CALL SECOND(TIME)                                                 FK2.596
      PRINT 14,TIME                                                     FK2.597
      IF (NF.EQ.NNFY.AND.MORE2.EQ.0) GO TO 2600                         FK2.598
      CALL NXTFRM(SPECS)                                                FK2.599
 2600 CONTINUE                                                          FK2.600
       PRINT 38,STA(1)                                                  FK2.601
      DO 2650 I=1,NNFY                                                  FK2.602
      NFP=NFY(I)                                                        FK2.603
      FYP(I)=FREQ(NFP)                                                  FK2.604
      PMAXDB(I)=10.0*ALOG10(FKPMAX(I)/PMAXREF)                          FK2.605
       PRINT 39,I,NFP,FYP(I),FKPMAX(I),PMAXDB(I)                        FK2.606
 2650 CONTINUE                                                          FK2.607
      IF (IFKYPL.EQ.1) CALL YPLOT(PMAXDB,1,NNFY,1,30.,-30.,STA(1),1,FYP)FK2.608
 2671 IF (MORE2.NE.0) GO TO 198                                         FK2.609
 2672 CALL GOSEND(SPECS)                                                FK2.610
      GO TO 2710                                                        FK2.611
 2675  PRINT 40,J,STATN(J),STAT                                         FK2.612
 2710 CONTINUE                                                          FK2.613
      CALL SECOND(TIME)                                                 FK2.614
      PRINT 14,TIME                                                     FK2.615
                                                                        FK2.616
                                                                        FK2.617
    1 FORMAT (F5.0,4I5)                                                 FK2.618
    2 FORMAT (I5,10F5.0)                                                FK2.619
    3 FORMAT (15I5)                                                     FK2.620
    4 FORMAT (8I5,3F5.0,A10)                                            FK2.621
    5 FORMAT (16I5)                                                     FK2.622
    6 FORMAT (16F5.3)                                                   FK2.623
    7 FORMAT (10F8.4)                                                   FK2.624
    8 FORMAT (A10,10I2,4F5.0)                                           FK2.625
   14 FORMAT (15X,*TIME = *,F15.4)                                      FK2.626
   15 FORMAT (1H0,///,17H                 ,33X,*THE DATA CAME FROM *,A10FK2.627
     1,/,50X,*NUMBER OF POINT IN TIME DOMAIN = *,I4,/,50X,*ICOHER = *,I1FK2.628
     1,/,50X,*IFKPSD = *,I1,/,50X,*STA = *,A10,/,50X,*SEISMOMETER SPACINFK2.629
     1G IN KM = *,F6.3,/,50X,*INITIAL KX AND KY = *,F7.2,/,50X,*DELTA K FK2.630
     1= *,F7.3,/,50X,*COORDINATES OF THE SEISMOMETER IN KM = *,2F7.3,/) FK2.631
   16 FORMAT (1H0,49X,*ICONVEN = *,I2,/,50X,*IFKPLOT = *,I2,/,50X,*NVSDPFK2.632
     1L = *,I2,/,50X,*GAIN = *,E12.3,//)                                FK2.633
   17 FORMAT (1H0,10X,*END OF FILE MARK ENCOUNTED*,//)                  FK2.634
   18 FORMAT (1H0,10X,*STATION *,A10,I3,* TIME CORRECTION IS *,F8.3,* SEFK2.635
     1CONDS, WHICH CORR. TO *,I5,* POINTS ADV. IN DIGITAL DATA.*)       FK2.636
   19 FORMAT (2X,5I6,3X,5I6,3X,5I6,3X,5I6)                              FK2.637
   20 FORMAT (1H0,10X,*THE PROGRAM SKIPS THE RECORD *,A10,I3,* AS REQUESFK2.638
     1TED.*)                                                            FK2.639
   21 FORMAT (1H0,/,10X,*THE DIGITAL DATA FROM THE STATION *,A10,* GIVE FK2.640
     1NB512=0 WHEN MORE=0.*)                                            FK2.641
   22 FORMAT (1H0,5X,*NO. OF 512PTS DATA BLOCK = *,I5,*,RUNNING AVE. OVEFK2.642
     1R *,I4,* POINTS.*,/)                                              FK2.643
   23 FORMAT (1H0,2X,*SM1*,//,24(2X,12E10.2,/))                         FK2.644
   24 FORMAT (3F5.0)                                                    FK2.645
   25 FORMAT (1H0,* AMPLIFIER GAIN = *,F6.2,*  VCO FULL SCALE = *,F5.1,*FK2.646
     1 RC CUT = *,F5.1,*  W ENERGY = *,E10.3)                           FK2.647
   26 FORMAT (1H0,2X,*SM2*,//,24(2X,12E10.2,/))                         FK2.648
   27 FORMAT (//,2X,*NB512 = *,I5)                                      FK2.649
   28 FORMAT (3X,*95 PERCENT CONFIDENT LIMIT*,/)                        FK2.650
   29 FORMAT (10(3X,2F5.2))                                             FK2.651
   30 FORMAT (1H6)                                                      FK2.652
   31 FORMAT (1H1,1X,*FREQUENCY WAVENUMBER POWER SPECTRAL DENSITY AT FREFK2.653
     1QUENCY = *,F7.2,*     AT*,A10,/,2X,*MAXIMAL PSD = *,E12.3,/,2X,*NOFK2.654
     1TE THAT THE VALUES PRINTED ARE (-10)(PSD/PMAX1) IN DB.*,/,2X,*X295FK2.655
     1 = *,F9.3,2X,*DELTA K = *,F9.3,//,2X,*NFY = *,I3,////////////)    FK2.656
```

```
 32 FORMAT (64X,1H0)
 33 FORMAT (2X,123H  . . . . . . . . . . . . . . . . . . . . . . . . . .
  1  . . . . . . . . . . . . . . . . . . . . . . . . . . . . . . . . .
  1  .  .)
 34 FORMAT (1H0,1X,41(I3))
 35 FORMAT (1H0,*0*,41(I3),* 0*)
 36 FORMAT (1H0,2X,*VELOCITY (KM/SEC) = *,5F10.3)
 37 FORMAT (1H0,2X,*AZIMUTH (DEGREE)  = *,5F10=3)
 38 FORMAT (1H1,4X,A10,/)
 39 FORMAT (2I5,*  FREQUENCY = *,F7.2,*  MAXIMUM FKPSD = *,E12.3,F10.3
  1,* DB*)
 40 FORMAT (1H0,///,*   THE PROGRAM STOPS DUE TO STATN(*,I2,*) = *,A10
  1,*   WHICH CONFLICTS WITH STAT = *,A10)
 41 FORMAT (1H0)
    STOP
    END


    SUBROUTINE AMPVCO(VS,NPTF,GAIN,VCOFS,RCCUT)

C.....SUBROUTINE AMPVCO CORRECTS THE GAIN AND THE LOW-PASS FILTER OF THE
C     AMPLIFIER AND THE VCO FULL SCALE.
C     THE LOW-PASS FILTER AT AS110 IS 2-POLE RC FILTER.

    COMMON /BLK1/FREQ(226)
    DIMENSION VS(226)
    GAIN=GAIN/20.0
    GAIN=10.0**GAIN
    A=GAIN*2048.0/VCOFS
    DO 1 I=1,NPTF
    B=FREQ(I)/RCCUT
    B2=B*B+1
    VS(I)=VS(I)*B2/A
    VS(I)=VS(I)*1.0E+09
  1 CONTINUE
    RETURN
    END


    SUBROUTINE ANTIALI(VS,PI2,NBW,BWCUT,NPTF)

C.....SUBROUTINE ANTIALI IS USED TO COREECT MODULUS OF THE TRANSFER
C     FUNCTION OF ARBITRARY LOW PASS BUTTERWORTH FILTER SUCH AS THE
C     ANTI-ALIASING FILTER USED IN THE HAVILAND HALL.
C     NBW = NUMBER OF FILTER STAGE
C     NPOLE = NUMBER OF POLE OF THE FILTER.

    COMPLEX VS
    COMMON /BLK1/FREQ(226)
    DIMENSION VS(226)
    NPOLE=4
    DO 1 I=1,NPTF
    N=2*NPOLE
    A=FREQ(I)/BWCUT
    A=A**N
    B=SQRT(1+A)
    B=B**NBW
    VS(I)=VS(I)*B
  1 CONTINUE
    RETURN
    END
```

```
      SUBROUTINE CMXDIV(IN,IM,DET,IDIM,V)

C     REPLACES B BY (A INVERSE)*B.  DESTROYS A.
C     A IS N BY N, B IS N BY M.   A AND B ARE STORED IN V(N,N+M).

      COMPLEX SAVE,PIVOT,DETERM,DET,V,CABS
      DIMENSION V(IDIM,1)
      INTEGER P
      N=IN
      M=IM
C
      NM1=N-1
      NP1=N+1
      NPM=N+M
      DETERM=(1.0E0,0.0E0)
      P=1
  202 CONTINUE
      IMIN=P+1
C                              FIND PIVOT
      RPIVOT=0.0E0
      DO 209 I=P,N
      RSAVE=CABS(V(I,P))
      IF (RSAVE .LE. RPIVOT) GO TO 209
      RPIVOT=RSAVE
      IBIG=I
  209 CONTINUE
      IF (RPIVOT .GT. 0.0E0) GO TO 210
      DETERM=(0.0E0,0.0E0)
      GO TO 290
C                              ROW EXCHANGE AND ROW REDUCTION
  210 PIVOT=V(IBIG,P)
      DETERM=DETERM*PIVOT
      DO 219 J=P,NPM
      SAVE=V(IBIG,J)/PIVOT
      V(IBIG,J)=V(P,J)
      V(P,J)=SAVE
  219 CONTINUE
      IF(IBIG .NE. P) DETERM=-DETERM
      IF (P .GE. N) GO TO 250
      V(P,P)=(1.0E0,0.0E0)
C                              BLOCK REDUCTION
      DO 239 I=IMIN,N
      DO 238 J=IMIN,NPM
      V(I,J)=V(I,J)-V(I,P)*V(P,J)
  238 CONTINUE
      V(I,P)=(0.0E0,0.0E0)
  239 CONTINUE
      P=P+1
  249 GO TO 202
C                              BACK SUBSTITUTION
  250 CONTINUE
      IF (M .LE. 0) GO TO 290
      DO 259 K=NP1,NPM
      DO 253 P=1,NM1
      I=N-P
      DO 252 J=I,NM1
      V(I,K)=V(I,K)-V(J+1,K)*V(I,J+1)
  252 CONTINUE
  253 CONTINUE
  259 CONTINUE
C
```

```
  290 CONTINUE
      DET=DETERM
      RETURN
      END


      SUBROUTINE CONFLIM(TERM2,TERM3,NPTF)
C.....THIS ROUTINE CALCULATES THE CONFIDENT LIMITS OF COHERENCE ESTIMATE
      COMMON /BLK2/COH(226)
      COMMON /BLK13/ERRBU(164),ERRBD(164)
      DIMENSION W(164)
      DO 2 NF=1,NPTF
      A=(1.0+COH(NF))/(1.0-COH(NF))
      W(NF)=0.5*ALOG(A)
      B=W(NF)-TERM2
      CU=B+TERM3
      CD=B-TERM3
      ERRBU(NF)=TANH(CU)
      ERRBD(NF)=TANH(CD)
    2 CONTINUE
      RETURN
      END


      SUBROUTINE FFT(A,M,N,PI)

C.....THIS FFT SUBROUTINE PERFORMS THE FORWARD FAST FOURIER TRANSFORM
C     ONLY. AFTER COOLEY,LEWIS,WELCH,OBTAINED FROM L.R. RABINER AND B.
C     GOLD---- THEORY AND APPLICATION OF DIGITAL SIGNAL PROCESSING.
C.....N=2**M
C.....A(N) = THE ARRAY OF DATA TO BE TRANSFORMED.

      COMPLEX A(N),U,W,T
      NV2=N/2
      NM1=N-1
      J=1
      DO 7 I=1,NM1
      IF (I.GE.J) GO TO 5
      T=A(J)
      A(J)=A(I)
      A(I)=T
    5 K=NV2
    6 IF(K.GE.J) GO TO 7
      J=J-K
      K=K/2
      GO TO 6
    7 J=J+K
      DO 20 L=1,M
      LE=2**L
      LE1=LE/2
      U=(1.0,0.)
      W=CMPLX(COS(PI/LE1),SIN(PI/LE1))
      DO 20 J=1,LE1
      DO 10 I=J,N,LE
      IP=I+LE1
      T=A(IP)*U
      A(IP)=A(I)-T
   10 A(I)=A(I)+T
   20 U=U*W
      RETURN
```

```
      END

      SUBROUTINE FKPLOT(FRECCY,ICONVEN,NAV,PMAX1)

C.....THIS SUBROUTINE CONTOURS THE FREQUENCY WAVE               NSITY
C     AT A SELECTED FREQUENCY ON A KX-KY PLANE.

      COMMON /BLK7/X(41),Y(41)
      COMMON /BLK8/Z(41,41)
      COMMON /BLK9/NKX,NKY
      COMMON /BLK10/ZLEVEL(10),NL
      COMMON /BLK11/LINE(2)
      COMMON /BLK12/VEL(5),NVEL,AZIM(5)
      DIMENSION BUFXYZ(100),SPECS(35)
      SPECS(1)=1.0
      SPECS(2)=1.5
      SPECS(3)=X(NKX)
      SPECS(4)=X(1)
      SPECS(5)=Y(NKY)
      SPECS(6)=Y(1)
      SPECS(7)=5.0
      SPECS(8)=5.0
      SPECS(11)=1.0
      SPECS(12)=99.
      SPECS(9)=2.0
      SPECS(10)=2.0
      CALL GDLILI(SPECS)
      SPECS(30)=97.
      SPECS(31)=NKX
      SPECS(32)=NKY
      SPECS(33)=FLOAT(NL)
      LENGTH=67
      CALL CONLI(X,Y,Z,ZLEVEL,BUFXYZ,LENGTH,SPECS)
      SPECS(17)=0.15
      SPECS(18)=0.15
      SPECS(19)=0.0
      SPECS(20)=0.0
      SPECS(21)=1.0
      SPECS(22)=6.1
      SPECS(23)=6.6
      SPECS(29)=3.0
      RULE=1.0
      CALL SIGVAL (RULE,FRECCY,0,SPECS)
      SPECS(22)=6.9
      CALL TITLEG(RULE,2HHZ,SPECS)
      SPECS(22)=7.4
      SPECS(28)=0.0
      VALUE=NAV
      CALL DECVAL(RULE,VALUE,SPECS)
      SPECS(22)=4.5
      IF (ICONVEN.EQ.0) CALL TITLEG(RULE,4HH.R.,SPECS)
      IF (ICONVEN.EQ.1) CALL TITLEG(RULE,5HCONV.,S
      SPECS(22)=2.5
      CALL TITLEG(RULE,LINE,SPECS)
      SPECS(17)=0.1
      SPECS(18)=0.1
      SPECS(19)=0.0
      SPECS(24)=0.0
      SPECS(28)=1.0
      CALL NODLIB(SPECS)
      SPECS(26)=0.0
```

```
      CALL NODLIL(SPECS)
      SPECS(17)=0.15
      SPECS(18)=0.15
      SPECS(24)=0.2
      CALL TITLEG(14HKX (CYCLES/KM),SPECS)
      SPECS(26)=0.4
      CALL TITLEL(14HKY (CYCLES/KM),SPECS)
      SPECS(22)=6.1
      SPECS(23)=6.0
      SPECS(17)=0.1
      SPECS(18)=0.1
      CALL TITLEG(RULE,11HLEVELS (DB),SPECS)
      SPECS(23)=4.0
      CALL TITLEG(RULE,17HVELOCITY (KM/SEC),SPECS)
      SPECS(17)=0.1
      SPECS(18)=0.1
      SPECS(22)=6.3
      SPECS(28)=1.0
      DO 5 L=1,NL
      SPECS(23)=5.7-0.2*FLOAT(L-1)
      VALUE=ZLEVEL(L)
      CALL DECVAL(RULE,VALUE,SPECS)
    5 CONTINUE
      SPECS(28)=3.0
      DO 6 L=1,NVEL
      SPECS(23)=3.8-0.2*FLOAT(L-1)
      VALUE=VEL(L)
      CALL DECVAL (RULE,VALUE,SPECS)
    6 CONTINUE
      SPECS(22)=7.0
      SPECS(23)=1.0
      DO 7 L=1,NVEL
      SPECS(23)=3.8-0.2*FLOAT(L-1)
      VALUE=AZIMU(L)
      CALL DECVAL(RULE,VALUE,SPECS)
    7 CONTINUE
      SPECS(22)=6.3
      SPECS(23)=1.5
      SPECS(24)=4.0
      CALL SIGVAL(RULE,PMAX1,IPOWER,SPECS)
      SPECS(22)=6.1
      CALL TITLEG(RULE,13HPMAX =       E,SPECS)
      SPECS(22)=7.4
      SPECS(28)=0.
      VALUE=FLOAT(IPOWER)
      CALL DECVAL(RULE,VALUE,SPECS)
      RETURN
      END

      SUBROUTINE GEOPHON(DATA,PI2,DMPFT,RD,RS,NPTF)

C.....SUBROUTINE GEOPHON IS USED TO CORRECT THE VELOCITY SENSITIVITY,
C     DAMPING RESISTANCE,AND GENERATOR CONSTANCE.
C.....WG = NATURAL FREQUENCY OF THE SEISMOMETER (IN HZ).
C     GS = GENERATOR CONSTANCE OF THE SEISMOMETER (IN VOLT/METER/SEC).
C     RS = COIL RESISTANCE.
C     RD = DAMPING RESISTANCE.
C     DMPFT =  DAMPING FACTOR.

      COMPLEX DATA,E,PH
      COMMON /BLK1/FREQ(226)
```

```
      DIMENSION PHASE(257)
      DIMENSION DATA(512)
      DATA WG/4.5/,GS/77.17/
      DATA LAB/10HPHASE TEST/
      WS=WG*PI2
      WS2=WS*WS
      RO2=2.0*DMPFT
      RD=RD*1000.0
      RS=RS*1000.0
      DO 1 I=2,NPTF
      WE=PI2*FREQ(I-1)
      WE2=WE*WE
      A=WE2-WS2
      A2=A*A
      B=RO2*WS*WE
      B2=B*B
      C=SQRT(A2+B2)
      AMP=WE2/C
      PHASE(I)=ATAN2(B,A)
      PA=PHASE(I)
      E=CMPLX(0.0,PA)
      PH=CEXP(E)
C     PRINT 2,PHASE,PA,PH,AMP,DATA(I)
    2 FORMAT (5X,8E12.3)
      DATA(I)=DATA(I)/(AMP*PH)
      IF (RD.GE.999000.0) GO TO 1
      R=RS+RD
      DATA(I)=DATA(I)*R/RD
    1 CONTINUE
      RETURN
      END


      SUBROUTINE HAMMIN(NPTT,PI2,W,ENW)
      DIMENSION W(NPTT)
      ALFA=0.54
      ALFA1=1.0-ALFA
      A=FLOAT((NPTT-1)/2)
      ENW=0.0
      DO 5 M=1,NPTT
      B=FLOAT(M-1)
      ARG=PI2*(B-A)/FLOAT(NPTT)
      W(M)=ALFA+ALFA1*COS(ARG)
      ENW=ENW+W(M)*W(M)
    5 CONTINUE
      RETURN
      END


      SUBROUTINE PLOTCOH(LABEL1,L,NPTF)

C.....THIS SUBROUTINE PLOTS THE COHERENCE BETWEEN TWO SEISMOMETER
C     OUTPUTS.

      COMMON /BLK1/X(226)
      COMMON /BLK2/Y(226)
      COMMON /BLK13/ERRBU(164),ERRBC(164)
      DIMENSION SPECS(30),LINE(4)
      SPECS(1)=1.0
      SPECS(2)=1.5
      SPECS(3)=25.0
      SPECS(4)=0.3
```

```
      SPECS(5)=1.0
      SPECS(6)=0.0
    5 SPECS(7)=7.675
      SPECS(8)=5.2
      SPECS(10)=10.0
      SPECS(11)=1.0
      SPECS(12)=99.
      CALL AXLGLI(SPECS)
      SPECS(25)=-0.15
      CALL SAXLGT(SPECS)
      SPECS(27)=-0.15
      CALL SAXLIR(SPECS)
      SPECS(13)=FLOAT(NPTF)
      SPECS(14)=1.0
      SPECS(15)=1.0
      SPECS(30)=97.
      CALL SLLGLI(X,Y,SPECS)
      DO 10 I=1,NPTF
      Y(I)=ERRBU(I)
   10 CONTINUE
      SPECS(16)=17.0
      SPECS(17)=0.05
      SPECS(18)=0.05
      CALL PSLGLI(X,Y,SPECS)
      DO 11 I=1,NPTF
      Y(I)=ERRBU(I)
   11 CONTINUE
      CALL PSLGLI(X,Y,SPECS)
   15 SPECS(17)=.1
      SPECS(18)=.1
      SPECS(19)=0.0
      SPECS(21)=1.0
      SPECS(24)=0.0
      SPECS(29)=2.0
      CALL NOLGB(SPECS)
      SPECS(20)=0.0
      SPECS(26)=0.0
      SPECS(28)=1.0
      CALL NODLTL(SPECS)
      SPECS(17)=0.15
      SPECS(18)=0.15
      SPECS(24)=0.2
      CALL TITLEB(14HFREQUENCY (HZ),SPECS)
      SPECS(20)=90.0
      SPECS(26)=0.4
      CALL TITLEL(9HCOHERENCE,SPECS)
      SPECS(17)=0.15
      SPECS(18)=0.15
      SPECS(19)=0.0
      SPECS(20)=0.0
      SPECS(21)=1.0
      SPECS(22)=2.0
      SPECS(23)=6.6
      RULE=1.0
      LINE(1)=LABEL1
      LINE(2)=0
      CALL TITLEG(RULE,LINE,SPECS)
      SPECS(22)=4.5
      SPECS(28)=0.
      VALUE=FLOAT(L)
      CALL DECVAL(RULE,VALUE,SPECS)
      RETURN
```

```
      END                                                               PLCOH.77
                                                                        PLCOH.78

      SUBROUTINE PLOTVS                                                 PLVS.2
                                                                        PLVS.3
C.....THIS SUBROUTINE PLOTS THE VELOCITY SPECTRAL DENSITY IN LOG*LOG    PLVS.4
C.....SCALE.                                                            PLVS.5
                                                                        PLVS.6
      DIMENSION SPECS(30),LINE(4)                                       PLVS.7
      COMMON /BLK1/X(226)                                               PLVS.8
      COMMON /BLK11/STAT(2)                                             PLVS.9
      COMMON /BLK14/Y(226),NREC,NPTF                                    PLVS.10
      SPECS(1)=1.0                                                      PLVS.11
      SPECS(2) =1.5                                                     PLVS.12
      SPECS(3)=25.0                                                     PLVS.13
      SPECS(4)=0.3                                                      PLVS.14
      DO 8 I=1,NPTF                                                     PLVS.15
      IF (Y(I).GT.1.0E+03) GO TO 6                                      PLVS.16
      IF (Y(I).LT.1.0E-01) GO TO 9                                      PLVS.17
    8 CONTINUE                                                          PLVS.18
      SPECS(5)=1.0E+03                                                  PLVS.19
      SPECS(6)=1.0E-01                                                  PLVS.20
      GO TO 5                                                           PLVS.21
    6 SPECS(5)=1.0E+04                                                  PLVS.22
      SPECS(6)=1.0                                                      PLVS.23
      GO TO 5                                                           PLVS.24
    9 SPECS(5)=1.0E+01                                                  PLVS.25
      SPECS(6)=1.0E-03                                                  PLVS.26
    5 SPECS(7)=7.875                                                    PLVS.27
      SPECS(8)=5.2                                                      PLVS.28
      SPECS(11)=1.0                                                     PLVS.29
      SPECS(12)=99.                                                     PLVS.30
      CALL AXLGLG(SPECS)                                                PLVS.31
      YMAX=SPECS(5)                                                     PLVS.32
      YMIN=SPECS(6)                                                     PLVS.33
      DO 10 I=1,NPTF                                                    PLVS.34
      IF (Y(I).GT.YMAX) Y(I)=YMAX                                       PLVS.35
      IF (Y(I).LT.YMIN) Y(I)=YMIN                                       PLVS.36
   10 CONTINUE                                                          PLVS.37
      SPECS(25)=-0.15                                                   PLVS.38
      CALL SAXLGT(SPECS)                                                PLVS.39
      SPECS(27)=-0.15                                                   PLVS.40
      CALL SAXLGR(SPECS)                                                PLVS.41
      SPECS(13)=FLOAT(NPTF)                                             PLVS.42
      SPECS(14)=1.0                                                     PLVS.43
      SPECS(15)=1.0                                                     PLVS.44
      SPECS(30)=97.                                                     PLVS.45
      CALL SLLGLG(X,Y,SPECS)                                            PLVS.46
   15 SPECS(17)=.1                                                      PLVS.47
      SPECS(18)=.1                                                      PLVS.48
      SPECS(9)=10.0                                                     PLVS.49
      SPECS(19)=0.0                                                     PLVS.50
      SPECS(21)=1.0                                                     PLVS.51
      SPECS(24)=0.0                                                     PLVS.52
      SPECS(29)=2.0                                                     PLVS.53
      CALL NOLGB(SPECS)                                                 PLVS.54
      SPECS(20)=0.0                                                     PLVS.55
      SPECS(26)=0.0                                                     PLVS.56
      CALL NOLGL(SPECS)                                                 PLVS.57
      SPECS(17)=0.15                                                    PLVS.58
      SPECS(18)=0.15                                                    PLVS.59
```

```
      SPECS(24)=0.2
       CALL TITLEB(14HFREQUENCY (HZ),SPECS)
      SPECS(20)=90.0
      SPECS(26)=3.4
      CALL TITLEL(30HVSD (MILLIMICRON/SEC/SQRT(HZ)),SPECS)
      SPECS(17)=.15
      SPECS(18)=0.15
      SPECS(19)=0.0
      SPECS(20)=0.0
      SPECS(21)=1.0
      SPECS(23)=0.8
      RULE=1.0
      SPECS(22)=2.15
      SPECS(28)=0.0
      VALUE=NREC
      CALL DECVAL(RULE,VALUE,SPECS)
      LINE(1)=STAT(1)
      LINE (2)=10H   RECORDS
      LINE(3)=0
      SPECS(22)=0.5
      CALL TITLEG(RULE,LINE,SPECS)
      RETURN
      END


      SUBROUTINE SYMCONT(P,NKX,NKY)

C.....THIS SUBROUTINE PLOTS THE FKPSD BY SYMBOLS AT A FREQUENCY
C     COMPONENT.

      COMMON /BLK10/PLEVEL(10),NPLEV
      DIMENSION P(41,41),KEY(41)
      DATA K1,K2,K3,K4,K5,K6/1H0,1H*,1H/,1H=,1H$,1H+/
      DATA K7/1H /
      PRINT 750
  750 FORMAT (1H0)
      PRINT 760, (PLEVEL(I),I=1,NPLEV)
  760 FORMAT (1H1,*  CONTOUR LEVELS = *,7E12.3)
      PRINT 762
  762 FORMAT (1H0,/////////////////)
      PRINT 700
  700 FORMAT (64X,1H0)
      PRINT 761
  761 FORMAT (2X,123H  .   .   .   .   .   .   .   .   .   .   .   .   .   .   .
     1  .   .   .   .   .   .   .   .   .   .   .   .   .   .   .   .   .
     1  .   .)
      DO 100 JKY=1,NKY
      JY=NKY-JKY+1
      DO 200 KX=1,NKX
      IF (P(KX,JY).GE.PLEVEL(1)) GO TO 10
      IF (P(KX,JY).GE.PLEVEL(2)) GO TO 20
      IF (P(KX,JY).GE.PLEVEL(3)) GO TO 30
      IF (P(KX,JY).GE.PLEVEL(4)) GO TO 40
      IF (P(KX,JY).GE.PLEVEL(5)) GO TO 50
      IF (P(KX,JY).GE.PLEVEL(6)) GO TO 60
      KEY(KX)=K7
      GO TO 200
   60 KEY(KX)=K6
      GO TO 200
   50 KEY(KX)=K5
      GO TO 200
   40 KEY(KX)=K4
```

```
      GO TO 200
   30 KEY(KX)=K3
      GO TO 200
   20 KEY(KX)=K2
      GO TO 200
   10 KEY(KX)=K1
  200 CONTINUE
      IF (JY.EQ.21) GO TO 151
      PRINT 150,(KEY(J),J=1,NKX)
  150 FORMAT (1H0,1X,41(2X,A1))
      GO TO 100
  151 PRINT 152,(KEY(J),J=1,NKX)
  152 FORMAT (1H0,*0*,41(2X,A1),* 0*)
  100 CONTINUE
      PRINT 761
      PRINT 700
      RETURN
      END


      SUBROUTINE YPLOT(Y,IB,IE,IK,PMAX,PMIN,TITLE,L,X)

      DIMENSION X(1)
      DIMENSION Y(1),KMAP(100),ISCALE(11)
      DATA KBLANK,KY/1H ,1H*/
      DATA ISCALE/ 0,10,20,30,40,50,60,70,80,90,100/
      DO 2 I=1,100
    2 KMAP(I)=KBLANK
C....PRINT BEGINNING OF GRAPH
      C=100.0/(PMAX-PMIN)
      B=C*PMIN
      SCALE=1.0/C
      PRINT 5,TITLE,L,IB,IE,IK,PMAX,PMIN
    5 FORMAT (1H1,10X,*YPLOT......*,A10,I5,/,10X,*IB=*,I5,2X,*IE=*,I5,2X
     1,*IK=*,I5,2X,*PMAX=*,E12.3,2X,*PMIN=*,E12.3,///)
      PRINT 6, (ISCALE(I),I=1,11)
    6 FORMAT(11X,5(I2,8X),1X,I2,5(7X,I3))
      DO 7 I=1,2
    7 PRINT 8
    8 FORMAT(13X,(11(1H. ,9X)))
      PRINT 12
   12  FORMAT (  6X,1HX,7X,100H......................................
     1.................................................... ,7X,1HY
     1Y)
C....PRINT BODY OF GRAPH
      DO 10 I=IB,IE,IK
      IY=C*Y(I)-B
C     CHECK THAT Y IS ON SCALE
      IF(IY .LT. 1 .OR. IY .GT. 100) GO TO 13
      KMAP(IY)=KY
      PRINT 9, X(I),(KMAP(J),J=1,100),Y(I),I
    9   FORMAT (  2X,F9.3,1X,1HI,100A1,1HI,2X,E10.3,1X,I4)
      GO TO 14
   13 PRINT 9, X(I),(KMAP(J),J=1,100),Y(I)
      GO TO 10
   14 KMAP(IY)=KBLANK
   10 CONTINUE
      RETURN
      END

62.50     6 2500    24     2
    5 -1.0 -3.0 -6.0 -9.0-12.0
```

```
     0       0       0
     1       0       1       1      12       0       0       3 10.0   0.50.007    E5.9W04
    20       1       2       3       4       5       6       7       8       9      10      11      12      13      14      15
    16      17      18      19      20
0.1200.0000.1200.0000.1200.0000.1200.0000.1200.0000.0000.0000.1200.0000.1200.000
0.1200.0000.0800.0000.1200.0000.1200.000
 -0.0190  0.0110  0.0000  0.0250  0.0190  0.0110 -0.0108  0.0063  0.0000  0.0177
  0.0108  0.0063 -0.0153 -0.0089  0.0000 -0.0125  0.0153 -0.0089 -0.0217 -0.0125
  0.0000 -0.0219  0.0217 -0.0125
 E5.9W0401 2 1 3                     1.0  3.4999.0 0.30
 E5.9W0402 2 1 3                     1.0 1.35 3.00 0.60
 E5.9W0403 2 1 3                     1.0 1.35 3.00 0.60
 E5.9W0404 2 1 3                     1.0 3.40999.0 0.30
 E5.9W0405 2 1 3                     1.0 1.35 3.00 0.60
 E5.9W0406 2 1 3                     1.0 3.40999.0 0.30
 E5.9W0407 2 1 3                     1.0 3.40999.0 0.30
 E5.9W0408 3 1 2 4                   1.0 4.30999.0 0.60
 E5.9W0409 3 1 2 4                   1.0 1.35999.0 0.60
 E5.9W0410 2 1 3                     1.0 3.40999.0 0.30
 E5.9W0411 2 1 3                     1.0 3.40999.0 0.30
 E5.9W0412 2 1 3                     1.0 1.35 3.50 0.60
     0       0       1       0      12       0       0       3 10.0   0.50.007    E5.9W05
     4       7       8       9      10
0.0000.0400.0000.0400.0000.0200.0000.0000.0000.0400.0000.0400.0000.0400.0000.000
0.0000.0000.0000.0400.0000.0400.0000.040
 -0.0190  0.0110  0.0000  0.0250  0.0190  0.0110 -0.0108  0.0063  0.0000  0.0177
  0.0108  0.0063 -0.0153 -0.0089  0.0000 -0.0125  0.0153 -0.0089 -0.0217 -0.0125
  0.0000 -0.0219  0.0217 -0.0125
 E5.9W0501 2 2 3                     1.0  3.4999.0 0.30
 E5.9W0502 3 2 3 4                   1.0 1.35 3.00 0.60
 E5.9W0503 2 2 3                     1.0 1.35 3.00 0.60
 E5.9W0504 2 2 3                     1.0 3.40999.0 0.30
 E5.9W0505 2 2 3                     1.0 1.35 3.00 0.60
 E5.9W0506 2 2 3                     1.0 3.40999.0 0.30
 E5.9W0507 2 2 3                     1.0 3.40999.0 0.30
 E5.9W0508 2 2 3                     1.0 4.30999.0 0.60
 E5.9W0509 2 2 3                     1.0 1.35999.0 0.60
 E5.9W0510 2 2 3                     1.0 3.40999.0 0.30
 E5.9W0511 2 2 3                     1.0 3.40999.0 0.30
 E5.9W0512 2 2 3                     1.0 1.35 3.50 0.60
114.0  5.0 30.0
```